A GEOCHEMICAL STUDY OF THE CONTROLS OF CRUDE OIL WATER UPTAKE ABILITY AT SURFACE CONDITIONS.

by

Edward L. Clarke, B.Sc.(HONS), M.Sc.,

A thesis submitted to the University of Newcastle upon Tyne
in partial fulfilment of the requirements for the degree of
Doctor of Philosophy in the Faculty of Science

Fossil Fuels and Environmental Geochemistry
(Postgraduate Institute): NRG
University of Newcastle upon Tyne, U.K.

December 1995

DECLARATION

I hereby certify that the work decribed in this thesis is my own, except where otherwise acknowledged, and has not been submitted previously for a degree at this or any other university.

Edward Clarke

ACKNOWLEDGEMENTS

I would like to express my sincere thanks and gratitude to the people, organisations and companies who have helped and encouraged me throughout my PhD studies here at the NRG. To begin with I would like to thank my two supervisors, Prof. Steve Larter and Dr. Martin Jones for their friendship, help and guidance throughout both my PhD and MSc studies. For funding and assistance I would like to thank Robert Johnson and all at "The PSTI" Edinburgh.

Dr. Nick Kernhagan (BP) is thanked for his help and advice for Karl Fischer operation. Dr. Ashley Wilson is acknowledged for his assistance in emulsion identification. In addition, the following are thanked for the donation of crude oil samples; CHEVRON (UK), Dr. Paul Mason (FINA), Dr. Tim Dodds (BP), Prof. Steve Rowland (Plymouth University), UNOCAL and Phillips Petroleum (Norway).

I would like to thank the following for assistance with my work; Dr. Paul Taylor for help with phenol extraction and analysis, as well as writing up. Dr. Stuart Petch for advise on many topics (especially diving). Dr. Andy Bishop for help with Wax extraction/analysis and advise. The following are thanked for their technical advise and help; Bernie Bowler, Ian Harrison, Rob Hunter, Mei Chen, Dr. P. Farrimond, Dr. Bryn Jones, Dr. Ian Head, Dr. Gordy Macleod, Anne Evens, Lexa Summerbell and Trevor Whitfield. Paul Donohoe is thanked for GCMS help and assistance, as well countless games of squash. Both Yvonne Hall and Anne Thwaites are gratefully thanked for their vital help in getting through the University bureaucracy while Barbara and Christine are thanked for their superb art work.

Special thanks goes to my fellow sufferers from the "write up room" experience, Wendy Quayle, Adrian Piper, Al Vincent and Dr. Stan Cooper who are all thanked for their camaraderie. Wendy is also thanked for her friendship/help and infectious laughter throughout the last five years. The following are thanked for their social intercourse during my stay at Newcastle. Dr. Derek "Baldy" Tobin, Dr. Linda Wainwright, Ashley Bigge, Helen Innes, Dr. Neil Gray, Dr. Andy Stott, Rich Stott, Davey Hill, Dr. Linda Stalker, Ben Stern, Dr. Greg Ewbank, Dr. Dan Stoddart, Dr. Bazza Bennet, Nyki Tessen and Suzanne & Andy McDonough. From outside the department I would like to thank Sarah, Eileen, Les & Gerry, Fred & Wendy, Andy & Sue, Sean and Cathy. Special thanks goes to Nimisha Gunja for her friendship, encouragement, M&S food supplies and general good taste.

Lastly, yet most importantly, I wish to express my thanks to my family for their total support and encouragement during this endless educational career. Mum and Dad I promise no more courses for a bit.

Abstract

The work contained within this thesis is an assessment of the water uptake ability of various crude oils, and an investigation of the relationship between water uptake and the chemical composition of crude oils.

Using the Karl Fischer titration technique it was possible to achieve rapid analysis of the rate of change of the water content of prepared crude oil/water blends with various added water quantities. A set of procedures, called Crude Oil Water Uptake Analysis (COWUA), were established using this apparatus and applied to a group of crude oils, with varying maturity and extent of biodegradation, from two main oil producing provinces, the U.K. North Sea and Santa Maria Basin, California. Water determination from the top and bottom of crude oil/water blends, combined with visual inspection, was used to characterise the water uptake of crude oils by their water retentive (rate of sedimentation of water and/or emulsion droplets) and emulsion formation/stabilisation (degree of oil/water separation) abilities.

Initial results identified that both of these properties altered with the extent of biodegradation of the crude oil in question. Non-biodegraded crude oils exhibited "poor" water retention (rapid water or emulsion sedimentation) and formed stable water-in-oil emulsions, while degraded crude oils exhibited higher water retentive capability (slower sedimentation) yet possessed varied emulsification ability.

Water retention was considered to be possibly due to either the physicochemical (viscosity, density *etc.*) or geochemical (crude oil compositional) properties of the crude oil. It was anticipated that the composition of crude oils, which exhibit "good" water retention would probably contain "emulsifiers", *i.e.*, asphaltene and wax sols as well as oil-soluble surfactants, such as C_0-C_3 alkylphenols. These emulsifiers promote stable oil/water interfaces and produce good interaction between the immiscible phases, therefore slowing, or preventing, water and/or emulsion droplet growth. However, bulk chemical analysis showed that the effectiveness of asphaltene and wax emulsifiers decreased with increasing biodegradation and that NSO compounds exhibited no association with increasing water retention. Since no relationship between these crude oil geochemical compositions and increased water retention could be detected it is suggested that physicochemical properties of crude oil/water blends are probably responsible for the rate of sedimentation of the water content.

The emulsion formation/stabilisation ability of crude oils analysed varied. Bulk chemical analysis of the major crude oil chemical groups (aliphatic and aromatic hydrocarbons, resins and asphaltenes) showed that crude oils which formed stable water-in-oil emulsions either possessed a composition conducive to asphaltene and

wax precipitation (as for the non-degraded North Sea crude oils) or possessed high NSO contents (as for both non-degraded and biodegraded Santa Maria Basin crude oils). However, where none of the above properties were exhibited, as for biodegraded North Sea crude oils, poor or no emulsion formation occurred.

Detailed analysis of the C_0-C_3 alkylphenols found that their concentration was severely reduced in crude oils which were characterised by poor, or no, emulsification. Therefore, the reduction of oil-soluble surfactants (such as C_0-C_3 alkylphenols), as well as asphaltene and wax sols, is related to poor emulsion formation/ stabilisation.

The importance of emulsifiers was further outlined by analysis of the organic matter extracted from the crude oil/water interfacial film present in the emulsions. All the above emulsifiers were found to be preferentially enriched, indicating their involvement in the formation and stabilisation of water-in-oil emulsions.

The effect of biodegradation upon water uptake was further investigated under controlled conditions, by the laboratory biodegradation of non-degraded and biodegraded North Sea crude oils. The subsequent emulsification of the non-degraded crude oil during biodegradation was not attributed to the presence of asphaltene and wax sols (biodegradation was considered to reduce the presence of these particles) but the result of significant surfactant generation. This phenomenon is associated with the rapid microbial degradation of the easily metabolisable components in the crude oil. Consequently, the observed lack of emulsification, for the previously biodegraded crude oil, was attributed to both the reduced presence of asphaltene and wax sols, as well as poor surfactant generation associated with slow degradation rates.

TABLE OF CONTENTS.

CHAPTER 3: ASSESSMENT OF THE WATER UPTAKE ABILITY OF CRUDE OILS.

CHAPTER 1:

INTRODUCTION

CHAPTER 1: INTRODUCTION.

1.1. General Introduction to Water Uptake Problems and the Aims of this Study.

Crude oil water uptake is the incorporation of water into a crude oil medium, predominantly in the form of water-in-oil emulsions (Sheu & Shields, 1995). This process, even when only involving small quantities of water, results in many costly problems within the petroleum industry caused by the presence of both water and associated salts (Speight, 1980; Taylor, 1992b). Water incorporation into crude oil may occur in many areas of the petroleum industry, however, it is most frequent during production. It is reported in the literature that the average ratio of oil to water, during production of petroleum accumulations, is approximately 1:1 while the average water content of produced crude oils frequently lies in the range of 10-50% (Aveyard *et al.*, 1990; Staiss *et al.*, 1991). However, with increasing depletion of crude oil reserves, and greater use of secondary and tertiary recovery techniques, the co-production of oil and water, and consequently associated problems, are increasing (Stosur *et al.*, 1990; Ng & Tsakiri, 1992). Problems associated with water uptake are common in many stages of the production and treatment of crude oil and are listed in Figure 1.1.

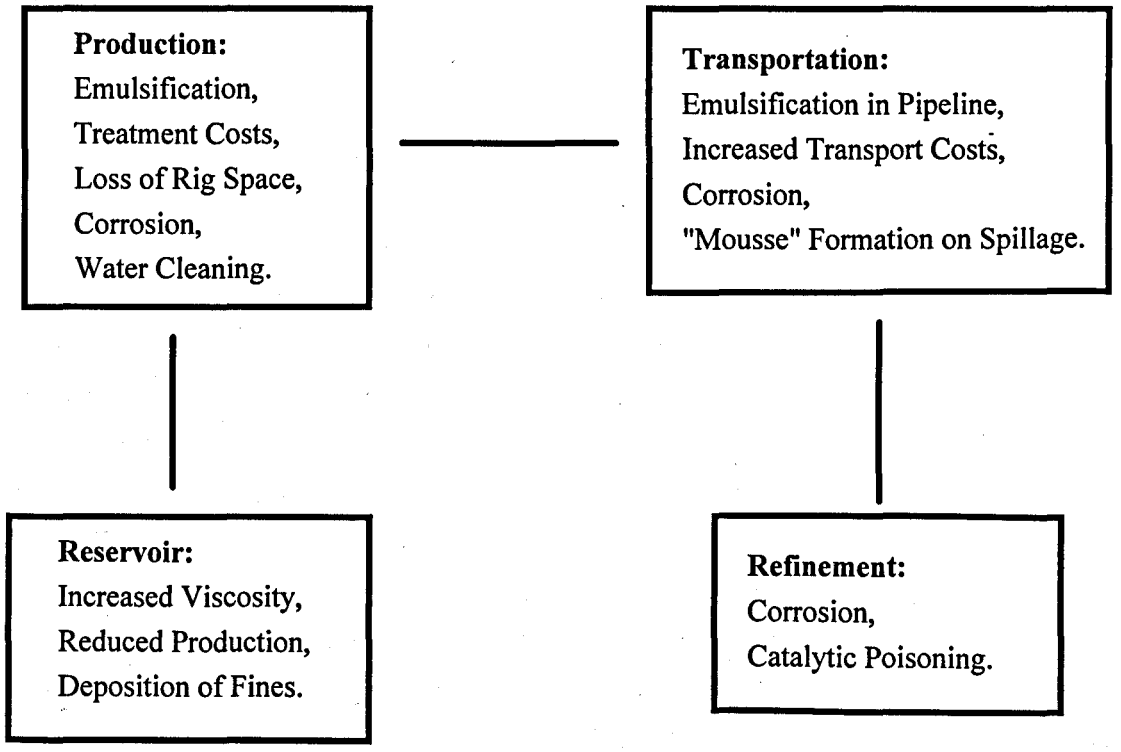

Figure 1.1. Water Uptake Problems in the Petroleum Industry.

During reservoir production, the incorporation of saline formation water increases the viscosity of the produced crude oil (Thompson *et al.*, 1985; Rønningsen, 1995). This slows the crude oil extraction rate, which in turn increases production costs due to reduced output. In addition, reduced rate of production may cause secondary problems, most notable of which is the deposition of fines, such as asphaltene and wax precipitates. The deposition of these fines will cause reduction in reservoir permeability, reducing production and possibly causing irreversible formation damage (Leontaritis, 1989; Philp & Bishop, 1995; Jamaluddin *et al.*, 1995).

One of the major problems associated with the co-production of crude oil and water occurs when the immiscible phases pass through the well head chokes and valves, where high shear action produces viscous water-in-oil emulsions (Aveyard *et al.*, 1990). These emulsions (emulsions are discussed in detail below), although thermodynamically unstable, are usually kinetically stable for long time periods (months to years; Eley *et al.*, 1988; Aveyard *et al.*, 1990). These emulsions are difficult to handle due to both their high viscosity and bulk (emulsions which contain 80% water exhibit a volume five times greater than that of the crude oil alone; Bridié *et al.*, 1980; Schramm, 1992). The creation of such troublesome emulsions increases costs due to greater processing and preparation time, which is necessary prior to crude oil transportation. In addition, the equipment needed for emulsion destabilisation, such as coalescers, as well as the standard water/oil separating vessels (referred to as "Free Water Knockout Vessels"; Giuliano, 1981), takes up valuable rig space. Johansen *et al.* (1989) suggested that prediction of whether or not a produced crude oil would form a stable emulsion could save vital rig space which could have more valuable uses.

Once the oil and water phases have been separated it is not a simple task to transport the crude oil and discard the water. The co-produced water will be an "industrial waste", containing pollutants. Consequently separated water has to be cleaned prior to dumping in order to meet environmental requirements (Staiss *et al.*, 1991; Madian *et al.*, 1995). Such processing will inevitably increase production costs still further.

Transportation, either by pipeline or tanker, is also greatly affected by water contamination. Obviously, the actual presence of water in crude oil lowers the volume of oil transported, thereby increasing costs. Even with advised maximum crude oil water contents of between 0.5 and 2.0%, for pipeline transportation (Speight, 1980; Giuliano, 1981), and 0.02% for tanker transportation (Staiss *et al.*, 1991), huge costs will be acquired solely for water conveyance. As well as transport costs the presence of saline water will cause pipeline corrosion (discussed below) and turbulence in the pipe induces water-in-oil emulsion formation, which increases viscosity and decreases

transportation efficiency (Rønningsen, 1995). However, it is possible that during transportation the water content of some heavy crude oils may be increased, due to their deliberate emulsification into oil-in-water emulsions (less viscous than water-in-oil emulsions due to the absence of rigid interfacial films) in order to improve the efficiency of heavy oil transportation (Schramm, 1992).

Other problems associated with transportation, either pipeline or tanker, is that of spillage. The successful clean up of crude oil spillages, as well as the limitation of their immediate damage to the environment, is influenced by their ability to form water-in-oil emulsions (frequently referred to as "chocolate mousses" in oil spill situations, Berridge *et al.*, 1968). Clean up operations, as for the Amoco Cadiz, are hampered by the high viscosity and large volume of these emulsions (Berridge *et al.*, 1968; Bridié *et al.*, 1980). In addition, the efficiency of bioremediation techniques is lessened due to the limited access of oxygen and nutrients to the emulsified oil, thereby preventing effective degradation of the spilt crude oil (Atlas *et al.*, 1981; Bragg *et al.*, 1992).

Once the crude oil arrives at the refinery intensive cleaning processes are performed to prevent metal corrosion problems which are related to the presence of water and associated salts, predominantly due to chloride ion attack (Speight, 1980). Such problems frequently affect pipelines in the production string, transportation (pipeline and tanker) and refinery processes. During refinement additional problems are caused by the formation, at distillation temperatures, of highly corrosive hydrogen chloride, which also poisons catalysts used during refinement (Speight, 1980; Aveyard *et al.*, 1990). The presence of salt, which partitions from the saline water to the crude oil, is generally considered to be the most problematic contaminant (Speight, 1980). To remove it prior to refinement, the crude oil is often emulsified with distilled water with subsequent emulsion de-stabilisation removing both the salts and water from the crude oil (Speight, 1980).

Consequently, prediction of the water uptake the ability of crude oils, from their geochemical compositions, would help the petroleum industry highlight possible production, transportation and refinery problems.

1.2. Crude Oil Water Uptake.

The incorporation of water into an immiscible crude oil medium represents the formation of an emulsion. Therefore, before assessment of crude oil water uptake ability may be attempted some understanding of emulsions and their terminology is required.

1.2.1. Introduction to Emulsion Principles and Terminology.

This section gives a basic introduction to emulsions and the nomenclature used in this study. It does not represent a comprehensive review of emulsion technology as that is beyond the scope of this work.

Emulsions, as defined in most text books, such as Becher (1966) and Myers (1991), are mixtures of two immiscible phases (usually an oil and water), where one phase is dispersed as droplets (0.1 μm to 10 μm in size) into the other, usually in the presence of a third, emulsifier phase. Emulsions are distinguished by the presence of large interfacial areas, however, they are perpetually driving to reduce such interfacial areas to their smallest possible value (acquired at total separation of the water and oil phases). Consequently, emulsions are naturally thermodynamically unstable (Myers, 1991). However, as mentioned above, these kinetically stable emulsions may persist for long time periods (Aveyard *et al.*, 1990). The classification of emulsion stability is frequently assessed by the consideration of several factors (discussed below), creaming (sedimentation), flocculation and coalescence (Schramm, 1992). However, for simplicity this study uses coalescence to characterise emulsion stability, by monitoring the ease, or rate of oil and water separation (Mikula, 1992).

Emulsions are predominantly split into two types depending upon which phase is dispersive and which is dispersed. Figure 1.2, displays the two main types of emulsion dispersions produced, water-in-oil and oil-in-water. One of the main factors determining the emulsion formation and stabilisation, as well as type formed, is the state and composition of the oil and water interface (Schramm, 1992).

The oil/water interface is the boundary between two liquid phases and is usually characterised by interfacial free energy, more commonly referred to as the interfacial tension (IFT; force per unit length around an interface in millinewtons per meter). The higher the interfacial tension (IFT) the more unstable the emulsion (the more immiscible are the oil and water phases) and the greater the drive to reduce the interfacial area (Myers, 1991). The IFT is the result of the sum of the surface tensions of both phases. In Figure 1.3a, the surface molecules for each phase are seen to be attracted back into their respective phase, resulting in the formation of a dense and stretched "skin", such as a meniscus, for each phase. If however, the surface molecules are attracted by the other phase, the tension is reduced and the "skin" becomes less dense and tight, reducing the IFT (Fig. 1.3b). Ultimately, the attraction from the opposite phase may equal that from the host phase and the molecules will then move freely between the two phases under Brownian motion. At this stage the phases are miscible and the IFT is 0, Figure 1.3c (Myers, 1991).

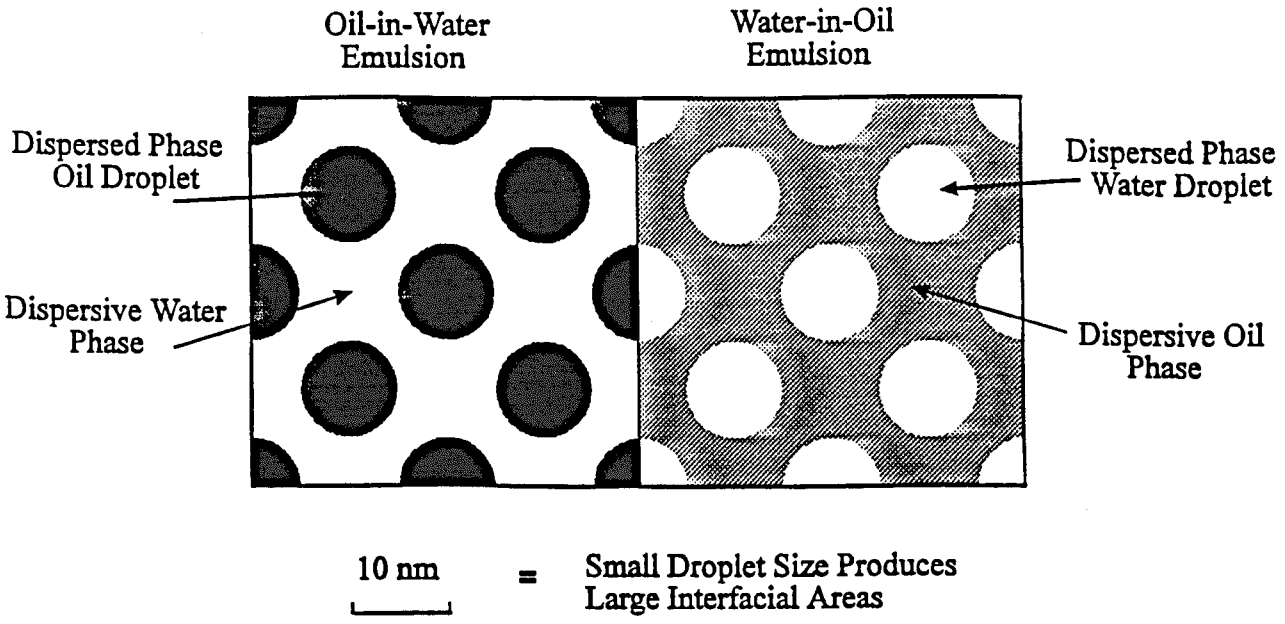

Figure 1.2, Illustration of the two main emulsion types (oil-in-water and water-in-oil) and associated nomenclature.

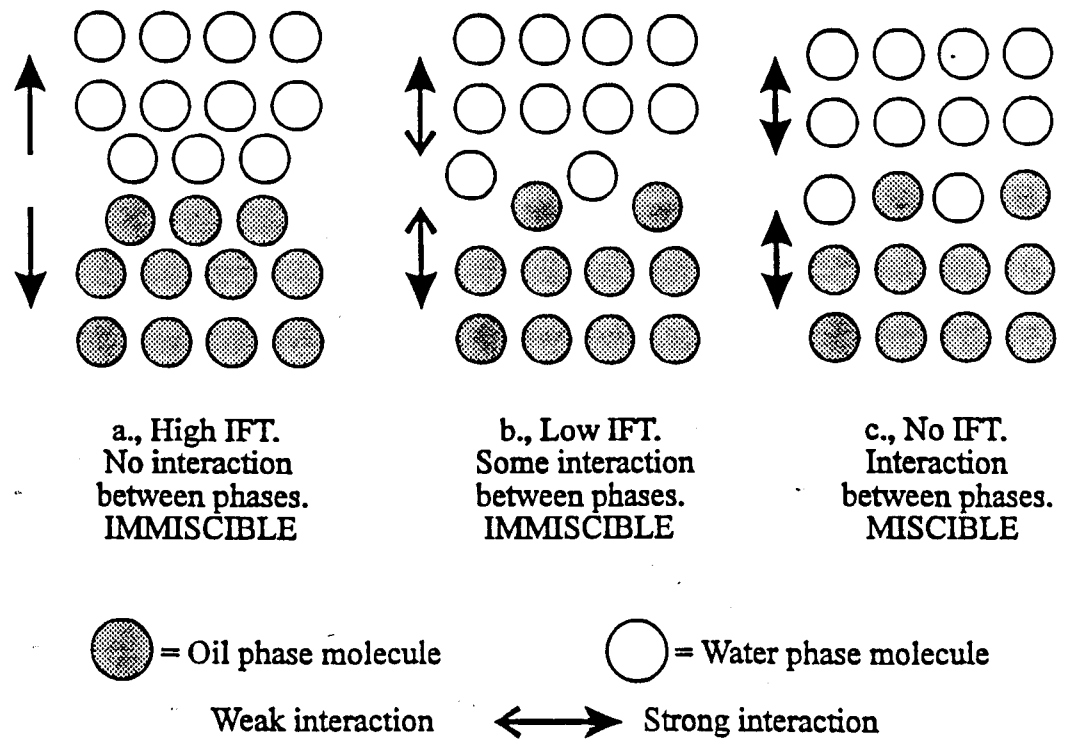

Figure 1.3 (a,b,c), Examples of three oil and water interfaces with different interfacial tensions (IFT).

The energy necessary for the emulsification of two immiscible phases is directly related to the IFT of a particular system, with higher IFT systems requiring greater energy for emulsification. This is illustrated in an example by Schramm (1992), showing that to emulsify a barrel (159 L) of oil with water, at a dispersed droplet size of approximately 0.64 μm and with an interfacial tension (IFT) of 35 mN m^{-1}, the amount of emulsification energy needed would be 2.6 x 10^4 J, shown in Figure 1.4. If this energy is not available, surfactants may be used to reduce the necessary energy requirements.

A surfactant has two main functions, increasing the ease of emulsion formation as well as helping to stabilise emulsions. Surfactants are able to perform these tasks because they are chemicals which possess both hydrophobic and hydrophilic constituents; consequently they have affinity for both the oil and water phases. As a result they partition to the oil and water interface with both chemical functions interacting with their preferred phases (Fig. 1.5; Myers 1991). This has the effect of reducing the IFT, making an emulsion more stable and resulting in a lower energy requirement for emulsification. Schramm (1992) estimated that a small addition (less than 0.5% of the total volume) of surfactant to the barrel of oil in the above example, would reduce the IFT from 35 mN m^{-1} to 0.35 mN m^{-1}, lowering the energy requirements by 100 fold to approximately 2.6 x 10^2 J (Fig. 1.4).

Although surfactants are amphiphilic by nature (interacting with both water and oil phases; Fig. 1.5), to stabilise emulsions they generally have to possess a greater affinity for one particular phase (Shaw, 1980). This characteristic will not only influence whether or not the surfactant may stabilise an emulsion, it will also affect the type of emulsion formed (water-in-crude oil emulsion or crude oil-in-water emulsion; Shaw, 1980). This latter characteristic is well described by one of Bancroft's rules, which states that which ever phase a surfactant is most soluble in, that phase will comprise the dispersing medium (Becher, 1966). Therefore, a surfactant, soluble in the crude oil (oil soluble surfactant) will help form water-in-crude oil emulsions and *vice versa.*

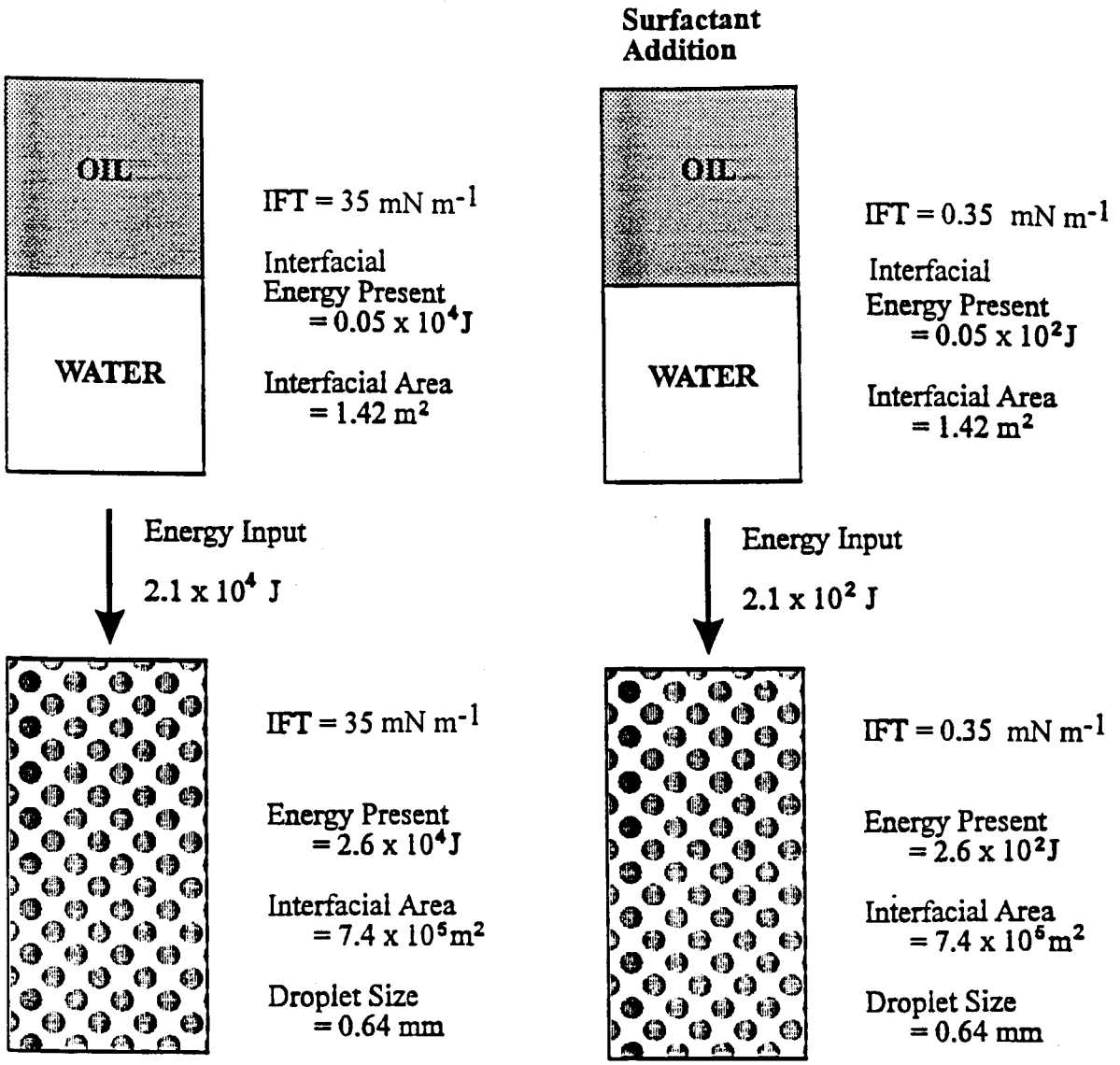

Figure 1.4, Example of the effect of surfactant addition on the required emulsification energy to form an oil-in-water emulsion (Schramm, 1992). Energy present is gained by multiplying the total area by the interfacial tension.

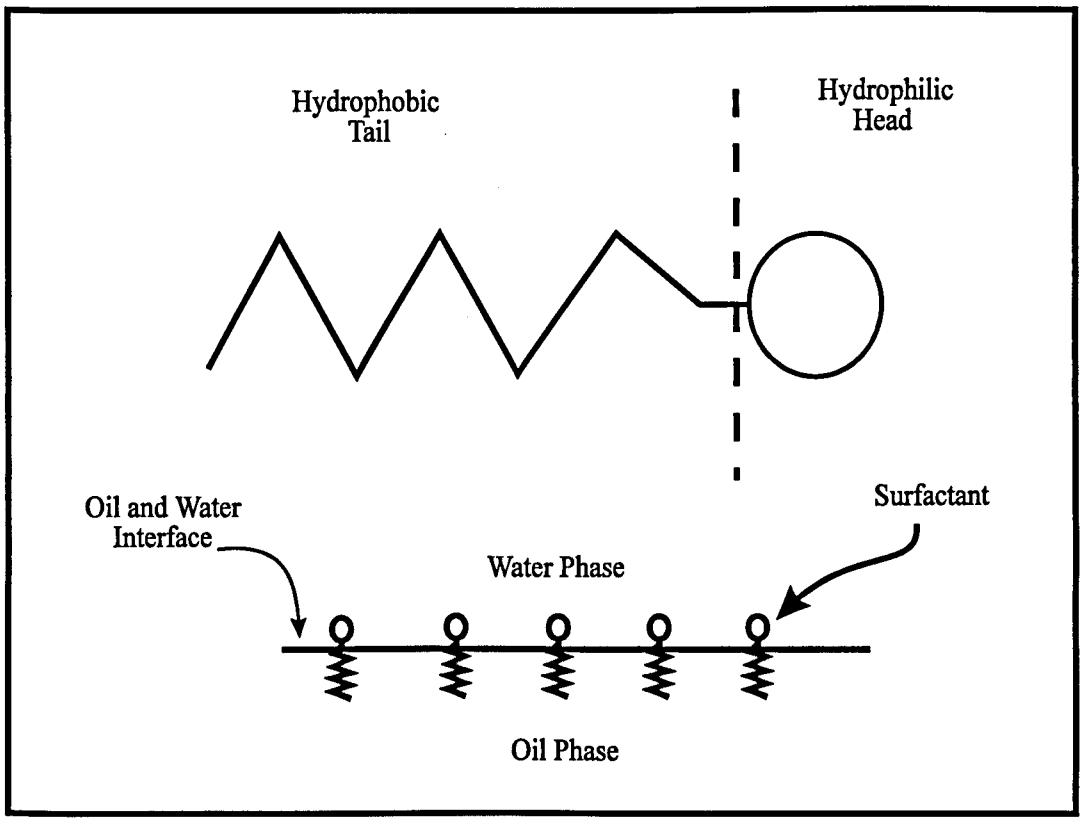

Figure 1.5. Schematic diagram of a surfactant, illustrating the amphiphilic nature and orientation of a surfactant molecule at an oil and water interface (Myers, 1991).

As well as reducing thermodynamic instability, by reduction of the IFT, surfactants may also increase the kinetic stability of a dispersed system. Surfactants orientate themselves perpendicular to the interface (hydrophilic functions towards the water, hydrophobic away). This ordered structure adds mechanical strength to the interface making kinetic destabilisation more difficult (Myers, 1991). It must be noted however, that the emulsion formation and stabilisation abilities of surfactants due to the reduction of the IFT, and increased mechanical strength, are not the only stabilising mechanism necessary for the formation of stable emulsions. There are many types of emulsion stabilisers, or emulsifiers, and their influence will vary with the type of emulsion formed (oil-in-water or water-in-oil).

1.2.2. Emulsion Stabilising Mechanisms.

The stabilisation mechanisms for the two main types of emulsion vary greatly. An oil-in-water emulsion is predominately stabilised by electrostatic forces, while a water-in-oil emulsion is predominantly stabilised by the mechanical strength of a rigid and protective interfacial film. As this study is concerned with the dispersion of water

into crude oil, only the stabilising mechanisms of water-in-oil emulsions are considered here.

Water-in-oil emulsions are highly viscous and persistent emulsions, which are prominent in both crude oil production and oil spillage scenarios (Bridié *et al.*, 1980; Aveyard *et al.*, 1990; Bobra *et al.*, 1992). They are primarily stabilised by the mechanical strength gained from the adsorption and accumulation of emulsifying agents, surfactants and sols (sols are fine grained solid particles which may be suspended in a colloidal solution; Fine & Beall, 1990), at the oil and water interface (Schramm, 1992). The influence of the sol groups, especially asphaltenes and waxes, has been shown to be fundamental to stability (Thompson *et al.*, 1985; Eley *et al.*, 1988; Schramm, 1992). Payne and Phillips (1985a) have suggested that both asphaltene and wax precipitates act together in the stabilisation of water-in-oil emulsions, although asphaltenes were considered to play the more important role. For both of these crude oil precipitates to be effective water-in-oil emulsion stabilisers three considerations have to be met. (1) the size of the precipitated sols has to be small relative to the water droplet they are stabilising; (2) the precipitated sols have to accumulate at the interface; (3) the sols have to be wetted by both phases (Schramm, 1992). Once the sols and surfactants reach the interfaces sterical rearrangement occurs, increasing interfacial rigidity still further (Bhardwaj & Hartland, 1994).

The build up of the interfacial film is not immediate as emulsifiers arrive at the interface at different rates. Surfactants diffuse to the oil/water interface within the first few seconds of emulsification to provide initial stabilisation. Aggregates, especially asphaltenes accumulate at the interface over a period of hours (Sheu *et al.*, 1992a). Sheu and Shields (1995, p.523) considered that this slower rate was "due to the complicated structural distribution of asphaltene molecules because asphaltenes represent a class of material rather than a pure substance". Bhardwaj & Hartland (1994), in Figure 1.6, illustrate that the interfacial tension of the oil and water interface decreases with time from emulsification, indicating that the complete build up of surfactants was not complete 60 hours after the initial blending and was therefore relatively slow.

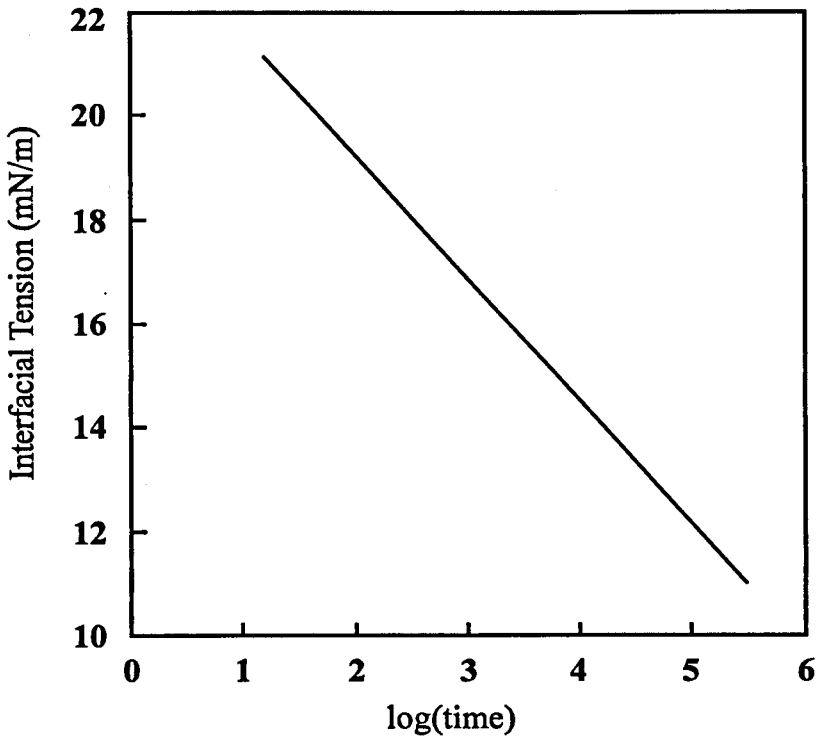

Figure 1.6. Variation in interfacial tension (mN m^{-1}) with log (time) for crude oil/brine at 20°C. Time in seconds. Taken from Bhardwaj & Hartland (1994).

As water-in-oil emulsions are strongly influenced by asphaltene and wax components both will be discussed in further detail below. The effect of oil soluble surfactants has already been discussed above; however, additional discussion will be made in Section 5.1.

1.2.2.1. Asphaltenes.

Asphaltenes were originally defined by Boussingault (1837) as material that precipitated out of petroleum upon the addition of petroleum ether. Today the definition has changed little and asphaltenes are generally classified as material that precipitates out of petroleums and sediment extracts (bitumen) upon the addition of an excess of light alkanes (Speight & Moschopedis, 1978).

Work by Lawrence and Killner (1948), Berridge *et al.* (1968) and Mackay *et al.* (1973), identified that the asphaltene group is of prime importance to water-in-oil emulsion stabilisation. In addition, Eley *et al.* (1976), using electron micrography, were able to identify the presence of asphaltene particles on the oil side of an oil and water interface, within a water-in-oil emulsion, estimating that they (asphaltene particles) were approximately 10-30 nm in diameter.

Van der Waarden (1957) suggested that the effectiveness of the asphaltene group, in the stabilisation of water-in-oil emulsions, was due to the "incipient" precipitation of the asphaltene fraction. As asphaltene precipitation has received extensive attention due to it's detrimental effects upon reservoir production, crude oil transportation and others (Leontaritis, 1989; de Boer *et al.*, 1995), conditions under which precipitation occurs have been well documented. Wilhelms and Larter (1994b and literature cited therein) showed that in reservoir scenarios, the main factors controlling asphaltene precipitation are (in order of importance) pressure, temperature, crude oil composition and the nature of the asphaltene. Earlier work by Leontaritis (1989) also considered electrokinetic effects upon asphaltene precipitation caused by the neutralisation of charges on asphaltene micelles during rapid flow ("streaming"). In many experiments, performed at surface conditions (constant temperature and pressure) the main restriction upon asphaltene precipitation was considered to be the chemical composition of the crude oil. Precipitation being predominantly caused by the change in the solvent properties of the crude oil (referred to by Leontaritis (1989) as alteration of the "solvent power" of the crude oil), where the solvent (crude oil) is incapable of supporting the solute (asphaltenes) resulting in precipitation (Wilhelms & Larter, 1994a).

Work by Mackay *et al.* (1973), Eley *et al.* (1987) and others, has shown that the relative concentration of aliphatic and aromatic hydrocarbons in crude oil is of great importance to asphaltene precipitation because of their effect upon the solvent power of the crude oil. Bobra *et al.* (1992) used an aliphatic:aromatic hydrocarbon (Ali:Arom) ratio to indicate the occurrence of asphaltene precipitation in a model oil (artificially prepared oil). It was found that aliphatic hydrocarbon concentrations of between 50% and 95% (Ali:Arom ratios of 1 to 19), caused asphaltene precipitation coinciding with, and was adjudged responsible for, the formation of stable water-in-oil emulsions. However, the most stable emulsions were found by both Eley *et al.* (1988) and Bobra *et al.* (1992, Fig. 1.7) to occur at an aliphatic hydrocarbon concentration of 80% (Ali:Arom ratio = 4). This was attributed to the optimum size of the asphaltene particles precipitated at these conditions.

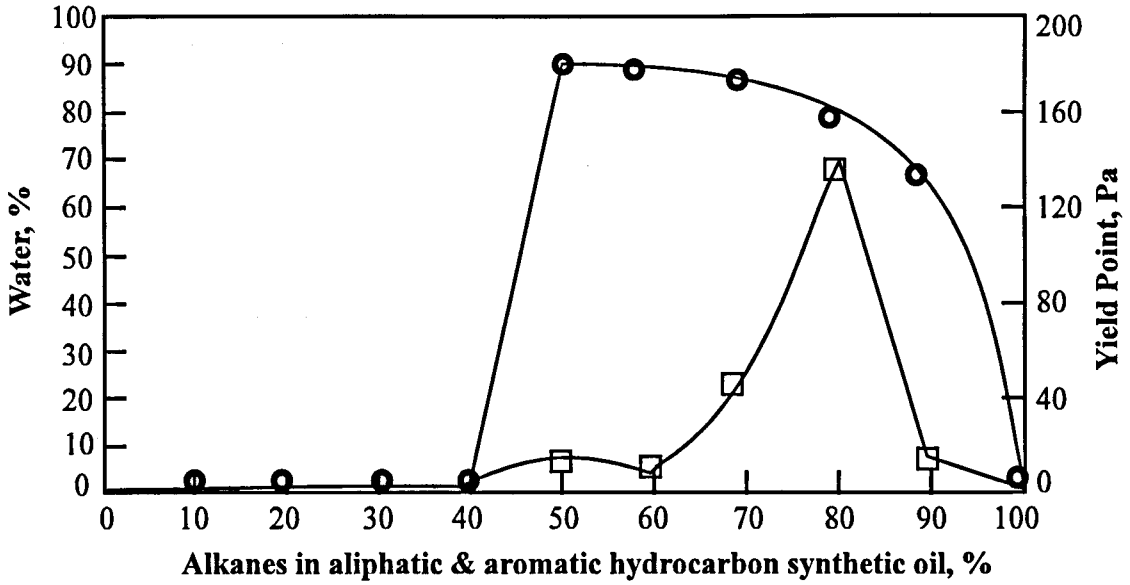

Figure 1.7. Water content (●) of stable emulsions formed, and yield point (□) of stable emulsions versus % alkane in synthetic oil (aliphatic and aromatic hydrocarbon mixture). Illustrates that the most stable water-in-oil emulsion occurs at a Ali:Arom ratio of approximately 4. Taken from Bobra et al. (1992). (The alkane percentage only represents the amount of alkanes in an aliphatic and aromatic hydrocarbon mixture which does not include the emulsifier content).

Although asphaltene precipitates are regarded as the main stabilisers of water-in-oil emulsions due to their mechanical strength (Payne & Phillips, 1985a; Eley *et al.*, 1988; Bobra *et al.*, 1992), their surfactant ability may also have some stabilising effect. It is reported that asphaltenes are able to influence water-in-oil emulsions by lowering oil/water interfacial tensions (Anderson & Birdi, 1991; Sheu *et al.*, 1992a & b; Bobra *et al.*, 1992). It was also found that in model oils, asphaltenes only have to be present at low concentrations, approximately 0.025 mg ml^{-1} (Bobra *et al.*, 1992), to aid stabilisation. Any further increase in the asphaltene content appeared to have no additional stabilising effects (*i.e.*, interfacial tension reduction). This phenomenon was also recognised by Sheu *et al.* (1992a & b), who attributed it to the attainment of a critical micelle concentration (CMC; Fig. 1.8). A critical micelle concentration (CMC) is the concentration at which the asphaltenes (or any surfactant) predominantly form discrete aggregates (while still in dispersion in the crude oil). Therefore, when the asphaltene concentration is larger than the CMC, the asphaltene distribution will be predominantly in micelle form, with only minor asphaltene quantities existing as "monomers" (i.e., capable of interaction at the oil/water interface) (Myers, 1991). Anderson & Birdi (1991) found that the CMC value, and therefore the quantities of asphaltene micelles and monomers, will vary with the crude oil chemical composition, although monomer concentration is generally low (Sheu *et al.*, 1992a). However, the low monomer concentration is able to maintain an interfacial tension of approximately

20-30 mN m^{-1}, even after attainment of the CMC (Bobra *et al.*, 1992). Such interfacial tensions are equal to those of stable water-in-oil emulsions (Shaw, 1980; Taylor, 1992b). Therefore, in addition to asphaltene sols, it is suggested that asphaltene monomers or asphaltene precursor entities (APEs; Wilhelms & Larter, 1994a), acting as surfactants, are also effective water-in-oil emulsion stabilisers.

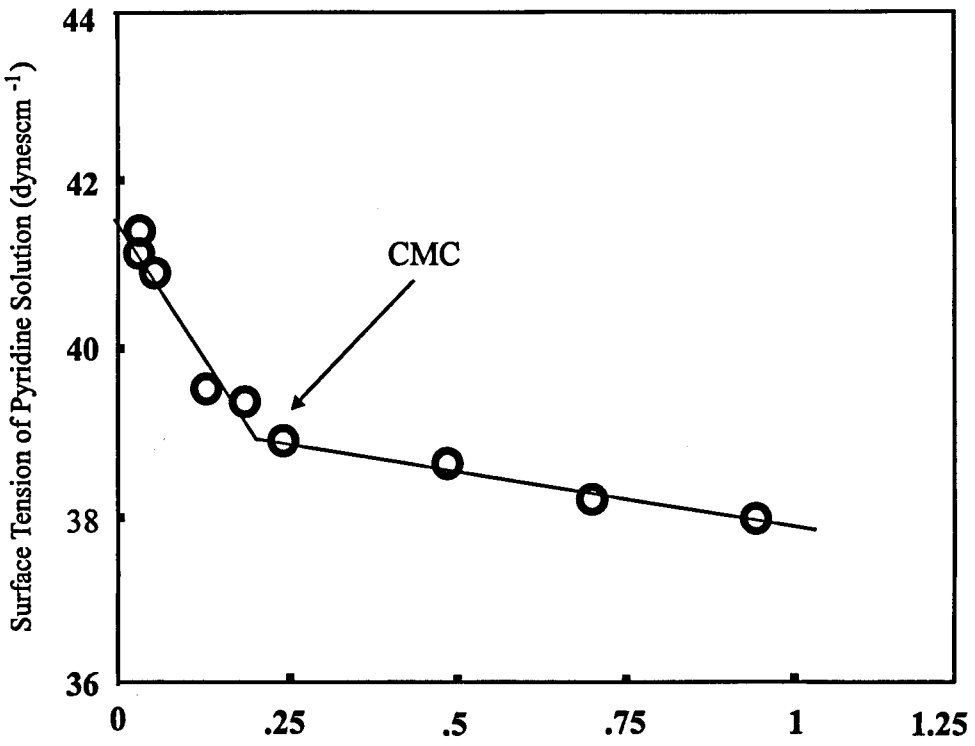

Figure 1.8. Illustration of the surfactant behaviour of the asphaltene group by the variation of the surface tension (dynecm^{-1}) of a pyridine solution with increasing asphaltene concentration (wt%). CMC = critical micelle concentration. Taken from Sheu et al. (1992a).

Papirer *et al.* (1982) and Siffert *et al.* (1984), suggested that different asphaltenes will possess different surfactant ability. They found that asphaltenes with the best emulsifying ability possessed large imbalances between their inherent acid and basic components (producing asphaltenes with an amphiphilic character indicative of surfactants) and low hydrogen bonding ability (preventing aggregation of asphaltene thereby aiding their accumulation at the oil/water interface). In addition, it was also found that a greater degree of emulsification was associated with asphaltenes that accumulated at the oil and water interface in regular laminae. Such ordered accumulations ensured rigid film development and therefore mechanically stable water-in-oil emulsions (Siffert *et al.*, 1984). This regular structure is attributed to the

surfactant nature of the asphaltenes which causes orientation at the interface (discussed above), hydrophilic group towards the water, hydrophobic towards the oil (Fig. 1.5; Myers, 1991).

1.2.2.2. Wax.

Waxes, or petroleum waxes, are defined as high molecular weight alkanes (greater than n-C_{40}, Philp & Bishop, 1995) although later work in this study will class waxes as n-alkanes which are solid at room temperature (*n*-C_{18} +). They are predominantly sourced from reworked continental organic matter, common to crude oils generated from Type I and Type III source rocks (Tissot & Welte, 1984). However, some waxy crude oils are also generated from Type II source rocks (Tissot & Welte, 1984) possibly originating from, (1) high molecular weight precursors such as polyisoprenyl alcohol and bacterial carotenoids, (2) decomposition of asphaltenes and (3) oligomerisation of low molecular weight precursors (del Rio & Philp, 1992). The petroleum waxes which occur in crude oils are classified according to their average molecular mass. Hanstveidt (1992) lists three types of petroleum waxes common to crude oil. "Paraffin wax" which possesses an *n*-alkane distribution of *n*-C_{18} to *n*-C_{50}, which is also associated with smaller amounts of iso- and cyclo-alkanes. "Intermediate wax" which consist of predominantly *n*-C_{22} to *n*-C_{60} *n*-alkanes. Lastly "microcrystalline wax" which contains *n*-C_{23} to *n*-C_{85} *n*-alkanes as well as large quantities of iso- and cyclo-alkanes. Bobra (1990) only lists two types of petroleum waxes; "paraffin wax", with *n*-alkane distribution of *n*-C_{20} to *n*-C_{40}, and "microcrystalline wax", predominantly consisting of iso-alkanes with 35 to 70 carbon atoms.

Precipitation of waxes, either in reservoirs (due to decreases in reservoir pressure) or production equipment (due to decreases in temperature), is of great interest to the petroleum industry. It has been estimated that losses attributed to wax precipitation annually cost billions of dollars (Misra *et al.*, 1995). Consequently, the conditions under which wax precipitation occurs have been extensively investigated. It has been reported that problems associated with production and transportation are attributed to "macrocrystalline" waxes (predominantly *n*-alkanes), while "microcrystalline" waxes (predominantly branched alkanes) contribute most to the tank bottom sludges (storage tanks etc.). Investigation by del Rio *et al.* (1992), using high temperature gas chromatography (HTGC; described in Section 4.2.3), found that wax deposits from Oklahoma crude oils were characterised by high molecular weight hydrocarbons. Bishop *et al.* (1994), using a novel wax concentration/precipitation

technique, coupled with HTGC (discussed in detail in Section 4.2.3), also identified that wax deposits contained high molecular weight hydrocarbons (HMWHCs) with distributions commonly possessing a maximum peak height at *n*-C_{45}. Bishop *et al.* (1994) subsequently analysed the crude oils associated with the wax deposits (which in conventional gas chromatographic analyses showed no sign of HMWHCs), and highlighted an HMWHC distribution of up *n*-C_{70}, with a maximum peak height at *n*-C_{30}. Therefore, HMWHCs are present in low concentration implying that wax deposits are built up slowly and are possibly common to most crude oils (Philp & Bishop, 1995).

It is the precipitation of these waxes which probably influences emulsion stability. This is supported by Eley *et al.* (1976) who were able to identify the presence of wax platelets at oil and water interfaces by use of electron micrography. However, the ability of the wax to influence emulsion stability, was found to be related to the temperature history of the crude oil, which affected the size of the wax particles (Bridié *et al.*, 1980; Graham *et al.*, 1983 & Thompson *et al.*, 1985). Slow cooling was shown to give large wax crystal formation, while rapid cooling (conditions found during petroleum production) produced small wax crystals. The significance of this being that large crystals do not assist with the formation of stable water-in-oil emulsions, whereas small crystals, formed during production, do (Fig. 3.4.1). Bridié *et al.* (1980) and Thompson *et al.* (1985) also found that removal of the wax fraction from a crude oil would inhibit the formation of stable water-in-oil emulsions. However, Bobra *et al.* (1992) indicated that although waxes were important stabilisers they were also dependent upon a small quantity of asphaltenes being present to achieve emulsion stability, while the asphaltene fraction was capable of stabilising water-in-oil emulsions by itself. Using a model oil consisting of aliphatic & aromatic hydrocarbons and emulsifying agents (resins and asphaltenes which were precipitated from a Californian crude oil using ethyl acetate), Bobra *et al.* (1992) was able to produce a stable water-in-oil emulsion without the apparent presence of waxes. Therefore, it was concluded that waxes were not essential to stabilise crude oil/water emulsions. However, a recent paper by Bishop *et al.* (1994), has shown the difficulty of separating asphaltenes and waxes by standard precipitation techniques. In Figure 1.9 it is seen that an isolated asphaltene fraction still contains a prominent distribution of *n*-C_{14} to *n*-C_{90} aliphatic hydrocarbons. Consequently, the precipitation of both wax and asphaltene fractions at surface conditions is probably concurrent and therefore, as reported by Payne and Phillips (1985a), their effects upon emulsion stability are likely to be indistinguishable, although they also reported that asphaltenes were probably the dominant stabilisers.

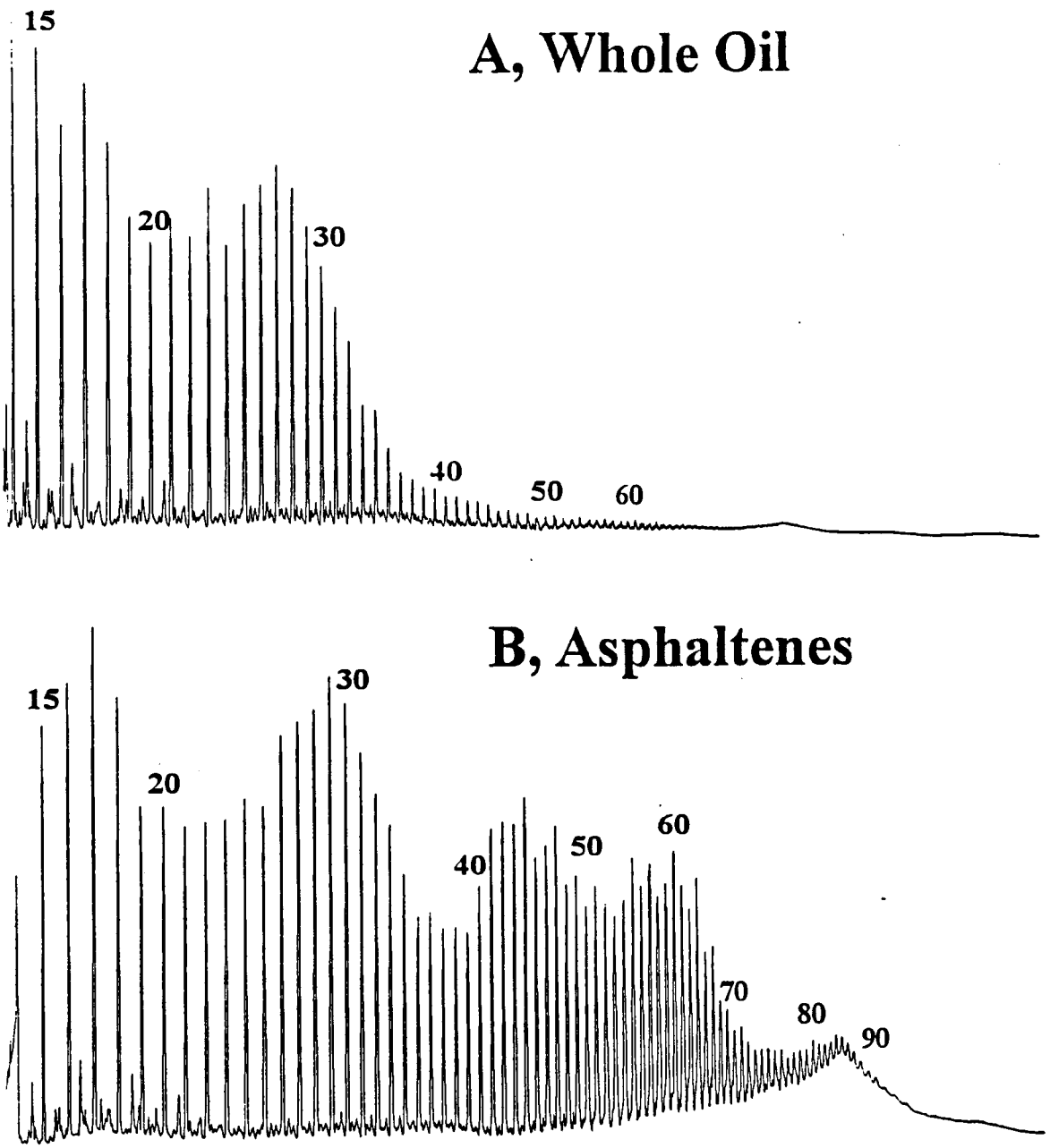

Figure 1.9, High Temperature Gas Chromatography (HTGC) of Oil # 1665 A, whole oil fraction, B, asphaltene fraction. Alkane carbon numbers are identified. Taken from Philp & Bishop, 1995.

The above work indicates the importance of precipitated waxes in aiding emulsion stabilisation. However, even when in liquid form waxes, as viscosifiers, may produce some stabilising influence. As viscosifiers, waxes will slow the separation (coalescence; definition given in Section 1.2.2.3) of the water and oil phases, therefore aiding emulsion stability (Johansen *et al.*, 1989).

1.2.2.3. Post Emulsification Processes.

Immediately after the formation of a water-in-oil emulsion the dispersion will begin to alter, eventually culminating in the complete separation of the water and oil phases. The rate of separation identifies the kinetic stability of the emulsion, slow separation being indicative of a stable emulsion while rapid separation being indicative of an unstable emulsion.

The two main alteration processes which occur after dispersion are flocculation and coalescence (definitions below and illustrated in Fig. 1.10).

Flocculation is a reversible aggregation of the dispersed phase droplets, due to the force of gravity, resulting in agglomeration, or grouping, in which all the droplets remain as independent entities (Cavello & Chang, 1990). The droplets do not coalesce due to the presence of an interfacial film between the oil and water phases. Therefore, the flocculants will still be classed as emulsions. Eventually the inherent thermodynamic instability of the emulsion (see above), as well as gravity, thins the interfacial films, eventually rupturing them, causing coalescence and the formation of separate oil and water layers (Myers, 1991).

There are two types of flocculation, creaming and sedimentation, which differ according to the relative densities of the dispersed and dispersing phases. Creaming refers to the accumulation of the dispersed phase droplets, which are less dense than the dispersing phase. Therefore, creaming is a flocculation process which is characteristic of oil-in-water emulsions. Sedimentation is the same process however, the dispersed droplets are denser than the dispersive phase and therefore, accumulate at the base of the blend. Sedimentation is a flocculation process characteristic of the emulsion phase of water-in-oil emulsions and subsequently encountered during this study.

Coalescence is the irreversible reduction of interfacial area. Consequently, the droplets merge to form a single phase, reducing the interfacial area between the dispersed (water) and dispersing (oil) phases. Coalescence is the result of either (1) lack of the formation of an interface; (2) rupture of the interfacial film. Gravity will then separate the coalescing fractions resulting in individual water and oil phases

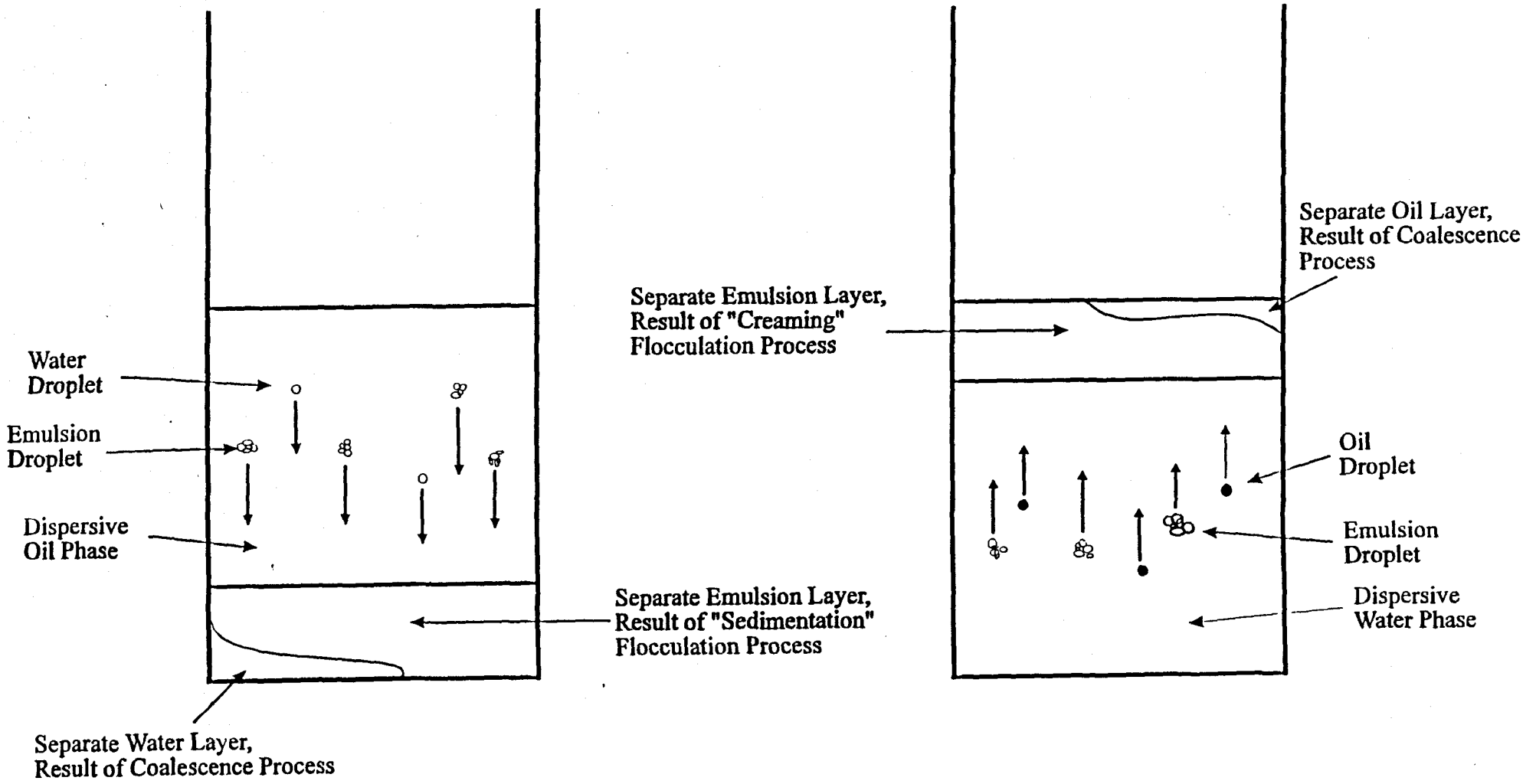

Figure 1.10, Illustration of Coalescence and Flocculation emulsion alteration processes for water-in-oil and oil-in-water emulsions.

(Cavello and Chang, 1990). Whether or not coalescence is preceded by a flocculation process (sedimentation or creaming) is dependent upon the availability of the emulsion stabilisers discussed above (asphaltene sols, wax sols and oil soluble surfactants; Cavello & Chang, 1990).

1.3. Thesis Outline.

Characterisation of crude oil water uptake ability is achieved by quantitatively monitoring both the rate of sedimentation of water and/or emulsion droplets as well as the degree of emulsion formation/stabilisation, which occurs when a crude oil is blended with different quantities of water.

As discussed above, sedimentation is a flocculation process which describes the separation of an emulsion phase (emulsion droplets) from the majority of the dispersive crude oil medium. In this work, sedimentation, and the rate of sedimentation, is not concerned with emulsion stability but is used to describe the separation of water (either emulsion or water droplets) from the top of the crude oil/water blends (see below). The relative rate of sedimentation of emulsion and/or water droplets in the crude oil/water blends will be described in terms of "crude oil water retention ability".

Assessment is achieved by measurement of the variation of the water content at the top of crude oil/water blends by use of a Karl Fischer Titration technique. The results are used to provide information of use in predicting problems associated with crude oil transportation and refinement, by indicating whether or not crude oil will retain water for substantial lengths of time (increasing transportation costs and the amount of water arriving at the refinery *etc.*, Section 1.1).

The ability to form stable water-in-oil emulsions is monitored by visual assessment of the crude oil/water blends. Results from these observations may be related to well head or oil spillage scenarios, where the formation of water-in-oil emulsions produces increased costs.

Chemical analysis of crude oils investigates any association between the emulsifier content of crude oils (asphaltene and wax sols, as well as surfactants (NSO compounds)) and water uptake, as these chemical groups are of prime importance in the formation of stable water-in-oil emulsion (above; Schramm, 1992). In addition, the effect of biodegradation upon the concentration of these emulsifiers is also addressed.

It is hoped that the characterisation of relationships between crude oil chemistry and water uptake ability may provide some explanation of the variation in water uptake ability of different crude oils. In addition, it is hoped to provide some predictive geochemical technique which may indicate the occurrence of future crude oil water uptake problems.

CHAPTER 2:

METHOD DEVELOPMENT.

A RAPID TECHNIQUE FOR THE ASSESSMENT OF THE WATER UPTAKE ABILITY OF CRUDE OILS OF DIFFERENT CHEMICAL COMPOSITION.

CHAPTER 2: METHOD DEVELOPMENT. A RAPID TECHNIQUE FOR THE ASSESSMENT OF THE WATER UPTAKE ABILITY OF CRUDE OILS OF DIFFERENT CHEMICAL COMPOSITION.

2.1. Method Selection.

The assessment of the water uptake ability of a crude oil was achieved by the measurement of its water content variation with increasing time, after the crude oil was initially blended with distilled water. The assessment of crude oil water uptake ability is therefore based upon the rate of water content change.

There are four basic techniques which are listed in the Institute of Petroleum (Great Britain) "Standard methods for analysis and testing of petroleum and related products" (1990) publication, for determination of the water content in non-aqueous samples. These techniques are "distillation" (Institute of Petroleum Standard (IP) #74 & 358), "centrifugation" (IP#359), "height measurement" (IP#290) and "titration" (IP#356).

Distillation analysis, also known as Dean & Stark analysis (Mikula, 1992), involves the distillation of water from the sample into a graduated receptacle. Distillation requires a sample mass of 5 g or more. As distillation is a large scale, irreversible technique, altering the sample during analysis, it is not possible to analyse water variation with time from blending, because all the sample would be consumed in one analysis.

The centrifuge technique is an inaccurate method, yielding approximate water content values. During centrifuge analysis, as with distillation, the sample is altered by the analytical procedure and therefore, water content variation in the crude oil/water blend, versus time from blending, can not be monitored.

Height measurement is a direct assessment of the amount of water separating from an oil and water blend, either by height of water column, or volume of water accumulated after blending. However, this is a slow and inaccurate analytical technique, allowing limited appreciation of water content variation with time.

The last technique is titration, otherwise known as Karl Fisher Titration (Scholz, 1984). This technique allows rapid and accurate analysis, while utilising a small sample size of approximately 100 µl. Consequently, water content variation with time from blending can be assessed. This technique was employed for the analysis of the water uptake ability of crude oils.

2.2. Crude Oil Water Uptake Analysis.

Crude Oil Water Uptake Analysis (COWUA) represents a set of procedures necessary for the assessment of the water uptake ability of crude oils using of the Karl Fischer Titration method. These procedures are shown in Figure 2.2.1, and range from apparatus preparation to presentation of results.

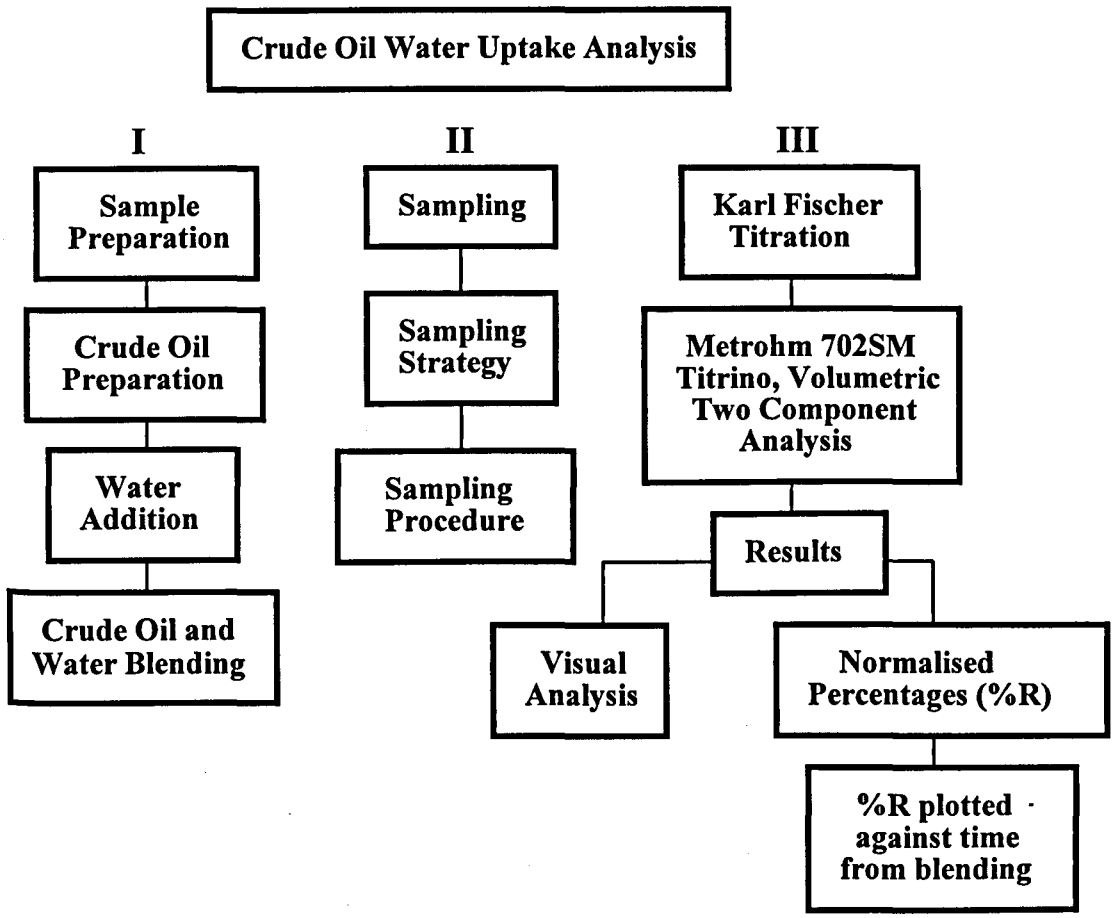

Figure 2.2.1. Flow diagram illustrating the three stages (I to III) of the Crude Oil Water Uptake Analysis.

2.2.1. Karl Fischer Titration.

The Karl Fischer Titration, first described by Fischer (1935), was a redox reaction whose original constituents, which formed the working reagent, were sulphur dioxide 0.5 ml l^{-1}, pyridine 1.7 ml l^{-1} and iodine 0.33 ml l^{-1} in methanol. The pyridine was essential to the reaction, keeping the reaction mixture within an optimum pH range (5-8) by acting as a basic buffer, neutralising produced acids. The Equations 1-3 show that the buffered alkyl sulphite acid was oxidised by iodine, which was

concomitantly reduced to iodide (Equation 3, B represents a basic buffer, R represents an alkyl group). The reaction was initiated by the presence of water. The amount of water present was calculated directly from the amount of iodine consumed.

To allow this reaction to go to completion a form of iodine addition mechanism was required, as well as monitoring the amount of iodine necessary to consume all the water present. Two methods can be used for this purpose; Coulometric and Volumetric (Scholz, 1984; MacLeod, 1991).

1. $2ROH + SO_2 \Leftrightarrow RSO_3^- + ROH_2^+$, Solvolysis
2. $B + RSO_3^- + ROH_2^+ \Leftrightarrow BH^+SO_3R^- + ROH$, Buffering
3. $H_2O + I_2 + BH^+SO_3R^- + 2B \Rightarrow BH^+SO_4R^- + 2BHI^-$, Redox

Coulometric analysis generates iodine, during analysis, at an anodic electrode. Water content is proportional to iodine consumption, while iodine generation is proportional to the amount of electrical charge used. Consequently, water content may be calculated from the electrical energy used to generate iodine, with a relationship of 1 mg (H_2O) being equal to 10.71 coulombs (Poynter & Barrios, 1994).

Volumetric analysis involves metering (from a burette) the amount of iodine necessary to consume the water. As the amount of iodine that reacts with a standard volume of water is known, it is possible to calculate the water content of any non-aqueous sample (Scholz, 1984).

The chemical reactions involved in both coulometric and volumetric detections are identical. The coulometric analysis generates accurate results for low water contents while using small sample size. As experimentation for assessment of water uptake ability would involve high water content, the accuracy of the coulometric analysis was not required. In addition, it was reported that the reliability of the coulometric apparatus may be affected by particulates present in crude oil samples (MacLeod, 1991).

2.2.2. Volumetric Analysis.

There are two types of Karl Fischer volumetric analysis, one component and two component (Scholz, 1984). One component analysis was the original type of volumetric analysis, the reagent containing all the chemicals necessary for Karl Fischer titration. Unfortunately, the shelf life of the one component mixture is short and therefore, a two component analytical system was developed, consisting of components A and B. Component A contained sulphur dioxide, pyridine and methanol, combining to act as the sample solvent in the titration vessel (Fig. 2.2.2).

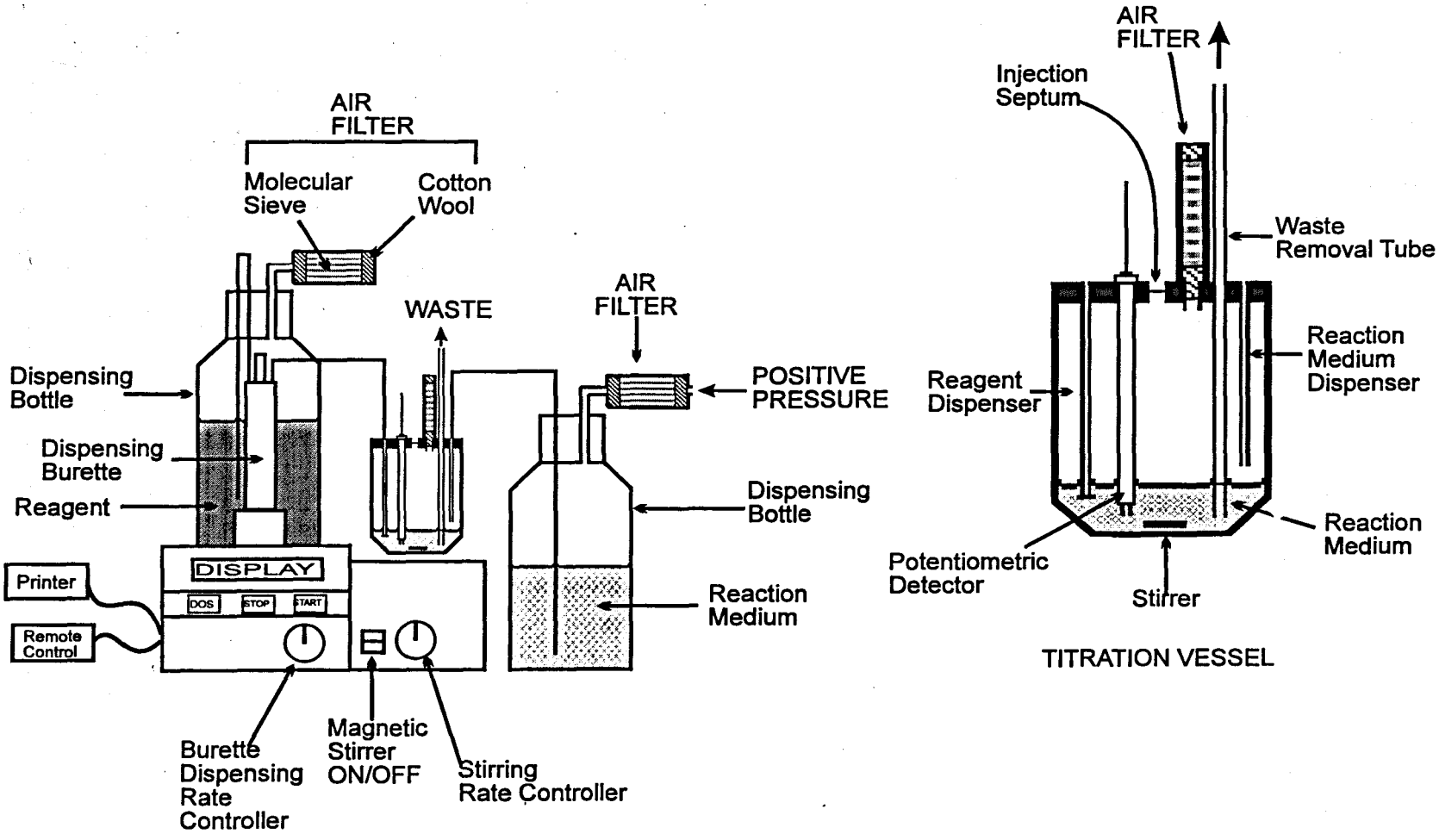

Figure 2.2.2. Metrohm 702SM Titrino adapted for Karl Fischer Titration.

Component B, contained iodine, pyridine and methanol, combining to act as the reagent. Component B was titred from the burette to the titration vessel (containing component A) when required.

The chemistry of the two methods is identical; however, the development of the two component system brought two major advantages. First, the rate of reaction is increased (therefore, titration time reduced) due to the high initial concentration of sulphur dioxide and buffer in the titration vessel. Second, the endpoint stability and therefore accuracy of the water determination is improved. Figure 2.2.3, taken from Scholz (1984), shows that the titration of 40 mg of water was faster. The Two Component analytical method was chosen for use.

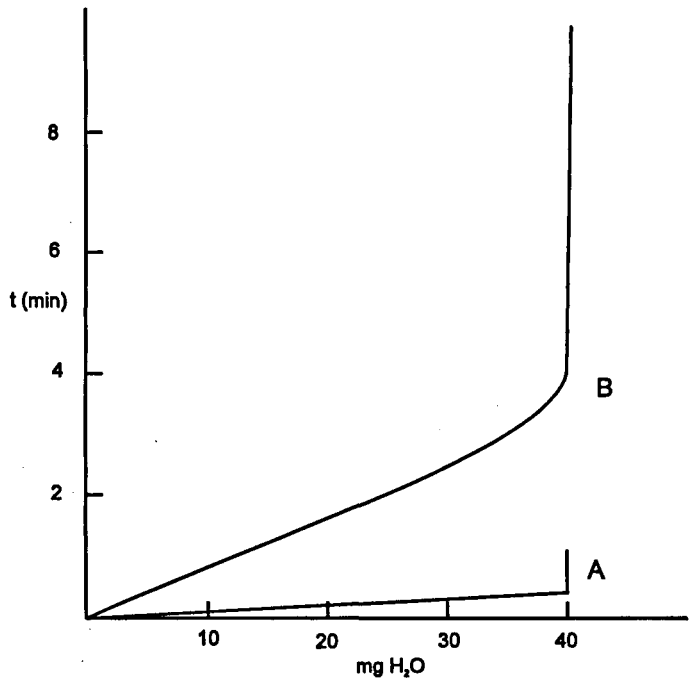

Figure 2.2.3. Titration of 40 mg of water with different Karl Fischer reagent. A = two component reagent; B = one component reagent. Adapted from Scholz (1984).

The components used were the Karl Fischer Titrant U, pyridine free, BDH catalogue #19260 (containing iodine and basic buffer) and Karl Fischer Solvent Solution, pyridine free, BDH catalogue #19266 (containing SO_2, methanol and a basic buffer). The Karl Fischer Titrant U, otherwise called the reagent, has an approximate reactivity with water of 1 ml reagent to 5 mg of water.

To perform the Karl Fischer water determinations with a volumetric, two component system, a Metrohm 702SM Titrino was selected (Fig. 2.2.2). This performs automatic endpoint determination (endpoint represents the completion of the titration) of the titrations by the use of a potentiometric detector.

A potentiometric detector was employed to avoid the reliance on visual endpoint determination in Karl Fischer titrations, thereby reducing probable human error. A double platinum electrode was attached to a voltmeter and then polarised by the application of a current. When a "wet" solution is present and there is an absence of iodine, a large potential difference between the electrodes exists. However, when the water content of the sample is eventually consumed during titration the iodine content will sharply rise, producing a rapid decrease in the applied voltage between the two electrodes consequently indicating the end of the titration. The amount of water present is then determined from the amount of iodine titred (Scholz, 1984; MacLeod, 1991).

2.2.3. Metrohm Apparatus.

The preparation of experimental consumables and adjustment of the titration conditions for the water determination analyses performed in this thesis are described in detail in Appendix 1, Sections A1.5 to A1.7. The method used followed the procedures described for the determination of "Water in crude oil by Karl Fischer Volumetric Titration" (ASTM 4277/87; IP 356/87), as well as valuable recommendations by Nick Kernhigan, BP (Sunbury).

2.2.3.1. Basic Preparations.

Basic preparations assess and maintain the materials and equipment, of the Metrohm, which are consumed and worn out by Karl Fischer titration. The reagent, reaction medium levels, condition of the septum in the titration vessel, electrode condition and state of the molecular sieve traps were all checked before analysis. In addition, the reactivity ratio of the reagent (*i.e.*, the amount of reagent that reacts with a given water quantity, on average 1 ml of reagent reacting with 5 mg of water) will vary with time and exposure to the atmosphere. To produce accurate titration results the reagent has to be re-calibrated daily when in use.

2.2.3.2. Titration Conditions.

Before analysis, the titration conditions of the Metrohm require adjusting to meet the requirements of the samples to be analysed, in this case crude oil. There are

two main problems associated with the analysis of the water content of crude oil when using Karl Fischer titration. These are the de-asphaltening of the crude oil, by solvent dilution, and interfering side reactions between the Karl Fischer reagents and components in the crude oil.

De-asphaltening of a crude oil occurs when the solubility potential of the crude oil is lowered (loss of solvent power, Section 1.2.2.1), either by changes in PVT conditions or changes in the composition of the oil. Such changes make the oil unable to support the high molecular mass asphaltenes in a colloidal or solution state, consequently asphaltene precipitation occurs (Kawanaka *et al.*, 1989; Wilhelms & Larter 1994b). Addition of the crude oil sample to the BDH solvent solution (SS), in the titration vessel, produces de-asphaltening. To prevent de-asphaltening, xylene (Xy), a good crude oil solvent, was mixed with the SS. The mixture, (SS:Xy; 40:60), known as the reaction medium, maintained the solubility balance of the crude oil and overcame prevent de-asphaltening.

An interfering side reaction may be classed as any reaction, between the sample and titration components (reagent and solvent solution), other than the actual Karl Fischer reaction. Interfering side reactions affected the water content determination by either generation or consumption of water. Water loss resulted in low water content determination while water addition resulted in two possible outcomes; a higher than expected water content was determined or, the slow addition of water prevented the titration from reaching an endpoint (Section 2.2.2). Such a condition is referred to as a "vanishing endpoint". Crude oils, due to their complex chemical nature, are susceptible to interfering side reactions (Scholz, 1984).

To reduce the risk of poor water determination, caused by complications, the Karl Fischer reaction was encouraged to reach an endpoint (EP) rapidly (Scholz, 1984, 1985). The endpoint (EP) occurs when the titration has reached completion. Rapid endpoint completion was achieved by the manipulation of three parameters in the Metrohm Karl Fischer program. The three parameters were: 1, endpoint limit; 2, dynamic limit and 3, the minimum titration rate. The first two parameters are illustrated in Figure 2.2.4.

The endpoint limit represents the point of cessation for reagent addition. Figure 2.2.4, shows that when the detected voltage falls below the endpoint limit of 250 mV, reagent addition and therefore titration, ceases. The limit was set at the high value of 250 mV to give early cessation of titration and help promote rapid endpoint determination.

Prior to the cessation of reagent addition, the rate of titration must be slowed to avoid passing the endpoint and overdosing the reaction with reagent, giving overestimation of the water content of the sample. The dynamic limit represents the

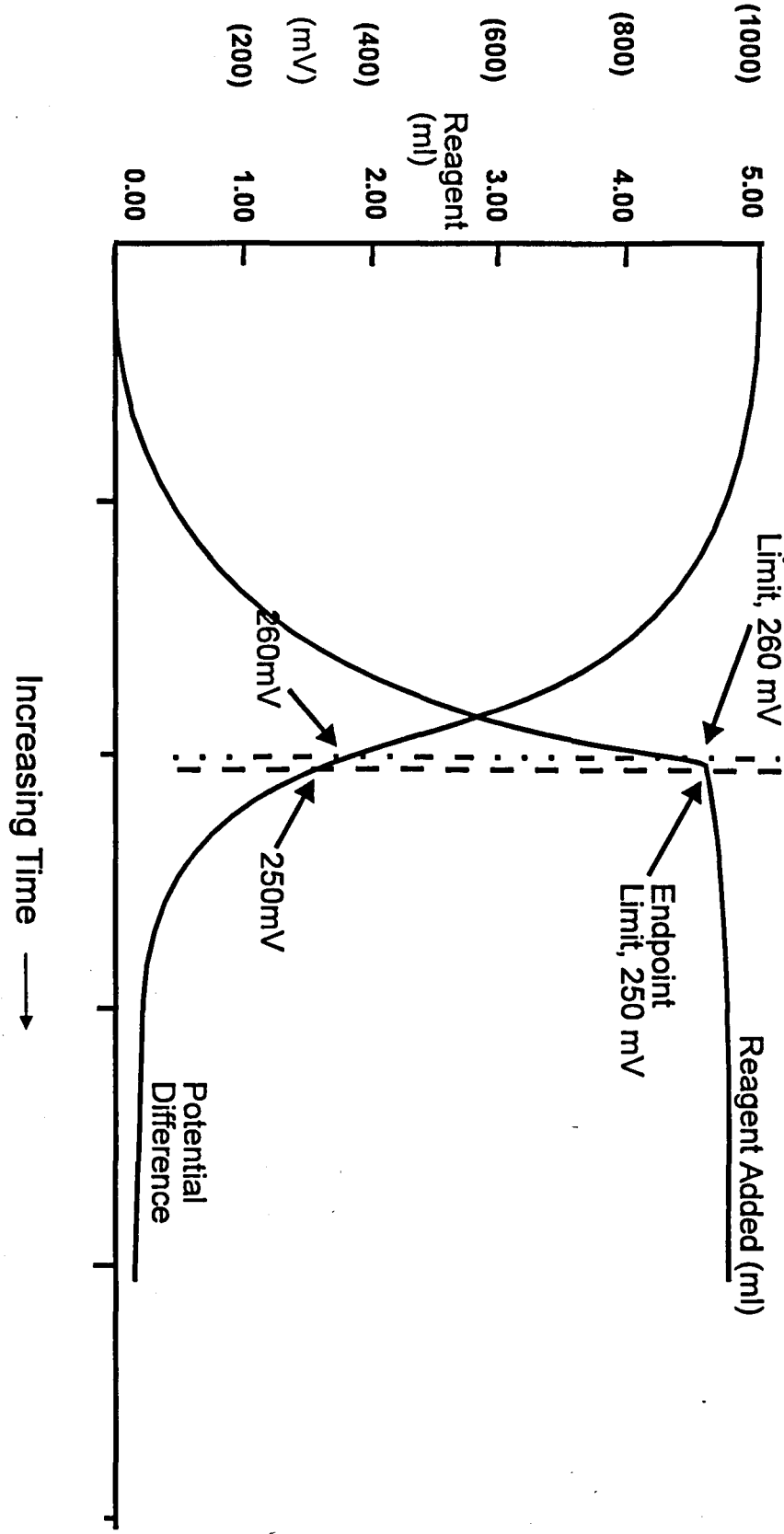

Figure 2.2.4. Effect of the Dynamic and Endpoint Limits upon Titration

voltage at which reagent addition was slowed in preparation for the endpoint limit. A balance between overdosing and achieving a rapid titration was required and the dynamic limit was set at 10 mV above the endpoint limit. In Figure 2.2.4, the slope of reagent addition decreases, indicating a decrease in the reagent addition rate, when the dynamic limit of 260 mV was reached (10 mV prior to the endpoint limit). This was relatively late for slowing the titration and some overestimation of water content was possible; however, the benefits from rapid endpoint determination and the consequential restriction of prohibiting side reactions was preferred.

Minimum titration rate represents the rate of titration at the beginning and end of analysis. As previously mentioned, to reduce complications (interfering side reactions) from influencing water content determination, analysis was rapid. Consequently, the minimum titration rate was high, at 45 $\mu l\ min^{-1}$.

2.2.4. Sample Preparation.

Sample preparation is divided into three parts; crude oil preparation, water addition and crude oil and water blending. These procedures are described in detail in Appendix 1, Section A1.8. As in Section 2.2.3, procedures were based around those described in the ASTM 4277/87 and IP 356/87 method, as well as additional recommendations (Kernhigan, N., pers. comm. 1991)

2.2.4.1. Crude Oil Preparation.

All crude oil samples used for analysis have to be representative of the entire sample batch, and not altered by storage effects such as gravity separation or oxidation. Homogenisation of the crude oil was achieved by use of an IKA Ultra-Turrax T25, high speed disperser and S25N-18G disperser attachment prior to further work (Fig. 2.2.5).

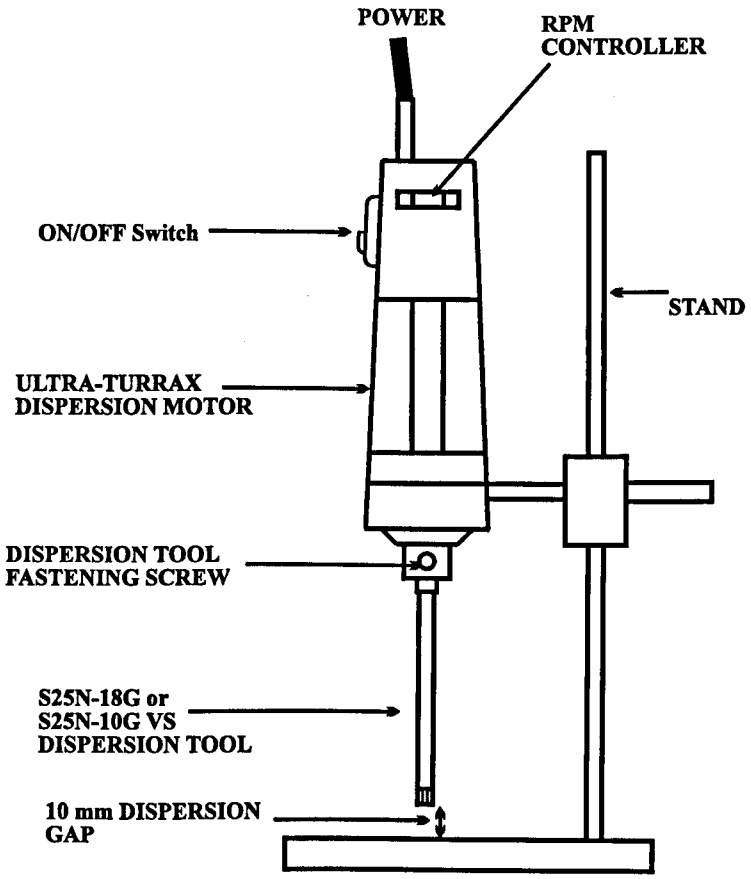

Figure 2.2.5. The IKA Ultra-Turrax T25 Disperser.

The Ultra-Turrax system was chosen for homogenisation procedure because of its capability of blending without aeration, and little or no heating. The S25N-18G disperser attachment allowed homogenisation of samples with a volume between 10 ml and 500 ml.

The S25N-18G dispersion tool, attached to the Ultra-Turrax T25 drive unit, was lowered into the bulk crude oil sample until it was estimated as being approximately 10 mm from the base of the crude oil container. The bulk sample was then homogenised, the blending rate being slowly increased from the minimum, 8,000 RPM, to approximately 18,000 RPM. This rate was maintained for 3 minutes and then slowly decreased to the minimum rate.

During operation, the high speed rotor of the Ultra-Turrax dispersion tool causes the crude oil to be sucked axially into the dispersion head, as depicted by Figure 2.2.6. The crude oil was then forced radially through the slots of the rotor-stator arrangement, shown in Figure 2.2.7, and passed through the shearing gap. Here the crude oil receives approximately 1000 times more energy than by stirring, in addition, the turbulence in the shearing gap produces excellent dispersion conditions. The result of this procedure was that the composition of the crude oil was homogeneous.

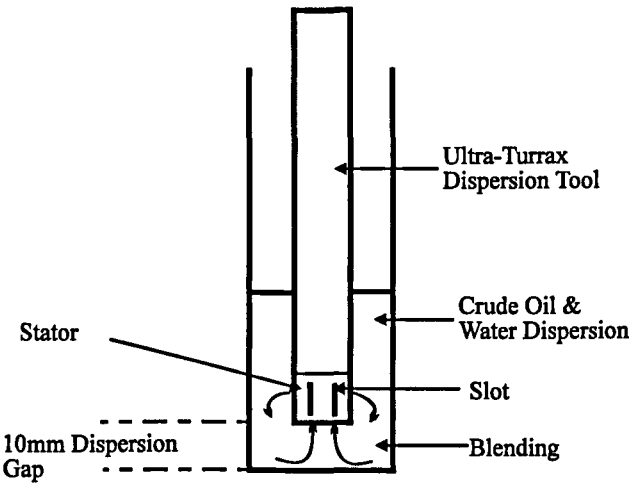

Figure 2.2.6. Ultra-Turrax blending action.

Once the sample had been homogenised crude oil aliquots, approximately 6 g in weight, were taken from the bulk sample for blending with water.

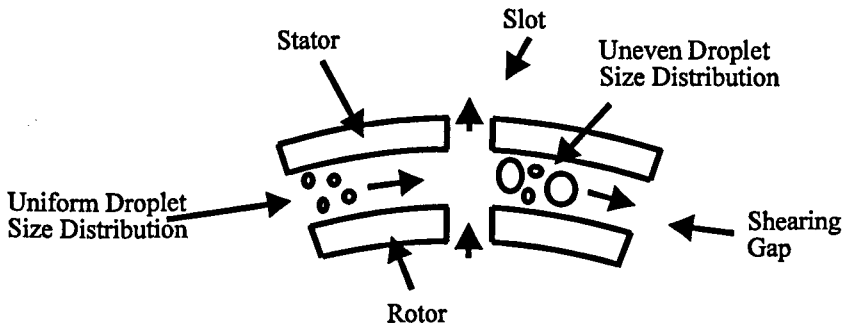

Figure 2.2.7. Illustration of the shearing gap in the Ultra-Turrax tool, emphasising the shearing and homogenisation action.

2.2.4.2. Water Addition.

The crude oil samples (approximately 6 g) were pipetted into a 28 ml vial and a quantity of distilled water added. The amount of water added was dependent upon the required crude oil water content, either 5%, 10%, 20% or 30% by weight.

2.2.4.3. Crude Oil and Water Blending.

The Ultra-Turrax high speed disperser was used to blend the crude oil and water phases. The procedure followed was the same as described in the Crude Oil Preparation (Section 2.2.4.1) however, a S25N-10G VS dispersion tool was used which can blend liquid volumes in the range of 3 to 10 ml. The aim of blending was to uniformly disperse the water phase, into the oil phase, as droplets with an even size distribution. The effectiveness of the Ultra-Turrax, for water droplet formation and distribution into North Sea crude oils, using varying blending times and speeds was assessed by Johansen *et al.* (1989). The results of that study are plotted in Figure 2.2.8. It was found that the water droplets maintained a narrow size range, even with large variation in both blending time (1 - 8 minutes) and rate (8,000 - 20,000 RPM). It was therefore considered that the blending procedure, of 18,000 RPM for 3 minutes, used for these experiments, was acceptable.

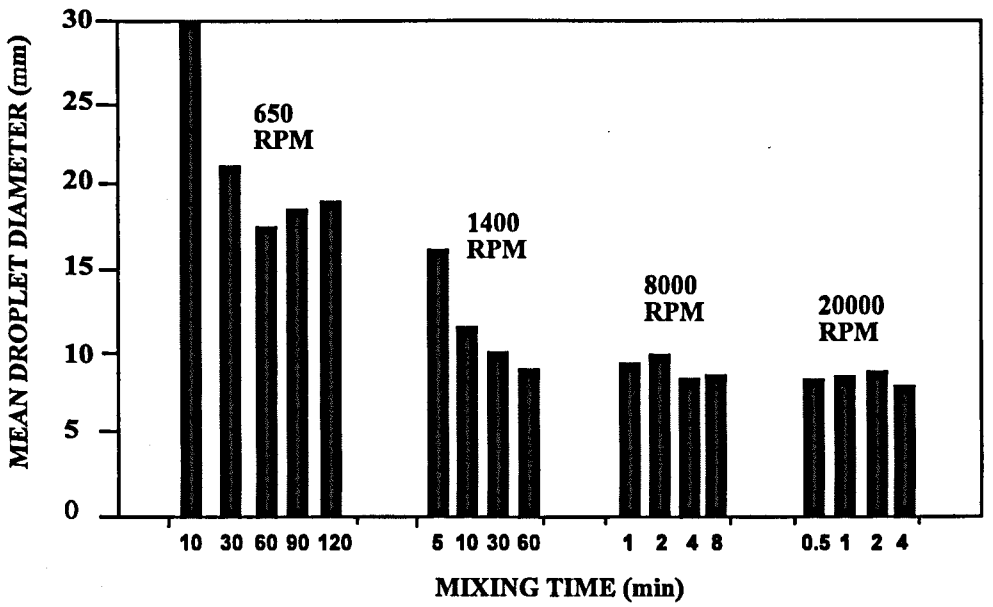

Figure 2.2.8. Illustration of the Ultra-Turrax blending efficiency at varying rates and times. Taken from Johansen et al. (1989).

2.2.5. Sampling.

Once the crude oil and water blends were prepared, they were immediately sampled according to the sampling strategy (Appendix 1, Section A1.9) and analysed by Karl Fischer titration (later modifications, made to the samping strategy, are given in Section 3.2). The results were calculated and plotted against time from blending. The blends were observed for any sample alteration such as water or emulsion

separation (sedimentation). These observations are used in conjunction with the Karl Fischer titration results.

2.2.5.1. Sampling Strategy.

Samples were taken from the top of the crude oil and water blends, as shown in Figure 2.2.9. The initial sampling frequency was high and is shown in Table 2.2.1.

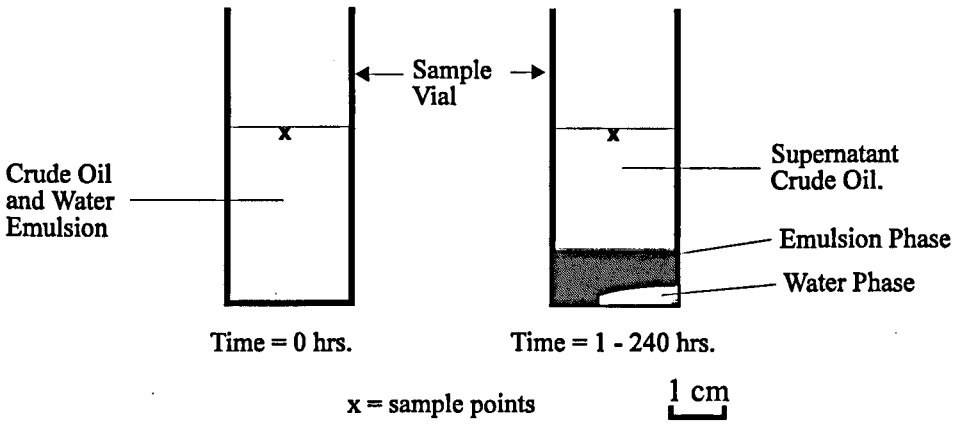

Figure 2.2.9. Sampling Procedure.

Sampling No.	Sampling Time (Hrs. Mins)	Sampling No.	Sampling Time (Hrs.Mins)	Sampling No.	Sampling Time (Hrs.Mins)
1	0' 3"	9	3' 0"	17	120' 0"
2	0' 6"	10	6' 0"	18	144' 0"
3	0' 9"	11	9' 0"	19	168' 0"
4	0' 12"	12	12' 0"	20	192' 0"
5	0' 21"	13	24' 0"	21	216' 0"
6	0' 30"	14	48' 0"	22	240' 0"
7	1' 0"	15	72' 0"		
8	2' 0"	16	96' 0"		

Table 2.2.1. Sampling Frequency.

2.2.5.2. Sampling Procedure.

Sampling procedure is described in greater detail in Appendix 1, Section A1.9.2. The titration vessel was filled to approximately 3 cm depth with the reaction medium. The water content of the reaction medium had to be neutralised and this was

achieved by titration. When the reagent dispensing rate had fallen to 3 μl min^{-1} or less, the reaction medium was considered to have been dried and sample analysis could begin. Consistently waiting for a dispensing rate of 3 μl min^{-1} or less, prior to sample analysis, improved the analytical precision of the Karl Fischer titration. Titration commenced when the Metrohm was started (press START button).

The crude oil/water blend was prepared by the procedure described in Section 2.2.4, and sampled immediately after blending. Accurate, precise and rapid sampling was achieved by clamping the sample vial, and a 250 μl Hamilton gas syringe, as shown in Figure 2.2.10. This arrangement ensured that the needle always sampled the same area of blend (*i.e.*, the top 1 mm of the blend). The syringe was lowered into the sample, placing the needle in the top 1 mm of the crude oil and water blend (Fig. 2.2.9). Approximately 100 μl of crude oil and water blend was sampled. The syringe and sample were weighed to 0.1 mg.

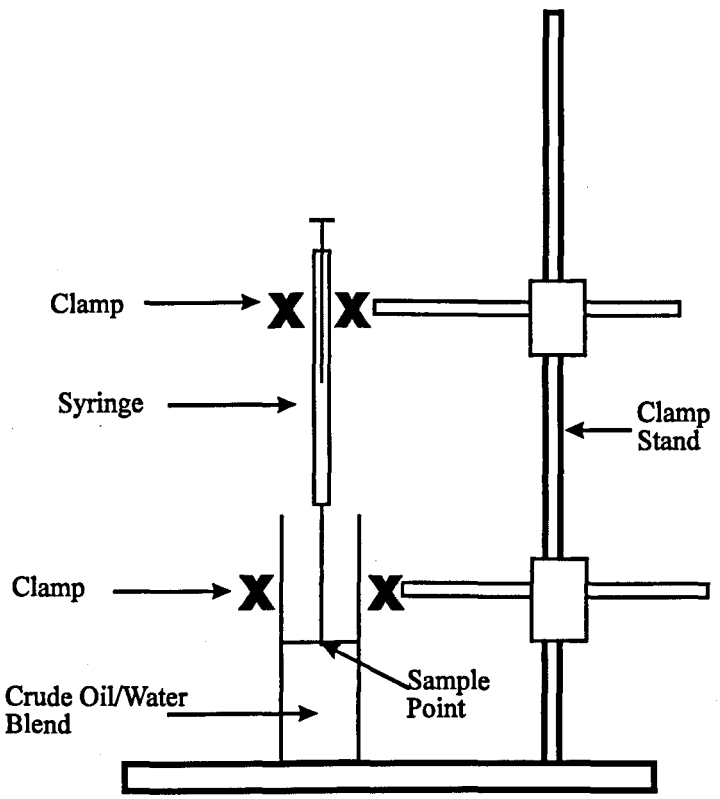

Figure 2.2.10. Sampling Procedure Set Up.

Prior to injection of the sample, the Metrohm's "START" button was pressed twice to give the prompt "sample weight" on display (Fig. 2.2.2). The method of injecting the sample into the reaction medium was a crucial stage in the analysis and was performed exactly as described below and illustrated in Figure 2.2.11.

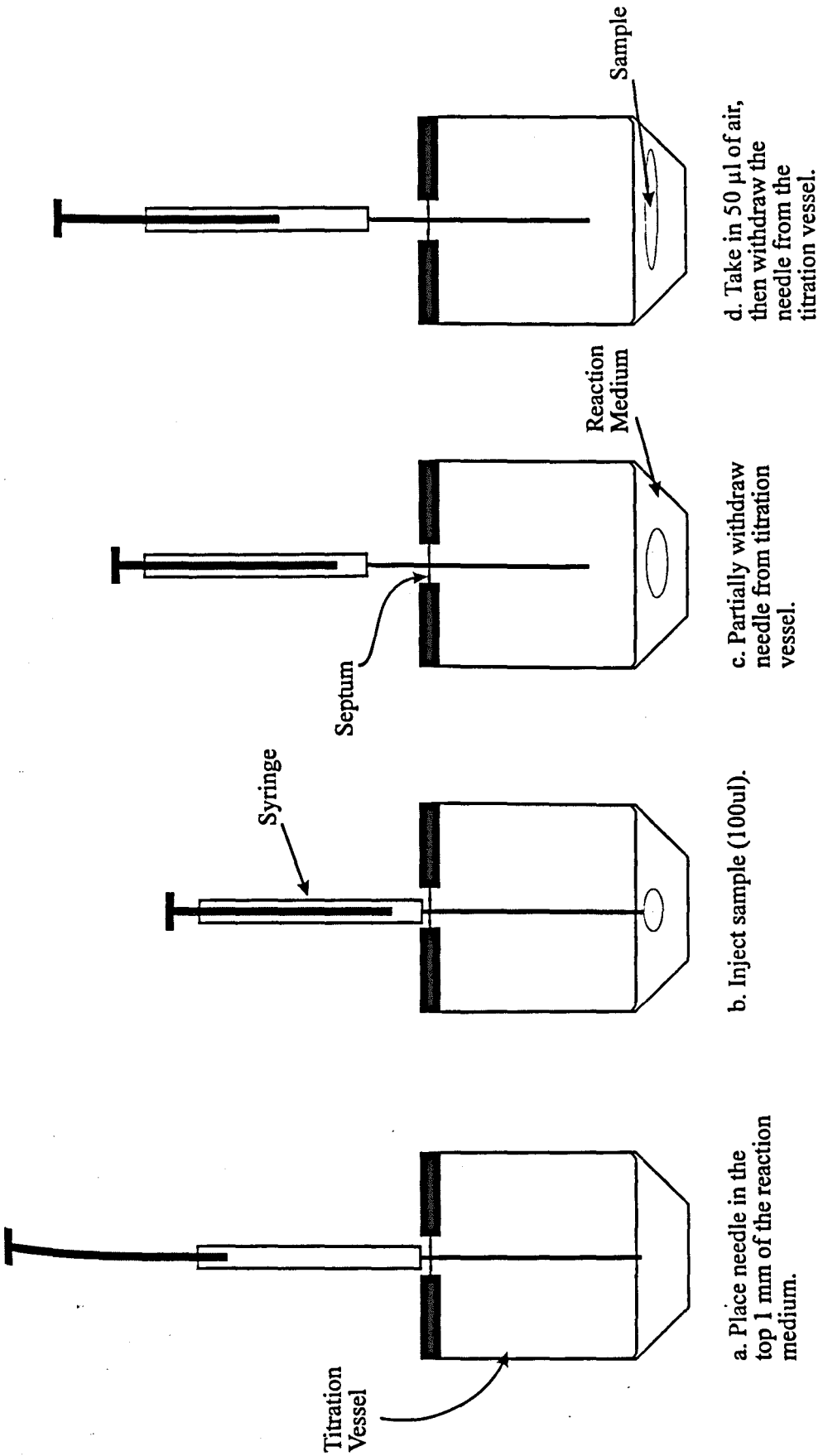

Figure 2.2.11(a,b,c,d). Injection procedure, steps a to d.

The syringe was pushed through the septum of the titration vessel, until the needle tip was in the dried reaction medium (Fig. 2.2.11a). The sample (100 µl) was then injected into the reaction medium (Fig. 2.2.11b). It was very important to ensure that the sample was injected directly into the reaction medium as this prevents loss of sample on the sides of the titration vessel. Sample loss would result in the underestimation of the water content of the sample.

The syringe was withdrawn from the reaction medium (Fig. 2.2.11c) but, before total removal from the titration vessel, approximately 50 µl of air was taken up into the syringe (Fig. 2.2.11d). Taking air into the syringe removes any drops of crude oil and water blend from the needle tip. If these drops were not removed they would be smeared onto the septum when the syringe was subsequently removed from the titration vessel. This would have resulted in inaccuracies in sample weight calculation and underestimation of the water content. The syringe was removed from the titration vessel and re-weighed. The sample weight was calculated and entered into the Metrohm and the "ENTER" button pressed so that the Karl Fischer water determination (titration) commenced. The titration endpoint was automatically determined and the water content of the sample calculated to 0.01 percent. The dried reaction medium was used for two titrations only, the Metrohm was then stopped (press STOP button) and the reaction medium was replaced, the fresh reaction medium being dried by titration (press START button).

Once the sample vial had been analysed it was put aside until its next sampling time and the next sample vial clamped, and the above procedure repeated.

2.2.5.3. Sample Alteration.

During the analysis period it was possible that the state of the sample could change (already illustrated in Fig. 2.2.9 and briefly addressed in Section 2.2.5) from well-dispersed emulsion into a mixture with several phases.

The sample, as soon as 1 hour after blending, (Section 3.3.2, Fig. 2.2.9), was capable of separating into different phases. The oil which accumulated at the top of the sample was referred to as the supernatant oil. In Section 3.3.1, it is shown that the supernatant oil predominantly contained oil but also contained a significant amount of water (water and/or emulsion droplets), which was sedimenting. The base of the sample was either an emulsion sediment or a separate water phase, however both were not mutually exclusive and could occur together (Section 3.3.2). The amount of emulsion/water phase at the base of the sample increased with time from blending, due to the sedimentation of emulsion/water droplets from the supernatant oil.

2.2.5.4. Results Presentation.

The results of the water content determinations, from the Crude Oil Water Uptake Analyses, were presented as normalised percentages (%R), plotted against time from blending. The normalised percentage of water (%R) was calculated from the water content determined by Karl Fischer titration, divided by the initial added water content of the crude oil and water blend in question. Examples of these calculations are shown in Figure 2.2.12. Also, Figure 2.2.12, illustrates an idealised drop in the normalised percentage (%R), with increasing time, for a crude oil and water blend.

The results obtained from the above sampling procedure produce information on the water retentive ability of the different crude oils. The water retentive ability is described as either "good", "moderate" or "poor", from assessment of crude oil/water blends with 30% added water contents. "Good" water retention is represented by a constant water content value of between 100-40%R. When water retention drops to 40%R or less, between 50 and 100 hours, it is described as having "moderate" water retention. However, values dropping below 40%R or less, before 50 hours, represent "poor" water retention. Examples of these three water retentive categories ("good, moderate and poor") are illustrated in Figure 2.2.13.

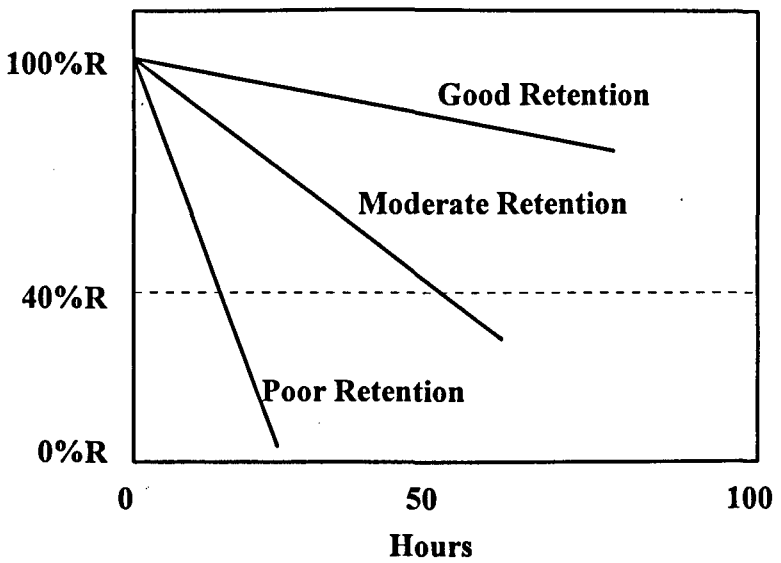

Figure 2.2.13. Illustration of examples of water dropout lines for the water retention categories "good", "moderate" and "poor". Normalised water percentages (%R), gained from samples taken from the top of the crude oil/water blends with 30% added water content, were plotted against time from blending (hours).

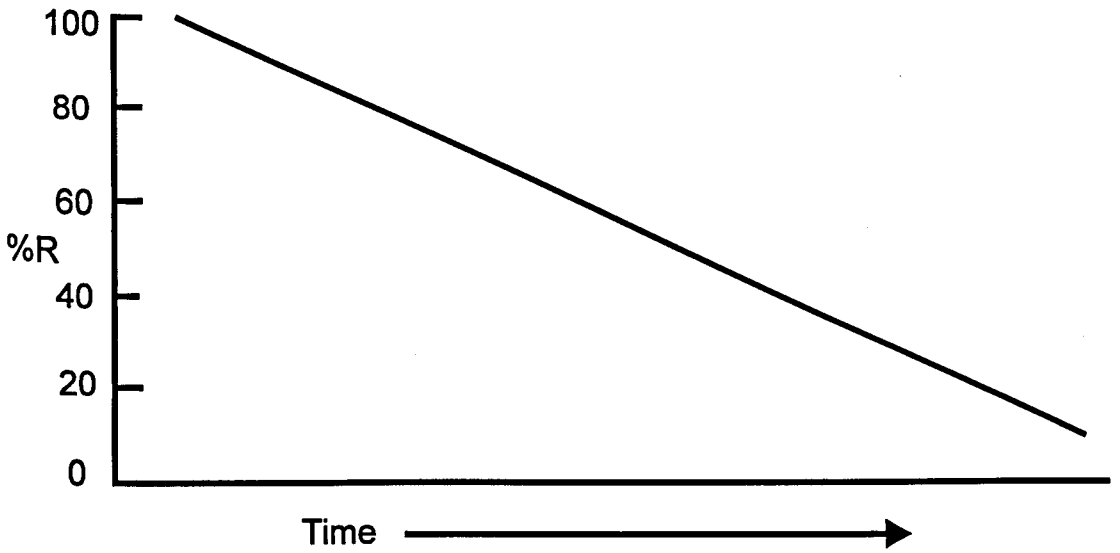

Figure 2.2.12. Idealised drop in %R (Normalised Percentage) with time from samples taken at the top of the blend/supernatant oil. In addition, examples of Normalised Water Content (%R) calculations are shown below.

$$\%R = \frac{\text{Measured Water Content (\%)}}{\text{Original Water Content (\%)}} \times 100\%$$

E.g., For a homogenisation with an initial 30% water content.
Measured Water Content by Karl Fischer Water Determination = 30%

$$\%R = \frac{30\%}{30\%} \times 100\%$$

%R = 100%R

E.g., For a homogenisation with an initial 20% water content.
Measured Water Content by Karl Fischer Water Determination = 5%

$$\%R = \frac{5\%}{20\%} \times 100\%$$

%R = 25%R

CHAPTER 3:

ASSESSMENT OF THE WATER UPTAKE ABILITY OF CRUDE OILS

CHAPTER 3: ASSESSMENT OF THE WATER UPTAKE ABILITY OF CRUDE OILS.

The assessment of the water uptake ability of various crude oils was achieved by the blending of oils with varying amounts of water. This enabled the characterisation of their water retention and emulsion formation/stabilisation properties. It was also found that both these characteristics were influenced by the extent of biodegradation of the crude oils.

3.1. Introduction.

Using Crude Oil Water Uptake Analysis (COWUA), described in Chapter 2, Section 2.2, the water uptake ability of various crude oils were assessed by monitoring their behaviour when blended with different quantities of water. After these initial experiments the factors which influenced the extent of crude oil water uptake were investigated. Therefore, the compositional effects of both crude oil and water phases were assessed in order to identify their roles in crude oil water uptake. Characterisation of these factors may help in the prediction of the water uptake ability of new crude oil accumulations. Factors which have been reported in the literature as influencing oil and water interactions are the emulsifiers (sols and surfactants) present in the crude oil (Papirer *et al.*, 1982; Siffert *et al.*, 1984; Thompson *et al.*, 1985; Eley *et al.*, 1987; Schramm, 1992), as well as the electrolyte content of the aqueous phase (Becher, 1966; Kizling & Kronberg, 1990; Aronson & Petko, 1993).

As previously described in Chapter 1, the asphaltene and wax emulsifiers in crude oils have been strongly associated with controlling the water uptake ability of crude oils by acting as sols (Graham *et al.*, 1983; Johansen *et al.*, 1989; Acevedo *et al.*, 1992; Bobra *et al.*, 1992). Payne and Phillips (1985a) reported that their effects upon emulsion stability are likely to be indistinguishable. However, Payne and Phillips (1985a) also suggested that the effect of the asphaltene group was dominant over the wax group. This investigation will attempt to assess individually how quantitative variation of both asphaltenes and waxes may affect emulsion stability. However, it will be remembered that it is probable that both fractions act together in the stabilisation of crude oil and water blends.

Distilled water was used for the majority of experiments in this work, but it was considered that use of saline water would make the experiments more representative of real life scenarios (Section 1.1). The literature has shown that the ionic content of the water phase is very important in controlling the water uptake

ability of crude oils. The ionic content influences emulsification, affecting both the type of emulsion formed and resultant emulsion stability (Oren & MacKay, 1977; Schramm, 1992). Ionic controls on emulsion stabilisation are, however, mostly concerned with oil-in-water emulsions, as water-in-oil emulsions are generally stabilised by rheological or steric effects (Eley *et al.*, 1987). However, it has been shown by Bhatnagar (1920), that water-in-oil emulsions are capable of producing a small electric current, therefore, it is possible that the stability of water-in-oil emulsions may be influenced by the ionic content of the water phase. In addition, Jones *et al.* (1978) highlighted that stability differences in water-in-oil emulsions were associated with the variation of the pH and salt content in the aqueous phase. Consequently, the electrostatic forces, so prevalent in oil-in-water emulsions, may also be influential in water-in-oil emulsions. Therefore, alteration of the electrolyte content of the aqueous phase may change the determined (distilled) water uptake characteristics of the crude oils analysed.

Use of synthetic seawater, instead of distilled water, altered both the electrolyte concentration and pH of the aqueous phase in the crude oil/water blends. Aronson & Petko (1993) identified that the presence of electrolytes in the aqueous phase of a crude oil/water blend increased the stability of water-in-crude oil emulsions by reduction of the degree of coalescence of water droplets. Three main reasons (discussed below) were given for this effect; prevention of Oswald Ripening of water droplets, reduction of the effect of van der Waals forces of attraction between the dispersed water droplets, and the increase of adsorbed emulsifier concentration at the crude oil and water interface.

Oswald Ripening is seen as the growth of large dispersed water droplets, at the expense of the smaller dispersed water droplets (Weers & Arlauskas, 1995, and literature cited therein). This occurs due to the diffusion of water from small water droplets, which have high chemical potentials (greater solubility), to large water droplets, which have low chemical potentials (lower solubility). Aronson & Petko (1993) found that the addition of an electrolyte decreased the degree of water coalescence by preventing water diffusion across the dispersive oil phase. This was attributed to the decrease of water solubility in oil, reducing the diffusive ability of water.

Reduction of van der Waals attractive forces between water droplets across the dispersive oil phase, according to Kizling & Kronberg (1990), is caused by the presence of electrolytes producing electronic properties in the water phase, equal to those of the oil phase. Consequently, the water droplets are just as attracted to the oil phase as to other water droplets. Therefore, increased electrolyte concentration in the

water phase decreases the attractive forces between water droplets, which lowers coalescence, thereby aiding emulsion stability.

The last mechanism which prevents water droplet coalescence, results from increasing the concentration of adsorbed emulsifier at the oil and water interface. Aronson & Petko (1993) found that small amounts of electrolyte in the water phase will reduce the aqueous solubility of emulsifiers, otherwise referred to as "salting out" (Price, 1976; Myers, 1991). Consequently, emulsifiers will be preferentially partitioned to the oil and water interface resulting in more stable oil/water interfacial films.

Alteration of the pH of the water phase has been used over many years to improve bitumen recovery, especially in heavy oil reservoirs such as those found in the Athabasca petroleum province (Brauer & Wasan, 1982; Stosur *et al.*, 1990). This technique is based on the formation of oil-in-water emulsions (Surkalo, 1990; Taylor & Schramm, 1990; González & Louvisse, 1991; Rudin *et al.*, 1994). This pH controlled effect is caused by the dissociation of surfactants, such as acids, at high pH, allowing the acidic ions to react with the water at the oil and water interface. This reduces the interfacial tension and improves emulsification (Jennings, 1975; Chan & Yen, 1982; Babu *et al.*, 1984). Although generally used for the formation of oil-in-water emulsions, this mechanism will affect the oil and water interface in either type of emulsion. Alteration of the pH in the aqueous phase will therefore affect the assessment of the water retention and water-in-oil emulsion formation/stabilisation properties of crude oils.

3.1.1. Sample Set.

Crude oils from a range of source rock depositional environments, maturities and biodegraded states, from two major petroleum provinces (North Sea and Santa Maria Basin, California), were used to study crude oil water uptake ability. These oils are listed in Table 3.1.1 which also lists source rock, maturity, reservoir and state of biodegradation data.

3.1.1.1. Santa Maria Basin (SMB) Crude Oils.

The crude oils generated from the Monterey and Point Sal Formations of the Santa Maria Basin (SMB) are sourced from a Type IIS, algal marine source rock (approximate TOC 5%), enriched in diatoms, indicative of a palaeo-upwelling

Name	Origin[1]	Source Rock (type #)[2]	Reservoir Age and Type.[3]	Generation Stage.[4]	Biodegraded State (API°)	C_{27}/C_{29} ααR[5]	*n*-C_{18} /Ph[7]	Ph/ $C_{30}\alpha\beta$[7]	$C_{32}\alpha\beta$S /S+R	$C_{29}\alpha\alpha\alpha$ S/S+R	MDR
A29	NS	KCF (II)	KU-chalk	EARLY	Non-degraded (35°)	0.95	2.04	11.44	0.62	0.57	2.71
B12	NS	KCF (II)	KU-chalk	EARLY	Non-degraded (35°)	1.05	2.53	12.85	0.61	0.46	nd
Kittiwake	NS	KCF (II)	JU-clastic	EARLY	Non-degraded (28°)	0.94	1.87	28.72	0.63	0.53	2.75
Ninian	NS	KCF (II)	JM-clastic	EARLY	Non-degraded (35°)	1.07	1.47	14.88	0.60	0.40	nd
NS1	NS	KCF (II)	Pal-clastic	EARLY	Non-degraded (28°)	1.09	1.34	15.85	0.61	0.54	2.90
NS2	NS	KCF (II)	JM-clastic	EARLY	Mildly degraded (29°)	1.00	0.20	15.39	0.62	0.44	3.30
NS3	NS	KCF (II)	Eoc-clastic	PEAK	Extensively degraded (14°)	0.53[6]	0.00	5.18	0.62	0.47	2.01
H1	SMB	MF (IIS)	Mio-clastic	PEAK	Non-degraded (25°)	2.11	1.41	7.07	0.51	0.58	3.28
H7	SMB	MF (IIS)	Mio-clastic	PEAK	Moderately-extensively degraded (24°)	1.95	0.00	0.00	0.55	0.59	3.13
Monterey	SMB	MF (IIS)	Mio-clastic	PEAK	Mildly degraded (22°)	1.45	0.64	2.48	0.56	0.61	2.77

*Table 3.1.1. Fundamental details of the crude oils analysed in this study. Biodegraded state classified using the Volkman et al. (1984) scheme. Bulk compositional data is provided in chapters 3 and 4. [1]; NS = North Sea, SMB = Santa Maria Basin. [2]; KCF = Kimmeridge Clay Formation, MF = Monterey Formation. [3]; KU = Upper Cretaceous, JU = Upper Jurassic, JM = Middle Jurassic, Pal = Paleocene, Eoc = Eocene, Mio = Miocene. [4] = generation stages estimated from Table 3.1.4. [5] = C_{27}/C_{29} values > 1 suggests possible marine organic matter dominance at source; < 1 suggests possible terrestrial organic matter dominance at source. [6] = value reduced by biodegradation of C_{27} ααα*R* sterane. [7] = biodegradation parameter, discussed in chapter 6. Maturity ratios and depositional indicators listed in Appendix 2.*

depositional environment (Tyson, 1995 and literature cited therein). A ternary cross plot of the C_{27}, C_{28} and C_{29} ααα*R* steranes, illustrated in Figure 3.1.1, shows that the SMB crude oils apparently come from a common origin. In addition, analysis of the C_{27}/C_{29} ααα*R* sterane ratios (Table 3.1.1) also suggests organic matter input is predominately from a marine origin (Peters & Moldowan, 1993).

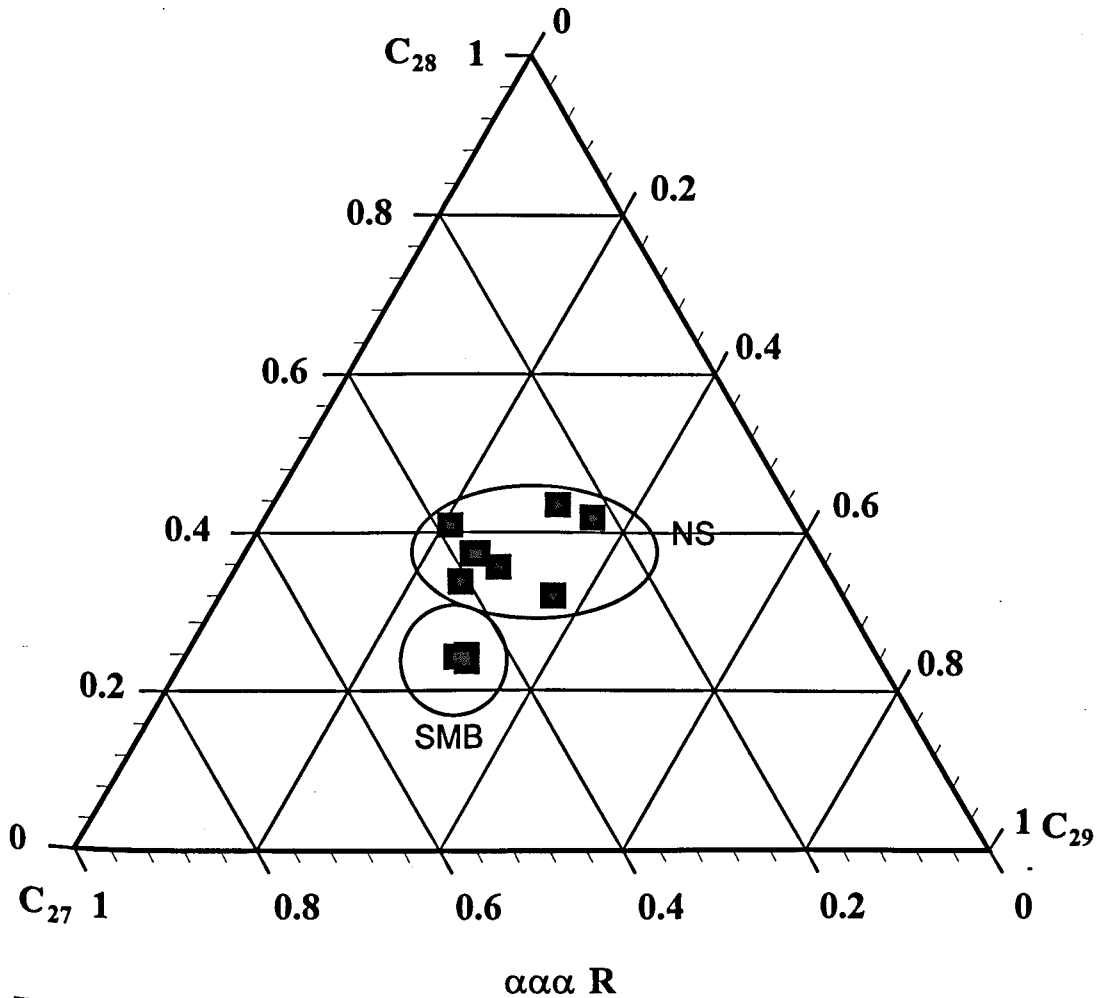

*Figure 3.1.1. Ternary plot (following Huang & Meinschein, 1979) illustrating the variation of sterane distributions (C_{27}, C_{28}, C_{29}, ααα*R*) for the North Sea (NS) and the Santa Maria Basin (SMB) crude oils.*

Deposition of the Santa Maria Basin source rock occurred in a highly reducing environment which resulted in the incorporation of large amounts of organic sulphur (8-14%) into the crude oil (Didyk *et al.*, 1978; Orr, 1986). Confirmation of the low redox potential (low Eh) at deposition is given by the plot of the relative percentages of the homohopanes (C_{31}-C_{35} regular hopanes) in Figure 3.1.2 with the homohopane index being high ($C_{35}/[C_{31}$-$C_{35}]$; Table A2.5; Peters & Moldowan, 1993; Moldowan & McCaffrey, 1995)

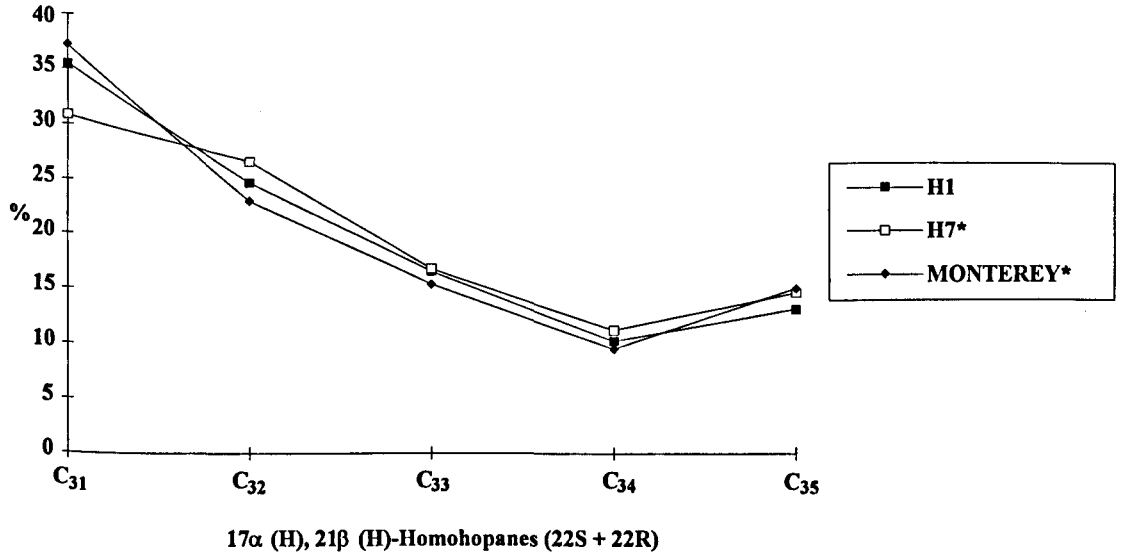

*Figure 3.1.2. The relative abundances (%) of C_{31}-C_{35} 17α(H), 21β(H) (22S+22R) hopanes (normalised to total C_{31}-C_{35} homohopanes) in the SMB crude oils analysed in this study. Note that the C_{35} homohopane percentages are greater than the C_{34} percentages, indicating that the source rock depositional environment was highly reducing. * = biodegraded crude oil.*

Due to the high organic sulphur content (>6%), the source rock has been designated as a Type IIS instead of Type II (Orr, 1986). The incorporation of large amounts of organic sulphur is influential on crude oil generation. Type IIS sourced crude oils differ from those generated from Type II source rocks, in that Type IIS sourced crude may be generated at lower temperatures (0.3% vitrinite reflectance; Taylor, 1994, and literature cited therein). Orr (1986) reported that this early generation of petroleum was attributed to weaker C-S bonds in the kerogen rather than the usual C-C and C-O bonds, which are broken at higher temperatures during crude oil generation from Type II source rocks. This was supported by Tissot *et al.* (1987) who found that activation energies for hydrocarbon generation from sulphur-rich Type II kerogens were lower than activation energies for hydrocarbon generation from normal Type II kerogens. However, recent work by Patience and Claxton (1993) has suggested that C-S bonds are no weaker than C-O bonds, and that early petroleum generation (characteristic of Type IIS kerogen) previously attributed to the weakening of C-C bonds due to sulphur incorporation, is unlikely. Which ever mechanism is responsible for early generation, the result is that Californian crude oils are frequently enriched with asphaltene, resins and aromatic sulphur. The average composition of these crude oils is approximately, 21% aliphatic hydrocarbons, 16% aromatic hydrocarbons and 63% NSO compounds. It is immediately apparent that these crude oils are enriched in the compounds ideal for water and crude oil interaction (Section 1.2.2).

3.1.1.2. North Sea Crude Oils.

In contrast to the heavy crude oils generated from the Santa Maria Basin, the crude oils of the North Sea petroleum province are generally sourced from the Upper Jurassic Kimmeridge Clay Formation (Cornford, 1990, and literature cited therein). It is seen in Figure 3.1.1 that all North Sea crude oils plot in the same region of a C_{27}, C_{28} and C_{29} αααR sterane ternary cross plot implying a similar origin (Peters & Moldowan, 1993). Deposition predominantly occurred in a marine "seaway" with input from bacterially degraded marine algal debris and degraded terrestrial humic matter (Cornford, 1990). The use of the C_{27}/C_{29} αααR sterane ratio also indicates a mixed marine and terrestrial organic matter input with Table 3.1.1 showing ratio values of approximately 1.

These Kimmeridge Clay Formation (KCF) source rocks constitute the major oil generating source rocks of the North Sea. They are organic rich (average TOC 2-9%) laminated mudstones, classified as Type II source rocks (Hallam, 1987). Analysis of the relative percentages of the homohopanes, in Figure 3.1.3, suggest varied depositional redox potentials. The resultant petroleums are predominately light crude oils (approximate API° of 35°) with average compositions of 60% aliphatic hydrocarbons, 30% aromatic hydrocarbons and 10% NSOs (Tissot *et al.*, 1974; Tissot *et al.*, 1978). Sulphur contents are approximately 0.65% (Tissot & Welte, 1984).

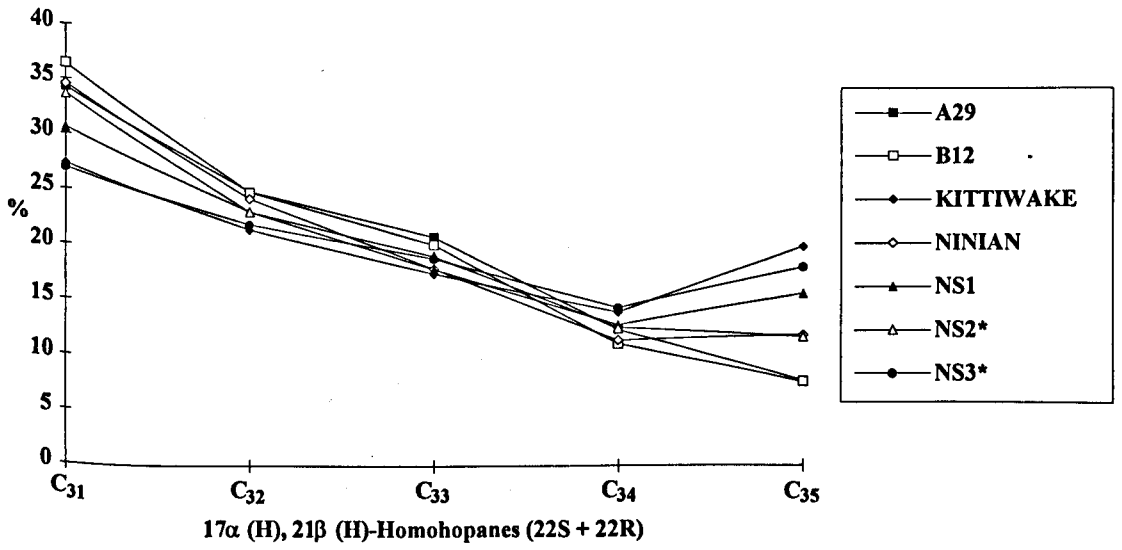

*Figure 3.1.3. The relative abundances (%) of C_{31}-C_{35} 17α(H), 21β(H) (22S+22R) hopanes (normalised to total C_{31}-C_{35} homohopanes) in the North Sea crude oils analysed in this study. Note the variable C_{35} homohopane percentages indicating different depositional redox potentials. * = biodegraded crude oils.*

As well as source rock and maturation differences, the two petroleum provinces are characterised by difference migration regimes, reservoir depths and reservoir histories. In addition, during analysis of crude oil water uptake ability, it should be remembered that the Santa Maria Basin sourced crude oils have a much higher surfactant (NSO) content than the North Sea crude oils.

3.1.1.3. Description of Crude Oils Analysed.

3.1.1.3.1. Eldfisk, A29 and B12 Crude Oils.

Both A29 and B12 crude oils are produced in block 2/7 of the North Sea from the Cretaceous chalk reservoirs of the Tor and Hod Formations (Hancock, 1990; Stoddart, 1993). From assessment of the biomarker and molecular maturity parameters, $C_{32}\alpha\beta S/S+R$, $C_{29}\alpha\alpha\alpha S/S+R$ and MDR, reported in Table 3.1.1, as well as other parameters listed in Table A2.6 (Appendix 2), it may be seen that A29 and B12 are mature crude oils generated during early to peak generation stages. Generation was estimated by comparison of the maturity ratios with the generation curve in Figure 3.1.4. In addition, the high n-C_{18}/Ph ratios (Table 3.1.1) indicate that both crude oils are "non-degraded", according to the Volkman *et al.* (1984) biodegradation scale, discussed in Chapter 6 (other biodegradation parameters are reported in Table A2.5).

3.1.1.3.2. Kittiwake Crude Oil.

The Kittiwake crude oil, as with the majority of North Sea crude oils, was sourced from the KCF (Fig. 3.1.1) however, homohopane index results presented in the graph in Figure 3.1.3, indicate that redox potentials at deposition were lower than those for the majority of North Sea crude oils (Peters & Moldowan, 1991).

Kittiwake is produced in block 21/18 of the North Sea, from the Upper Jurassic clastic reservoirs of the Fulmar Formation (Brown, 1990). Assessment of the maturity parameters (Tables 3.1.1 & A2.6), indicates that the Kittiwake crude oil is mature, from the early oil generation stage. Kittiwake is classed as a "non-degraded" crude oil, displaying a high n-C_{18}/Ph ratio.

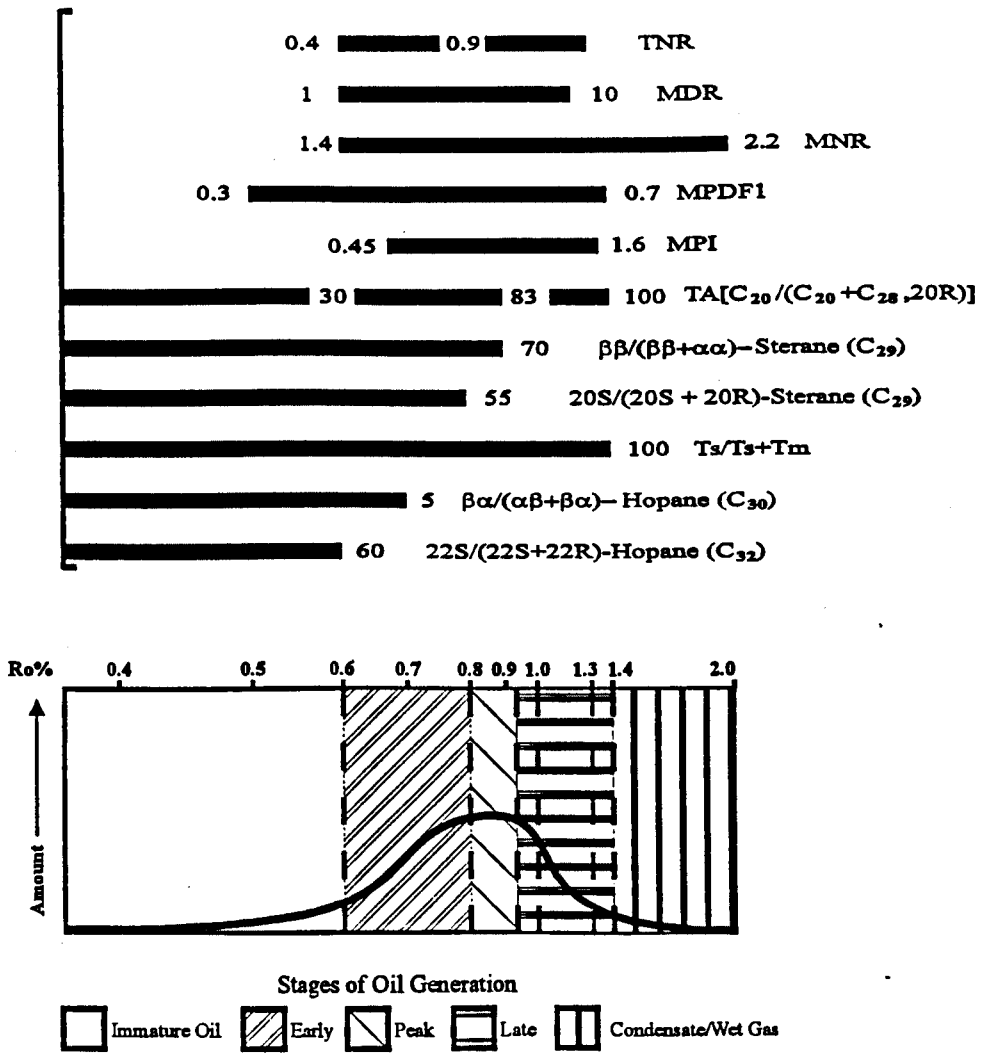

Figure 3.1.4. The approximate range of biomarkers and additional maturity parameters are shown versus oil generation stages. Lines do not represent a linear change in each parameter up to its maximum value. After Mackenzie et al. (1982).

3.1.1.3.3. Ninian Crude Oil.

Ninian crude oil is produced from the Middle Jurassic clastic reservoirs of the Brent Group, from block 3/3 of the North Sea (Brown, 1990). Examination of maturity parameters (Tables 3.1.1 & A2.6) suggests the oil was expelled from the source rock at the early generation stage. In addition, the Ninian crude oil is also classified as "non-degraded".

3.1.1.3.4. NS1 Crude Oil.

The NS1 crude oil is a confidential sample and therefore, both its block number and reservoir name are not presented. However, it may be reported that this crude oil was produced from a clastic, Paleocene reservoir of the North Sea. Both biomarker and molecular maturity parameters indicate that this crude oil probably migrated from the source rock at the early oil generation stage. NS1 is also identified as "non-degraded". Assessment of the homohopane indices shows that the source rock was probably deposited under highly reducing conditions (Peters & Moldowan, 1991; Figure 3.1.3).

3.1.1.3.5. NS2 Crude Oil.

The NS2 crude oil is a confidential sample and both its block number and reservoir name are not presented however, it may be reported that it is produced from the clastic Middle Jurassic reservoirs of the Brent Group (Horstad *et al.*, 1995). It was estimated that the NS2 crude oil is from the early generation stage (Table 3.1.1 & A2.6). However, it was found that the crude oil had been "mildly" biodegraded, according to the Volkman *et al.* (1984) scale, with the loss of *n*-alkanes illustrated by reduction of the *n*-C_{18}/Ph ratio from ≥ 1 to 0.20 (Table 3.1.1). However, no reduction in isoprenoid values was observed with the Ph/$C_{30}\alpha\beta$ ratio remaining constant relative to all previous samples except B12 (above). A geological study of the North Sea region in which the NS2 reservoir is located, indicates biodegradation is attributed to the incursion of oxygen rich, meteoric waters (Horstad *et al.*, 1995).

3.1.1.3.6. NS3 Crude Oil.

The NS3 crude oil is also a confidential sample and consequently, location and reservoir names are not given. The NS3 crude oil is produced from a clastic Eocene reservoir in the North Sea petroleum province. Maturity parameters indicate that the NS3 crude oil is mature migrated from the source rock during the early/peak oil generation stages (Tables 3.1.1 & A2.6). Assessment of the biodegradation parameters identifies that the oil is "extensively" degraded, with both *n*-alkanes and isoprenoids being strongly reduced (*n*-C_{18}/Ph & Ph/$C_{30}\alpha\beta$ ratios exhibiting 0 and 5.18, respectively for degraded samples compared to the approximate non-degraded values of 2 and 12, respectively, A2.5). In addition, the source correlation parameter, $C_{27}\alpha\alpha\alpha R/C_{29}\alpha\alpha\alpha R$ ratio (0.53), has been reduced relative to other North Sea crude oil values (approximately 1), indicating possible biodegradation of the $C_{27}\alpha\alpha\alpha R$ regular sterane. An aerobic biodegradation mechanism is considered responsible for the alteration of the NS3 crude oil as investigation has highlighted the passage of oxygen rich, meteoric waters through the NS3 reservoir (Mason *et al.*, 1995).

3.1.1.3.7. H1 Crude Oil.

The Santa Maria Basin crude oil, H1, is produced from the clastic Miocene reservoirs of the Monterey and Point Sal Formations (Taylor, 1994). Maturity analysis indicates that the H1 crude oil is mature and was probably expelled from the source rock during the early and peak oil generation stages (Table 3.1.1). The oil is identified as "non-degraded" with no recognisable alteration to the aliphatic hydrocarbons.

3.1.1.3.8. H7 Crude Oil.

The H7 crude oil is also produced from the clastic Miocene reservoirs of the Monterey and Point Sal Formations (Taylor, 1994) and has also been identified as a mature crude oil (early/peak oil generation stage). However, the H7 crude oil is classified as "moderate-to-extensively" degraded, with extensive reduction of both the n-alkane and isoprenoid groups (both groups are not detected, Table 3.1.1).

3.1.1.3.9. Monterey Crude Oil.

The Monterey crude oil is sourced from the clastic Monterey Formation and is classed a mature crude oil, being expelled from the source rock during the early and peak oil generation stages. Assessment of its biodegradation parameters indicates that the crude oil is probably "mildly" degraded with the *n*-alkanes having been reduced (n-C_{18}/Ph approximately 0.64 compared to 2 for a non-degraded equivalent, Table 3.1.1) however, no alteration is observed for the isoprenoids.

3.2. Experimental.

The experimental procedures used in this chapter are illustrated in Figure 3.2.1.

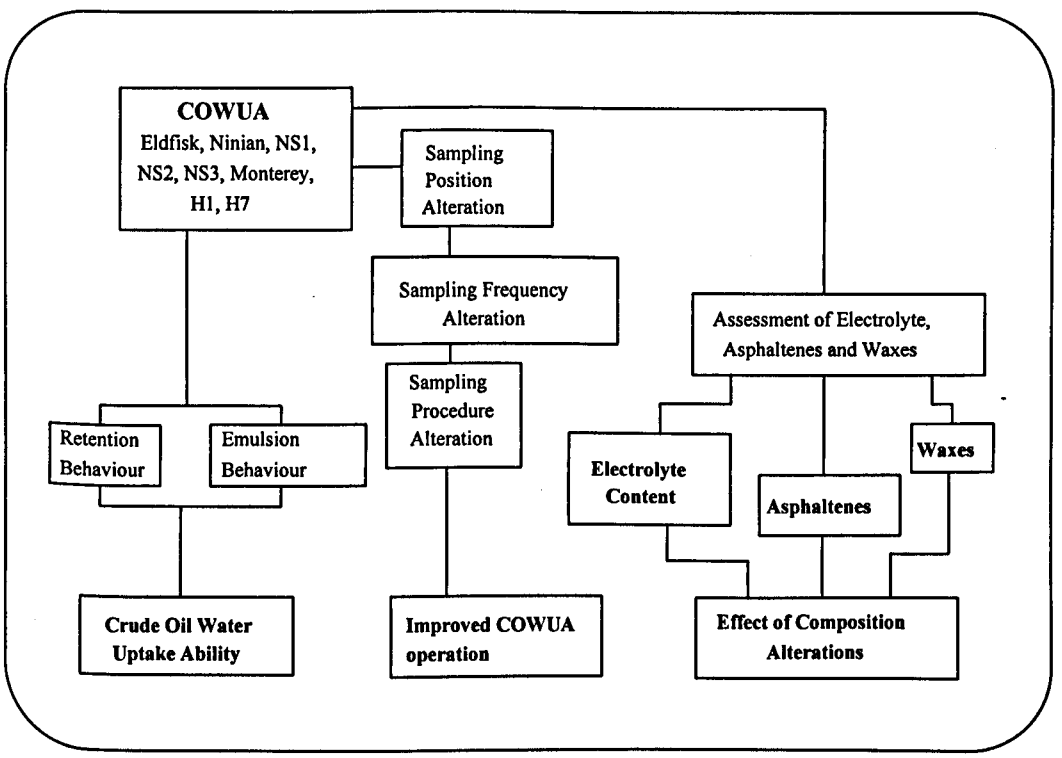

Figure 3.2.1. Experimental procedures used in this chapter.

3.2.1. Crude Oil Water Uptake Analysis.

Initial experiments followed the procedure established in Chapter 2, Section 2.2, in which the water uptake ability of various crude oils was assessed. This procedure, known as Crude Oil Water Uptake Analysis (COWUA), was altered during analysis to improve accuracy and ease of use. Alterations made to the COWUA included those to the sampling position, sampling frequency and sampling procedure.

3.2.1.1. Sampling Position.

The number of sampling positions for the crude oil and water blends was increased to two, since it was quickly realised that one sampling position could not fully characterise the water uptake ability of the crude oil. The ability of crude oil to retain water can be best assessed by measuring the variation of the water content at the top of the blend. The emulsion formation/stabilisation ability of crude oil can be best assessed by measuring the water content at the bottom of the blend as either the emulsion and/or water phase will accumulate there. The sampling positions are illustrated in Figure 3.2.2. If no sampling position is indicated, samples will have been taken from the top of the crude oil/water blend.

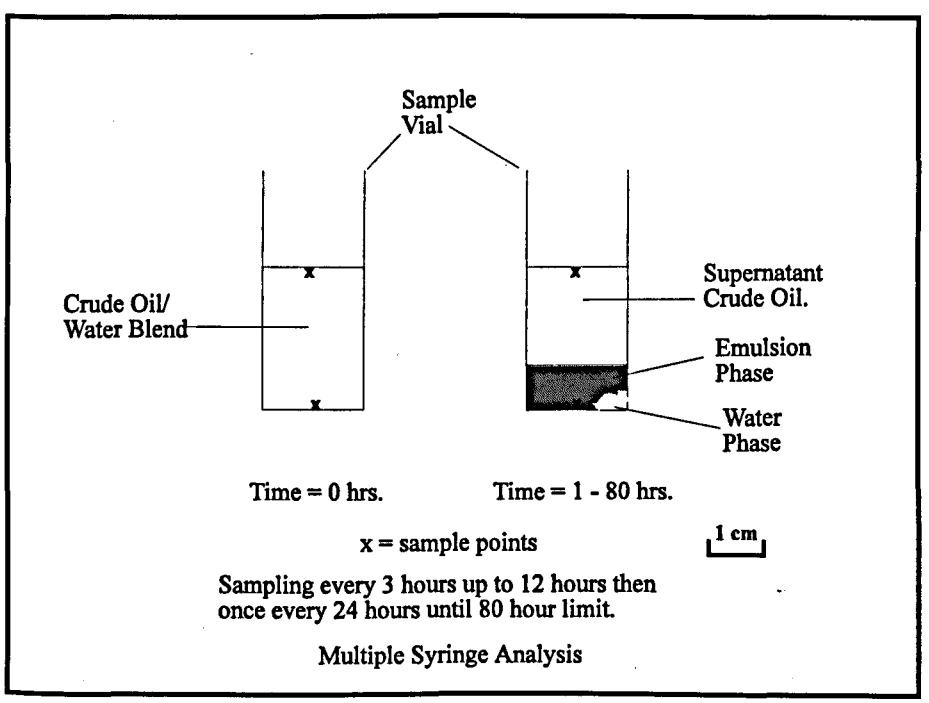

Figure 3.2.2. Illustration of changes to sampling position, sampling frequency and sampling procedure (Sections 3.2.1.1 to 3.2.1.3).

3.2.1.2. Sampling Frequency.

Sampling of each crude oil/water blend was altered from that shown in Table 2.2.1, to a sample every three hours during the first 12 hours, followed by one sample every subsequent 24 hours (Fig. 3.2.2). Sampling ceased approximately 80 hours after the crude oil and water phases had been blended.

3.2.1.3. Sampling Procedure.

Early work found that crude oil/water blends with 5% water contents produced erroneous normalised water percentages (Figs. 3.2.3 & 3.2.4). In Figure 3.2.3, the averaged water sedimentation curves for NS3 crude oil/water blends (5, 10, 20 & 30% water contents), sampled from the top of the blends, may be observed. It may be seen that the blends with 10, 20 & 30% water content exhibit initial normalised water percentage (%R) of approximately 100%R, as expected. However, the averaged water sedimentation curve for the 5% initial water content blend, exhibits initial %Rs of approximately 200%R. The same observations were obtained for the averaged water sedimentation curves for the Eldfisk (A29) crude oil/water blends. In Figure 3.2.4 initial normalised water percentages of approximately 100%R were obtained from crude oil/water blends with 10, 20 and 30% initial water contents. However crude oil/water blends with 5% water contents show normalised water contents of approximately 180%R.

Tests established that the extreme normalised water percentages, seen in Figures 3.2.3 and 3.2.4, were caused by the water contamination of the syringes used for sampling. In Figures 3.2.5 and 3.2.6, it may be seen that initial normalised water percentages of 180%R (Fig. 3.2.5) and 200%R (Fig. 3.2.6) are obtained from crude oil/water blends (NS3 & Eldfisk (A29), respectively) with 5% initial water content, when sampled with "contaminated syringes" (syringes that were previously used to sample blends with high (*e.g.*, 30%) water content) despite cleaning. However, normalised initial water contents of approximately 90%R for the NS3 blend (Fig. 3.2.5) and 100%R for the Eldfisk (A29) blend (Fig. 3.2.6) are obtained when clean sampling syringes were used to sample blends with 5% water contents. Crude oil and water analyses using multiple syringes (one syringe for each water quantity) was found to correct this problem. The initial re-use of syringes was a consequence of the large number of samples being analysed combined with a lack of syringes. The inefficient cleaning of syringes between analyses was a direct result of the initial high sampling rate. The water sedimentation curves for both NS3 and Eldfisk crude

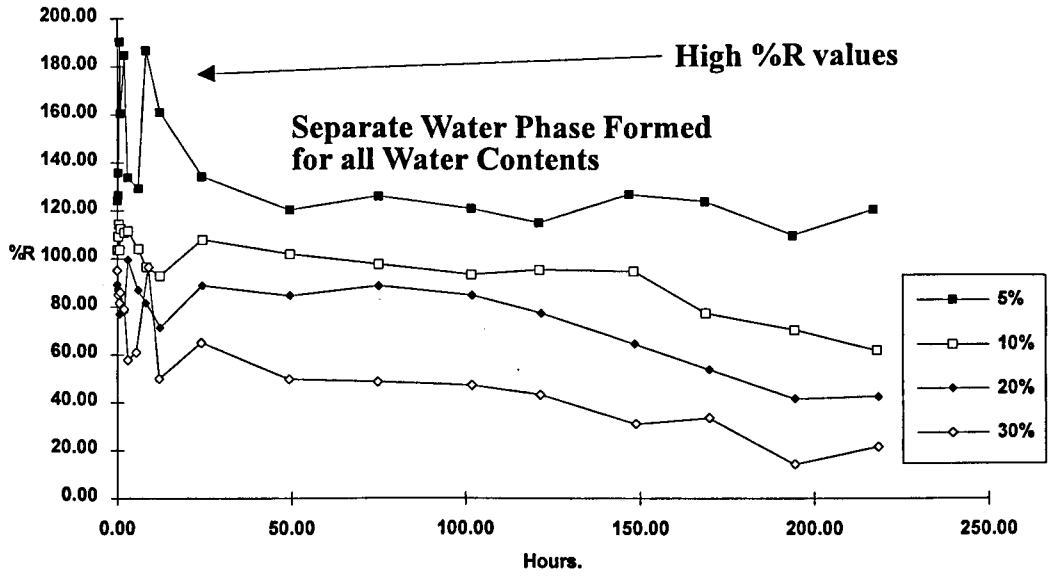

Figure 3.2.3. Averaged sedimentation curves for NS3/water blends with initial water content of 5%, 10%, 20% and 30%. It may be seen that the %R readings for the 5% water content sample are high.

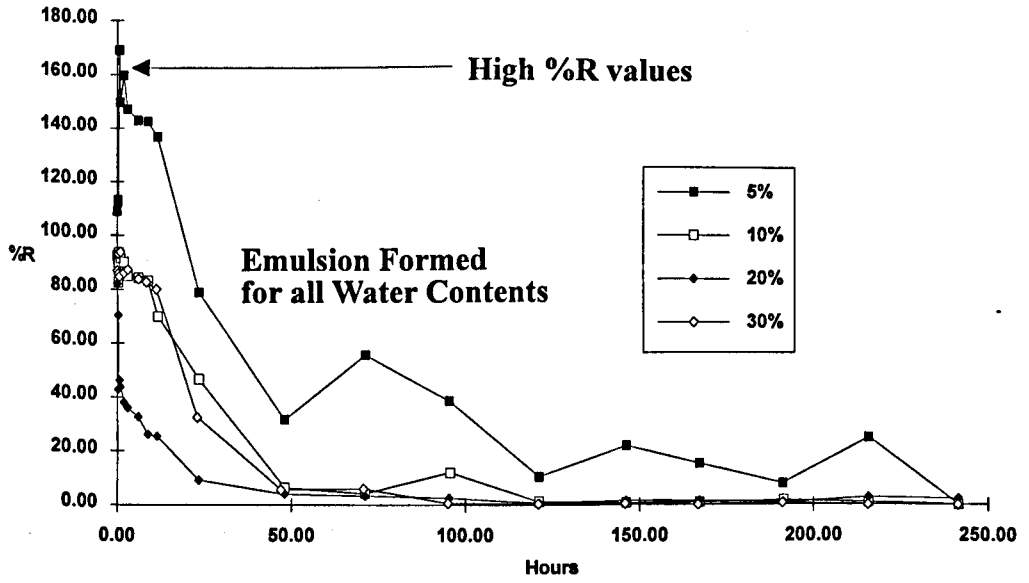

Figure 3.2.4. Averaged sedimentation curves for Eldfisk/water blends with initial water content of 5%, 10%, 20% and 30%. It may be seen that the %R readings for the 5% water content sample are high.

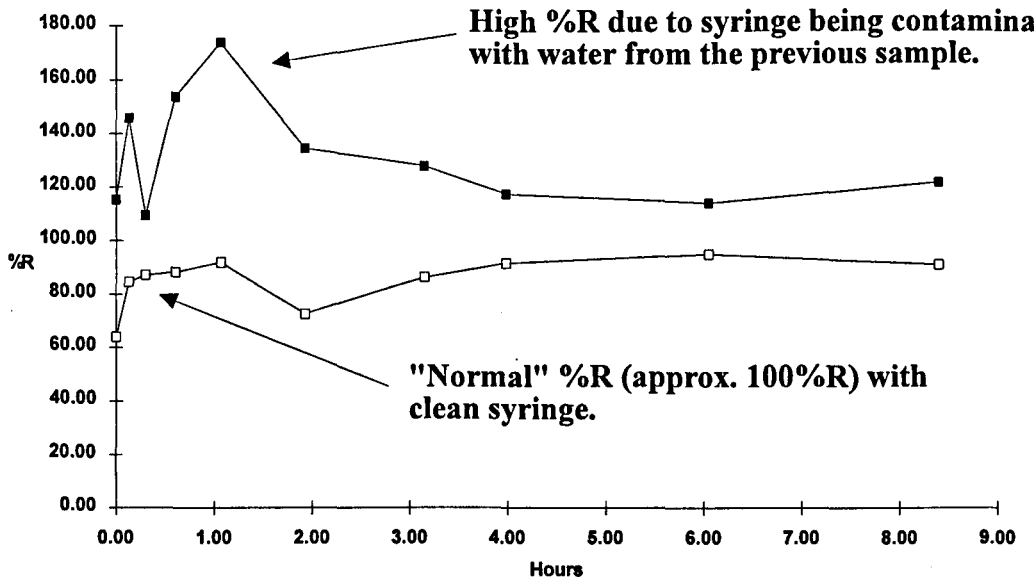

Figure 3.2.5. Effect of syringe contamination on NS3/water blends with 5% water content.

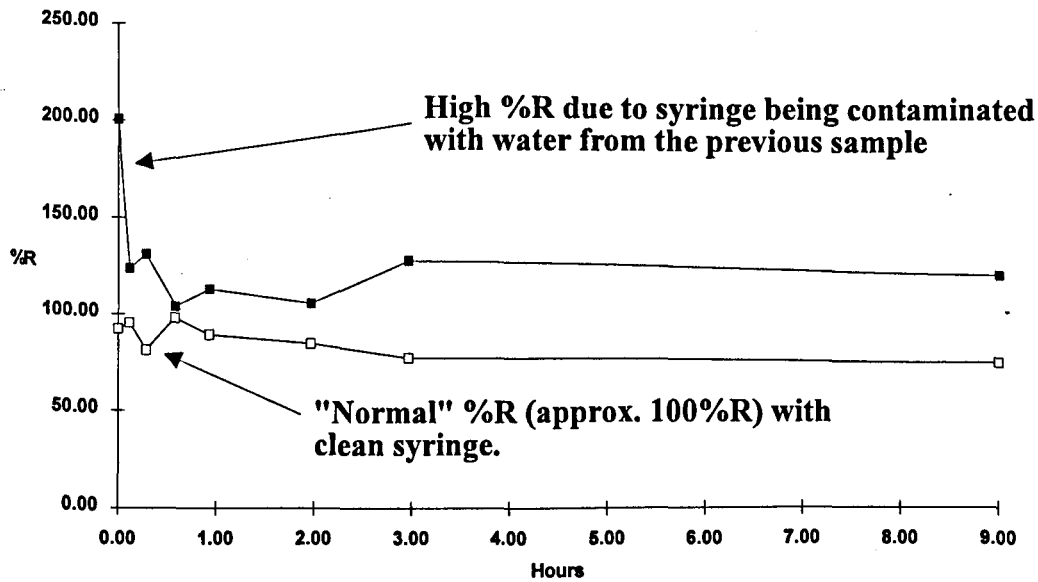

Figure 3.2.6. Effect of syringe contamination on Eldfik/water blends with 5% water content.

oil/water blends were therefore corrected using the multiple syringe sampling procedure, results being illustrated in Figures 3.2.7 and 3.2.8 respectively (these water sedimentation curves will be discussed in Section 3.3.1).

3.2.2. Emulsion Analysis.

Emulsions, produced during crude oil and water blending, were characterised by Freeze-Fracture Replication (FFR) and transmission electron microscopy (Robards & Sleytr, 1985; Wilson, 1989). This process, highlighted in Figure 3.2.9, characterised the emulsion by rapidly freezing it in "slushed" nitrogen (a part liquid part solid mixture which prevents bubble formation around the emulsion), fracturing the frozen emulsion and then evaporating a Pt/C mix onto the fractured surface. The Pt/C mixture formed a replica of the fractured surface of the emulsion. The replica was then viewed with a transmission electron microscope (TEM), allowing visual characterisation of the state of the emulsion (i.e., oil-in-water or water-in-oil).

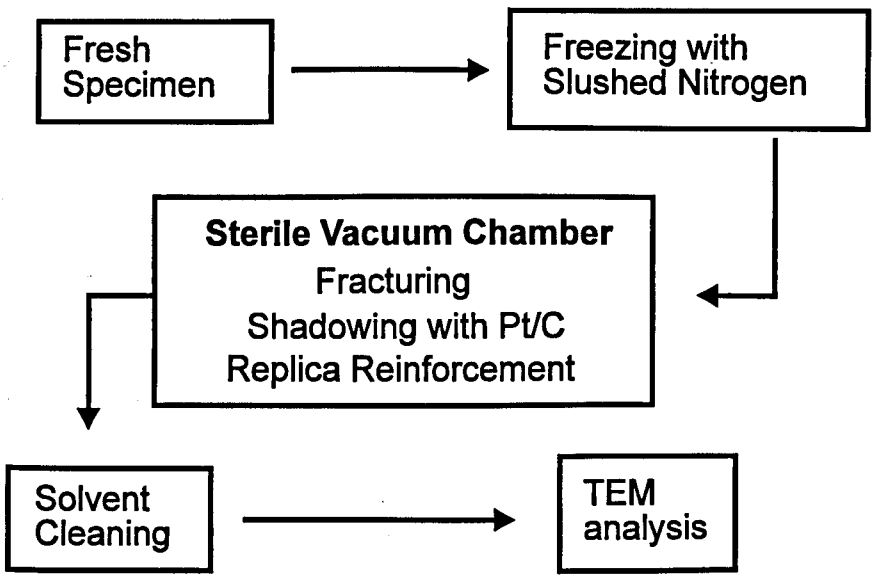

Figure 3.2.9. Method of Freeze-Fracture Replication (FFR) used to identify emulsion type (Wilson, 1989).

3.2.3. Alteration of Asphaltene Content.

Asphaltenes were isolated from the Monterey crude oil by using the following procedure. Approximately 1 g of crude oil was dissolved in 1 ml of dichloromethane (DCM), before adding a forty fold excess of *n*-heptane (*i.e.*, ≈ 40 ml). The liquid was

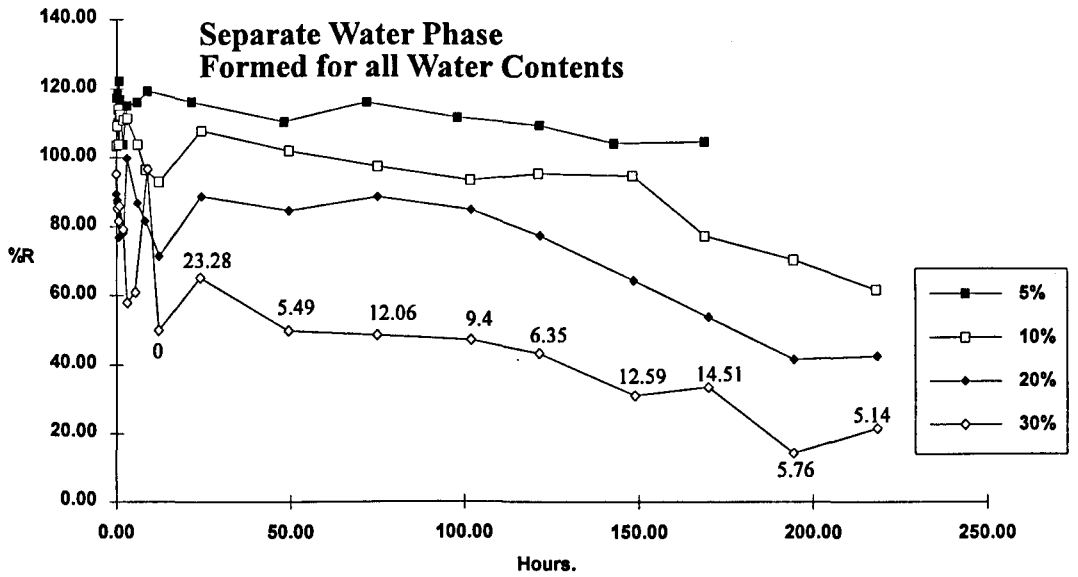

Figure 3.2.7. Corrected average sedimentation curves for NS3/water blends with initial water content of 5%, 10%, 20% and 30%. Standard deviation for 30% water content blend are reported where possible. Statistical data for all sedimentation curves is given in Appendix 3, Tables A3.4a and A3.4b.

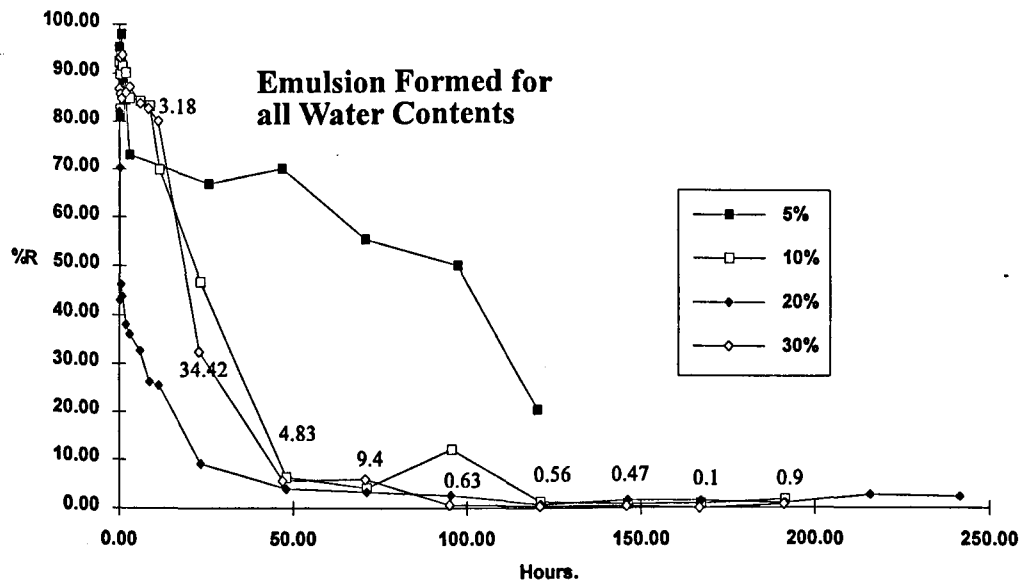

Figure 3.2.8. Corrected average sedimentation curves for Eldfisk/water blends with initial water content of 5%, 10%, 20% and 30%. Standard deviation for 30% water content blend are reported where possible. Statistical data for all sedimentation curves is given in Appendix 3, Tables A3.1a and A3.1b.

stirred for 30 minutes before being left to stand for between 8 and 12 hours, to allow the precipitate to settle out. The contents were then filtered through a sinter funnel (grade 4) to collect the maltene fraction. The asphaltene precipitate was retrieved by washing it through the sinter funnel, into a separate flask, with DCM:methanol (93:7). This precipitation process was then performed twice more on the collected maltene fraction before the maltene and asphaltene fractions were concentrated by rotary evaporation, transferred to vials, evaporated to dryness and weighed.

A series of "oils" of varying asphaltene content was prepared by mixing separated asphaltenes and maltenes in different proportions. Blending was achieved by mixing the two fractions, with their respective solvent systems (maltenes = heptane solution; asphaltenes = DCM/MeOH (93:7) solution), to the relevant ratio, and then evaporating off the solvent by use of a rotary evaporator.

Experiments were carried out for these reconstituted crude oils with asphaltene content of 20, 10, 5 & 0%. These reconstituted "crude oils" were blended with distilled water to give an initial added water content of 10% and analysed immediately by COWUA (Chapter 2). These blends were compared with standard Monterey crude oil/water blends, also with 10% initial added water content, in which the composition of the crude oil had not been altered. The normalised water contents were plotted against time from blending in the standard manner.

3.2.4. Wax Addition.

The waxes used for these experiments were octadecane 97% (*n*-C_{18}, MP 29-30°C: Aldrich) and tetracosane (*n*-C_{24}, MP 49-51°C: FLUKA) standards. The waxes were added (between 0.4 & 1.8wt%) to NS3 crude oil after first being melted, and then poured into the crude oil. This mix was then gently heated (30°C) to prevent the wax from solidifying. The crude oil and wax mix was then blended with an Ultra-Turrax disperser and S25N-10G VS dispersion tool, at approximately 9,000 RPM for 1 minute. The crude oil and wax blend was then heated gently, at approximately 30°C for 5 minutes, to aid mixing. The blends were then homogenised with distilled water to give an added water content of 30% (this procedure is described in Sections 2.2.4.2 & 2.2.4.3). All samples were visually monitored for the formation of any separate water layers with time from blending. Results were compared to unaltered NS3 crude oil and distilled water blends, also with 30% added water contents.

3.2.5. Blending Crude Oil with Synthetic Seawater.

A synthetic seawater solution was prepared and used for these experiments. The synthetic seawater had a pH of approximately 8 and a total electrolyte concentration of approximately 36 gl^{-1} (3.6wt% of the aqueous phase). The solution contents are listed in Table 3.2.1. Most crude oils in the sample set were blended with the synthetic seawater to an initial added water content of 30%. All blended samples were analysed by COWUA (Sections 2.2 & 3.2.1) and the results plotted against time from blending.

COMPONENTS	GRAMS/LITRE	N(mol/l)
NaCl	27.9809	$4.788 * 10^{-1}$
$MgCl_2$	3.7768	$3.97 * 10^{-2}$
$CaSO_4$	1.4607	$1.0729 * 10^{-2}$
$MgSO_4$	1.8059	$1.5011 * 10^{-2}$
K_2SO_4	0.6108	$3.505 * 10^{-3}$
$NaHCO_3$	0.1744	$2.08 * 10^{-3}$
KCl	0.1499	$2.01 * 10^{-3}$
TOTAL	35.9594	

Table 3.2.1. Synthetic seawater electrolyte composition.

3.3. Results.

The assessment of the water uptake ability of crude oil may be divided into two parts; the water retention ability of crude oil and the ability of crude oil to form stable emulsions. The ability of crude oil to retain water can be best assessed by measuring the variation of the water content at the top of the blends. The emulsion formation/stabilisation ability of crude oil can be best assessed by observation of blend alterations (such as emulsion and/or water separation) as well as measuring the water content at the bottom of the blend where the separating fractions (emulsion and/or water) will accumulate. These results are followed by analysis of the effects upon the water uptake ability of crude oils by; 1) altering the asphaltene content of crude oils, 2) wax additions to the crude oil, and 3) alteration of the electrolyte content of the aqueous phase.

3.3.1. Water Uptake Analysis - Water Retention.

Water retention analyses were performed for eight crude oils from the two petroleum provinces, *i.e.*, the North Sea and Santa Maria Basin. Table 3.3.1, summarises a water retention classification (based on 30% added water) obtained for each crude oil. The table also lists other water additions (5,10 & 20%) made for each oil, as well as the number of analyses made for each addition (represents number of analyses which were averaged for water sedimentation curves). The measured normalised water percentage (%R), for each water addition, are plotted against time from blending and displayed as water sedimentation curves. Even though water retention classification is based upon the 30% water addition only, sedimentation curves for other water additions (5,10 & 20%) are reported when used, in order to aid classification.

Crude Oil	Origin (API°) and degree of Biodegradation*	Water Additions (%)	Analyses per Water Addition	Water Retention Class**
Eldfisk (A29)	North Sea (35°), Non-degraded (1)	5, 10, 20, 30	4	Poor
Ninian	North Sea (35°), Non-degraded (1)	5, 10, 20, 30	2	Poor
NS1	North Sea (28°), Non-degraded (1)	30	2	Poor
NS2	North Sea (29°), Mild degradation (2)	30	2	Poor
NS3	North Sea (14°), Extensive degradation (6)	5, 10, 20, 30	4	Good
Monterey	Californian (22°), Mild degradation (2)	5, 10, 20, 30	4	Moderate
H1	Californian (25°), Non-degraded (1)	30	2	Poor
H7	Californian (24°), Moderate-extensive degradation (5)	30	2	Moderate

*Table 3.3.1., Water retention classification of crude oils analysed (Good, Moderate, Poor, ** = classifications based on 30% added water, are described in Table 3.3.2 as well as Section 2.2.5.4 & Fig. 2.2.13), water additions analysed and the number of analyses per water addition. Statistical data for 30% added water blends is reported when possible on sedimentation curves. All statistical data is reported in Appendix 3, Tables A3.1 to A3.6.* = Volkman et al. (1984) scale of biodegradation was used and the relevant scale numbers are bracketed (classification is described in Section 6.1 & Table 6.1.2).*

The average water sedimentation curves obtained from the Crude Oil Water Uptake Analysis (COWUA) of the Eldfisk crude oil and water blends (5, 10, 20 & 30% added water), sampled from the top of the crude oil/water blends, are illustrated in Figure 3.2.8. It may be seen that crude oil/water blends with 5% water contents, display a slower sedimentation rate than the other added water quantities (10, 20 & 30%). The normalised water content (%R) for the 5% added water blends went from approximately 100%R to 40%R in 100 hours (equivalent to the "good to moderate" boundary, defined in Table 3.3.2). However, the sedimentation curves for the crude oil/water blends with 10, 20 & 30% added water content were indicative of a crude oil with a "poor" water retention ability (normalised water contents (%R) dropping to 40%R or less before 50 hours). According to the water retention classification (based on 30% added water), the crude oil water retentive ability of the Eldfisk (A29) crude oil, when blended with water, was classed as "poor". An emulsion phase (sediment) was observed for all Eldfisk crude oil/water blends from approximately 24 hours onwards.

Water Retention Category	Definition
Poor	Normalised water content (%R) dropping from 100%R to 40%R, or less, before 50 hours
Moderate	Normalised water content (%R) dropping from 100%R to 40%R, or less, during 50 to 100 hours.
Good	Normalised water content (%R) maintained between 100%R and 40%R for 100 hours.

Table 3.3.2. Definition of the water retention categories based upon the 30% added water content. Further explanation is given in Section 2.2.5.4 and Figure 2.2.13.

Figure 3.3.1 displays the averaged water sedimentation curves for the Ninian crude oil and water blends (5, 10, 20 & 30% added water content). The sedimentation curve for the 5% water content blend is unreliable (due to high initial %Rs) and was attributed to sampling problems (Section 3.2.1.3) however, due to the limited sample available the curve is reported. In view of the unreliability of the 5% water content blend, the water retentive character of the Ninian crude oil is assessed from the crude oil/water blends with 10, 20 & 30% water contents only. The water sedimentation curves for the different water contents are very similar. The normalised water percentages dropped from 125%R to 10%R in less than 50 hours, a dropout rate indicative of a crude oil which exhibits a "poor" water retention ability when blended with water. Therefore, the Ninian crude oil is classed as having "poor" water retention ability.

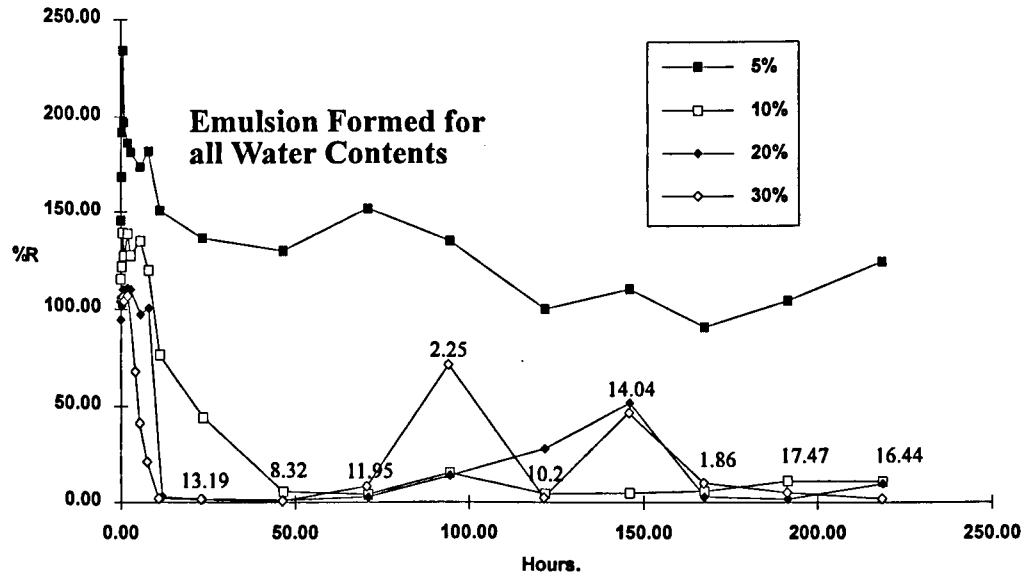

Figure 3.3.1. Averaged sedimentation curves for Ninian/water blends with initial water content of 5%, 10%, 20% and 30%. +/- errors for 30% water content blend are reported where possible. Statistical data for all sedimentation curves is given in Appendix 3, Tables A3.2a and A3.2b.

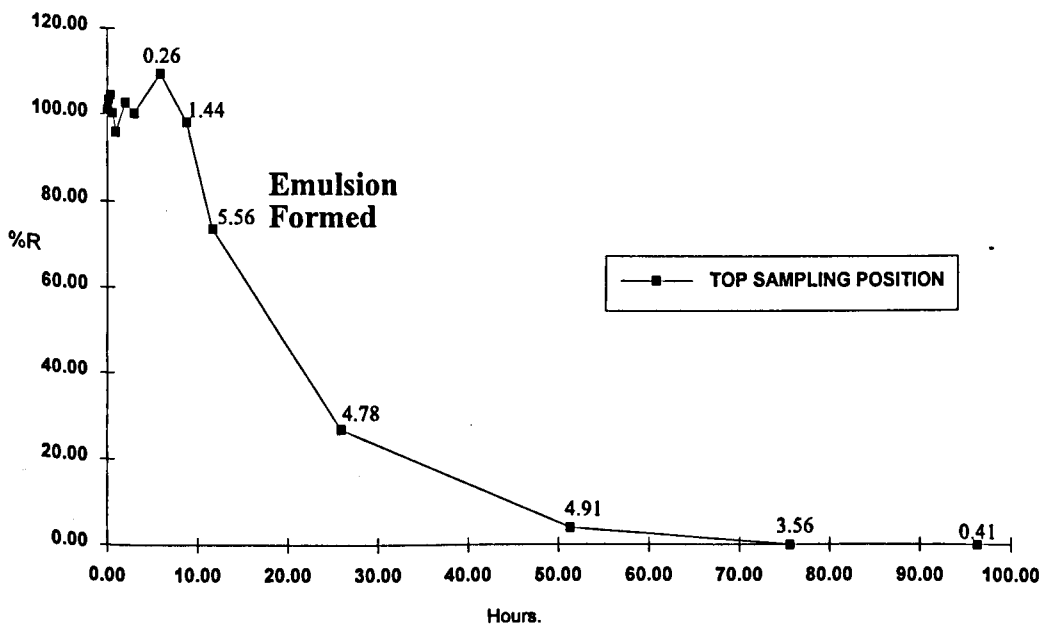

Figure 3.3.2. Averaged sedimentation curves for NS1/water blends with initial water content of 30%. Sampling positions are illustrated in Figure 3.2.2. +/- errors for 30% water content blend are reported where possible. Statistical data for all sedimentation curves is given in Appendix 3, Tables A3.3..

Assessment of the averaged water sedimentation curve for the NS1 crude oil/water blends (Fig. 3.3.2), with 30% added water content, found that the normalised water percentages dropped rapidly from approximately 100%R to less than 10%R in the first 50 hours. The NS1 crude oil is therefore classed as exhibiting "poor" water retentive ability.

The averaged water sedimentation curves for the NS2 crude oil/water blends, with 30% initial added water content, in Figure 3.3.3, were obtained from samples taken from both the top and bottom of the blends. These sampling positions are illustrated in Figure 3.2.2. The samples taken from the top of the crude oil/water blend indicated that the NS2 crude oil exhibited "poor" water retention, with normalised water percentages dropping from approximately 100%R to 25%R in less than 50 hours. The samples taken from the bottom of the crude oil/water blend display normalised water percentage readings which, after 10 hours, increase from 100%R to approximately 210%R, at 50 hours. As well as some emulsification, the formation of a separate water layer, at the base of the crude oil/water blend, was also observed.

The averaged water sedimentation curves (Fig. 3.2.7) for the NS3 crude oil/water blends (5%, 10%, 20%, 30% added water content), from samples taken from the top of the crude oil/water blend, highlight that the crude oil displays "good" water retention ability (constant normalised water content value of between 100%R and 40%R from 0 to 100 hours; Table 3.3.2 & Fig. 2.2.13). In Figure 3.2.7 it may be seen that all averaged water sedimentation curves, except for the crude oil/water blends with 30% water content, maintained 40%R or more throughout the entire analytical period.

The averaged sedimentation curves for the Monterey crude oil/water blends (5%, 10%, 20%, 30% initial added water contents), illustrated in Figure 3.3.4, show that all blends are indicative of crude oils with "moderate" water retention ability (normalised water percentages (%R) dropping to 40%R or less in 50 to 100 hours of analysis; Table 3.3.2 & Fig. 2.2.13) when blended with water. The initial normalised water contents for the 5% added water content blend was high, but within analytical error (standard deviation reported in Appendix 3, Table A3.5a), peaking at 130%R during the first 12 hours of analysis.

The H1 crude oil/water blend, with initial 30% added water content, was sampled from both the top and bottom of the blend. Results, displayed in Figure 3.3.5, demonstrate that samples from the top of the blend indicate that the H1 crude oil has a "poor" water retentive ability when blended with water. The normalised water content dropped from approximately 100%R to 0%R in less than 50 hours. Assessment of the samples from the bottom of the crude oil/water blend found that the normalised water

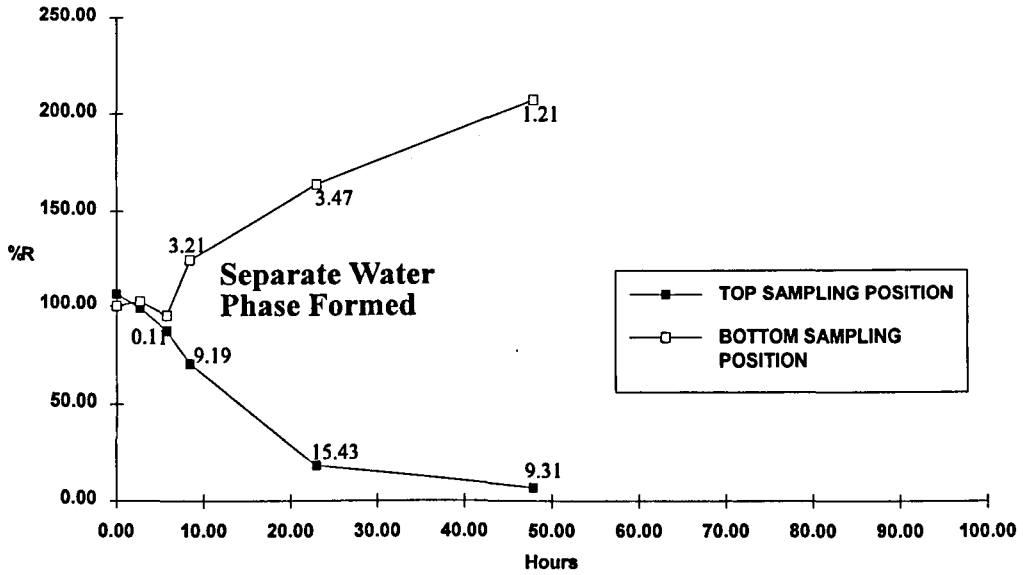

Figure 3.3.3. Averaged sedimentation curves for NS2/water blends with initial water content of 30%. Sampling positions are illustrated in Figure 3.2.2. +/- errors for 30% water content blend are reported where possible. Statistical data for all sedimentation curves is given in Appendix 3, Tables A3.3..

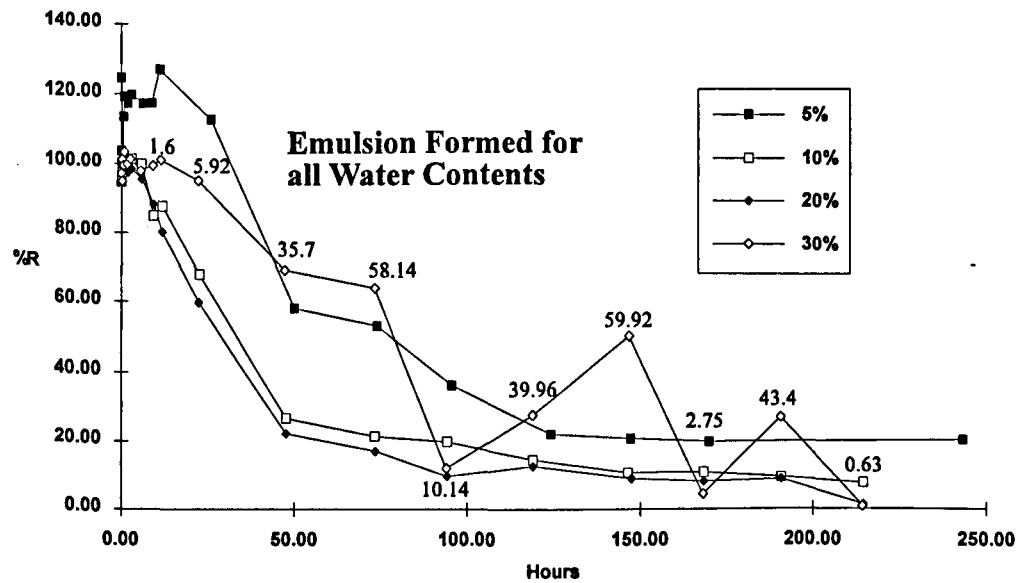

Figure 3.3.4. Averaged sedimentation curves for Monterey/water blends with initial water content of 30%. Standard deviations for 30% water content blend are reported where possible. Statistical data for all sedimentation curves is given in Appendix 3, Tables A3.5a and A3.5b.

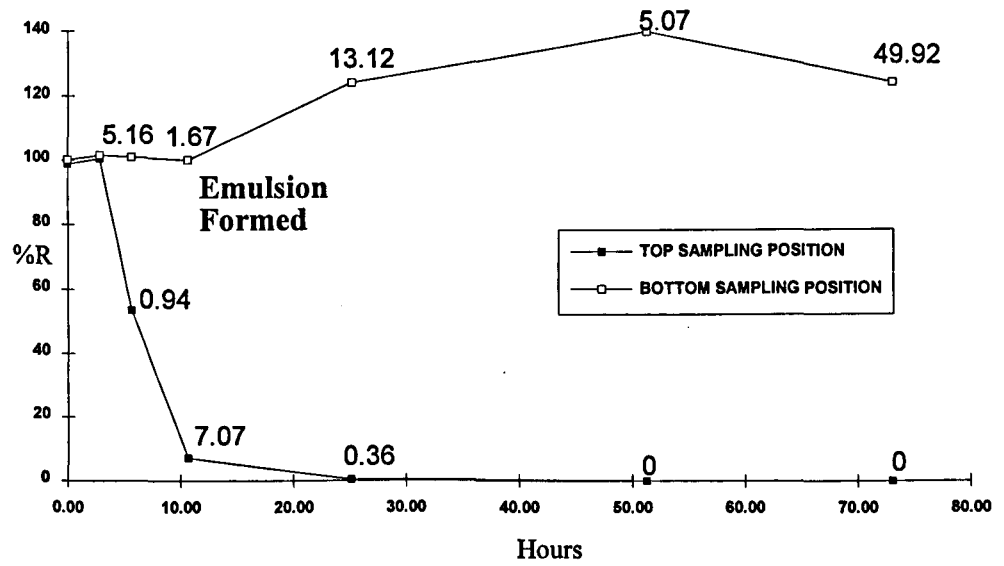

Figure 3.3.5. Averaged sedimentation curves for H1/water blends with initial water content of 30%. Sampling positions are illustrated in Figure 3.2.2. +/- errors for 30% water content blend are reported where possible. Statistical data for all sedimentation curves is given in Appendix 3, Tables A3.6.

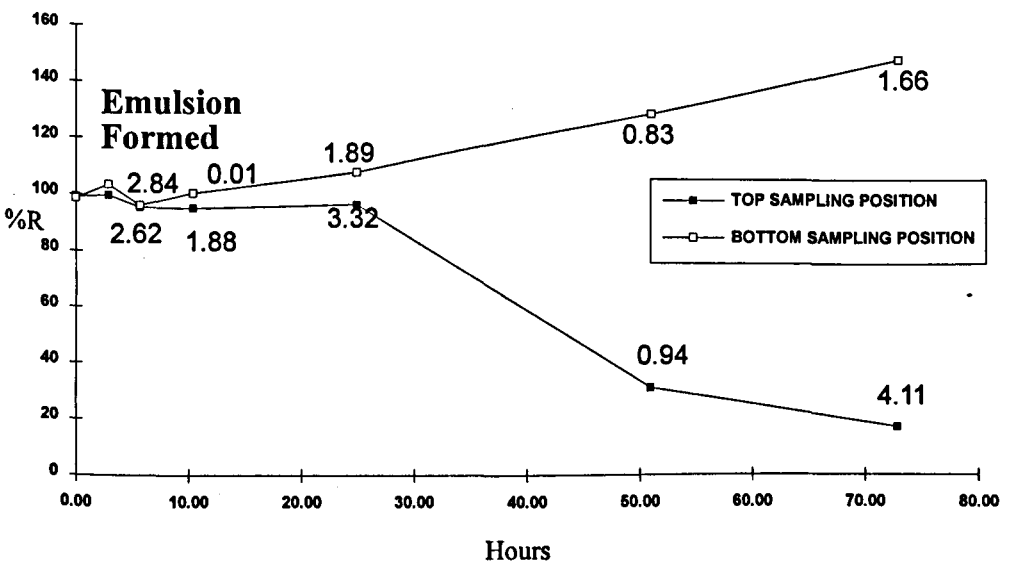

Figure 3.3.6. Averaged sedimentation curves for H7/water blends with initial water content of 30%. Sampling positions are illustrated in Figure 3.2.2. +/- errors for 30% water content blend are reported where possible. Statistical data for all sedimentation curves is given in Appendix 3, Tables A3.6.

percentage, after the initial 10 hours, increased from 100%R to approximately 130%R after 50 hours, and is associated with the formation of an emulsion.

The water sedimentation curve for the H7 crude oil/water blends, with initial added 30% water content, is displayed in Figure 3.3.6 and is seen to be on the boundary between "poor" and "moderate" water retention. It is assumed that all blends with water contents less than 30% would have been characterised by "moderate" water retention. This characteristic has been observed for Eldfisk, Ninian & NS3 crude oil/water blends (5, 10, 20 & 30% added water) where the 30% water additions exhibited the fastest water dropout, followed by the 20% water addition, 10% water addition and finally the 5% water addition, which displayed the slowest water sedimentation (Figs. 3.2.8, 3.3.1 & 3.2.7). Therefore, the overall water retentive character for H7 crude oil is classed as "moderate" when blended with water. Assessment of the samples from the bottom of the crude oil/water blend found that the normalised water percentage, after the initial 10 hours, increased from 100%R to approximately 140%R after 50 hours and is associated with the formation of an emulsion.

3.3.2. Water Uptake Analysis - Emulsion Formation/ Stabilisation.

Examination of the crude oil/water blends during analysis showed that the blends altered (possibly within the first few hours of analysis) from homogenised crude oil/water blends to fractionated samples, containing a supernatant oil with either an emulsion phase (also referred to as "emulsion sediment" in later chapters) or water layer, or combination of both, below the supernatant oil. This alteration is schematically illustrated in Figures 3.2.2 and 2.2.9, and discussed in Section 2.2.5.3. All crude oil/water blends were found to form supernatant oil layers, but the appearance of the emulsion and/or water layer, was variable (Table 3.3.3).

Crude Oil	Origin (API°) and degree of Biodegradation*	Water-in-Oil (W/O) Emulsion.
Eldfisk	North Sea (35°), Non-degraded (1).	Forms viscous W/O emulsion
Ninian	North Sea (35°), Non-degraded (1).	Forms viscous W/O emulsion
Kittiwake**	North Sea (28°), Non-degraded (1).	Forms viscous W/O emulsion
NS1	North Sea (28°), Non-degraded (1).	Forms viscous W/O emulsion
NS2	North Sea (29°), Mild degradation (2).	Forms both W/O emulsion and water layer
NS3	North Sea (14°), Extensive degradation (6).	Separate Water Layer
Monterey	California (22°), Mild degradation (2).	Forms viscous W/O emulsion
H1	California (25°), Non-degraded (1).	Forms viscous W/O emulsion
H7	California (24°), Moderate-extensive degraded (5).	Forms viscous W/O emulsion

*Table 3.3.3. The ability of crude oils to form stable emulsions. * = degree of biodegradation characterised by the Volkman et al. (1984) scale (Chapter 6). The relevant scale numbers are bracketed. ** = not assessed for water retention.*

The emulsions formed during COWUA were analysed by Freeze-Fracture Replication (FFR) to identify whether the emulsion type was either water-in-crude oil or crude oil-in-water. In Picture 3.3.1 (a TEM photograph of an emulsion from a Ninian crude oil/water blend), a water droplet, approximately 3 μm in size, is surrounded by a dispersive crude oil phase (the crude oil was distinguished by its "rough, irregular" appearance. Wilson *pers com.,* 1992). The emulsion is therefore a water-in-crude oil type, *i.e.*, water dispersed in a crude oil medium. Picture 3.3.2 illustrates the different emulsion formation/stabilisation ability of four of the crude oils analysed.

The crude oils which formed water-in-oil emulsions, when blended with distilled water, were Eldfisk, Ninian, Kittiwake, NS1, Monterey, H1 and H7. The emulsion layers were visible in the first 24 hours (a more exact time cannot be reported as initial emulsion formation time was variable and difficult to spot, however emulsions were clearly visible after 24 hours for the crude oils mentioned above).

Picture 3.3.1. A transmission electron microscope (TEM) photograph of a Freeze-Fracture Replication (FFR) from a crude oil (Ninian)/water blend. The circular object at the centre of the picture represents a water droplet (approximately 3 μm diameter) and is surrounded by a dispersive crude oil medium. The blend is therefore identified as a water-in-oil emulsion. Arrows depict laminations in the crude oil phase. Photograph courtesy of Ashley Wilson.

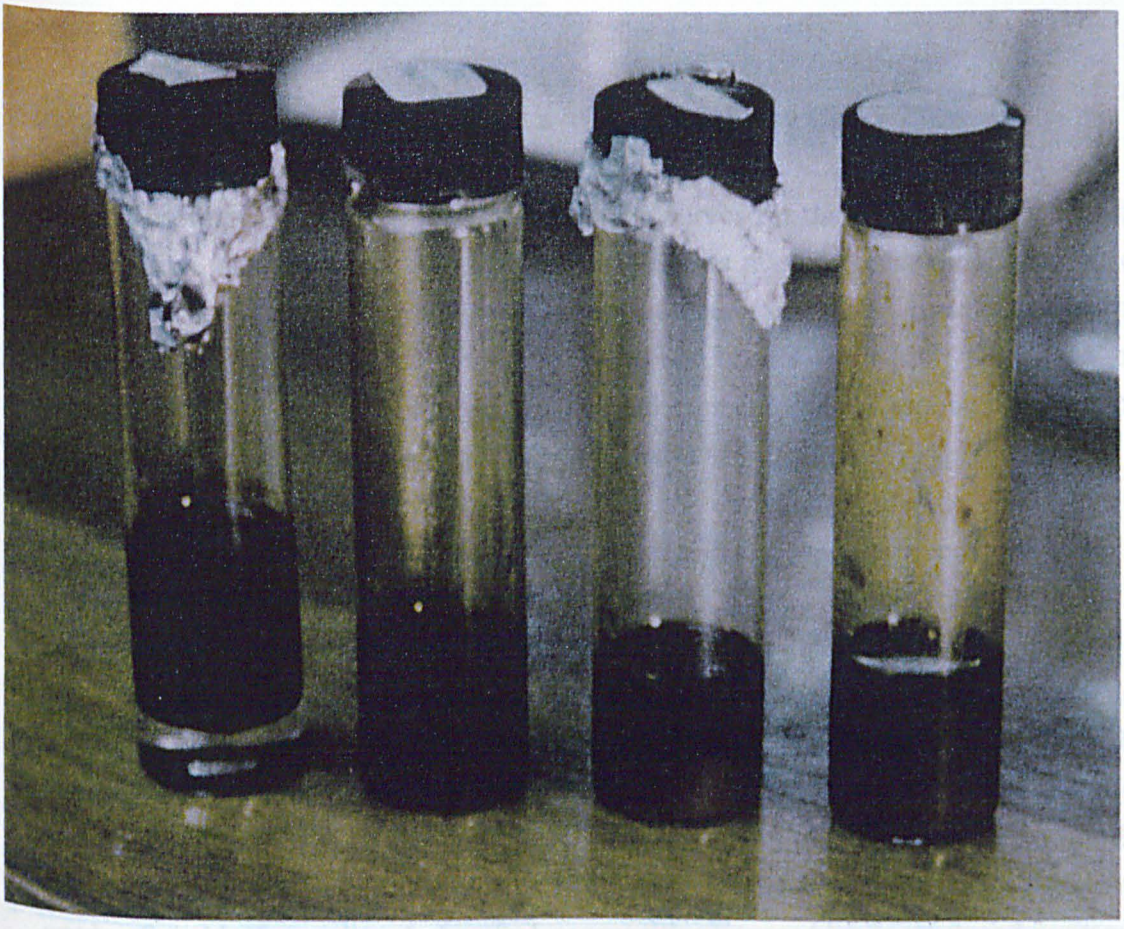

Picture 3.3.2. Photograph illustrating the variable emulsion formation/stabilisation ability of North Sea crude oils. Crude oil/water blends for non-degraded oils, vials A, B, & C, have formed stable water-in-oil emulsions (see Picture 3.3.1). The crude oil/water blend for biodegraded crude oil, vial D, has not emulsified, producing a separate water layer.

The crude oil which formed a separate water phase but no emulsion, when blended with distilled water, was the NS3 crude oil. NS3 blends frequently displayed a separate water phase within 1 hour of blending.

The crude oil which formed both water-in-oil emulsion and separate water phases, when blended with water, was the NS2 crude oil.

3.3.3. Effect of Asphaltene Content on Water Uptake by Crude Oils.

In Figure 3.3.7, the water sedimentation curves for the crude oil/water blends, whose crude oils have had their asphaltene contents altered (containing 0, 5, 10 or 20% asphaltene content) are compared to an averaged (average of five sedimentation curves) sedimentation curve for crude oil/water blends, in which the crude oil compositions are unaltered (Monterey crude oil containing 10% asphaltene content). All the crude oil/water blends contain 10% added water content.

It may be seen in Figure 3.3.7 that all the crude oil/water blends with reconstituted crude oil compositions, except the 20% asphaltene content sample, produced sedimentation curves indicative of "poor" water retention ability (normalised water content (%R) dropping to 40%R or less before 50 hours). The reconstituted crude oil sample with 20% asphaltene content, produced crude oil/water blends with sedimentation curves indicative of "good" water retention ability (the sedimentation curve remains above 40%R from 0 to 100 hours). The %R value of approximately 220%R, at 50 hours, is considered to be unreliable and is possibly the result of sampling a water droplet inside the crude oil/water blend. The Monterey crude oil (with the unaltered chemical composition)/water blends produced averaged sedimentation curves showing "poor" water retention (normalised water contents dropping to 40%R or less in 50 to 100 hours).

3.3.4. Effect of Wax Addition on Water Uptake.

The influence of wax addition on crude oil emulsification behaviour was tested on an oil (NS3) which did not emulsify (any subsequent emulsification being attributed to wax addition). The resultant effects of octadecane (n-C_{18}) additions (0.4wt%, 0.9wt% or 1.8wt%) on crude oil emulsion formation/stabilisation ability are schematically illustrated in Figure 3.3.8. It is seen that different degrees of emulsion formation/ stabilisation resulted from the additions of octadecane. The original NS3 crude oil and water blend, with an initial added 30% water content, formed a separate

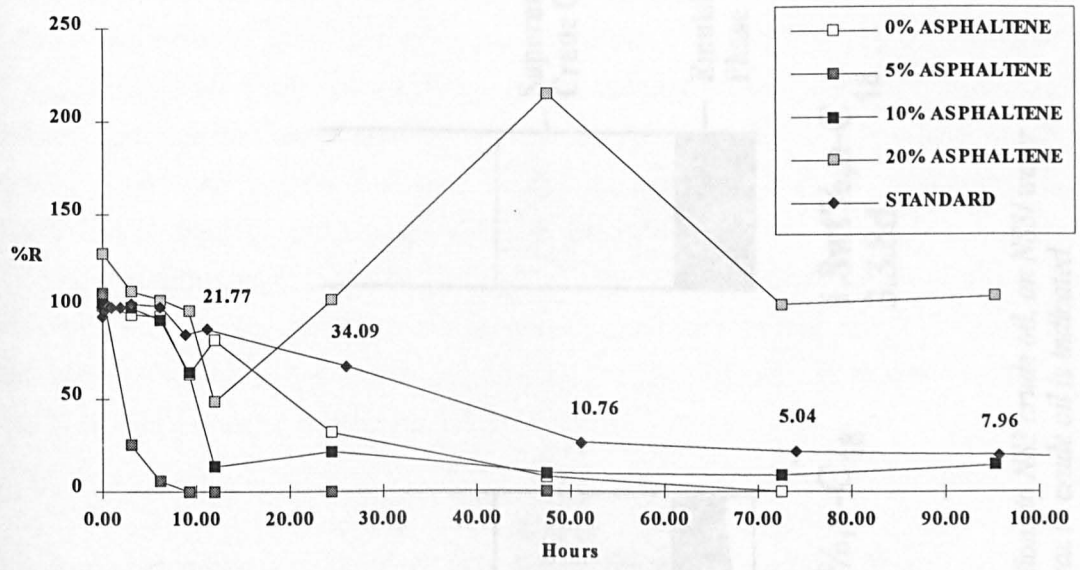

Figure 3.3.7. Water sedimentation curves for Monterey water blends with 10% water contents. The four blends which have had their asphaltene contents altered to 0%, 5%, 10% and 20% asphaltene content are labelled accordingly. The one blend which contains an unaltered crude oil composition is labelled "standard". The standard deviation of the unaltered blend is reported where possible, unreported standard deviation values are listed in Appendix 3, Table A3.5a.

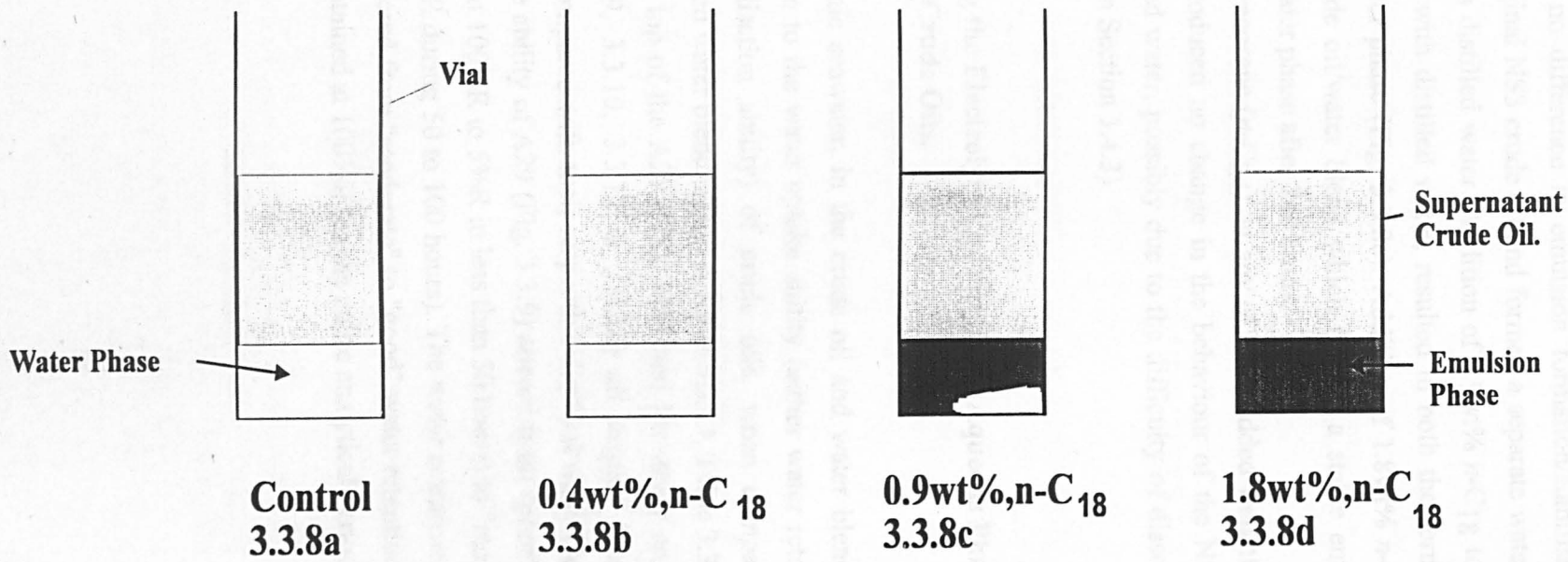

Figure 3.3.8. Schematic illustration of the effect of n-C_{18} wax additions to NS3 crude oil, on NS3/ water blends with 30% water content. Weight percent (wt%) of added wax in crude oil is indicated.

water phase with no emulsion (Fig. 3.3.8a). Addition of 0.4wt.% of octadecane to an NS3 crude oil sample (which was then blended with distilled water to give a water content of 30%) showed no difference in emulsion formation/stabilisation ability when compared to the original NS3 crude oil and formed a separate water layer (Fig. 3.3.8b) when blended with distilled water. Addition of 0.9wt% *n*-C_{18} to NS3 crude oil, followed by blending with distilled water, resulted in both the formation of an emulsion and separate water phase (Fig. 3.3.8c). Addition of 1.8wt% *n*-C_{18} to NS3 crude oil, produced a crude oil/water blend which formed a stable emulsion (Fig. 3.3.8d) with no separate water phase after 240 hours.

The addition of tetracosane (*n*-C_{24}), at any of these added weight percents, to NS3 crude oil samples produced no change in the behaviour of the NS3 crude oil when blended with distilled water, possibly due to the difficulty of dissolving *n*-C_{24} in the bulk oil (discussed in Section 3.4.3).

3.3.5. Effect of Increasing the Electrolyte Content of the Aqueous Phase upon the Water Uptake Ability of Crude Oils.

The use of synthetic seawater, in the crude oil and water blends, generally resulted in some alteration to the water uptake ability (either water retention and/or emulsion formation/stabilisation ability) of crude oils, when compared to their respective crude oil/distilled water blends (Figs. 3.3.9 to 3.3.13, Table 3.3.4).

Samples from the top of the A29, NS1, NS3 and Monterey crude oil/saline water blends (Figs. 3.3.9, 3.3.10, 3.3.12 & 3.3.13) all display increased water retention abilities when compared with their respective distilled water blends (Section 3.3.1). The water retentive ability of A29 (Fig. 3.3.9) altered from "poor" (normalised water contents falling from 100%R to 5%R in less than 50 hours) to "moderate" water retention (100%R to 50%R during 50 to 100 hours). The water retentive ability of the Monterey (Fig. 3.3.13) altered from "moderate" to "good" water retention (normalised water contents being maintained at 100%R for the entire analytical period).

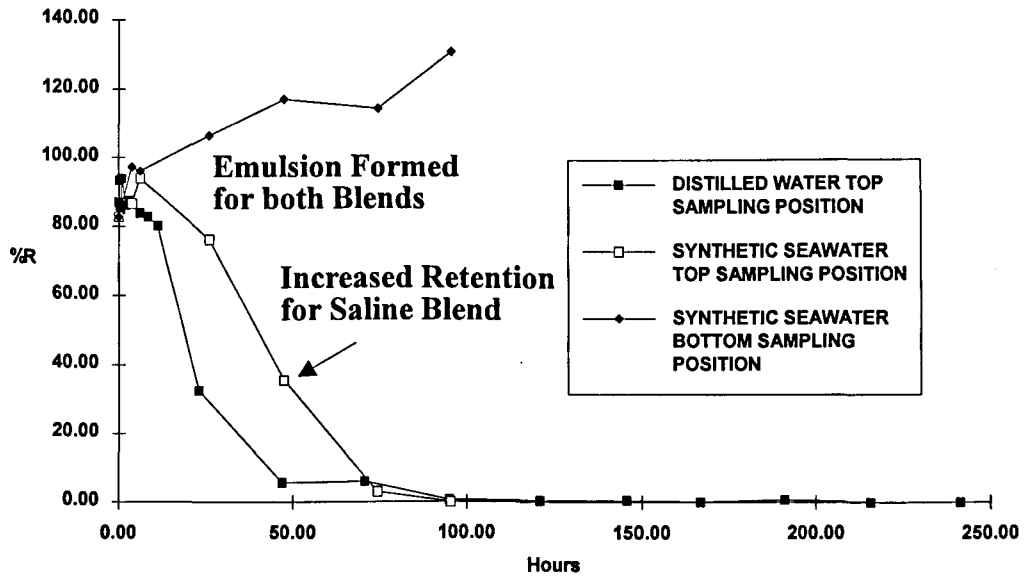

Figure 3.3.9. Comparison of sedimentation curves for Eldfisk/water blends with 30% water content using synthetic seawater abd distilled water. Sampling positions are illustrated in Figure 3.2.2. It may be seen that the water retention has increased for the saline blend when compared to the distilled water blend.

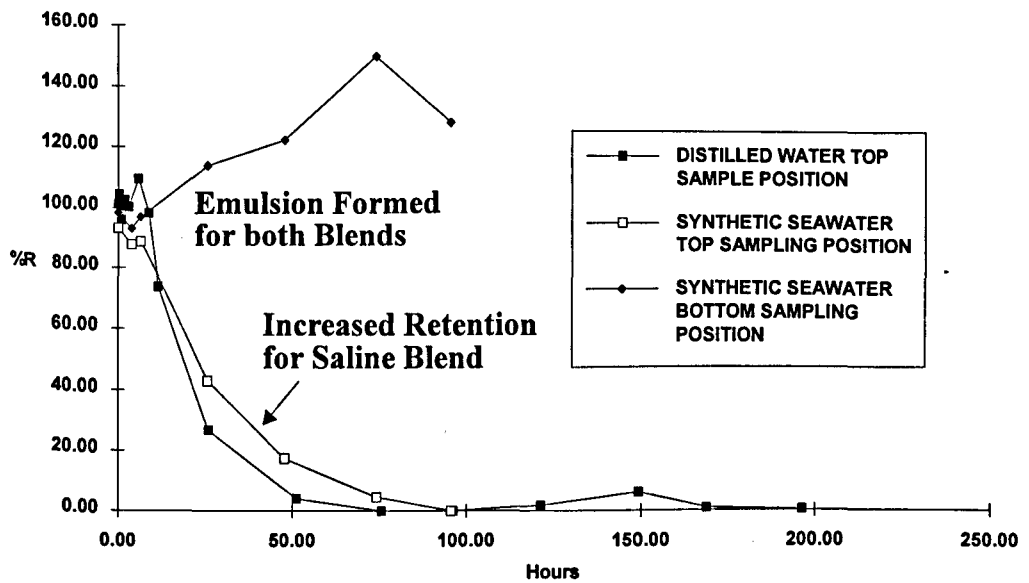

Figure 3.3.10. Comparison of sedimentation curves for NS1/water blends with 30% water content using synthetic seawater abd distilled water. Sampling positions are illustrated in Figure 3.2.2. It may be seen that the water retention has increased for the saline blend when compared to the distilled water blend.

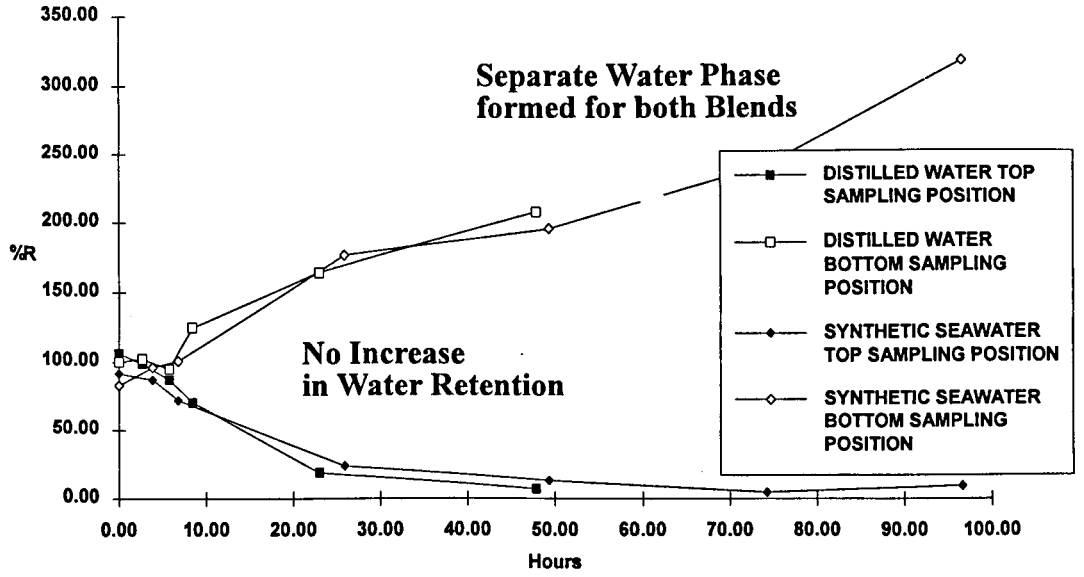

Figure 3.3.11. Comparison of sedimentation curves for NS2/water blends with 30% water content using synthetic seawater abd distilled water. Sampling positions are illustrated in Figure 3.2.2. The water retention for both saline and distilled water blends are similar.

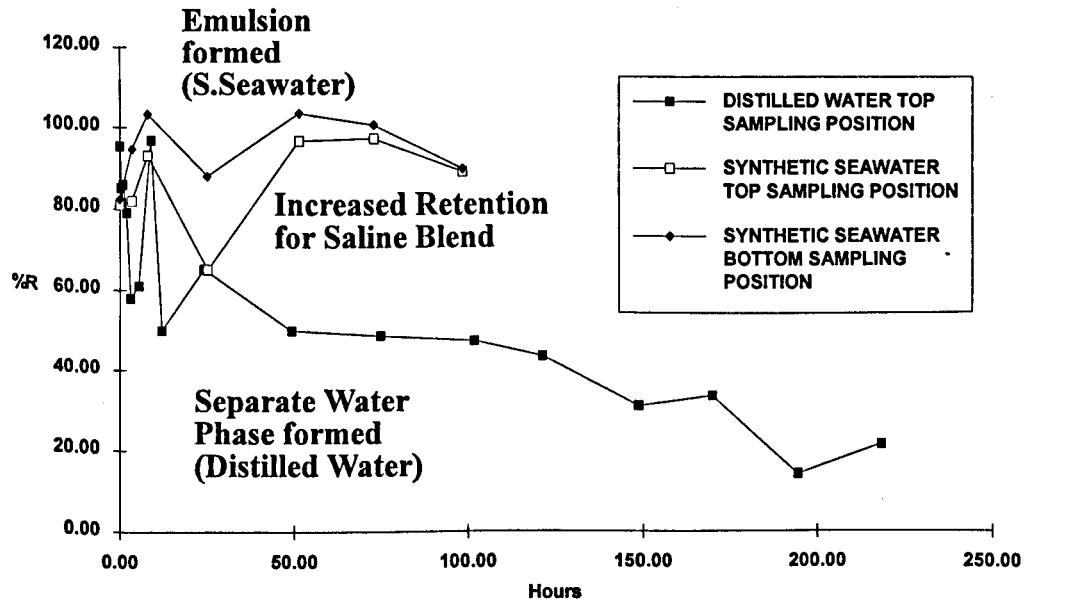

Figure 3.3.12. Comparison of sedimentation curves for NS3/water blends with 30% water content using synthetic seawater abd distilled water. Sampling positions are illustrated in Figure 3.2.2. The water retention for the saline blend is greater than that for the distilled water blend. In addition, the saline blend produced an emulsion.

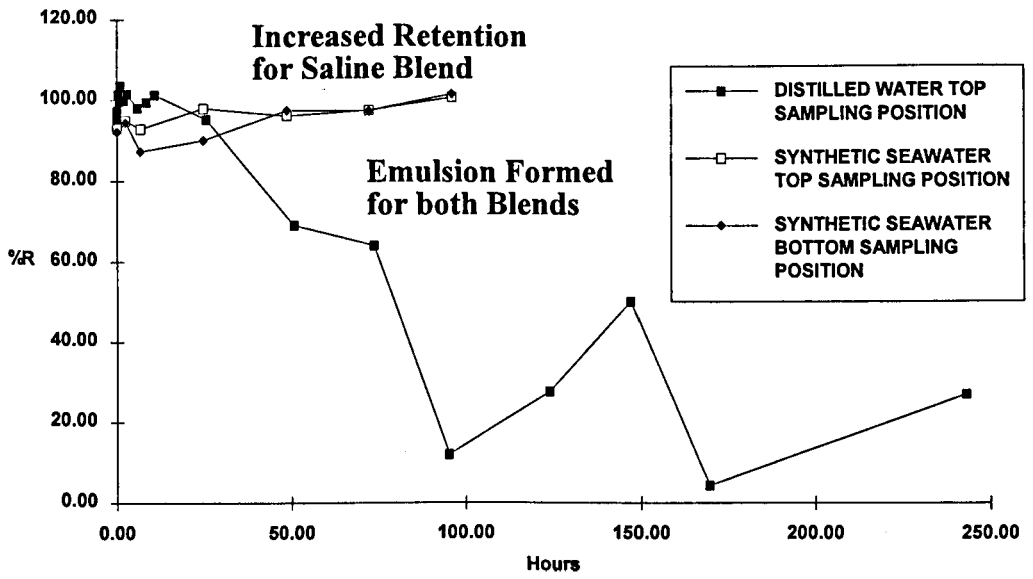

Figure 3.3.13. Comparison of sedimentation curves for Monterey/water blends with 30% water content using synthetic seawater abd distilled water. Sampling positions are illustrated in Figure 3.2.2. It may be seen that the water retention has increased for the saline blend when compared to the distilled water blend.

Crude Oil	Alteration of Water Retention Ability with Increasing Salinity.	Alteration of Emulsion Formation/ Stabilisation Ability with Increasing Salinity.
A29	Increased: From Poor to Moderate	No Change: Emulsion Formed
NS1	Slight Increase: Poor	No Change: Emulsion Formed
NS2	No Change: Poor	No Change: Emulsion and Water Layer Formed
NS3	Increased: Good	Changed: Emulsion Formed instead of a Water Layer
Monterey	Increased: From Moderate to Good	No Change: Emulsion Formed

Table 3.3.4. Comparison of the water retention and emulsion formation/ stabilisation abilities for crude oil samples blended with distilled water and saline water phases.

Although both NS1 and NS3 crude oils exhibited increased water retention when blended with saline water, their classifications remained the same, *i.e.*, "poor" and "good" respectively. The sedimentation curve for the NS1 crude oil/saline water blend (Fig. 3.3.10) dropped from 100%R to 20%R during the initial 50 hours compared to 100%R to 10%R for the distilled water blend. The NS3 crude oil saline water blend (Fig. 3.3.12) did not display any sedimentation, maintaining a normalised water content of 100%R, as opposed to the distilled water blend which displayed sedimentation from 100%R to 60%R after 24 hours.

Comparison of the water retention and emulsion formation/stabilisation abilities of the distilled water and saline water blends for the NS2 crude oil, found that both were almost identical. In Figure 3.3.11, the normalised water percentages for both distilled water and saline water blends, sampled from the top of the blends, both dropped from 100%R to 20%R in less than 50 hours (indicative of "poor" water retention).

Assessment of emulsion formation ability of crude oils found that only the ability of the NS3 crude oil altered when blended with saline water, with no change observed for A29, NS1, NS2 and Monterey crude oils when they were blended with saline water. All of these latter oils, apart from NS2 crude oil (forming both water and emulsion phases), formed stable water-in-oil emulsions. The emulsification ability of the NS3 crude oil changed, from no emulsion formation, when blended with distilled water (Table 3.3.3), to good emulsion formation in the saline water blend.

3.4. Discussion.

3.4.1. Water Uptake Analysis.

The Crude Oil Water Uptake Analysis (COWUA), performed in this chapter, characterised the water uptake ability of crude oils by their water retention (sedimentation rate of water and/or emulsion droplets from the top of the crude oil/water blends) and emulsion formation/stabilisation (degree of oil and water phase separation) properties. It is anticipated that an appreciation of the chemical controls affecting both these properties may explain their observed variation with different crude oils.

The water retentive ability of crude oil is affected by both the physicochemical properties of the crude oil in question and its ability to form a rigid and protective interfacial film with the water phase, thereby influencing droplet growth. The physicochemical properties of the crude oil (viscosity and density) will directly affect the rate at which the water and/or emulsion droplets fall, or sediment through the crude oil phase. For example water droplets will sediment through low viscosity, low density crude oil at a greater rate than through high viscosity, high density crude oil. This investigation has found some evidence for this by identifying that the increasing API gravity of the crude oil relates with increasing crude oil water retention, illustrated in Figure 3.4.1. However, since many factors influence crude oil API gravity (source rock type, maturation history, reservoir conditions etc.) it could not be reliably concluded whether the relationship was attributed to geochemical or physicochemical properties. As well as water retention being related to API gravity, it may also be tentatively related to the extent of biodegradation of each crude oil. It may be seen that the biodegraded crude oils NS3 and H7 plot to the left of the graph (Fig. 3.4.1), being characterised by "moderate" to "good" water retention. Therefore, biodegradation may effect the water retentive ability of the crude oil, possibly due to chemical alteration of the crude oil affecting its ability to form stable interfacial films. The importance of interfacial film formation upon droplet growth has been previously highlighted by Aveyard *et al.* (1990, p36) who reported that the fastest rate of emulsion resolution (separation) was achieved when a "zero energy barrier" to droplet growth existed (*i.e.*, lack of an oil/water interfacial film). Therefore, if a crude oil is unable to form an interfacial film due to compositional alteration, droplet growth will be unimpeded, potentially increasing the rate of sedimentation. As a physicochemical study of crude oils is not part of this work, investigation will concentrate upon the effect of biodegradation upon crude oil geochemistry and investigate if it is related to water retention.

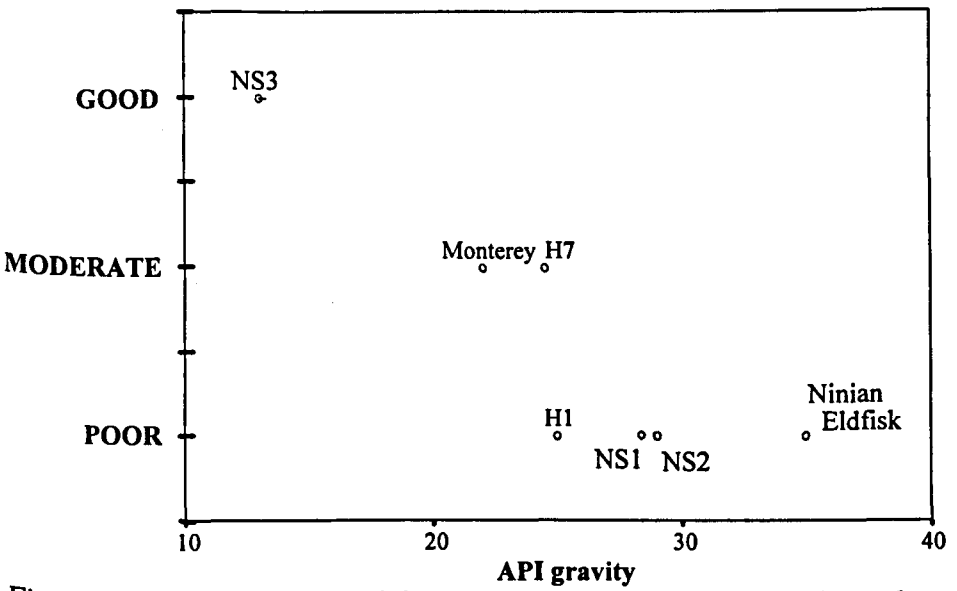

Figure 3.4.1. Comparison of the water retentive ability (Good, Moderate & Poor as defined in Section 2.2.5.4, Fig. 2.2.13) and API gravity of the crude oils analysed.

Crude oil emulsion formation/stabilisation was also found to be tentatively related to the extent of crude oil biodegradation. Observation of the oil/water blends during COWUA showed that the ability of crude oils to form stable water-in-oil emulsions was variable (emulsion type was identified by FFR in Section 3.3.2). The emulsion stabilities of the North Sea crude oil/water blends were found to decrease with increasing extent of biodegradation however, no such trend was seen for SMB crude oils (Table 3.3.3). The non-degraded North Sea crude oils (*viz.* Eldfisk, Ninian & NS1) and SMB crude oils were all found to form stable, viscous, water-in-crude oil emulsions (Table 3.3.3). However, biodegraded North Sea crude oils either formed separate water phases which were associated with very weak emulsions (i.e., NS2) or formed a separate water layer with no associated emulsification (i.e., NS3). Therefore, non degraded North Sea crude oils, and SMB crude oils are capable of forming rigid and protective interfacial films while the biodegraded North Sea crude oils are generally not.

In order to investigate the effect of biodegradation upon the water uptake ability, the bulk chemistry of the different crude oils was assessed. Due to the similarity of the source and maturity properties between the North Sea crude oils analysed, and also between the Santa Maria Basin crude oils analysed (Section 3.1.1), differences in their compositions may be tentatively related to the extent of biodegradation.

Crude Oil (API°)	Biodegraded State.**	Ali. HC, %	Arom. HC, %	Resins %	Asph %	Wax[a] wt%
Eldfisk (35°)	Non-degraded (1)	48	33	16	3	1
Kittiwake (28°)*	Non-degraded (1)	37	48	12	3	0.70
Ninian (35°)	Non-degraded (1)	38	40	16	6	**nd**
NS1 (28°)	Non-degraded (1)	42	30	23	5	0.42
NS2 (29°)	Mild degradation (2)	38	40	17	5	0.66
NS3 (14°)	Extensive degradation (6)	26	52	19	3	0.46
H1 (25°)	Non-degraded (1)	20	23	44	13	0.45
Monterey (22°)	Mild degradation (2)	18	33	38	11	**nd**
H7 (24°)	Moderate-extensive degradation(5)	13	18	51	18	0.20

*Table 3.4.1. Crude oil bulk chemistry determined by Iatroscan-FID (Section 4.2.2). Ali. = aliphatic; HC = hydrocarbons; Arom. = aromatic; Asph = asphaltenes. * = not assessed for water retention ability. ** = the extent of crude oil biodegradation was assessed by use of the Volkman et al. (1984) biodegradation scale and the relevant scale numbers are bracketed. [a] = Determination of wax concentration was performed by the wax concentration/precipitation technique of Bishop et al. (1994), discussed in Section 4.2.3.* **nd** *= not determined.*

As discussed in Chapter 1, Section 1.2.2, the governing factors affecting the formation of stable water/oil interfacial films is the presence of emulsifiers (asphaltenes and waxes sols as well as surfactants) in the crude oil (Schramm, 1992). However, the presence of these emulsifiers is strongly affected by biodegradation. In general, increasing biodegradation results in the removal of non-polar *n*-alkanes (including wax sols, Section 4.4.2; Hanstveit, 1992) and produces a more polar oil, increasing the solubility of asphaltenes in crude oil. Consequently, wax sols are removed while asphaltenes are less likely to precipitate from the crude oil. Therefore, it is probable that biodegradation results in a reduced likelihood of wax and asphaltene sols occurring at the oil/water interfaces, potentially reducing interfacial film stability between the phases.

Comparison of the bulk chemistry of non-degraded and degraded crude oils, from each sample province (North Sea and Santa Maria Basin), identifies these biodegradational trends. The aliphatic hydrocarbon content in North Sea crude oils decreases with increasing biodegradation, from approximately 37-48% to 26% (although this trend is difficult to determine for NS2 & Kittiwake crude oils). In addition, the measured wax content also displays some decrease, from approximately 0.7-1% to approximately 0.46% for NS3 however, it must be noted that the NS1 wax

content (non-degraded oil) is low and does not support this trend. The Santa Maria Basin crude oils show more clear trends for aliphatic hydrocarbon reduction, from 20% to 13% as well as wax content reduction, from 0.45% to 0.2%. While the effect of biodegradation on the presence of sols in crude oil offers an explanation for the emulsification behaviour of the biodegraded crude oil NS3, as well as the non-degraded North Sea crude oils, it does not satisfactorily explain the behaviour of; first, the NS2 crude oil, the bulk chemistry of which gives no indication of reduced sol content, yet forms a poor emulsion and water phase. Second, Santa Maria Basin oils, all of which form stable water-in-oil emulsions despite bulk chemical analysis indicating that the presence of asphaltene and wax sols is low.

In addition, reduced sol content would not explain the observed trends for the water retention data reported earlier. Reduction of asphaltene and wax sols should decrease interfacial film stability (therefore produce"poor" water retentions) yet biodegraded crude oils, especially NS3, are generally characterised by "good" to "moderate" water retention. However, before the influence of crude oil chemical composition upon water retention is discounted completely surfactant analysis is required.

The effect of biodegradation upon surfactants (the NSO compounds in crude oils (asphaltene and resins)), is to increase them relative to aliphatic and aromatic hydrocarbon contents (Connan, 1984). It was initially considered that such an increase would be beneficial to increased interfacial film stability and therefore increased water retention.

Investigation of the influence of individual surfactant groups, such as phenols, carboxylic acids *etc.*, upon water-in-oil emulsion formation/stabilisation, cannot be carried out with this limited chemical analysis. However, assessment of the total concentration of the NSO compounds (asphaltene and resins) is possible. Table 3.4.1 indicates that there is no trend of NSO enrichment with increasing biodegradation for both North Sea crude oils (approximately 15-28% NSO) and Santa Maria Basin crude oils (approximately 50-60% NSO). However, it is noted that high abundances of polar compounds in the Santa Maria Basin crude oils is possibly responsible for formation of water-in-oil emulsions, regardless of the extent of biodegradation of the crude oil.

Therefore, bulk chemical assessment of crude oils has demonstrated no clear relationship between crude oil chemical composition and water retention. It is suggested that either: (1) there is no relationship; or (2) subtle compositional alteration has occurred with biodegradation. Johansen *et al.* (1989) also suggested that alteration to emulsifiers may be subtle and not detected by "gross weight" determinations. Therefore, although analyses have implied that the presence of sols is not related to crude oil water retention, it is possible that surfactants may have been

subtly altered by biodegradation, thereby altering the water retention ability of crude oils. It is therefore probable that bulk chemical assessment may not be an effective method of discriminating crude oil water uptake potentials, and that more subtle analytical techniques are required (performed in Chapter 5).

Conversely, bulk chemical assessment has identified some correlation between crude oil geochemistry and emulsion formation/stabilisation behaviour. It is tentatively suggested that the lack of emulsion stability exhibited by biodegraded North Sea crude oils is due to the reduction of their ability to precipitate asphaltene and wax sols. However, the stable water-in-oil emulsions obtained from the biodegraded Santa Maria Basin crude oils, which also have reduced asphaltene precipitation ability and wax content, are attributed to the high concentration of NSO groups, increasing oil and water interaction. However, a more detailed analysis of the presence of asphaltene and wax sols, as well as surfactants, is necessary to confirm the tentative conclusions above. In addition, clarification is also required to explain the relationship between bulk chemical composition and the emulsion formation/ stabilisation behaviour of the NS2 and Kittiwake crude oils (Section 4.4.2.1).

3.4.2. Water Uptake Analysis - Asphaltene Fraction Influence.

Assessment of the effect of crude oil asphaltene content on the water uptake ability of Monterey crude oil (Fig. 3.3.7) was inconclusive. Reconstituted crude oil samples (with added asphaltene content of 0%, 5% & 10%) when blended with distilled water, produced water sedimentation curves indicating a "poor" water retentive crude oil. Although the sedimentation curve for the unspiked Monterey crude oil (natural 10% asphaltene content) was indicative of a crude oil with "poor" water retention its overall retention was greater than for the reconstituted oils (0%, 5% & 10% added asphaltene content). Therefore, even though the two crude oil samples (original and reconstituted) had the same "asphaltene content" (10%) their retention behaviour was different. From this, it appears that the experiments were unable to recreate the Monterey crude oil water uptake characteristics and so experimentation, assessing the influence of different asphaltene quantities on the water uptake ability of crude oils, was unsuccessful. It was considered possible that once the asphaltene fraction was precipitated it could not be fully re-dispersed into the crude oil phase in its original state. Previous work by Lhioreau *et al.* (1967), referred to by Wilhelms & Larter (1994b), also suggested that precipitation of asphaltenes was irreversible, and that asphaltenes cannot be re-dispersed into their original form.

3.4.3. Water Uptake Analysis - Wax Fraction Influence.

The effect of octadecane (n-C_{18}) and tetracosane (n-C_{24}) wax additions upon the emulsion formation/stabilisation ability of a biodegraded North Sea crude oil (NS3), Figure 3.3.8, was variable. The results show that increasing amounts of n-C_{18} (0.4, 0.9, & 1.8wt%) progressively improves the ability of the NS3 crude oil to form stable water-in-oil emulsions. The addition of 0.4wt% n-C_{18} produced no alteration to emulsion formation ability, however, an addition of 0.9wt% n-C_{18} produced partial emulsification. Finally, an addition of 1.8wt% of n-C_{18} to NS3 crude oil produced a stable water-in-oil emulsion when blended with distilled water. These results indicate that n-C_{18} wax is an effective emulsion stabiliser.

The influence of wax was also investigated by Thompson *et al.* (1985), by altering the wax concentration in crude oil samples. The wax concentration in crude oil samples was lowered by removal of wax by centrifuging crude oils at varying temperatures (the lower the temperature the more wax is present as a solid form and therefore removed by centrifuging). To increase the wax content of crude oil, extracted wax concentrates were incorporated into unaltered crude oil samples. The effect of wax content upon water-in-crude oil emulsion stability versus time was assessed and is shown in Figure 3.4.1. Thompson *et al.* (1985) also found that the reduced amount of water separation was related to the increasing wax concentration of the crude oil (Fig. 3.4.1). However, it should be realised that improved emulsion stability, due to wax addition does not imply that the wax component is solely responsible for emulsion formation and stability, as emulsion stabilisation cannot be attributed to one component, such as waxes (Schramm, 1992).

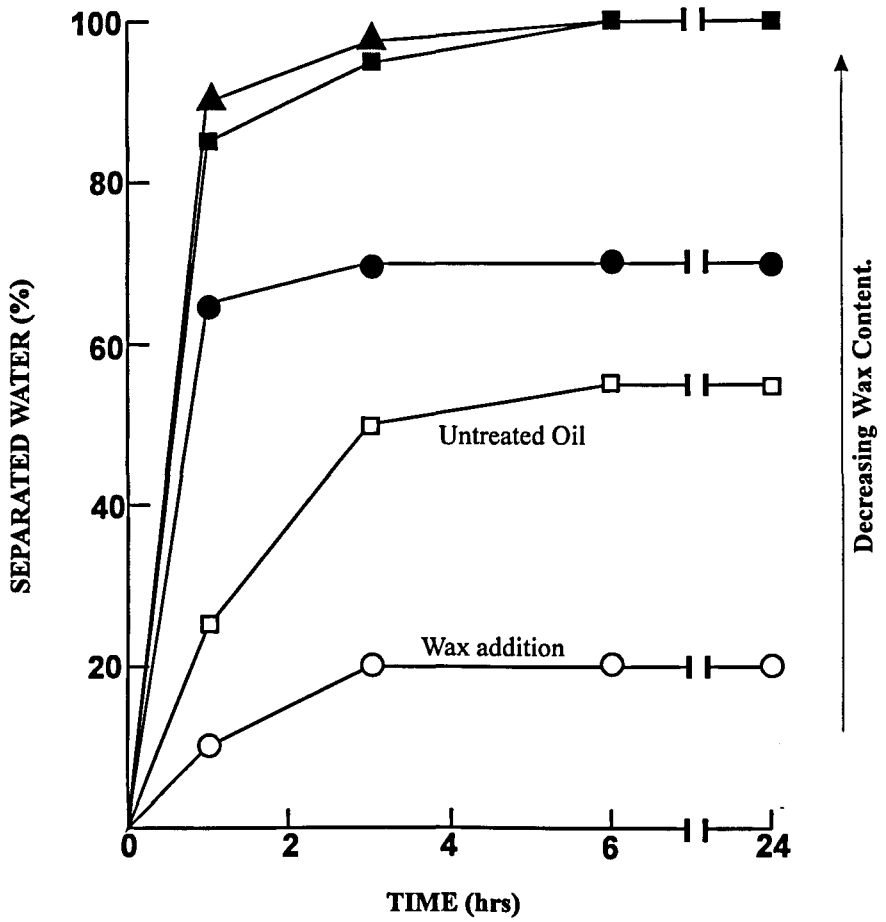

Figure 3.4.1. Influence of wax content upon emulsion stability. (□) *Untreated oil. Wax removed by centrifugation:* (■), *0°C;* (▲), *20°C and* (●), *35°C.* (○), *Wax added to oil. Taken from Thompson et al. (1985).*

Addition of *n*-C_{24} to NS3 crude oil did not improve emulsion stability. This would suggest either a fundamental difference in properties of *n*-C_{24} compared with *n*-C_{18} or, much more likely, poor dissolution of the *n*-C_{24} into the oils. This is further suggested as Thompson *et al.* (1985) used wax extracts which probably contained high molecular weight waxes with carbon numbers greater than 24. Poor solvation of the *n*-C_{24} alkane in crude oil was attributed to the blending preparations being unable to incorporate the wax. During wax addition it was hoped that a combination of the solvation ability of the crude oil and an increase in crude oil temperature would be sufficient to incorporate the wax into the crude oil. However, as experimentation had to avoid chemical and rheological alterations to the crude oil, other than those from the wax addition, solvents and high temperatures (>30°C) were not applied to aid wax incorporation.

3.4.4. Influence of the Electrolyte Content of the Aqueous Phase on the Water Uptake Ability of Crude Oils.

The use of synthetic seawater instead of distilled water, as the aqueous phase in crude oil and water blends, changed both the electrolyte content and pH of the dispersed aqueous phase. As the effect of pH on emulsion stabilisation is not influential until the pH is equal to, or greater than, 10 (Oren & MacKay, 1977), the alteration of the pH from 7 to 8, caused by the use of synthetic seawater, was not expected to influence the water uptake ability of the crude oils. However, alteration of the electrolyte content was expected to increase the stability of crude oil and water emulsions due to reduction of water droplet coalescence (Section 3.1). All the crude oils blended with synthetic seawater, except one (NS2), displayed some degree of increased water uptake ability compared to crude oil/distilled water blends.

As well as crude oil water retention alteration the emulsion formation/ stabilisation ability of the NS3 crude oil also increased, producing water-in-oil emulsions instead of separate water layers. It could not be explained why the water uptake ability of the NS2 crude oil did not increase.

It was concluded that the use of saline aqueous phases will increase the water uptake ability of the crude oils.

3.5. Conclusions.

This chapter has described the development and use of a working method for the characterisation of crude oil water uptake ability. It has shown that water uptake may be subdivided into two categories; firstly water retention (sedimentation rate of water and/or emulsion droplets from the top of the crude oil/water blend), assessed by measuring the variation of water content at the top of the crude oil/water blends, and secondly emulsion formation/stabilisation (degree of oil and water separation), which was assessed by visual inspection of the crude oil/water blends.

Results identified that both water retention and emulsion formation/ stabilisation properties varied with the extent of biodegradation of crude oil. Non-biodegraded crude oils were characterised by "poor" water retention (rapid sedimentation of water and/or emulsion droplets) and also by the formation of stable water-in-oil emulsions (identified by Freeze Fracture Replication). Biodegraded crude oils generally exhibited "moderate to good" water retention (slow sedimentation of

water and/or emulsion droplets); however, their emulsion formation/stabilisation ability varied.

Water retention was considered to be affected by either the physicochemistry (viscosity *etc.*) or chemical composition of the crude oil. Work subsequently investigated the relationship between water retention and crude oil bulk chemical composition and its variation with biodegradation. Of particular interest was the presence of emulsifiers (asphaltene and wax sols, as well as surfactants) which promote stable oil/water interfacial film formation. No relationship between chemical composition of crude oil and its water retentive ability could be identified. However, it is possible that biodegradation may have subtly altered the chemistry of the crude oil (in particular surfactants), alterations which may not have been identified by bulk chemical analysis. Therefore, a more detailed study of surfactant compounds was recommended (Chapter 5).

Crude oil emulsion formation/stabilisation was considered to be predominantly controlled by the presence of emulsifiers and analysis was able to identify correlations between variable emulsifier content (due to biodegradation) and the emulsion formation /stabilisation behaviour of crude oils. The formation of stable emulsion for the non-degraded North Sea crude oils was attributed to the presence of asphaltene and wax sols while the reduction of these precipitates probably accounted for the poor emulsion formation of the biodegraded crude oil, NS3. The stable water-in-oil emulsions of the Santa Maria Basin crude oils was explained by the high concentrations of NSO compounds (50-60%). However, it was not possible to explain the emulsion formation/stabilisation behaviours of all crude oils and it is therefore suggested that more detailed analyses may explain such anomalies (Chapters 4 & 5).

Alteration of the bulk chemistry of the crude oil, using wax additions was successful. Wax additions were shown to be influential emulsion stabilisers, with additions promoting emulsion formation and stability in the previously non-emulsifying, and biodegraded North Sea crude oil, NS3. However, the analysis of the asphaltene additions to Monterey crude oil was found to be inconclusive in assessing emulsion formation/stabilisation, possibly due to the inability to re-disperse the extracted asphaltene fraction (Section 3.4.2).

As well as assessment of the effect of crude oil compositional controls upon water uptake, assessment of water compositional controls was also performed. Results were found to corroborate reports from the literature, with increased electrolyte concentration increasing both water retention and emulsion formation/stabilisation ability. Thus it is concluded that crude oils in real life situations, involving seawater, formation water *etc.*, would probably display greater water uptake than experiments with distilled water.

CHAPTER 4:

GEOCHEMICAL ANALYSIS OF EMULSIFIERS AND THEIR INFLUENCE UPON CRUDE OIL WATER UPTAKE ABILITY

CHAPTER 4: GEOCHEMICAL ANALYSIS OF EMULSIFIERS AND THEIR INFLUENCE UPON CRUDE OIL WATER UPTAKE ABILITY.

Work in this chapter has firstly been able to identify that the stability of water-in-oil emulsions, isolated from crude oil/water blends, is associated with the preferential enrichment of both asphaltene and wax components. Secondly, further work has corroborated findings in Chapter 3, highlighting that the effect of biodegradation reduces the presence of asphaltene and wax sols within the crude oil and thereby reduces their ability to stabilise water-in-oil emulsions.

4.1. Introduction.

In the last chapter variations of the bulk composition of the crude oil suggested that asphaltene solubility and wax content in the crude oil was altered by the degree of biodegradation. The variation in the bulk chemistry and behaviour of the oils affected the ability of the oil to precipitate asphaltene and wax sols consequently reducing their ability to stabilise water-in-oil emulsions.

This chapter presents a more detailed study of the presence and behaviour of asphaltenes and wax sols in crude oils and their effects on water uptake ability. In addition to more indepth analysis of the effects of biodegradation upon the presence of sols in crude oils, work will also chemically analyse water-in-oil emulsion samples, extracted from crude oil/water blends, for the presence of both asphaltene and wax components.

4.2. Experimental.

This chapter will follow the analytical procedures highlighted in Figure 4.2.1 in an attempt to characterise the emulsion formation/stabilisation ability of crude oils by studying the chemistry of their whole oil and blend fractions.

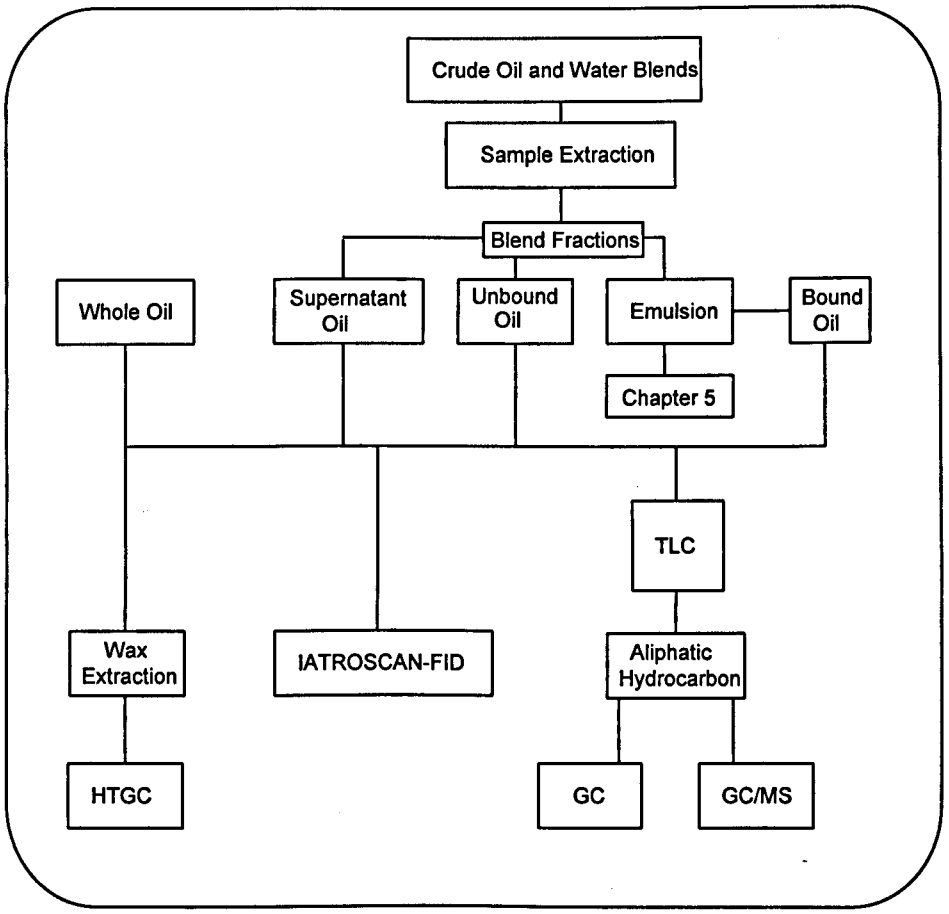

Figure 4.2.1. Analytical flow chart of the methods used in this chapter.

4.2.1. Sample Preparation.

Separation of the crude oil/water blends produced four fractions (also referred to as the blend fractions) for analysis. These fractions were supernatant oil, unbound oil and the emulsion fractions; the emulsion fraction consisted of the bound oil fraction as well as water phase (Fig. 4.2.2), the water phase was not analysed. The emulsion fraction was employed in alkyphenol analyses and is discussed in Chapter 5.

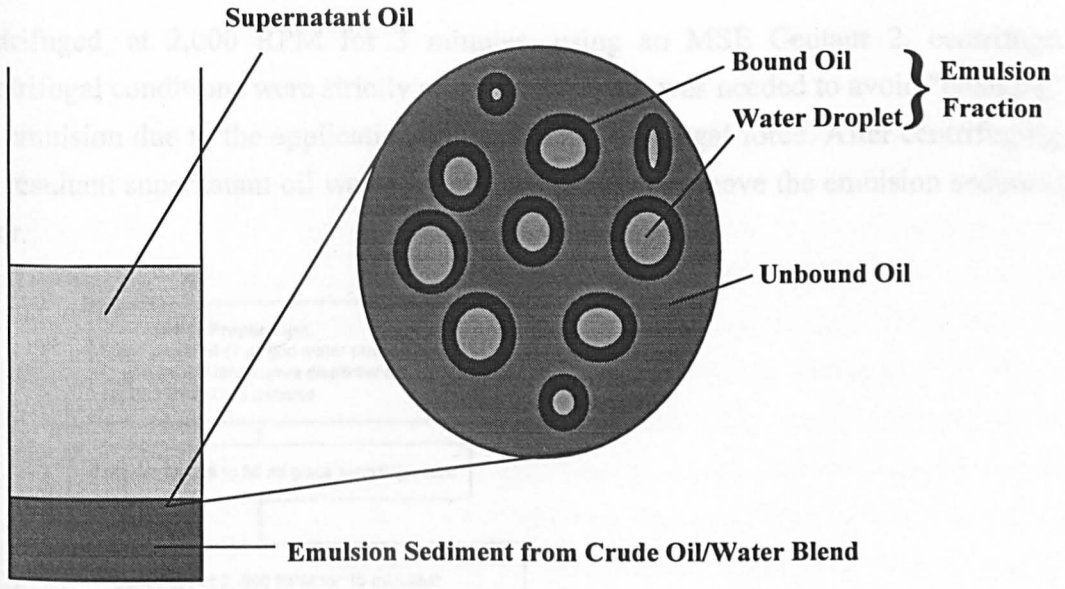

Figure 4.2.2. Illustration of the blend fractions obtained from crude oil/water blends. The emulsion sediment contains the unbound oil fraction, bound oil fraction and aqueous phase.

The supernatant oil fraction represents the crude oil which separated from the emulsion sediment due to gravity (normal, or increased due to centrifuging). The term "emulsion sediment" refers to the product caused by flocculation of the emulsion droplets in the crude oil/water blends. The sediment contains the unbound oil fraction, bound oil fraction and aqueous phase. The unbound oil fraction represents the crude oil trapped in the emulsion sediment, which is not part of the crude oil/water interfacial film. The emulsion fraction represents the organic matter in the crude oil/water interfacial film, as well as the dissolved organic matter in the water phase. The bound oil fraction represents the organic matter present in the crude oil/water interfacial film and is extracted from the emulsion fraction.

As well as fractions extracted from the crude oil/water blends (supernatant oil, unbound oil, emulsion, bound oil fractions), the whole oil fractions (oil which had not been blended with an aqueous phase) were also analysed by the procedures described below.

4.2.1.1. Extraction of Blend Fractions.

The extraction of the four blend fractions (supernatant oil, unbound oil, emulsion and bound oil) was based on the procedure described by Acevedo *et al.* (1992), illustrated in Figure 4.2.3. The crude oil/water blends were prepared as described in Chapter 2, Section 2.2.4, and in Appendix 1, Section A1.8. Once blended, the blend fractions were isolated. The crude oil and water blends were

centrifuged, at 2,000 RPM for 3 minutes, using an MSE Centaur 2, centrifuge. Centrifugal conditions were strictly adhered to as care was needed to avoid "breaking" the emulsion due to the application of too much centrifugal force. After centrifuging, the resultant supernatant oil was carefully pipetted off to leave the emulsion sediment layer.

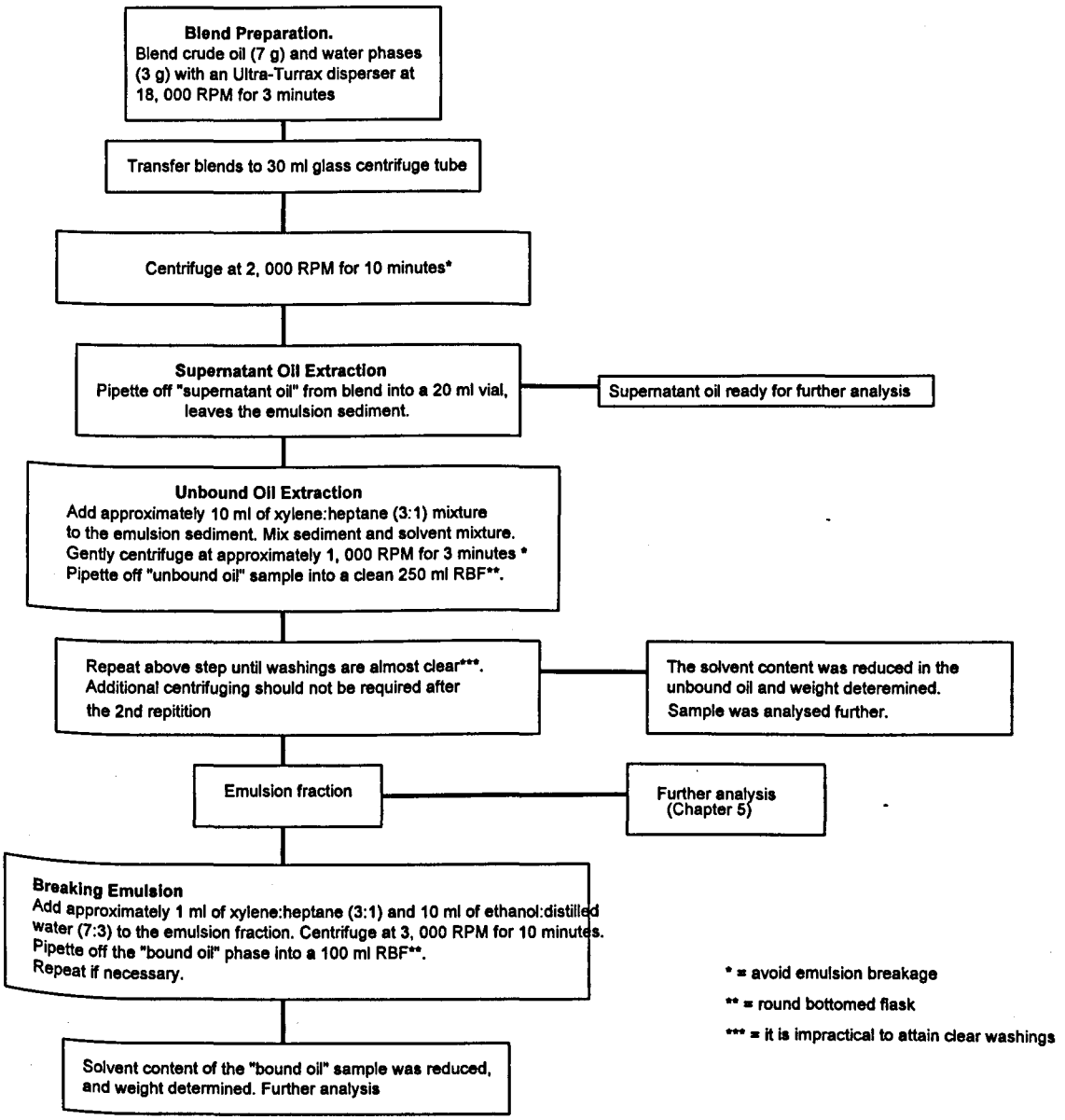

Figure 4.2.3. Procedure for extraction of the supernatant oil, unbound oil, emulsion and bound oil fractions (blend fractions) from the crude oil/water blends.

The extraction of the unbound oil sample was achieved by washing the emulsion sediment with a solvent mixture of xylene (Xy) and heptane (Hep), at a ratio of 3:1. Approximately 10 ml of solvent mixture was added to the sediment, the sediment/solvent mixture was agitated and then allowed to settle (solvent phase rising

to the top of the mixture). In some cases the sediment/solvent mixture was highly viscous and gentle centrifuging, at 1,000 RPM for 1 minute, was required to help separate the solvent (unbound oil extract) from the sediment. Centrifuging should not be necessary after the first two extractions as removal of the bulk of the unbound oil significantly lowers the viscosity of the sediment/solvent mixture, aiding rapid separation. The unbound oil fraction was then pipetted into a clean 250 ml round bottomed flask (RBF). The emulsion sediment was washed several times until the washings were almost clear. It was impractical to wait until the washings were totally clear as the time needed would have been prohibitive. The extracted unbound oil fraction was then reduced by rotary evaporation to approximately 2 ml. A known proportion of sample was pipetted into a weighed vial and taken to dryness under a stream of nitrogen. The weight of the total unbound oil fraction was then calculated prior to further analysis.

After the removal of the unbound oil fraction from the emulsion sediment, the remnant phase is referred to as the emulsion fraction. This fraction may be analysed, as with C_0-C_3 alkylphenol analysis (Chapter 5), or separated into the bound oil fraction (organic matter of the interfacial film) and aqueous phase.

Prior to the extraction of the bound oil fraction, approximately 1 ml of the Xy:Hep (3:1) solvent mixture was added to the emulsion fraction. The emulsion was destabilised by the addition of 10 ml of an ethanol:distilled water solution (7:3). The mixture was centrifuged at 3,000 RPM for 10 minutes to aid separation. The bound oil sample is pipetted into a vial. The broken emulsion was washed twice more with 1 ml of Xy:Hep (3:1) mixture, the washings were pipetted into the vial. A known proportion of sample is then pipetted into a weighed vial and taken to dryness under a stream of nitrogen. The weight of the total bound oil sample was calculated prior to further analysis.

4.2.2. Iatroscan-FID Analysis.

Iatroscan analysis was carried out on a Mk 4 Iatroscan fitted with a Flame Ionisation Detector (FID) and coupled to a Perkin Elmer LC100 integrator. Type S III silica Iatroscan rods were used. Hydrogen pressure was set at 0.9 kg cm^{-2}, air flow was set at 1,800 ml min^{-1}. The samples were diluted with dichloromethane, 5 - 10 mg of sample per 1 ml dichloromethane (DCM). 3 µl of sample was spotted on each silica rod. The rods were then developed with increasingly polar solvents (*n*-hexane to 100% development, cyclohexane to 50% development and finally 30% development in dichloromethane: methanol (95:5)) prior to analysis on the Iatroscan-FID.

4.2.3. Wax Extraction and Analysis.

Wax extraction and analysis (Fig. 4.2.4) was based on the method developed by Bishop *et al.* (1994) and del Rio *et al.* (1992). This procedure analysed whole oil samples only.

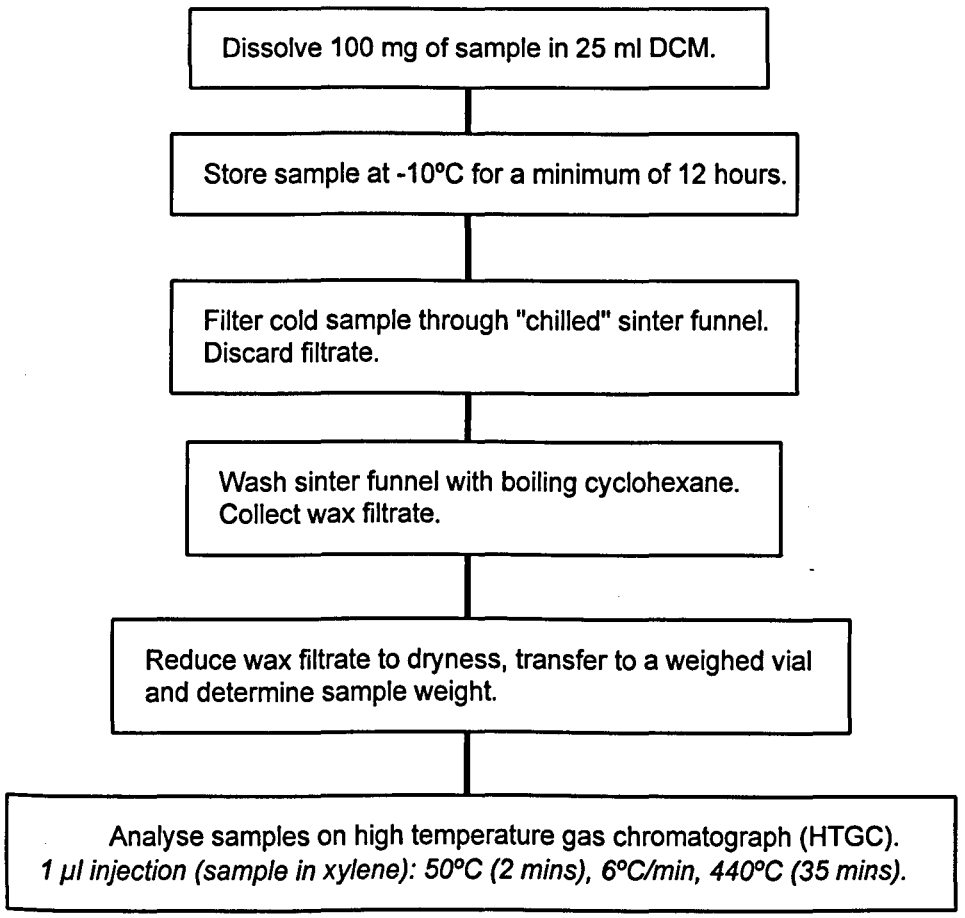

Figure 4.2.4. Wax extraction and analysis procedure, adapted from Bishop et al. (1994) and del Rio et al. (1992).

To a clean 100 ml conical flask (CF) add 100 mg of whole oil sample. Dissolve the oil in 25 ml of room temperature, laboratory distilled dichloromethane (DCM). The liquid was stirred for 5 to 10 minutes, or until the sample was dissolved. The mixture was stored at -10°C for a minimum of 12 hours, allowing the wax to precipitate and settle out.

Into a clean sinter funnel (grade 4) pour 50 ml of cold (-10°C) DCM, collecting the filtrate over a 2 minute period. The "chilled" sample was then filtered through the cold sinter funnel (prevents the re-dissolution of the wax) over a 2 minute period. Wash the 100 ml CF with 10 ml of cold DCM, the washings were then filtered

through the cold sinter funnel. Discard the collected solvent fraction and replace the 500 ml RBF with a clean 250 ml RBF.

Prepare 100 ml of boiling, distol grade, cyclohexane. To a clean 250 ml CF, add 100 ml of distol grade cyclohexane and a magnetic stirring bar. Place the 250 ml CF onto a combined hot plate/stirrer, situated in fume cupboard. Attach a water cooled condenser to the 250 ml CF and, while stirring, gently heat the cyclohexane until the cyclohexane begins to boil. Rinse the 100 ml CF with 50 ml of boiling cyclohexane, adding washings to the sinter funnel. Allow the hot cyclohexane washings to sit in the sinter funnel for approximately 2 minutes, without the vacuum on, to dissolve the wax crystals. Apply the vacuum and retrieve the wax fraction. Add the remaining 50 ml of boiling cyclohexane to the sinter funnel and retrieve. Remove the 250 ml RBF and reduce filtrate to dryness by rotary evaporation. Wash the 250 ml RBF with 1 ml of room temperature cyclohexane and add to a weighed vial. Wash the 250 ml RBF twice more with 1 ml hot cyclohexane (heated as above), and also add to the weighed vial. Take the sample to dryness under a stream of nitrogen and re-weight the vial to determine the sample weight. Dilute the sample with distol grade xylene (1 mg of sample requires 50 µl of xylene). In addition, an internal standard (heptadecylcyclohexane) was added prior to gas chromatographic analysis, 5 µg per 1 mg sample.

High temperature gas chromatography (HTGC) of the wax extracts was performed on a Carlo Erba 5160 gas chromatograph. On-column injection was used with no secondary cooling. The instrument was fitted with a flame ionisation detector (FID), at a temperature of 450°C. The chromatographic column used was a SGE aluminium clad, HT-5, fused silica column (12 m x 0.5 mm, film thickness 0.15 µm). Hydrogen pressure was 10 kPa. The temperature program started at 10°C for 2 minutes, increased to 440°C at 6°C/min, with the final temperature being maintained for 35 minutes. Prior to analysis, the gas chromatographic column was condition by slowly increasing the final temperature from 300°C to 440°C, over three conditioning runs. Before analysing the wax extracts, the column was calibrated with Fisons wax standards, P Wax and FT Wax. Injected sample size was 1 µl.

4.2.4. Aliphatic Hydrocarbon Fraction Separation and Analysis.

Wax extraction and analysis (described in Section 4.2.3) could not be applied to the bound oil fractions due to their small sample size (1-10 mg). However, thin-layer chromatographic (TLC) separation of the bound oil aliphatic hydrocarbon fraction, followed by gas chromatographic analysis, gave some indication of the

presence of the waxes. In addition, the aliphatic hydrocarbon fractions of the whole oil, supernatant oil and unbound oil fractions were also analysed by this method.

The TLC plates, 20 cm x 20 cm, were coated (0.5 mm thickness) with silica gel (Kiesel gel, 60G) and activated at 120°C for 4 hours. The plates were then cleaned in ethyl acetate and reactivated at 120°C for 2 hours. Plates were separated into two sections for the development of the crude oil sample (section width approximately 15 cm) and reference compound mixture (approximate section width 5 cm: reference compound mixture consisted of tetradecane (100 mg), phenyl dodecane (100 mg) and anthracene (100 mg) in 10 ml DCM). Approximately 10-20 mg of crude oil sample was spotted onto each plate along with approximately 2 mg of reference compound mixture. Plates were developed in light petroleum ether (BP 40°C to 60°C) until the solvent front was approximately 0.5 cm from the top of the plate. The reference compound section was sprayed with rhodamine 6G and visualised under a UV light to identify the aliphatic hydrocarbon band of the sample, which approximated to the tetradecane reference compound. The aliphatic hydrocarbon band was scraped off the plates and desorbed from the silica using petroleum ether. Samples were reduced by rotary evaporation to approximately 2 ml and pipetted into a vial.

The aliphatic hydrocarbon fraction was analysed on Carlo Erba 5160 gas chromatograph. On-column injection was used and the instrument was fitted with a flame ionisation detector (FID). The aliphatic hydrocarbon fractions were analysed on a HP-5 coated fused silica column (30 m x 0.25 mm, with a film thickness of 0.25 μm). The temperature programme used to assess the presence of high molecular weight wax in the aliphatic hydrocarbon fraction, was from 50°C for 2 mins, increasing at 4°C/min to 310°C which was maintained for 20 mins. Gas chromatographic analysis of aliphatic hydrocarbon fractions (whole oil, supernatant oil and unbound oil fractions) used a final temperature of 300°C for 20 minutes. Hydrogen carrier gas pressure was 50 kPa. Before injection the samples were diluted in dichloromethane (10 mg aliphatic hydrocarbons in 1 ml DCM). Injection of 0.5 μl sample was performed with secondary cooling.

4.3. Results.

The results presented in this section are for crude oils which have been analysed by all the procedures described in the experimental section of this chapter. These crude oils are A29, Kittiwake, NS1, NS2, NS3, H1 and H7. Details of the

source rock, maturity and biodegradation state of each crude oil are given in Chapter 3.

4.3.1. Iatroscan-FID Analysis.

4.3.1.1. Analysis of the Chemical Composition of Whole Oil Fractions.

The results from the Iatroscan-FID bulk chemical analyses of whole oil fractions are displayed in Figure 4.3.1. The effects of biodegradation on the two sets of crude oils, North Sea and Santa Maria Basin (SMB), may be seen. The non-degraded North Sea crude oils, A29 and NS1 are dominated by, in order of abundance, the aliphatic hydrocarbons (42-48%), aromatic hydrocarbons (approximately 30-33%), resins (16-23%) and asphaltenes (3%). The effect of biodegradation on North Sea crude oils (NS2 & NS3) shows that aliphatic hydrocarbon concentrations are reduced (approximately 45% to 38% & 26% respectively) with the aromatic hydrocarbon group becoming dominant (approximately 40% to 52%). The asphaltene (3% to 5%) and resin (17% to 19%) concentrations appear to be relatively unchanged. In addition, the aliphatic hydrocarbon reduction for the NS2 crude oil (approximately 45% to 38%) is less than that for the NS3 crude oil (approximately 45% to 26%), a probable indication that the NS2 crude oil has been degraded to a lesser degree than the NS3 crude oil.

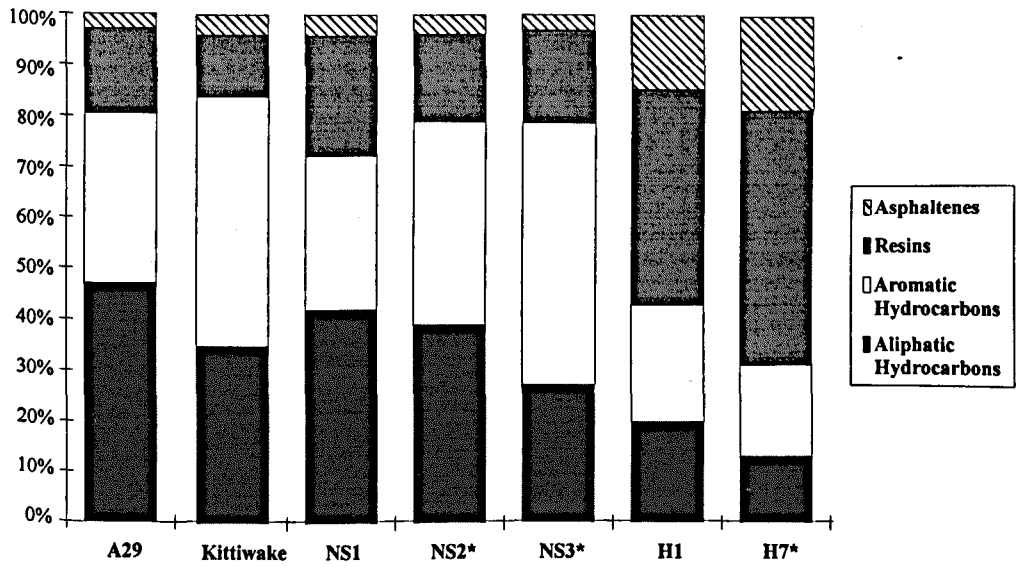

*Figure 4.3.1. Histograms of the whole oil chemical compositions, determined by Iatroscan-FID. Biodegraded whole oils are highlighted by *.*

Kittiwake, a non-degraded crude oil, displays a bulk chemistry similar to that of the biodegraded crude oil NS2 (Table 4.3.1). Iatroscan-FID analysis has therefore not been able to distinguish the non-biodegraded state of Kittiwake crude oil from the biodegraded state of the NS2 crude oil. However, assessment of the aliphatic hydrocarbon gas chromatograms for the crude oils (Fig. 4.3.2), indicates that although the total aliphatic hydrocarbon concentration of the Kittiwake and NS2 crude oils are similar, the molecular constituents are different. The aliphatic hydrocarbon distribution of NS2 crude oil is dominated by the isoprenoids, pristane and phytane, emphasising that *n*-alkanes from *n*-C_{13} to *n*-C_{27} have been reduced. However, the aliphatic hydrocarbon gas chromatogram for Kittiwake crude oil is dominated by the low molecular weight aliphatic hydrocarbons, with an *n*-alkane distribution of *n*-C_{10} to *n*-C_{38} and maximum peak height at *n*-C_{12}.

Crude Oil	Ali. HC, %	Arom. HC, %	Resins %	Asph %	Ali:Arom Ratio *	Wax wt%	n-C_{30} (10^{-4} mg)
A29	48	33	16	3	1.45	1.00	8
Kittiwake	37	48	12	3	0.77	0.70	0.6
NS1	42	30	23	5	1.40	0.42	0.6
NS2	38	40	17	5	0.95	0.66	1.6
NS3	26	52	19	3	0.50	0.46	0.4
H1	20	23	44	13	0.87	0.45	0.8
H7	13	18	51	18	0.72	0.20	0.08

*Table 4.3.1. Bulk chemical results for whole oil fractions. Results gained from Iatroscan-FID, aliphatic hydrocarbon gas chromatography and wax extraction analyses. * = ratio from Bobra et al. (1992). Ali. HC = aliphatic hydrocarbons; Arom. HC = aromatic hydrocarbons; Asph. = asphaltenes.*

The composition of the non-degraded Santa Maria Basin (SMB) crude oil, H1 (Table 4.3.1, Fig. 4.3.1), is dominated by (in order of abundance) resins (44%), aromatic hydrocarbons (23%), aliphatic hydrocarbons (20%) and asphaltenes (13%). Comparison of the H1 and H7 Iatroscan-FID results in Figure 4.3.1, indicates that biodegradation has reduced both the aliphatic and aromatic hydrocarbon concentrations (20% to 13%, & 23% to 18% respectively), while the resin and asphaltene concentrations have increased (44% to 51% & 13% to 18% respectively). Consequently, the order of dominance for the biodegraded Santa Maria Basin (SMB) crude oil, H7, is resins, asphaltenes and aromatic hydrocarbons, and lastly aliphatic hydrocarbons.

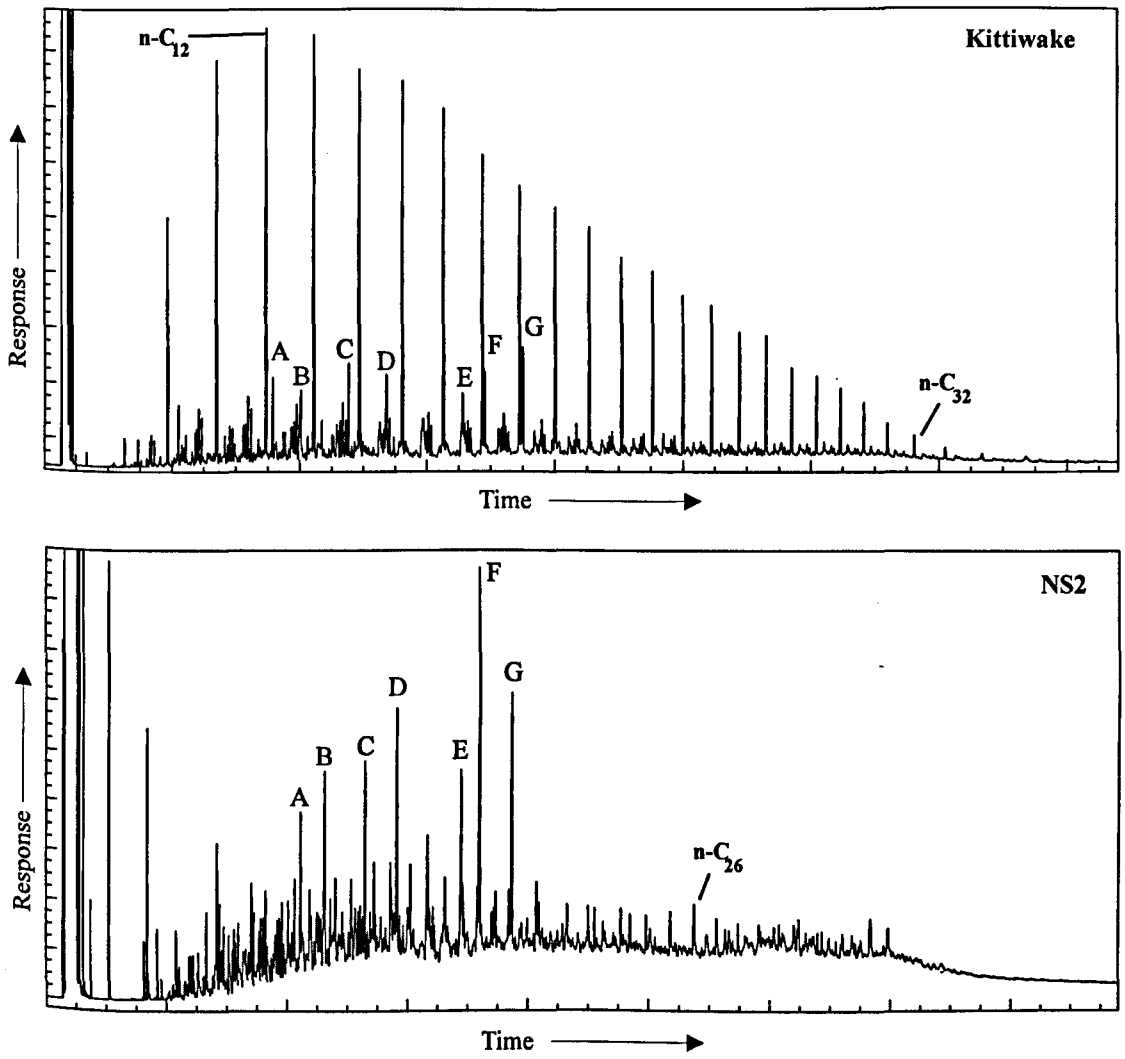

Figure 4.3.2. Comparison of the aliphatic hydrocarbon gas chromatograms for the Kittiwake and NS2 crude oils. Regular acyclic isoprenoid peak assignments (and abbreviations) are as follows: ***A*** *= 2,6,10-trimethyldecane (i-C_{13});* ***B*** *= 2,6,10-trimethylundecane (i-C_{14});* ***C*** *= 2,6,10-trimethyldodecane (farnesane, i-C_{15});* ***D*** *= 2,6,10-trimethyltridecane (i-C_{16});* ***E*** *= 2,6,10-trimethylpentadecane (norpristane, 1-C_{18});* ***F*** *= 2,6,10, 14-tetramethylpentadecane (pristane, Pr);* ***G*** *= 2,6,10, 14-tetramethylhexadecane (phytane, Ph).*

4.3.1.2. Analysis of the Chemical Composition of Blend Fraction and Comparison with the Bulk Chemistry of the Whole Oil Fractions.

Iatroscan-FID results for blend fractions (supernatant oil, unbound oil & bound oil fractions), as well as whole oil fractions, for most crude oils, are displayed in Figure 4.3.3 (only the whole oil & bound oil fraction are displayed for Santa Maria Basin crude oils).

The whole oil, supernatant oil and unbound oil fractions for A29, NS1 & NS2 crude oils, are seen to possess similar compositions. For example, the chemical composition for the fractions of A29 crude oil all possess aliphatic hydrocarbon concentrations of approximately 46%, aromatic hydrocarbon compositions of approximately 34% and total NSO concentrations of approximately 20%. Therefore, in future discussion, the whole oil fraction will also represent the supernatant and unbound oil fractions (Section 4.4.2).

The chemical compositions of all the extracted bound oil fractions are dominated by asphaltene and resin groups (Figs. 4.3.3 & 4.3.4).

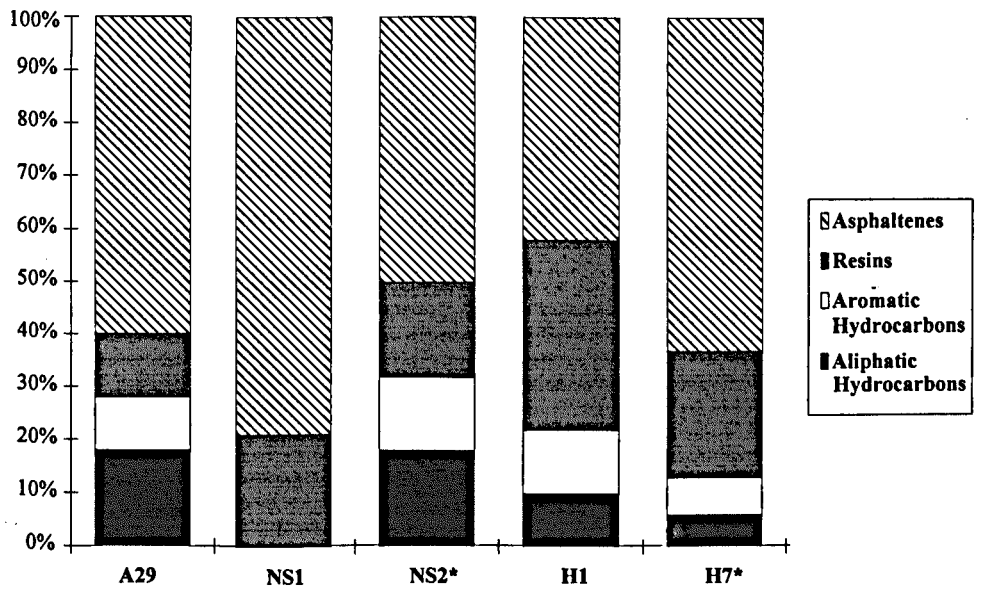

*Figure 4.3.4. Histogram of the chemical composition of the bound oil fractions. Determined by Iatroscan-FID. Biodegraded oils are highlighted by *.*

Comparison of the asphaltene concentration of the whole oil and emulsion/bound oil fractions, indicates a significant increase in the emulsion/bound oil fraction. Overall, the approximate change in asphaltene concentration, for North Sea crude oils, is from 4% to 60%. In addition, aliphatic hydrocarbon concentrations

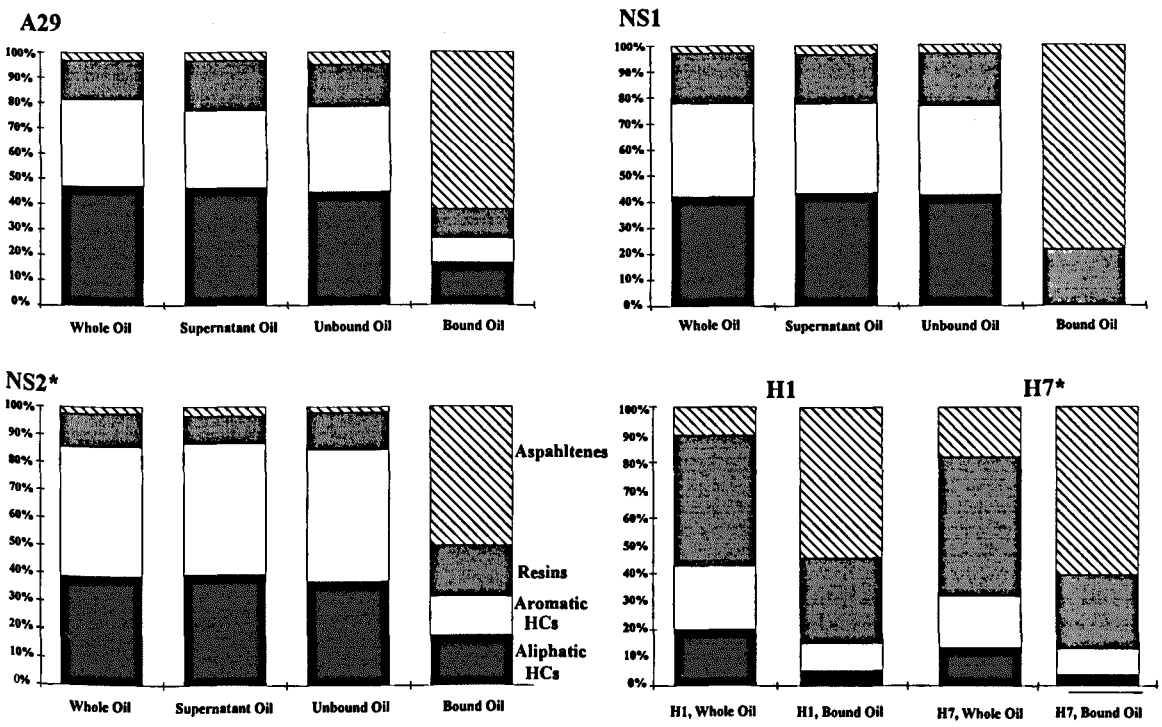

*Figure 4.3.3. Histograms of the chemical composition (Iatroscan-FID) of the whole oil and blend fractions (supernatant oil, unbound oil & bound oil fractions) for the A29, NS1, NS2, H1 and H7 crude oils. * = biodegraded crude oils. HCs = hydrocarbons.*

drop from 30-40% to 0-17%, and the aromatic hydrocarbon concentrations from 35-45% to 0-10%.

The asphaltene concentrations for SMB crude oils are from approximately 16%, in the whole oil fractions, to 58%, in the bound oil fractions. The aliphatic and aromatic hydrocarbons drop from approximately 17% and 21% to 8% and 9% respectively.

4.3.2. Wax Analysis.

4.3.2.1. Analysis of the Extracted Wax Content of Whole Oil Fractions.

Analysis of *n*-C_{30} peaks in the high temperature gas chromatograms, for the wax extracts, from biodegraded and non-degraded crude oils (Figs. 4.3.5 to 4.3.7), was made to assess the effect of biodegradation upon crude oil wax content. Examination of the non-degraded North Sea crude oils, illustrated in Figure 4.3.5, found that the *n*-C_{30} peak responses approximated to weights which varied from 8 x 10^{-4} to 0.6 x 10^{-4} mg. The *n*-C_{30} peaks for degraded North Sea crude oils, NS2 and NS3 illustrated in Figure 4.3.6, possessed values of 1.6 x 10^{-4} and 0.4 x 10^{-4} mg respectively. Therefore, no clear indication of the effect of biodegradation upon North Sea crude oil wax content was found, with the *n*-C_{30} peak for the NS3 oil reducing relative to non-degraded North Sea crude oil, while the *n*-C_{30} peak for the NS2 oil was uneffected. A clearer relationship between biodegradation and wax content was observed for the SMB crude oils, H1 and H7 (Fig. 4.3.7). The H7 *n*-C_{30} peak is reduced by an order of magnitude in comparison to the H1 peak, dropping from the non-degraded value of 0.8 x 10^{-4} mg to the biodegraded value of 0.08 x 10^{-4} mg.

Although the wax contents were reduced by biodegradation no preferential removal was observed. Therefore, wax distributions for all crude oils (both North Sea & SMB) had maximum peak heights at approximately *n*-C_{30}. All the wax fractions analysed for non-degraded North Sea crude oils possess *n*-alkane distributions of approximately *n*-C_{15} to *n*-C_{60}. The distributions for wax fractions extracted from biodegraded North Sea crude oils ranged from *n*-C_{21} upto *n*-C_{70} and have lost the sub *n*-C_{21} *n*-alkanes. The Santa Maria Basin crude oils (Fig. 4.3.7) show slight differences to the North Sea crude oil wax extract distributions. H1 strongly resembles the North Sea non-degraded crude oils with a distribution from *n*-C_{16} to *n*-C_{54}, with a maximum peak height at *n*-C_{31}. The wax extract high temperature gas chromatogram, for the H7 crude oil shows that the waxes have been strongly reduced, although, unlike the reduced wax distribution for biodegraded North Sea crude oils,

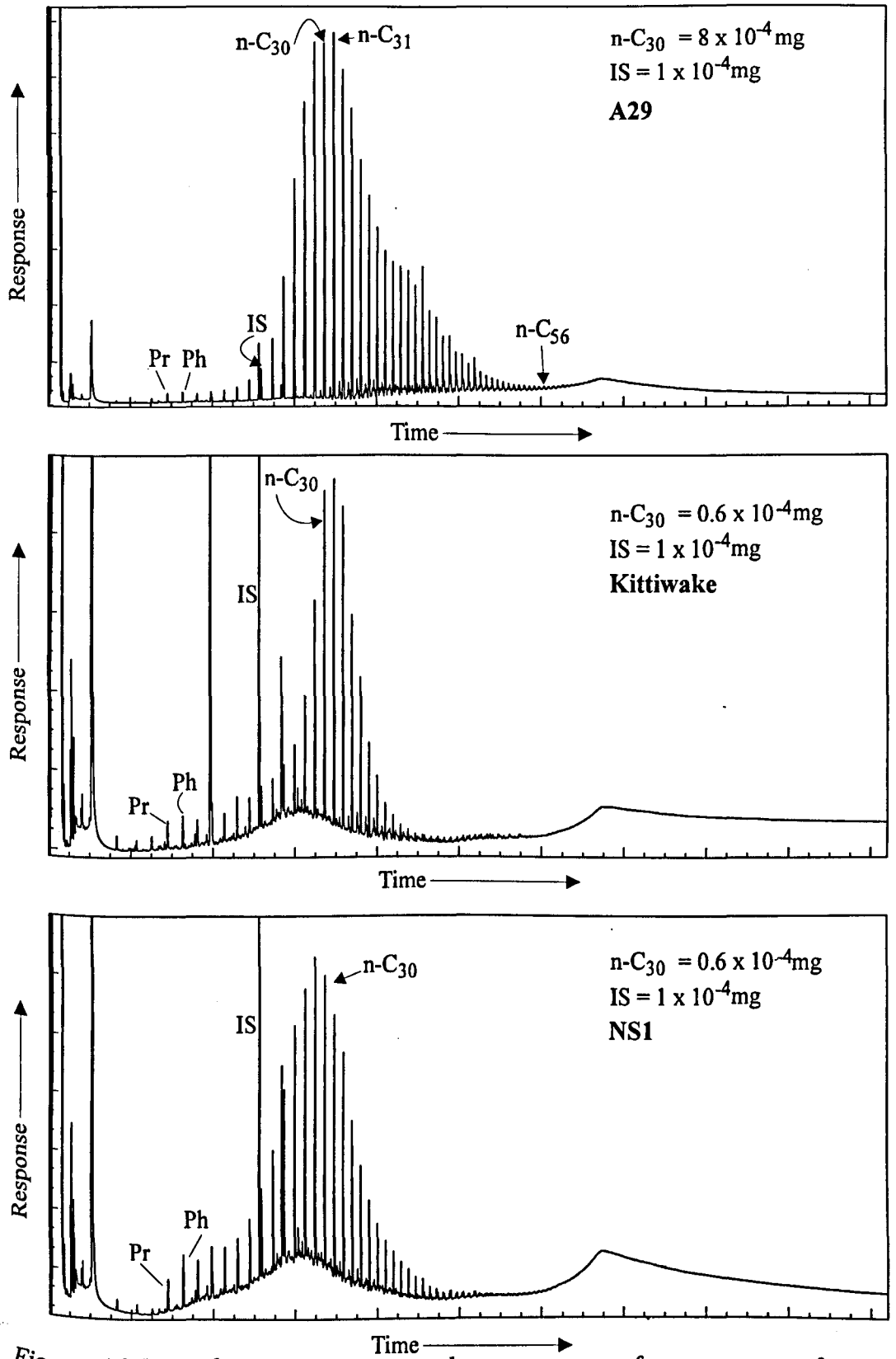

Figure 4.3.5. High temperature gas chromatograms of wax extracts from non-degraded North Sea crude oils (A29, Kittiwake, NS1). The equivalent weight of the n-C_{30} peak is shown. IS = internal standard (heptadecylcylohexane). Pr = pristane; Ph = phytane.

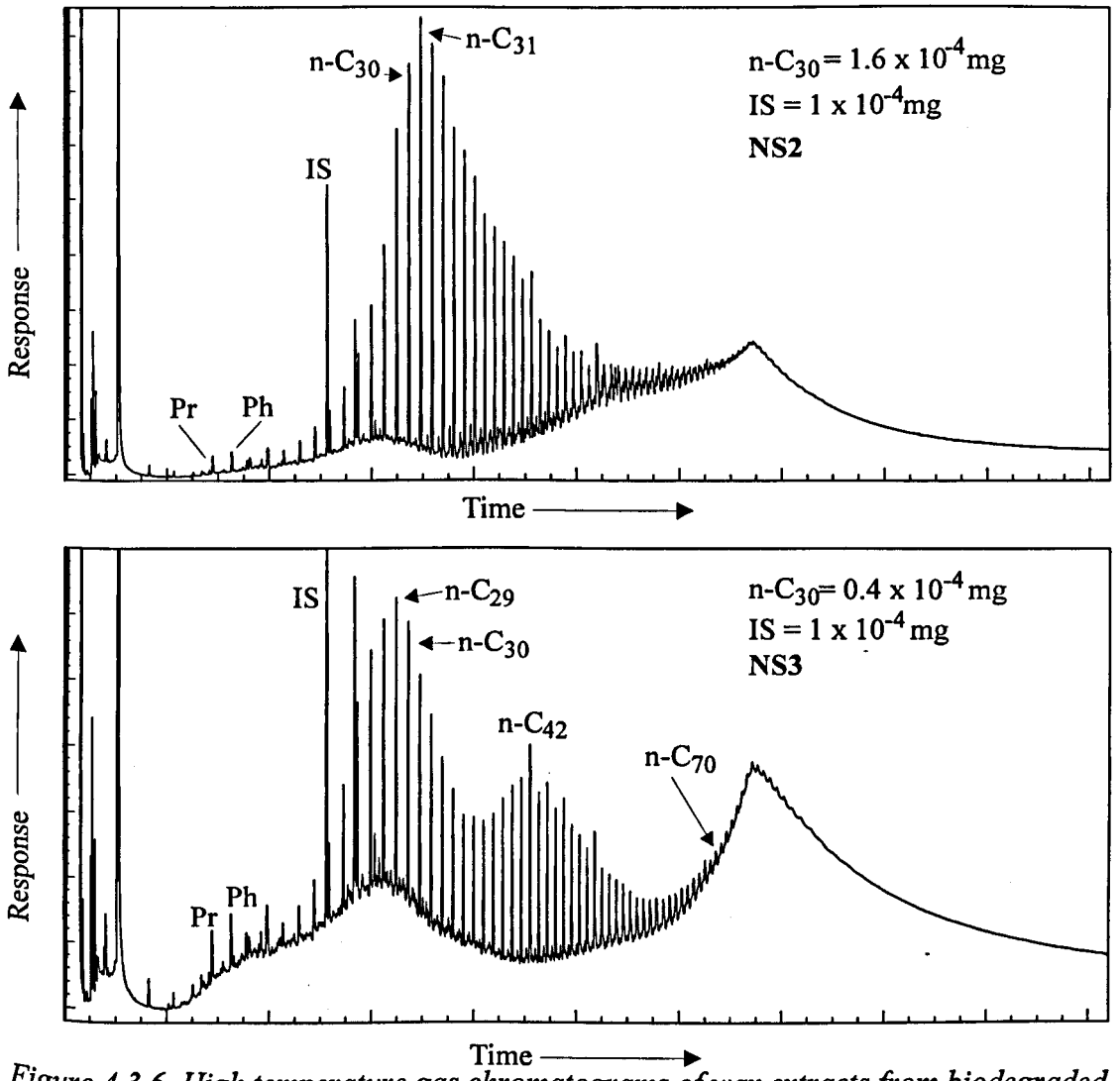

Figure 4.3.6. High temperature gas chromatograms of wax extracts from biodegraded North Sea crude oils (NS2, NS3). The equivalent weight of n-C_{30} peak is shown. IS = internal standard (heptadecylcyclohexane). Pr = pristane; Ph = phytane.

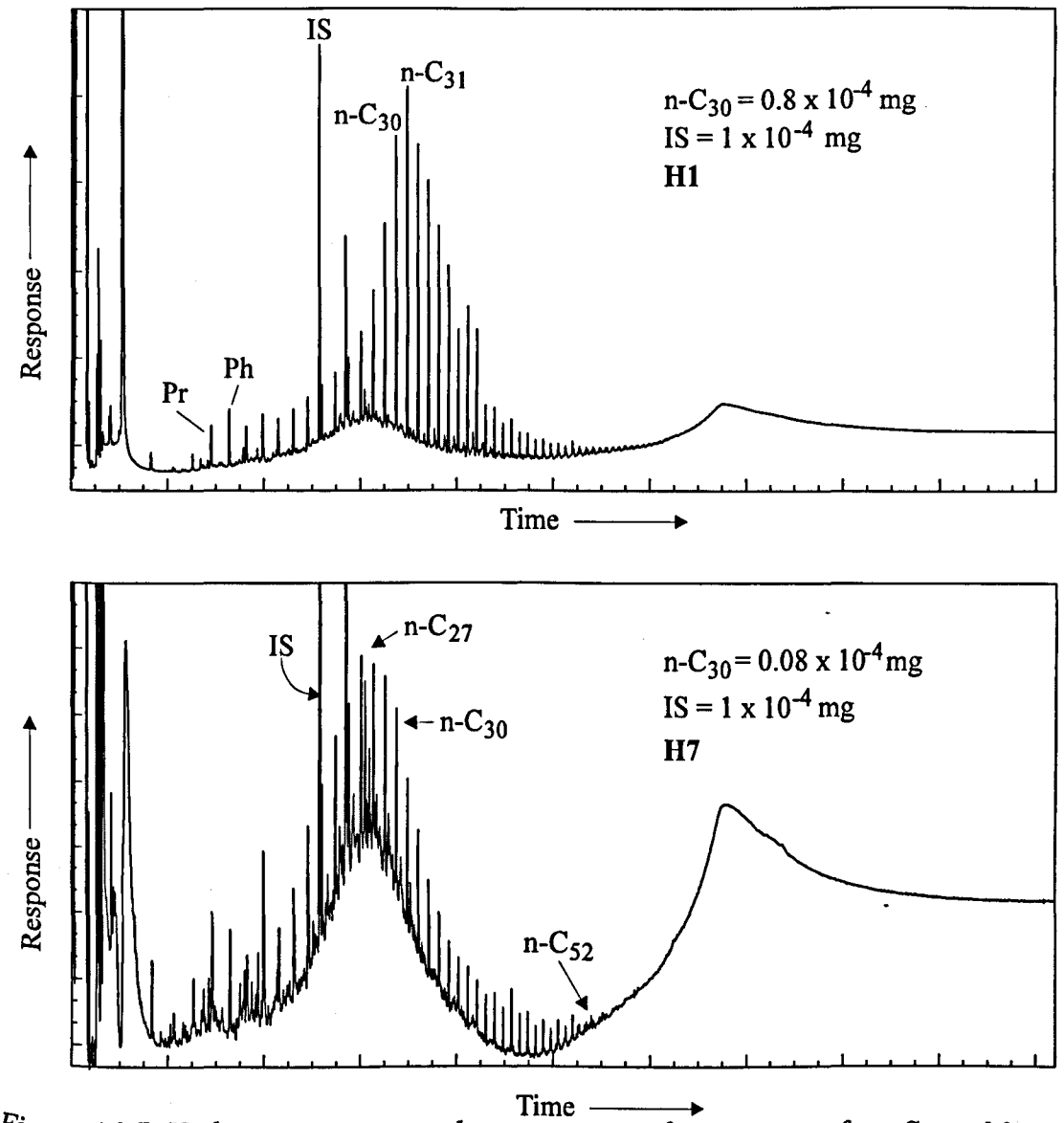

Figure 4.3.7. High temperature gas chromatograms of wax extracts from Santa Maria Basin crude oils (H1 & H7). The equivalent weight of n-C_{30} peak is shown. IS = internal standard (heptadecylcyclohexane). Pr = pristane; Ph = phytane.

waxes are still present below *n*-C_{21}. The wax distribution for H7 is from *n*-C_{15} to *n*-C_{52}, displaying a maximum peak height at *n*-C_{27}.

4.3.2.2. Analysis of the Aliphatic Hydrocarbon Fractions from Bound Oil Samples.

Results from the gas chromatographic analyses of the aliphatic hydrocarbon extracts from the whole oil and bound oil fractions, for several crude oils, are illustrated in Figures 4.3.8 to 4.3.10. In Figure 4.3.8, the A29 whole oil and bound oil aliphatic hydrocarbon distributions are compared. The whole oil has an aliphatic hydrocarbon distribution of *n*-C_{12} to *n*-C_{38}, with a maximum peak height at *n*-C_{15}. The A29 bound oil fraction displays a bimodal aliphatic hydrocarbon distribution ranging from *n*-C_{11} to *n*-C_{44}, with maximum peak heights at *n*-C_{16} and *n*-C_{37}. The bound oil fraction is therefore enriched in high molecular weight hydrocarbons.

In Figure 4.3.9, the aliphatic hydrocarbon gas chromatograms of the whole oil and bound oil fractions for the biodegraded NS2 crude oil may be seen. It is seen that enhancement of the high molecular weight hydrocarbons (HMWHCs), in the bound oil fraction, has occurred. The *n*-alkane distribution for the whole oil fraction ranges from approximately *n*-C_{13} to *n*-C_{28} (identification is difficult due to biodegradation), while the aliphatic hydrocarbon distribution for the bound oil fraction is from *n*-C_{12} to *n*-C_{44}. Due to biodegradation both the aliphatic hydrocarbon distributions are dominated by isoprenoids.

Figure 4.3.10, displays the aliphatic hydrocarbon chromatograms for the whole oil and bound oil fractions from the biodegraded H7 crude oil. Again the high molecular weight n-alkanes have been enhanced. The whole oil aliphatic hydrocarbon distribution is from *n*-C_{11} to *n*-C_{27} while the aliphatic hydrocarbon distribution for the bound oil fraction is from *n*-C_{10} to *n*-C_{43}. The dominant peaks for both whole oil and bound oil distributions are the isoprenoids.

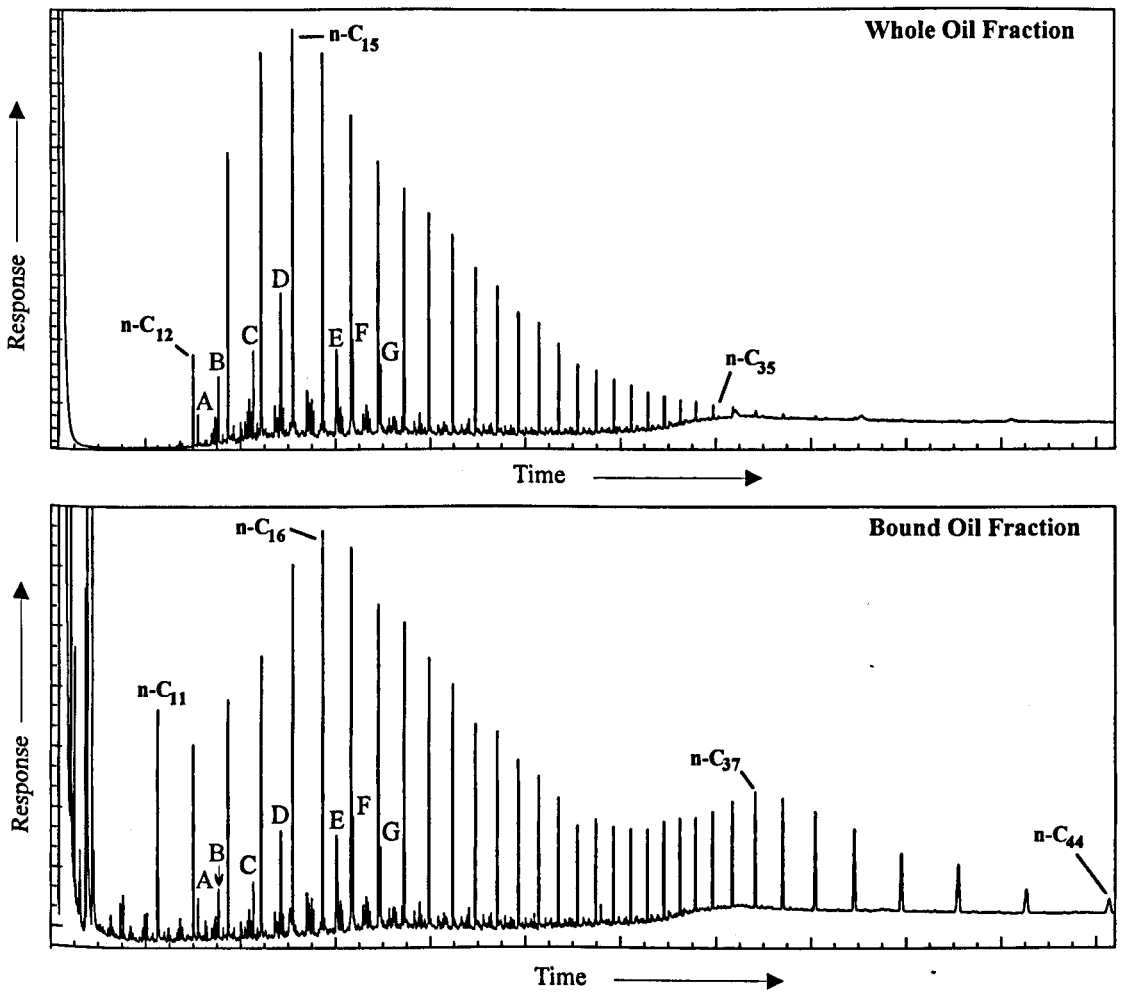

Figure 4.3.8. Comparison of gas chromatograms of aliphatic hydrocarbon distributions for whole oil and bound oil fractions from the A29 crude oil. Chromatograms illustrate the increase of wax in the bound oil fraction. Regular acyclic isoprenoid peak assignments (and abbreviations) are as follows: ***A*** *= 2,6,10-trimethyldecane (i-C_{13});* ***B*** *= 2,6,10-trimethylundecane (i-C_{14});* ***C*** *= 2,6,10-trimethyldodecane (farnesane, i-C_{15});* ***D*** *= 2,6,10-trimethyltridecane (i-C_{16});* ***E*** *= 2,6,10-trimethylpentadecane (norpristane, 1-C_{18});* ***F*** *= 2,6,10, 14-tetramethylpentadecane (pristane, Pr);* ***G*** *= 2,6,10, 14-tetramethylhexadecane (phytane, Ph).*

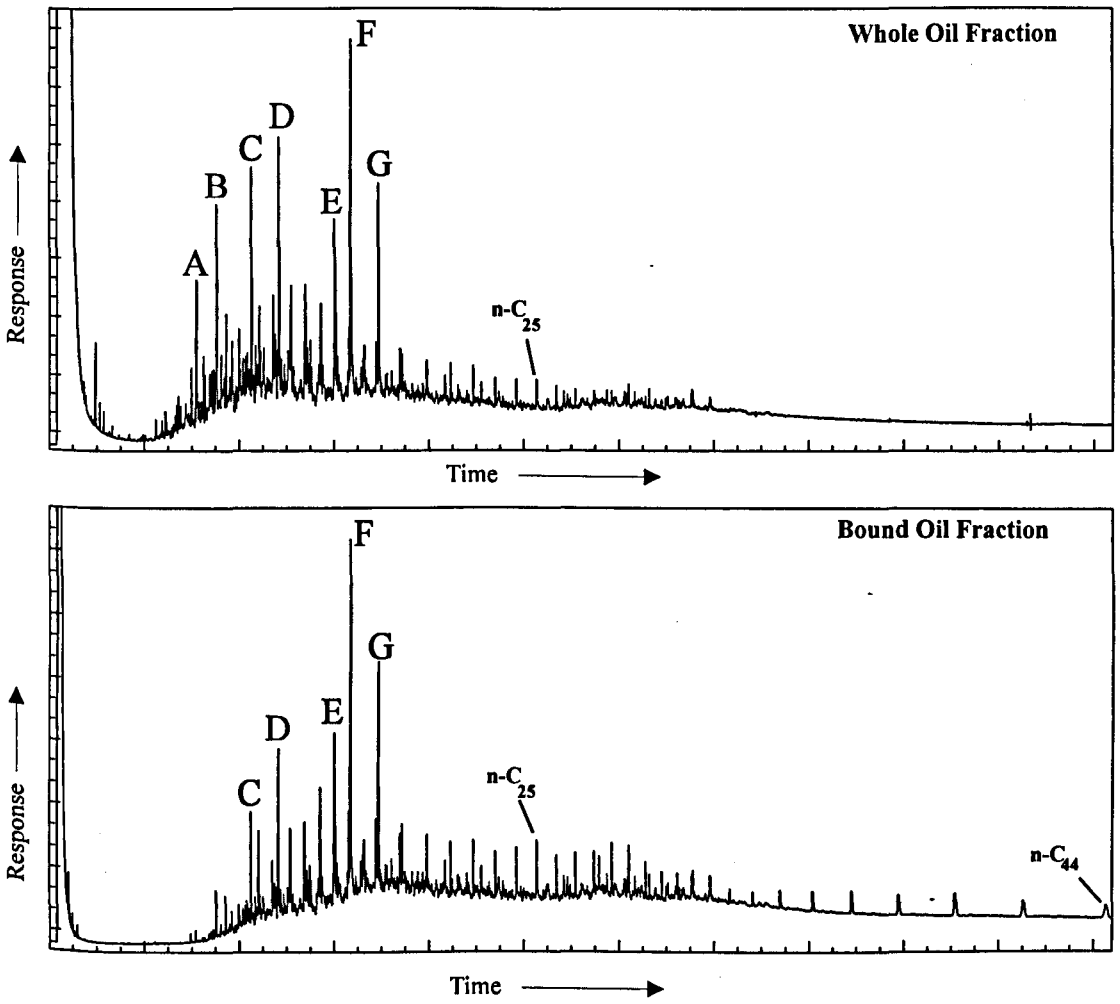

*Figure 4.3.9. Comparison of gas chromatograms of aliphatic hydrocarbon distributions for whole oil and bound oil fractions from the NS2 crude oil. Chromatograms illustrate the increase in wax in the bound oil fraction. Regular acyclic isoprenoid peak assignments (and abbreviations) are as follows: **A** = 2,6,10-trimethyldecane (i-C_{13}); **B** = 2,6,10-trimethylundecane (i-C_{14}); **C** = 2,6,10-trimethyldodecane (farnesane, i-C_{15}); **D** = 2,6,10-trimethyltridecane (i-C_{16}); **E** = 2,6,10-trimethylpentadecane (norpristane, 1-C_{18}); **F** = 2,6,10, 14-tetramethylpentadecane (pristane, Pr); **G** = 2,6,10, 14-tetramethylhexadecane (phytane, Ph).*

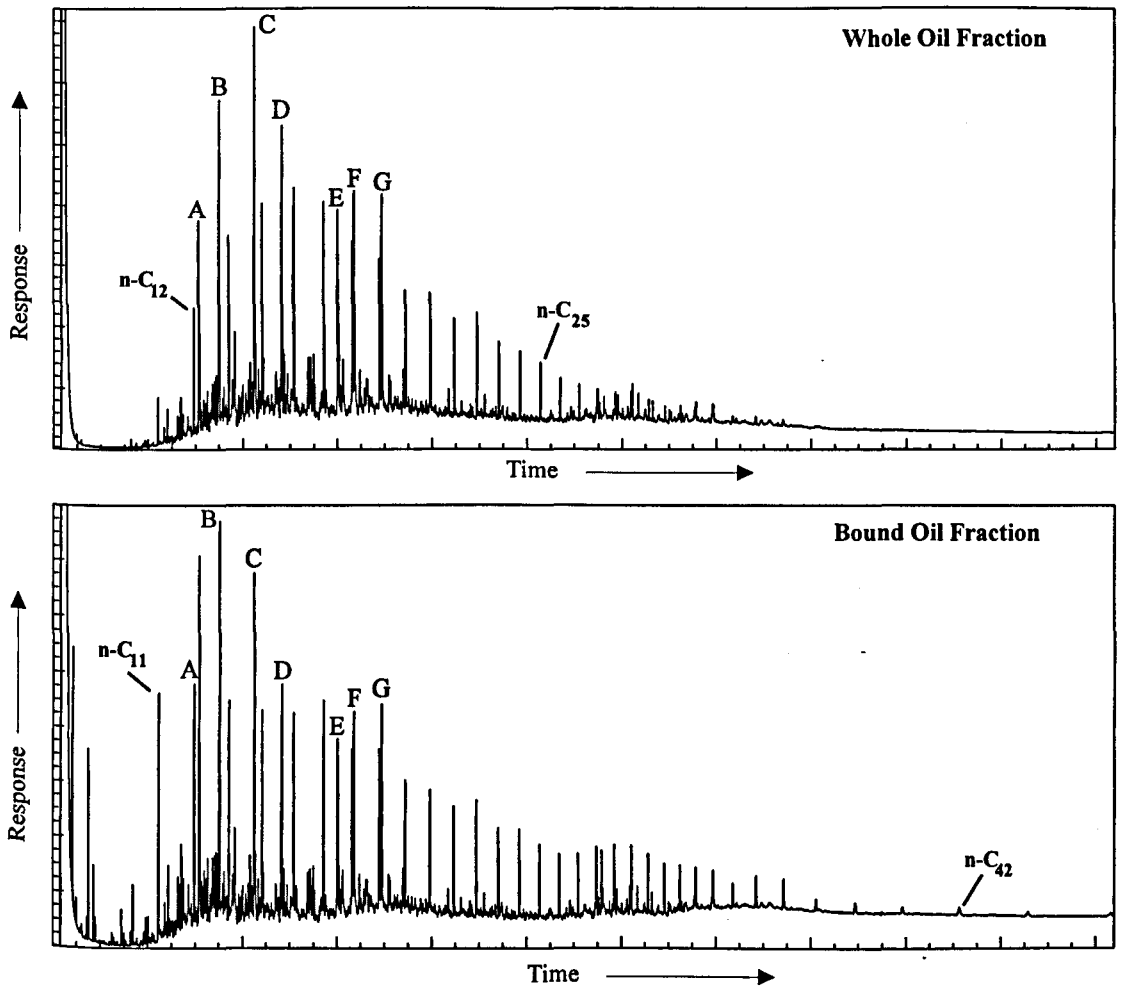

Figure 4.3.10. Comparison of gas chromatograms of aliphatic hydrocarbon distributions for whole oil and bound oil fractions from the H7 crude oil. Chromatograms illustrate the increase in wax in the bound oil fraction. Regular acyclic isoprenoid peak assignments (and abbreviations) are as follows: ***A*** *= 2,6,10-trimethyldecane (i-C_{13});* ***B*** *= 2,6,10-trimethylundecane (i-C_{14});* ***C*** *= 2,6,10-trimethyldodecane (farnesane, i-C_{15});* ***D*** *= 2,6,10-trimethyltridecane (i-C_{16});* ***E*** *= 2,6,10-trimethylpentadecane (norpristane, 1-C_{18});* ***F*** *= 2,6 10, 14-tetramethylpentadecane (pristane, Pr);* ***G*** *= 2,6,10, 14-tetramethylhexadecane (phytane, Ph).*

4.4. Discussion.

4.4.1. Emulsion and Bound Oil Fractions.

In Figure 4.3.4, it may be seen that the bound oil fractions are dominated by the asphaltene group, concentrations ranging from 50% to 79%, with the resin concentrations varying from 12% to 35%. On average the total NSO concentration for bound oil fractions was approximately 82% and in one instance (NS1), the bound oil phase consisted entirely of NSO compounds (100% concentration). For asphaltenes to remain in colloidal suspension or polymer solution, the resin content should be approximately double that of the asphaltene content (Leontaritis, 1988). Therefore, it appears likely that the majority of asphaltenes at the oil/water interface (bound oil fraction) have precipitated from the crude oil. Identification of the presence of asphaltene sols at the crude oil/water interface is in agreement with the general concepts for the formation and stabilisation of water-in-oil emulsions, discussed in Section 1.2.2.1 (Schramm, 1992; Acevedo *et al.*, 1992).

The wax extraction and analysis techniques, applied to whole oil fractions, could not be applied to the bound oil fractions due to their low extract weights (1 to 10 mg, Table 5.2.2). However, extraction and analysis of the aliphatic hydrocarbons from the bound oil fractions, by thin layer chromatography (TLC) coupled with gas chromatography (GC), was able to provide information upon wax content. Comparison of the aliphatic hydrocarbon gas chromatograms (Figs. 4.3.8 to 4.3.10) for the whole oil and bound oil fractions from the A29, NS1 and H7 crude oils, highlighted enrichment of low and high molecular weight *n*-alkanes in the bound oil fraction. The higher molecular weight waxes (above *n*-C_{30}), exhibited the greatest enrichment. N-alkane distributions for bound oil samples were found to be from *n*-C_{10} to *n*-C_{44} however, it was seen that wax peaks had not finished eluting by the end of the gas chromatographic temperature programme therefore, the *n*-alkane distributions are probably greater than *n*-C_{44}.

Due to the poor resolution of the aliphatic hydrocarbon peaks with increasing elution time, due to peak broadening, peak heights do not give clear indication of the enhancement of waxes. Therefore, a plot of the normalised peak areas (normalised to the largest peak area in the chromatogram) for both whole oil and bound oil fractions from the A29, NS2 and H7 crude oils, are seen in Figure 4.4.1, and provides a better indication of wax enhancement.

The normalised peak area distributions for whole oil and bound oil fractions of the A29 crude oil clearly indicate that the bound oil fraction is relatively enriched in high molecular weight waxes. The distribution has a maximum peak area at *n*-C_{39},

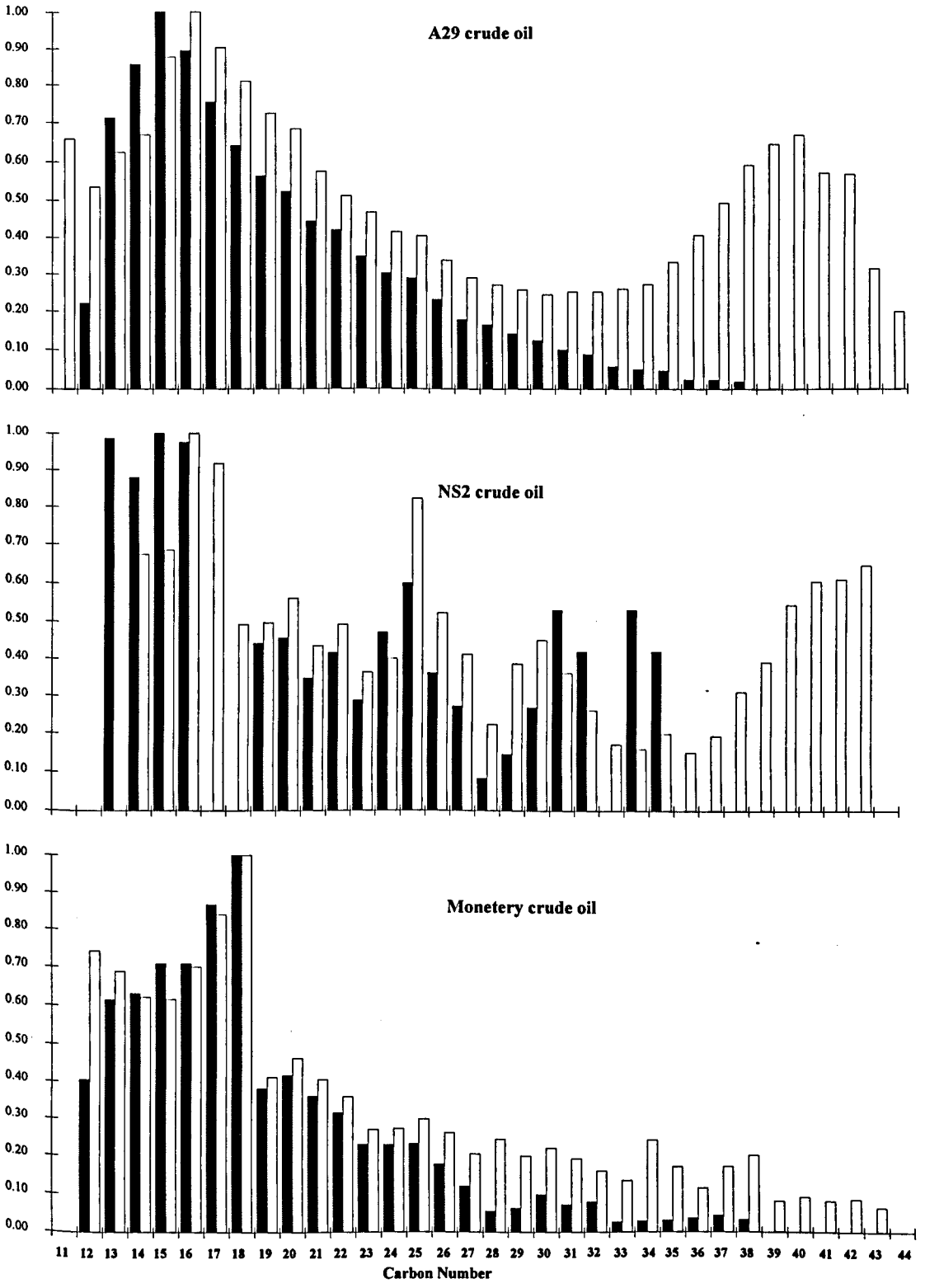

Figure 4.4.1. Comparison of the normalised peak areas (normalised to the largest peak area for each fraction) of aliphatic hydrocarbon distributions for whole oil and bound oil fractions from A29, NS2 and H7 crude oils. ■ *= whole oil fraction;* □ *= bound oil fraction.*

enhancement occurring from approximately n-C_{28} upwards. In the distributions for the NS2 crude oil, enhancement is less clear due to the effect of biodegradation. However, distribution for the whole oil sample is from n-C_{12} to n-C_{33} while high molecular weight enhancement, in the bound oil sample, is clearly evident from n-C_{35} to n-C_{43}. As with the distribution for the NS2 oil fractions, the H7 oil fractions have been affected by biodegradation and therefore, identification of enhancement is difficult. However, it is seen that enhancement has occurred in the bound oil fraction from approximately n-C_{28} upwards.

Iatroscan-FID and aliphatic hydrocarbon gas chromatographic analyses identified the preferential enrichment of both asphaltenes and waxes in the bound oil fractions. This research therefore agrees with the reported literature, which identified that the stabilisation of water-in-oil emulsions was dependent upon the presence of asphaltene and wax groups at the crude oil/water interfacial film (Graham *et al.*, 1983; Thompson *et al.*, 1985; Bobra *et al.*, 1992; Schramm, 1992).

4.4.2. Bulk Chemical Assessment of the Whole Oil, Supernatant Oil and Unbound Oil Fractions.

Work in Section 4.3.1.2 has already assumed that the whole oil, supernatant oil and unbound oil fractions were identical. However, as the latter two fractions have been blended with an aqueous phase it was considered necessary to assess if this would have altered their bulk compositions.

There were two mechanisms which may have altered the chemical composition of the supernatant oil and unbound oil fractions. These were; (1) the preferential adsorption of compounds to the oil/water interfacial film and (2) the loss of the water soluble fraction (WSF) to the aqueous phase. The unbound oil fraction was considered to have the greatest potential for alteration due to it's close proximity to the bound oil fraction (Fig. 4.2.2).

Assessment of the preferential adsorption of organics from the unbound oil to the oil/water interfacial film (bound oil phase) is assessed by a mass balance in Figure 4.4.2. It may be seen that subtraction of the approximate weights (small weights are subject to balance error and are reported as approximates) of each constituent group (aliphatic hydrocarbons etc.) in the bound oil (approximate total extract 10 mg, Table 5.3.1), from those of the unbound oil (approximate total extract from an initial crude oil quantity of 6 g = 2.8 g), has no significant effect upon the overall composition of the unbound oil fraction.

	Unbound Oil Composition (2,800 mg)*	-	Bound Oil Composition (10 mg)*	=	Altered Unbound Oil Composition (2,790 mg)*
Asphaltenes	3% (84 mg)	-	60% (6 mg)	=	2.8% (78 mg)
Resins	16% (448 mg)	-	10% (1 mg)	=	16% (447 mg)
Aromatic Hydrocarbons	34% (952 mg)	-	8% (0.8 mg)	=	34.1% (951.2 mg)
Aliphatic Hydrocarbons	47% (1316 mg)	-	12% (1.2 mg)	=	47.1% (1314.8 mg)

*Figure 4.4.2. Mass balance, showing the subtraction of the overall weights of the constituents of the bound oil fraction from those of the unbound oil fraction, both extracted from an A29 crude oil/water blend. Alteration to the composition of the unbound oil fraction is shown. * = approximate extract weights.*

Losses due to the water washing of water soluble fractions (WSFs) were also thought to be inconsequential in the fractions analysed. Work by Shiu *et al.* (1990) found that loss of WSFs was governed by the water:oil ratio, with the loss of WSF increasing with the water:oil ratio, as shown in Figure 4.4.3. The water:oil ratio for these crude oil/water blends was approximately 0.15 (3 ml water/ 7 ml oil) therefore, the loss of the WSF for the unbound oil, at this ratio, would be negligible. Water washing is discussed in more detail in Chapter 6.

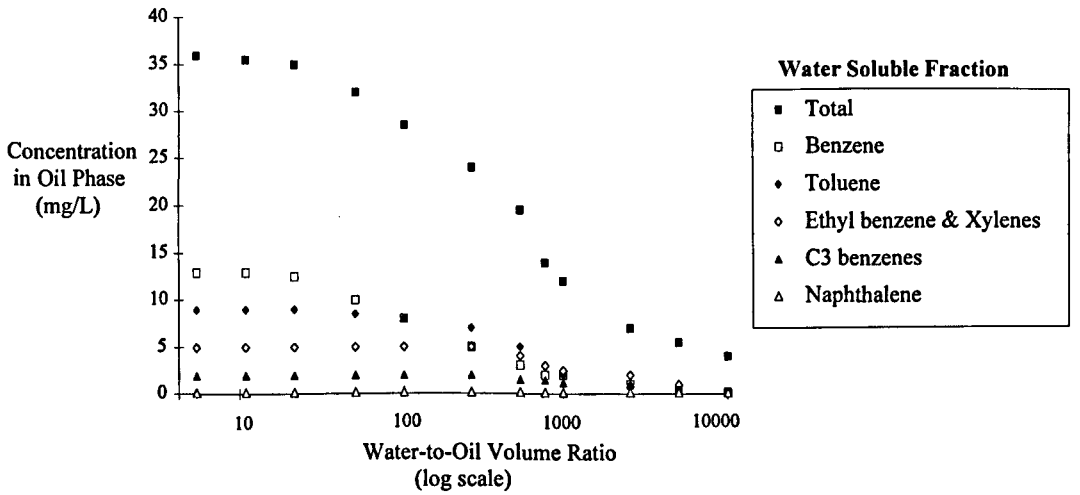

Figure 4.4.3. Illustration of the reduction in concentration of specific aromatic hydrocarbons (water soluble fraction) in Western Sweet Mixed Blend crude oil with increasing exposure to water (increasing water-to-oil ratio). Taken from Shiu et al. (1990).

Therefore, the supernatant and unbound oil fractions were expected to have bulk chemistries very similar to those of the whole oils. This was confirmed by results from Iatroscan-FID analysis, identifying that the bulk compositions of the whole oil, supernatant oil and unbound oil fractions (Fig. 4.3.3), from various crude oils, were similar. In addition, the molecular analysis of the aliphatic hydrocarbons from whole oil, supernatant oil and unbound oil fractions by gas chromatography (Fig. 4.4.4) for A29 crude oil, were also similar. The loss of n-C_{11} in the aliphatic hydrocarbon gas chromatograms for the supernatant and unbound oil fractions, in Figure 4.4.4, was attributed to evaporation during work up procedures.

4.4.2.1. Assessment of the Asphaltene Precipitation Potential of Whole Oil Fractions.

In addition to the bulk chemical analyses in Chapter 3 which were used to characterise the emulsion formation/stabilisation ability of crude oils, assessment of asphaltene precipitation potential was also performed by use of the aliphatic and aromatic hydrocarbon ratio employed by Bobra *et al.* (1992). According to Bobra *et al.* (1992), oils with aliphatic:aromatic hydrocarbon (Ali:Arom) ratios of less than 1, would be characterised by poor asphaltene precipitation and consequently poor emulsion formation/stabilisation properties (Chapter 1). Results from this investigation found that the crude oils A29 (Ali:Arom = 1.50), NS1 (Ali:Arom = 1.40), NS2 (Ali:Arom = 0.95) and NS3 (Ali:Arom = 0.50) were in agreement with the Bobra *et al.* (1992) hypothesis. When both the A29 and NS1 crude oils (Ali:Arom > 1) were blended with distilled water, stable water-in-oil emulsions were produced;

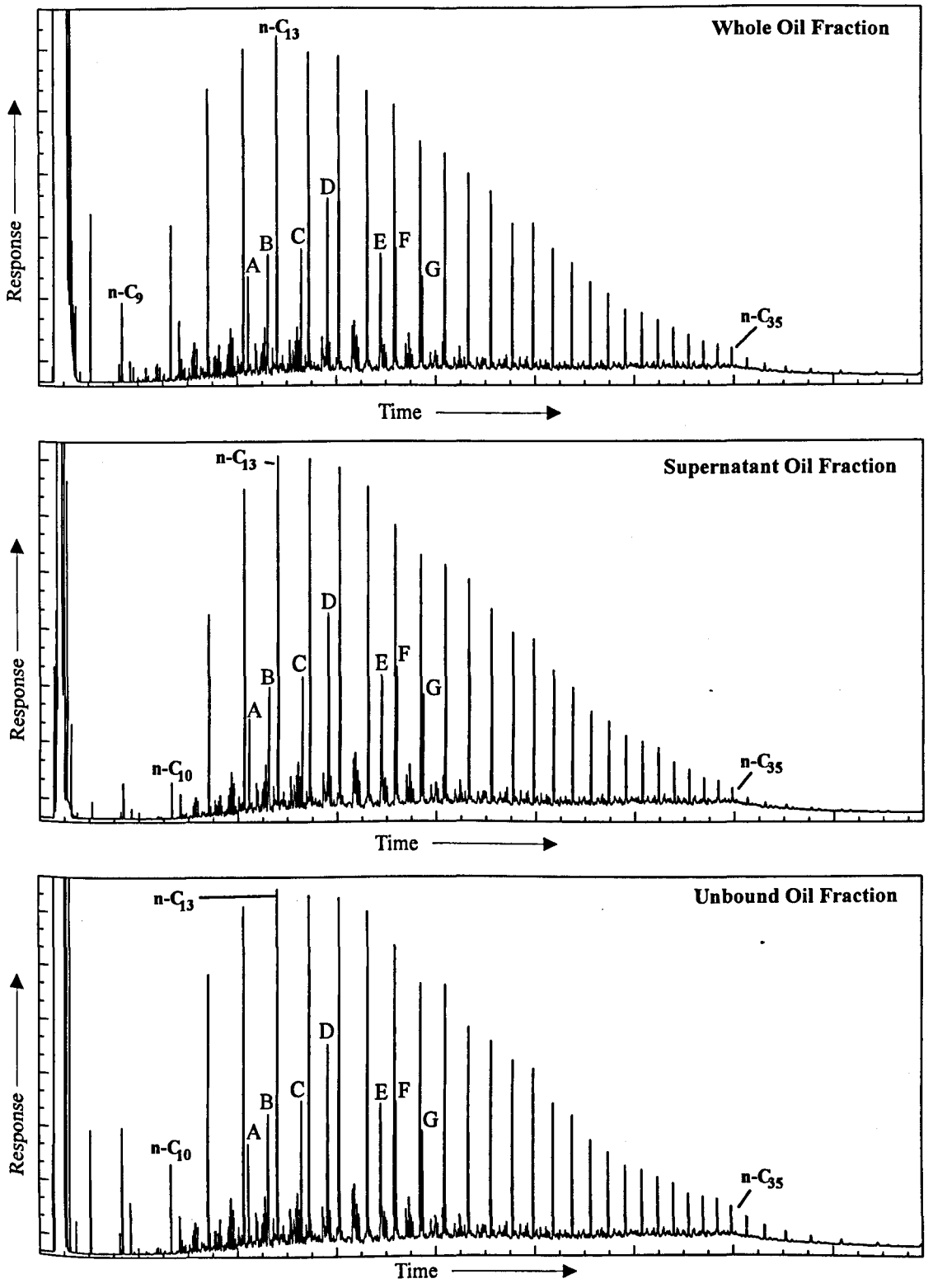

Figure 4.4.4. Comparison of the aliphatic hydrocarbon gas chromatograms for the whole oil, supernatant oil and unbound oil fractions from the A29 crude oil. F = pristane, G = phytane, A to E = other isoprenoids (Fig. 4.3.2).

while both the NS2 and NS3 crude oils (Ali:Arom < 1) produced poor (if any) emulsions. However, one North Sea crude oil (Kittiwake), and two SMB crude oils (H1 & H7) (Table 4.3.1), did not conform with this hypothesis, possessing Ali:Arom ratios of less than 1, yet forming stable, viscous, water-in-oil emulsions.

The high NSO contents of the two SMB crude oils was considered to be responsible for the formation of emulsions, promoting water/oil interactions and thereby stabilising emulsions (Chapter 3). However, a possible explanation of the ability of Kittiwake crude oil to form stable water-in-oil emulsions was gained by comparison of its chemical composition with that for the NS2 crude oil. It is seen in Figure 4.3.1 and Table 4.3.1, that the bulk chemistries of Kittiwake and NS2 crude oils possess some similarities. Both are dominated by the aromatic hydrocarbons (approximately 44%) followed in abundance by the aliphatic hydrocarbons (approximately 38%) and NSOs (approximately 15% - 22%). In addition, both have Ali:Arom ratios below 1, with wax extract concentrations of approximately 0.8wt%. However, work in Chapter 3 (Table 3.3.3), highlights that these two crude oils possessed different emulsion formation/stabilisation properties. The Kittiwake crude oil formed a stable, viscous water-in-oil emulsion while the NS2 did not, instead forming a weak emulsion associated with a separated water phase. These characteristics suggest that their different emulsion formation/stabilisation abilities may be attributed to subtle compositional differences not observed with Iatroscan-FID analysis.

In Figure 4.3.2, it is seen that the Kittiwake aliphatic hydrocarbon distribution is dominated by the low molecular weight constituents, with an n-alkane distribution from n-C_{10} to n-C_{34} and a maximum peak height at n-C_{12}. However, the aliphatic hydrocarbon distribution of the NS2 crude oil is dominated by isoprenoids, with a microbially reduced n-alkane distribution of n-C_{13} to n-C_{27}. This difference in the aliphatic hydrocarbon distribution (Kittiwake dominated by low molecular weight n-alkanes; NS2 dominated by isoprenoids) will probably affect the solubility of asphaltene particles in the crude oils. It is probable that a lower molecular weight aliphatic hydrocarbon mixture (Kittiwake), will promote asphaltene precipitation to a greater degree (promoting stable water-in-oil emulsions) than a higher molecular weight aliphatic hydrocarbon mixture with reduced n-alkanes (NS2). Standard asphaltene precipitation techniques illustrate this effect. It is seen that a greater amount of asphaltene precipitate is produced by the use of low molecular weight aliphatic solvents, such as pentane, than higher molecular weight aliphatic solvents, such as heptane (Speight *et al.*, 1984; Kawanaka *et al.*, 1989, Sheu *et al.*, 1992a). Consequently, the ability of Kittiwake to form a stable water-in-oil emulsion is possibly attributed to the composition rather than quantity of its aliphatic hydrocarbon

fraction. Therefore, it is suggested that an appreciation of the aliphatic hydrocarbon composition is required before prediction of the asphaltene precipitation of a crude oil may be made. Therefore, the Ali:Arom ratio hypothesis, suggested by Bobra *et al.* (1992), does not offer a subtle enough assessment of the asphaltene precipitation ability of the Kittiwake crude oil.

4.4.2.2. Assessment of the Wax Precipitation Potential of Whole Oil Fractions.

Chapter 3 identified that the emulsion formation/stabilisation ability of a crude oil was affected by the extent of biodegradation. Examination of total wax extracts was able to highlight a trend between the reduction of wax content and increasing biodegradation. The SMB crude oils, H1 and H7, display total wax concentrations of 0.45wt% and 0.20wt% respectively (Table 4.3.1), indicating wax reduction with increased biodegradation. Comparisons between the non-degraded North Sea crude oils, A29 and Kittiwake (1wt% and 0.7wt% wax concentrations respectively), and biodegraded North Sea crude oils, NS2 and NS3 (0.66wt% and 0.46wt% wax concentrations respectively) also shows a relationship between wax reduction with increasing biodegradation. The differences between total wax extract concentrations of the non-degraded Californian crude oils H1, and the non-degraded North Sea crude oils, A29 and Kittiwake, was assumed to be due to differences in source rock type and level of maturation.

As work by Thompson *et al.* (1985) has shown that the crude oil wax content is related to water-in-oil emulsion stability, it was probable that the poor emulsion formation/stabilisation of crude oils may be partly attributed to the reduction of the wax content, due to biodegradation processes (Section 3.4.3).

However, a more precise assessment of the variation of the wax content of the crude oil, with increasing biodegradation, is presented in this chapter by use of a novel wax concentration/precipitation technique (Bishop *et al.*, 1994) coupled with high temperature gas chromatography (HTGC; del Rio *et al.*, 1992). Assessment of the high temperature gas chromatograms of the wax extracts from crude oils (Figs. 4.3.5 to 4.3.7), indicated that biodegradation had a profound effect upon wax distribution and concentration. The n-C_{30} peak responses were observed to generally decrease with increasing biodegradation. SMB crude oils provide the best and most reliable example of this relationship with the n-C_{30} response in the H7 crude oil being an order of magnitude less than H1.

Non-degraded crude oils exhibit wax distributions from n-C_{18} to approximately n-C_{60}, with maximum peak heights at approximately n-C_{30}. In general, reduction of the wax contents for biodegraded crude oils exhibited no preferential removal, maximum peak heights were maintained at approximately n-C_{30}. However the NS3 crude oil exhibited a bimodal wax distribution with maximum peak heights at n-C_{28} and n-C_{42}. This additional peak maximum may be attributed to preferential wax removal. Work by Hanstveit (1992), studying the degradation of different waxes, found that waxes of up to n-C_{50} could be degraded, regardless of their type (paraffin, crystalline etc., Section 1.2.2.2). The only restriction upon the biodegradation of waxes appeared to be their availability. It is possible therefore, that the second maximum in the NS3 wax extract may represent wax which was protected from biodegradation. As the presence of high molecular weight aliphatic hydrocarbons in asphaltenes has already been described by Bishop *et al.* (1994, Section 1.2.2.1; Fig. 1.9) one possibility may be that the waxes have occluded into the asphaltenes making them unavailable for biodegradation.

In conclusion, it is suggested that the reduction of the wax content of North Sea crude oils, due to biodegradation, is a contributory factor to their poor emulsion formation/ stabilisation abilities.

4.5. Conclusions.

This work has identified that the stability of the water-in-oil emulsions, isolated from crude oil/water blends, is associated with the preferential enrichment of the asphaltene and wax groups at the water/oil interface. It is considered that their presence indicates the formation of a rigid and protective interfacial film, essential for the stabilisation of water-in-oil emulsions (Schramm, 1992). The build up of asphaltene and wax particles at the crude oil/water interface was predominantly attributed to precipitation from the crude oil (Eley *et al.*, 1987; Bobra *et al.*, 1992).

Additional assessment of asphaltene precipitation potential, to that performed in Chapter 3, was gained by use of the aliphatic and aromatic hydrocarbon ratio. Results agreed with findings in Chapter 3, that the process of biodegradation appeared to make the asphaltene group more soluble in the crude oil phase, and therefore less likely to aid emulsion stabilisation. However, it was noted that results from the use of this ratio should be viewed cautiously, as it does not take into account the state of the aliphatic hydrocarbons, which may alter the asphaltene precipitation potential.

More detailed assessment of the wax content of crude oils also agreed with conclusions from Chapter 3, with reduction in wax contents being related to increasing biodegradation. This would therefore reduce the wax sols ability to stabilise water-in-oil emulsions.

Asphaltene and wax observations possibly explain the poor emulsion formation/stabilisation abilities of the biodegraded North Sea crude oils, NS2 and NS3, which were probably unable to form rigid and protective interfacial films. However, as concluded in Chapter 3, the stability of biodegraded Santa Maria Basin crude oil emulsions was suggested to be due to greater surfactant interactions between the oil and water phases due to their high NSO concentrations. More detailed investigation of the NSO compounds, and their variation with biodegradation is given in the following chapter.

CHAPTER 5:

ASSESSMENT OF THE EFFECT OF ALKYLPHENOLS ON CRUDE OIL WATER UPTAKE ABILITY.

CHAPTER 5: ASSESSMENT OF THE EFFECT OF ALKYLPHENOLS ON CRUDE OIL WATER UPTAKE ABILITY.

This chapter investigates the effect of the C_0-C_3 alkylphenols on the water retention and emulsion formation and stabilisation ability of crude oil. This is achieved in two ways. Firstly, by assessment of the variation of alkylphenols (both qualitative and quantitative) in various crude oils, relating the results to water uptake ability as well as the biodegradation state of crude oils. Secondly, by studying the distribution of the C_0-C_3 alkylphenols in crude oil and water blends, especially the alkylphenol concentration and distribution in the water-in-oil emulsions.

5.1. Introduction.

The water uptake ability of crude oils has been categorised in Chapter 3 by the assessment of the water retention and water-in-crude oil emulsion formation/ stabilisation ability. The degree of water retention has been related to the biodegradation state of the crude oils, with both crude oil physicochemical properties and NSO content (Chapter 3) possibly influencing the degree of retention. The formation and stabilisation of water-in-crude oil emulsions has also been related to the degree of biodegradation and the resultant effects upon the presence of emulsifiers (asphaltene and wax precipitates, as well as the crude oil surfactants) at the oil and water interface. These emulsifiers have been reported in the literature as vital for the formation of the rigid and protective interfacial films, which are formed during oil/water blending in the laboratory, or during production, and stabilise water-in-oil emulsions (Bobra *et al.*, 1992, Schramm, 1992).

The previous chapter assessed the variation of the bulk chemistry of crude oils (in particular asphaltene and wax concentrations), in relation to their emulsion formation/stabilisation character and biodegradation state. In addition, assessment of the bulk chemical variation between the emulsion (bound oil) phase and whole oil phase was performed, emphasising the enrichment of asphaltene and wax groups at the crude oil/water interface. This chapter will perform detailed chemical assessment of a surfactant group attributed to stabilising water-in-oil emulsions, the C_0-C_3 alkylphenols (Layrisse *et al.*, 1984). In addition, work will attempt to relate alkylphenol concentrations and distributions to observed water retention ability in Chapter 3.

The ability of surfactants, such as phenols, to stabilise emulsions is based on their potential to interact with both crude oil and water phases (Israelachvili, 1991).

This amphiphilic nature is not uniform, and in general surfactants will react to a greater or lesser degree with one particular phase (Schramm, 1992). This characteristic will not only influence whether or not the surfactant may stabilise an emulsion, it will also affect the type of emulsion formed (water-in-crude oil emulsion or crude oil-in-water emulsion; Shaw, 1980). For the formation of water-in-oil emulsions the surfactant is generally soluble in the oil phase (Becher, 1966; Schramm, 1992). There are many crude oil soluble surfactants which are capable of interacting with both water and oil phases. In addition to phenols there are carboxylic acids, alcohols, esters, heterocyclic nitrogen compounds and resins (Acevedo *et al.*, 1985; Aveyard *et al.*, 1990; Schramm, 1992). The oil/water partition coefficients of alkylphenols (inferred from alkylphenol oil and water solubilities reported in Fig. 5.1.1) indicate that while soluble in both oil and water phases, they have a slightly greater affinity for the oil phase (Taylor, 1994). Therefore, phenols will be assessed as representatives of crude oil soluble emulsifiers due to their partition behaviour and ease of extraction and analysis.

Phenols are a group of monohydric aromatic alcohols which are common to crude oils (Fig. 5.1.2) and have been identified as water-in-oil emulsifying compounds (Tissot & Welte, 1984; Layrisse *et al.*, 1984; Hunter & White, 1992). Phenols have an electronegative hydroxyl group which imparts polarity upon the phenol molecule, allowing them to form hydrogen bonds with oil, water and solid phases (Taylor, 1994). In addition, their slight acidity allows them to react with bases, such as sodium hydroxide and potassium hydroxide, to form salts (Murray, 1977). This ability was utilised in the phenol extraction procedure described below. The ability of phenols to partake in acid/base and/or hydrogen bond interactions, with mineral, water or oil phases has led to their use in the assessment of crude oil migration and biodegradation (Sandvik *et al.*, 1992; Taylor, 1994; Larter & Aplin, 1995). Petroleum phenols which have been analysed previously and which are also analysed by this study, range from phenol (C_0) to C_3 alkylphenols and are hence forth referred to as C_0-C_3 alkylphenols, or just alkylphenols (C_0, C_1, C_2 & C_3 referring to the number of substituted alkyl carbons on the phenol aromatic ring; Fig. 5.1.2) unless specific isomers are discussed (Ioppolo *et al.*, 1992; Taylor, 1994). The specific alkylphenols analysed were; phenol, 2-methylphenol (*ortho*), 3-methylphenol (*meta*), 4-methylphenol (*para*), 2-ethylphenol, 2,5-dimethylphenol, 2,4-dimethylphenol, 2,6-dimethylphenol, 3,5-dimethylphenol, 4-ethylphenol, 3,4-dimethylphenol, 2-propylphenol, 3-isopropylphenol, 4-isopropylphenol, 2,4,6-trimethylphenol, 2,3,5-trimethylphenol, 2,3,6-trimethylphenol and 3,4,5-trimethylphenol.

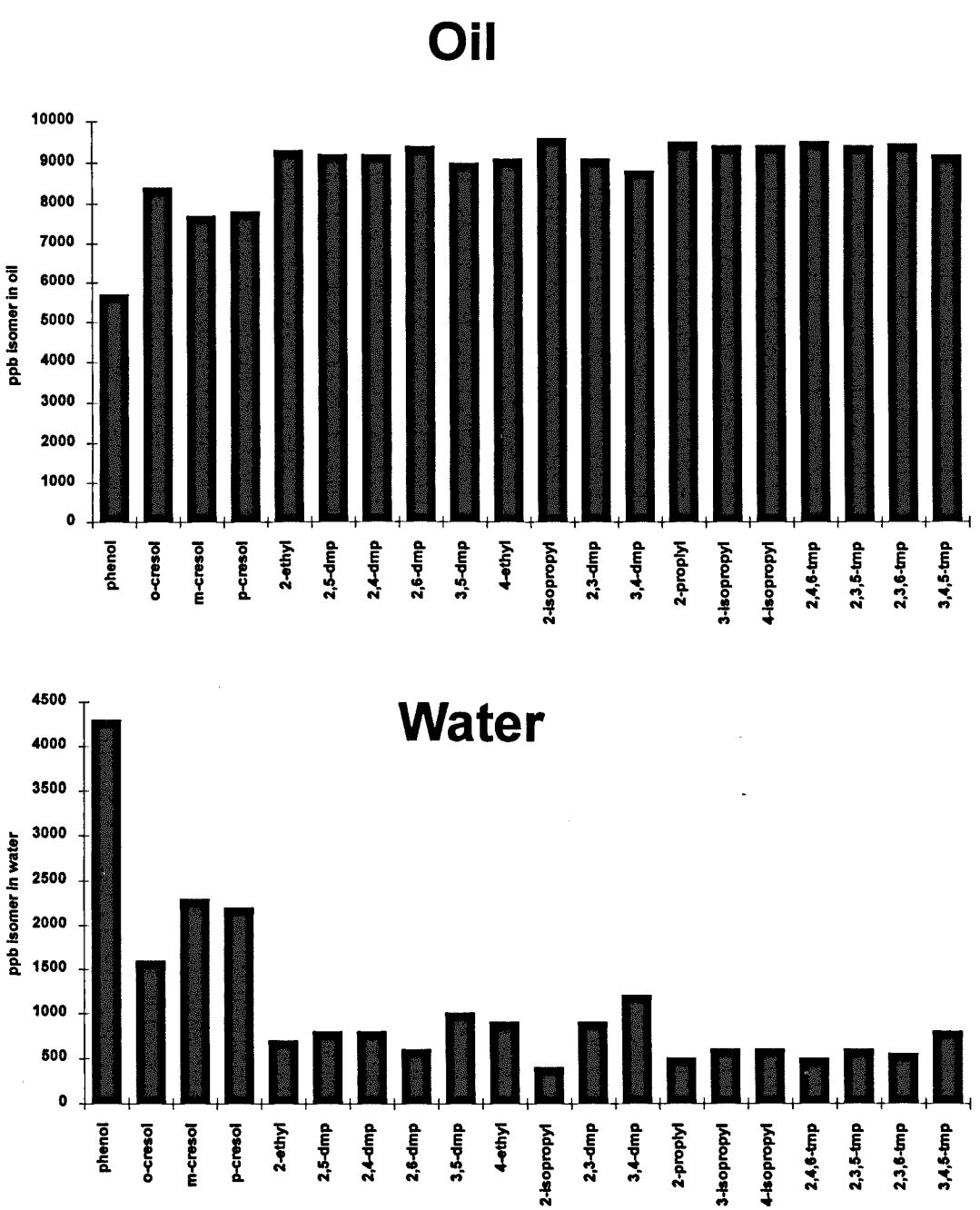

Figure 5.1.1. Estimated alkylphenol content of oil and water following equilibration of equal volumes of oil (initially containing 10 000 ppb of each isomer) and water (initially containing no isomers). Illustrates the overall preferential soluility of alkylphenols in oil. Taken from Taylor (1994).

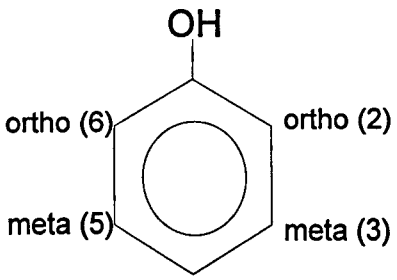

phenol,
C_0 = phenol

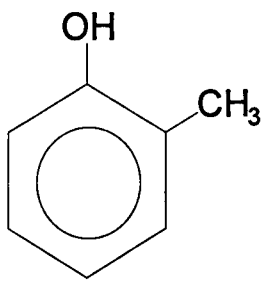

2-methylphenol,
C_1 = methylphenols

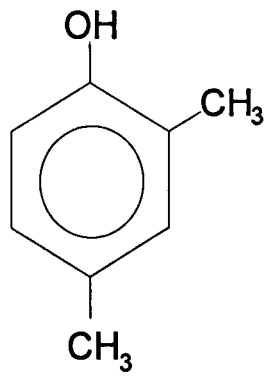

2,4-dimethylphenol,
C_2 = dimethylphenols, ethylphenols

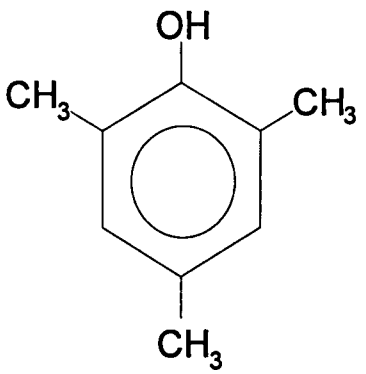

2,4,6-trimethylphenol,
C_3 = trimethylphenols, methyl and ethylphenols, propylphenols

Figure 5.1.2. Illustration of the phenol structure and notation as well as the four alkylphenol homolog groups (C_0-C_3) which are common to crude oils and were analysed in this study (Ioppolo et al., 1992).

As discussed above, the ability of the alkylphenols to stabilise water-in-crude oil emulsions depends upon their solubility in both phases (oil and water). The interaction of alkylphenols with various phases has been predominantly assessed by use of partition coefficients. Partition coefficients describe the partitioning of compounds between oil and water phases when equilibrium has been reached (Southworth *et al.*, 1983). Octanol-water partition coefficients (K_{OW}) are widely used as the standard measure for the partition ability of various compounds in varying situations, from oil spills to pharmaceuticals (Leo, 1971; Southworth *et al.*, 1983). The octanol/water partition coefficient (P or K_{OW}) is defined in Equation 5.1 (Lyman, 1982):

$$K_{OW} = \frac{\text{Conc. of solute in octanol phase}}{\text{Conc. of solute in aqueous phase}} \quad \{5.1\}$$

It is obvious that the partition coefficient of a particular solute is governed by its solubility in the solvents (octanol and water) and has been frequently related to its water solubility. Therefore, the water solubility of a solute may be used to estimate the K_{ow} of the solute (Chiou *et al.*, 1977). However, it is important to note that the partition coefficient of a solute is not the same as the ratio of the solubility of a solute in octanol and water phases because, in a binary system, octanol and water do not represent two pure phases. At equilibrium, the octanol phase will contain water and *vice versa* (Chiou *et al.*, 1982; Lyman, 1992). However, partition coefficients and water solubility may be correlated, hydrophobic solutes being represented by K_{ow} values of greater than 10 while hydrophilic solutes are represented by K_{ow} values of less than 10 (Lyman, 1992).

It has been found that both carbon number and steric arrangement alter the affinity of alkylphenols for the aqueous phase (Bizek *et al.*, 1992; Larter & Aplin, 1995). McAuliffe (1979) reported that water solubility for both aliphatic hydrocarbon and aromatic hydrocarbon groups decreases with increasing carbon number (Fig. 6.1.3), a similar trend has also been observed by Taylor (1994), with the partitioning of alkylphenols to the aqueous phase decreasing with increasing carbon number (Fig. 5.1.1). It was further shown, by Taylor (1994) and Macleod *et al.* (1993), that hindrance of the hydroxyl group of phenol, by substituted alkyl groups at the *ortho* position, would reduce the affinity of alkylphenols for the aqueous phase, consequently increasing their partition coefficient values. The effect of the position of an alkyl group, relative to that of a polar functionality, is not restricted to oxygen compounds and has also been recorded by Li & Larter (1993) for pyrrolic compounds.

The expected water solubility of the C_0-C_3 alkylphenols, as shown in the literature, will decrease in the following order:

$$C_0 > C_1 > C_2 > C_3 \quad \{5.2\}$$

This order is attributed to the alkyl groups which are both "electron releasing" and hydrophilic, reducing the polarity of the phenol group, thereby reducing partition capability and water solubility (Murray, 1977). On the basis of partition experiments, a second order of water solubility preference within the C_1, C_2 and C_3 alkylphenol groups would be seen, with "hindered alkylphenols" (*i.e.*, alkylphenols which have alkyl group substitution in the *ortho* position of the phenol ring) having lower aqueous solubilities than the non-hindered groups.

As well as alkylation of alkylphenols, the properties of the solvents (oil and water) will also greatly influence the affinity of alkylphenols for the water and oil phases. In partition coefficient assessment, the effect of different organic solvents

(such as octanol and hexane), has been shown to influence alkylphenol partition behaviour, due to the different hydrogen bonding abilities of polar (octanol) and apolar (hexane) organic solvent phases. Therefore, the partition coefficient for phenol, measured in a hexane-water system, is approximately two orders of magnitude lower than the phenol partition coefficient measured in an octanol-water system. The effect of solute-solvent interactions has also been noted by both Southworth *et al.*(1983) and Taylor (1994), when assessing the alkylphenol partition coefficients in crude oil-water systems. It was seen that heavy crude oils, containing higher percentages of polar NSO compounds, give higher oil/water partition coefficients than those observed with normal crude oils, which contain much lower percentages of NSO compounds. This was attributed to heavy crude oils having increased ability to form hydrogen bonds with phenols due to their greater overall polarity. This point is illustrated in Table 5.1.1, with data from Southworth *et al.* (1983).

Alkylphenols	Increasing organic solvent polarity →			
	Dodecane	Toluene	H-Coal*	SRC II*
C_0-alkylphenol	0.8	1.6	2.8	4.6
C_1-alkylphenol	0.76	7.4	10	16
C_2-alkylphenol	2.4	22	30	56
C_3-alkylphenol	25	100	100	210

Table 5.1.1. C_0-C_3 alkylphenol oil/water partition coefficients determined with different organic phases. ***After Southworth et al. (1983).*** *(* H-Coal was obtained from a coal liquefaction. SRC II was derived from oil shale).*

The solubility of the C_0-C_3 alkylphenols in aqueous phases, will be affected by the pH, salinity and temperature of the water.

An increase in the pH of the aqueous phase will increase the aqueous phase solubility of alkylphenols and therefore, decrease partition coefficients (Golumbic *et al.*, 1949). This increased phenol solubility was attributed to the ionisation of the phenols (ionised phenols preferring water; neutral or non-ionised phenols preferring the oil; Fig. 5.1.3). However, phenol ionisation is variable, dependent upon the degree of alkylation of the alkylphenol and pH. This variability is illustrated by the different pKa values of the phenol isomers, shown in Table 5.1.2.

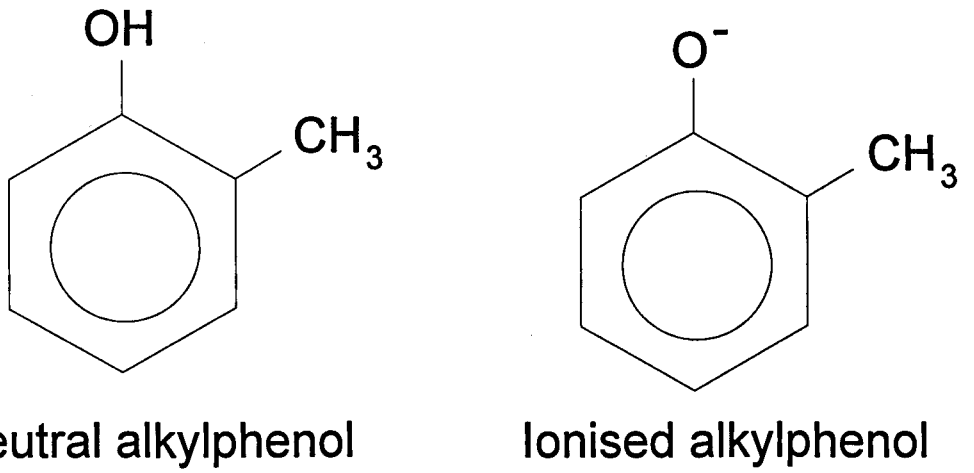

Figure 5.1.3. Neutral (preferentially partition into the oil phase) and ionised (preferentially partition into the aqueous phase) alkylphenols.

Phenol Compounds	pKa	MW
phenol	9.92	94.11
2-methylphenol	10.26	108.13
3-methylphenol	10.09	108.13
4-methylphenol	10.26	108.13
2-ethylphenol	10.20	122.17
2,5-dimethylphenol	10.40	122.17
2,4-dimethylphenol	10.60	122.17
2,6-dimethylphenol	10.62	122.17
3,5-dimethylphenol	10.20	122.17
4-ethylphenol	10.00	122.17
3,4-dimethylphenol	10.40	122.17
2-propylphenol	10.30	136.1
4-isopropylphenol	10.3	136.1
2,4,6-trimethylphenol	10.9	136.1
2,3,5-trimethylphenol	10.67	136.1
2,3,6-trimethylphenol	10.89	136.1
3,4,5-trimethylphenol	10.5	136.1

Table 5.1.2. pKa and molecular weight values for various alkylphenol isomers. Taken from Foley, 1988 and Varhanícková, 1995.

The pKa of a molecule represents the pH at which the neutral and ionised species of the molecule are in equal abundance. From the pKa data above it is concluded that low molecular weight (MW) alkylphenols will ionise to a greater degree than high MW alkylphenols, at a constant pH. This characteristic has proved useful. Foley (1988) recognised that the variable ionisation of alkylphenols could be used to separate cresols (methylphenols) and xylenols (dimethylphenols) in addition,

the phenol extraction technique developed by Taylor (1994), and used in this study, is also based on this phenomenon (see below).

Work by Taylor (1994) showed that below a pH of approximately 8, the phenols were dominated by the neutral, rather than ionised forms, and were therefore not affected by preferential partition from the oil phase into the aqueous phase. The samples in this study have been associated with distilled water, the pH will be 7 going to approximately 8 after equilibration (measured by pH paper) between the aqueous and oil phases. Therefore, it was considered that substantial ionisation and preferential partition of ionised alkylphenols into the aqueous phase had not occurred.

Increased salinity will cause alkylphenol partition coefficients to increase (Taylor, 1994). This is attributed to the "salting out" effect of the C_0-C_3 alkylphenols (Price, 1976).

It has been reported that increasing the temperature of a binary solvent system increases the solute concentration in the solvent with the lowest boiling point, thereby affecting partition coefficients (Leo *et al.*, 1971). Analysis of the C_0-C_3 alkylphenol concentrations in crude oil/water systems has observed that increases in temperature actually decreased the partition coefficients (Taylor, 1994). Therefore, all experiments in this study were performed at a constant temperature to avoid potential errors associated with changes to the partition coefficients.

All the above factors will effect the water solubility of alkylphenols and therefore, their partition coefficients. More importantly, they may also affect the ability of alkylphenols to stabilise water-in-oil emulsions by altering the relative oil and water solubilities of alkylphenols (oil soluble surfactants stabilise water-in-oil emulsions and *vice versa*; Bancroft's rule, Section 1.2.1; Shaw, 1980).

The main aim of this study was to assess the role of the alkylphenols as surfactants and mediators of water uptake by crude oil. This was achieved by studying the variation of C_0-C_3 alkylphenol concentrations and distributions in water/oil blend fractions, as well as in mature oils (whole oil). It was also hoped to examine the effect of biodegradation on the alkylphenol concentrations of crude oils and perhaps explain the relationship between the biodegradation state of a crude oil and its emulsion formation/stabilisation and water retention ability, described in Chapter 3. To achieve these goals the analytical method developed by Taylor (1994) was employed. This technique was applied to the crude oils in the sample set and the resultant alkylphenol distributions and concentrations were determined. Further, the fractions, separated from crude oil/water blends (supernatant oil, unbound oil, emulsion & bound oil; Section 4.2.1.1), were also analysed to assess the partitioning of the C_0-C_3 alkylphenols in the crude oil/water blends.

5.2. Experimental.

5.2.1. Phenol Extraction and Analysis.

This study was based upon the alkaline alkylphenol extraction and analysis procedures performed by Taylor (1994). For details the reader should refer to this work. The procedures are schematically illustrated in Figure 5.2.1.

Between 0.5 g and 1.0 g of either whole oil, supernatant oil or unbound oil fractions, or approximately 1-10 mg of bound oil/emulsion fractions (Table 5.2.2), was pipetted into a 100 ml round bottom flask (RBF) and diluted with 10 ml of toluene. 25 ml of methanolic potassium hydroxide solution (10% w/v) was added to the sample along with 8,145 ng of a 2-naphthol internal standard (4,072.5 ng of 2-naphthol for emulsion and bound oil fractions). This mixture was then shaken in a "Griffin flask shaker" for one hour. The mixture was poured into a 100 ml separating funnel and the 100 ml round bottom flask (RBF) was subsequently washed three times with 10 ml distilled water, each washing being added to the separating funnel. The separating funnel and contents were left overnight to allow the organic and aqueous phases to completely separate. After this time as much of the organic phase as possible was pipetted off without disturbing the aqueous phase. The aqueous phase was washed three times with hexane, each wash being pipetted off and added to the organic phase. The organic phase (containing the neutral and basic compounds) was discarded.

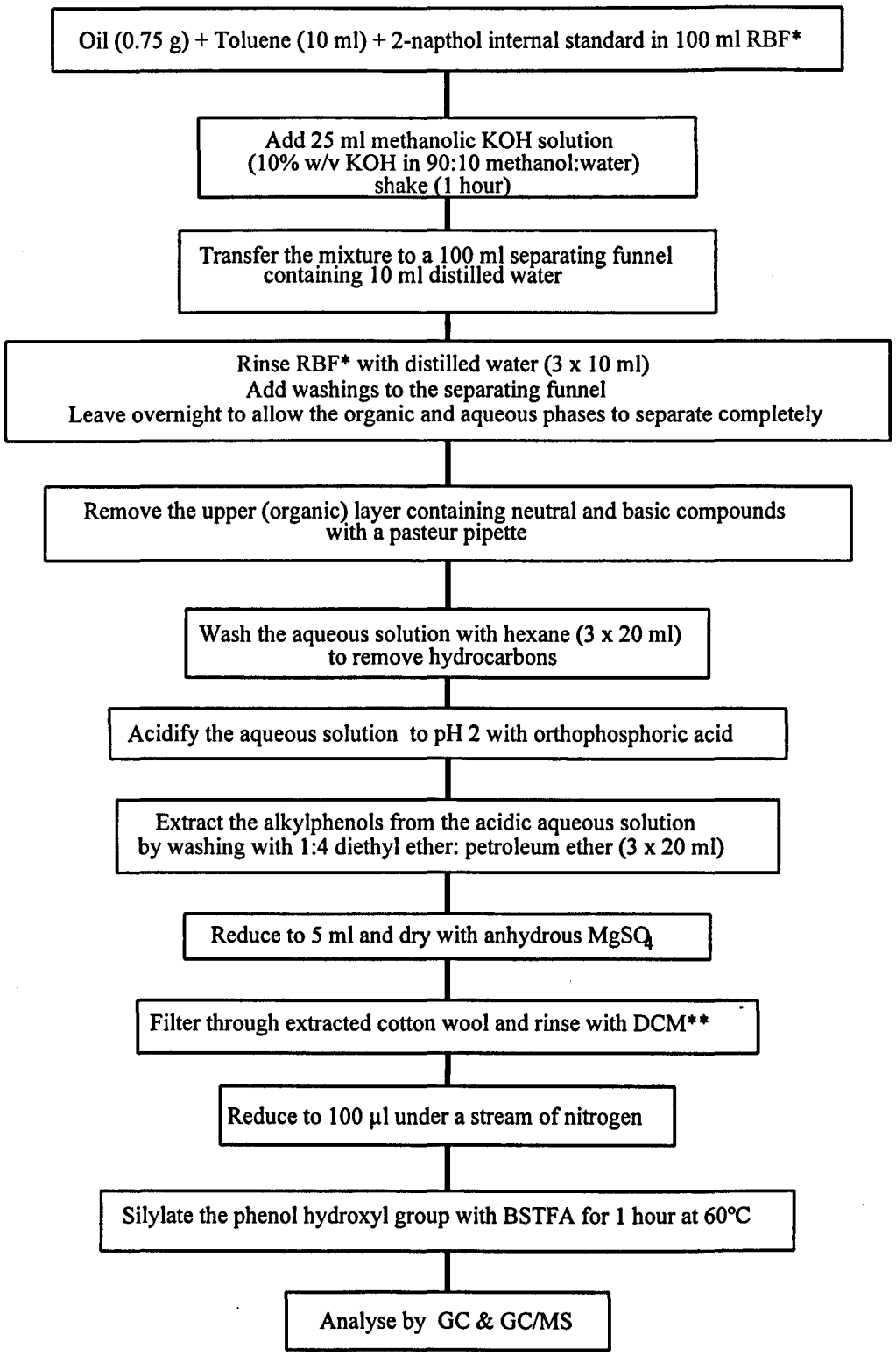

*Figure 5.2.1. Extraction and analysis procedure for assessment of C_0-C_3 alkylphenols (*RBF = round bottom flask; **DCM = dichloromethane). Taken from Taylor, 1994.*

The aqueous phase, containing the potassium phenolate salts, was transferred to a clean 100 ml RBF. This alkaline solution (approximate pH of 12) was then acidified with dilute phosphoric acid to a pH of less than 2. This acidified solution was then added to a clean 100 ml separating funnel. The acidified aqueous phase was then extracted three times with 20 ml of petroleum ether:diethyl ether (4:1) to remove the neutral alkylphenols. Solvent wash was pipetted into a clean 100 ml RBF and the solvent was subsequently reduced by rotary evaporation, to approximately 5 ml. Approximately 10 mg of solvent extracted anhydrous magnesium sulphate was added to the reduced solvent and left for 5 minutes to absorb any water contamination from the previous solvent/aqueous separation step. The anhydrous magnesium sulphate and solvent were separated by use of a short column, containing approximately a 1 cm plug of pre-extracted cotton wool. The sample was rinsed through the short column, with 10-20 ml of dichloromethane (DCM) into a clean 50 ml RBF to separate it from the magnesium sulphate. The phenol extract was now rotary evaporated to approximately 2 ml and transferred into a vial. The extract was further reduced to 100 µl by evaporation under a stream of nitrogen.

Before gas chromatography (GC) and gas chromatography/mass spectrometry (GC/MS) analyses, the phenol extract must be silylated, to maintain chromatographic resolution and protect the chromatographic columns. To silylate the phenol extract the reagent N,O-bis(trimethylsilyl)trifluoroacetamide (BSTFA) containing 1% trimethylchlorosilane (TMCS), Fluka Chemicals, was used. Approximately 50 µl was added to the 100 µl extract and heated for one hour, at 60°C, in a sealed vial. Samples were then diluted with DCM (500 µl for whole oil, supernatant oil and unbound oil; 50 µl for bound oil and emulsion samples) and then analysed directly by either GC or GC/MS techniques (Sections 5.2.2 & 5.2.3), with 1 µl injection.

Taylor (1994) found recoveries varied from 40% for phenol, 66% for C_1-alkylphenols, increasing up to 90% for C_3-alkylphenols. The 2-naphthol standard had a 90% recovery (Table 5.2.1). These recoveries compared well with a similar study by Pauls *et al.* (1990). These recovery percentages indicate that estimated C_0-C_3 alkylphenol concentrations, using this procedure, will be underestimates.

Phenol Compounds	% recovery	K_{ow}
phenol (non-hindered)	40.7	3.1
2-methylphenol (hindered)	66.1	15.6
3-methylphenol (non-hindered)	66.1	11.3
4-methylphenol (non-hindered)	66.2	10.9
2-ethylphenol (hindered)	76.1	61.9
2,5-dimethylphenol (hindered)	77.7	48.2
2,4-dimethylphenol (hindered)	79.8	45.4
2,6/3,5-dimethylphenol (hindered/non-hindered)	74.8	40.2
4-ethylphenol (non-hindered)	83.9	40.1
3,4-dimethylphenol (non-hindered)	82.0	32.5
2-propylphenol (hindered)	82.6	190.1
3-isopropylphenol (non-hindered)	87.8	116.4
4-isopropylphenol (non-hindered)	87.6	118.8
2,4,6-trimethylphenol (hindered)	48.8	104.6
2,3,5-trimethylphenol (hindered)	85.4	115.5
2,3,6-trimethylphenol (hindered)	67.5	103.5
3,4,5-trimethylphenol (non-hindered)	90.6	73.1
2-naphthol	90.8	

Table 5.2.1. The percent (%) recoveries and oil/water partition coefficients (K_{ow}) estimates, both determined by Taylor (1994), for the C_0-C_3 alkylphenols extracted and analysed in this study. The hindered/non-hindered state of each alkylphenol molecule is indicated.

5.2.1.1. Accuracy and Precision.

The above extraction procedure is designed to isolate C_0-C_3 alkylphenols from crude oil samples with weights of approximately 0.75 g. However, in Table 5.2.2, it is shown that total extract weights for the bound oil and emulsion samples varies between 1 and 10 mg. Consequently, these small sample weights have percentage errors ranging from 0.8% to 3.8% (Table 5.2.2) due to the limitations of the balance used. However, the calculated alkylphenol concentrations for bound oil and emulsion samples were at least an order of magnitude greater than the whole oil, supernatant oil and unbound oil alkylphenol concentrations (see below). Consequently, the conclusions reached in Sections 5.3 and 5.4, were not effected by the percentage errors for emulsion/bound oil sample weights. In addition, blank alkylphenol extraction runs were performed and the extraction process was not found to influence the C_0-C_3 alkylphenol concentrations and distributions for bound oil and emulsion samples.

	Crude Oil Fractions			
Crude Oils	Whole Oil	Supernatant Oil	Unbound Oil	Bound Oil/ Emulsion
Eldfisk A29	750	750	750	3.3 (2.4%)
Eldfisk B12	750	750	750	2.1 (3.8%)
NS1	750			10 (0.8%)
NS2	750	750	750	7.2 (1.1%)
NS3	750			
H1	750			4.2 (1.9%)
H7	750			3.3 (2.4%)

Table 5.2.2. Average sample weights (mg) for alkylphenol extraction. Low sample weights also show the percent error. The calculated standard deviation of the balance used was 0.08 mg. (percentage error = standard deviation [0.08 mg] divided by the mean sample weight).

5.2.2. Gas Chromatographic Analysis of Derivatised Alkylphenols.

The C_0-C_3 derivatised alkylphenol extracts were run on a Carlo Erba 5160 gas chromatograph. On-column injection was used and the instrument was fitted with a flame ionisation detector (FID). The hydrogen carrier gas pressure was 50 kPa. The chromatographic column used was an HP-1 coated, fused silica column (25 m x 0.32 mm, film thickness of 0.17 μm). All analyses were made using a temperature programme starting at 35°C for 10 min, increasing at 2°C min^{-1} to 120°C (0 mins) then increasing at 6°C min^{-1} to 300°C with the final temperature being maintained for 20 mins.

5.2.3. Gas Chromatography/Mass Spectrometry of Derivatised Alkylphenols.

For gas chromatography/mass spectrometry (GC/MS) analysis, samples were injected onto a Fisons 8000 Series gas chromatograph coupled to a Fisons Trio 1000 mass spectrometer. The gas chromatograph was fitted with an HP-1 fused silica column (25 m x 0.32 mm, with a film thickness of 0.25 μm). Cold on-column injection was used with a helium carrier gas pressure of 25 kPa. The GC/MS had an ionisation voltage of 70 eV and was fitted with a quadrupole mass filter, the electronmultiplier voltage was 7000 V. The filament current was 42 mA (amps), source current was 1400 mA and the trap current was 150 mA. Analysis was run in selective ion recording (SIR) mode, the selected ions being listed in Table 5.2.3. The

temperature programme used was the same as that in the gas chromatograph analysis (Section 5.2.2).

	Ions monitored by SIR analyses.	
	$(M-15)^+$	M^+
C_0-alkylphenol	151	166
C_1-alkylphenols	165	180
C_2-alkylphenols	179	194
C_3-alkylphenols	193	208
2-naphthol	201	216

Table 5.2.3. List of the molecular ions (M^+) and demethylated ions $(M-15)^+$ monitored in SIR analyses of C_0-C_3 alkylphenols and internal standard (2-naphthol).

Peaks were identified by co-injection of authentic reference compounds and the identified C_0-C_3 alkylphenol isomers were quantified by assessment of the peak areas of the fragmented silylated $(M-15)^+$ ions of the C_0-C_3 alkylphenols, relative to those of the 2-naphthol. In addition, the alkylphenol isomers 2,3-dimethylphenol and 2-isopropylphenol, analysed in the Taylor (1994) study, were not assessed here due to contamination problems. However, the two alkylphenol isomers 3,5 & 2,6-dimethylphenol, which co-eluted in the Taylor (1994) study, were resolved and assessed separately in this study.

5.2.4. Extraction of Blend Fractions from Crude Oil and Water Blends.

The blend fractions which were extracted from the crude oil/water blends and used in this chapter were the supernatant oil, unbound oil, emulsion and bound oil fractions. The supernatant oil fraction represented the crude oil which separated from the emulsion sediment due to gravity (normal, or increased due to centrifuging). The term "emulsion sediment" refers to product from the flocculation of the emulsion droplets in the crude oil/water blends. The sediment contains the unbound oil fraction, bound oil fraction and aqueous phase. The unbound oil fraction represented the crude oil trapped in the emulsion sediment which is not part of the crude oil/water interfacial film. The emulsion fraction represented the organic matter in the crude oil/water interfacial film, as well as the dissolved organic matter in the water phase. The bound oil fraction represented the organic matter isolated from the crude oil/water interfacial film.

As well as fractions extracted from the crude oil/water blends (supernatant oil, unbound oil, emulsion, bound oil fractions), the whole oil fractions (oil which has not been blended with an aqueous phase) were also analysed.

This procedure is described in detail in Chapter 4, Section 4.2.1.1.

5.3. Results.

5.3.1. Alkylphenol Distributions for North Sea Whole Oil and Blend Fractions.

5.3.1.1. North Sea Non-Degraded Crude Oil, A29.

The alkylphenol distributions for the whole oil and extracted crude oil/water blend fractions (supernatant oil, unbound oil and bound oil/emulsion defined in Section 5.2.4 and discussed in further detail in Section 4.2.1.1) of the A29 crude oil, are represented by the histograms in Figure 5.3.1. The overall C_0-C_3 alkylphenol yields for the supernatant and unbound oils (approximately 24,000 & 29,000 ng g^{-1} respectively, Table 5.3.1) are lower than the average total concentration (approximately 36,000 ng g^{-1}, Table 5.3.1) of the whole oil fractions. The whole oil, supernatant oil and unbound oil C_0-C_3 alkylphenol distributions are seen to be similar. The main alkylphenol groups are the C_1 and C_2 alkylphenols, with isomer concentrations between 2,000 and 4,000 ng g^{-1} for the whole oil and 1,500 and 2,500 ng g^{-1} for the supernatant and unbound oils. Phenol is more abundant in the unbound oil relative to whole oil and supernatant oil fractions. The C_3 alkylphenols are minor constituents in the whole oil, supernatant oil and unbound oil fractions with isomer concentrations averaging between 100-1,000 ng g^{-1}. The dominant C_0-C_3 alkylphenols are the *ortho*-cresol (2-methylphenol) and 2,4-dimethylphenol although phenol also becomes dominant (accompanied by a decrease in the ortho-cresol) in the unbound oil fraction.

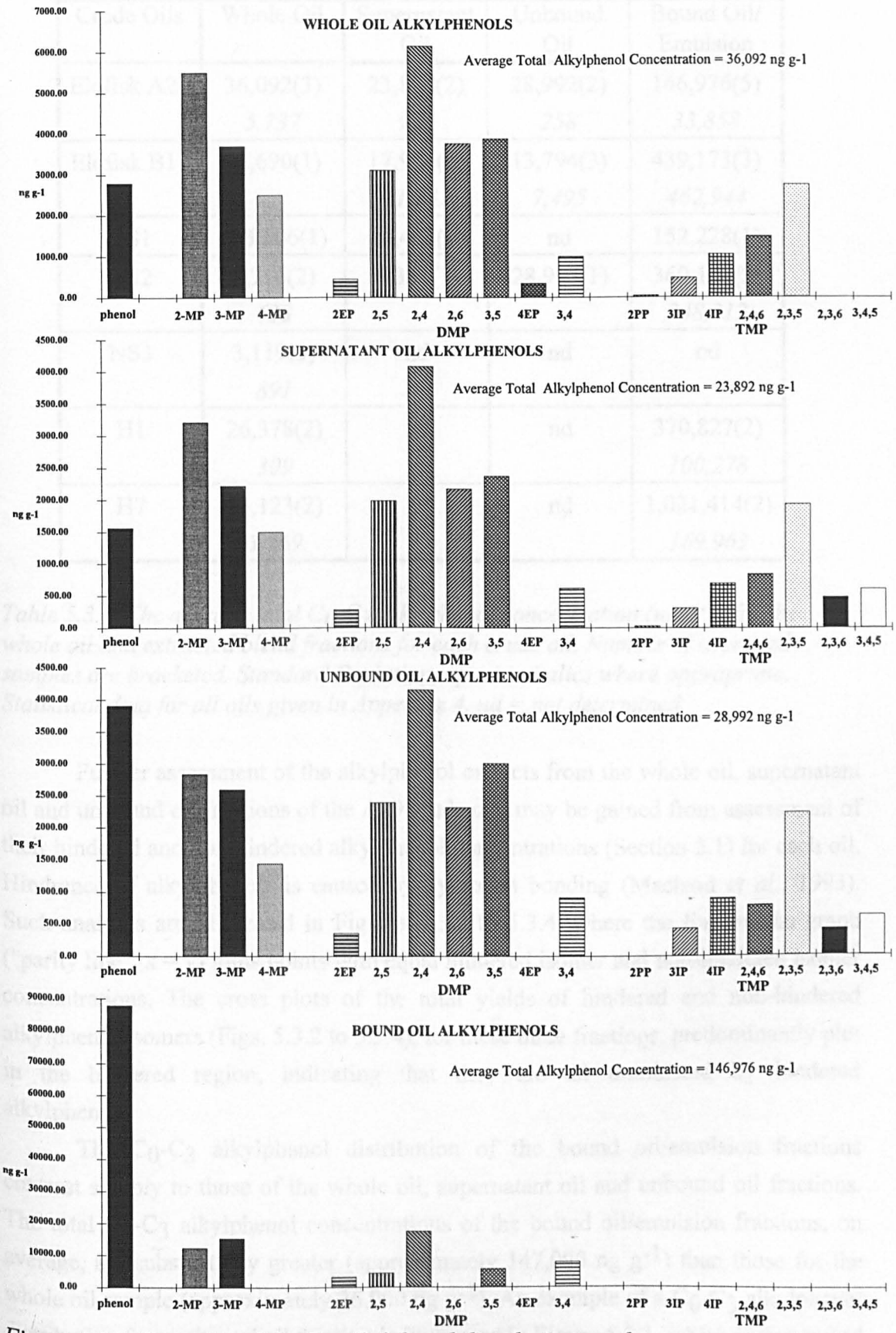

Figure 5.3.1. Examples of C_0-C_3 alkylphenol distributions and concentrations for the Eldfisk A29 whole oil, supernatant oil, unbound oil and bound oil fractions. Average total alkylphenol concentrations are also reported. MP = methylphenol; DMP = dimethylphenol; TMP = trimethylphenol.

Crude Oils	Whole Oil	Supernatant Oil	Unbound Oil	Bound Oil/ Emulsion
Eldfisk A29	36,092(3) *5,737*	23,892(2) *928*	28,992(2) *258*	146,976(5) *33,858*
Eldfisk B12	32,690(1)	17,917(3) *11,242*	13,794(3) *7,495*	439,173(3) *462,944*
NS1	103,506(1)	24,465(1)	nd	152,228(1)
NS2	4,716(2) *633*	4,353(1)	28,993(1)	360,154(3) *248,312*
NS3	3,119(3) *891*	nd	nd	nd
H1	26,378(2) *309*	nd	nd	370,827(2) *100,278*
H7	35,123(2) *3,269*	nd	nd	1,021,414(2) *169,963*

Table 5.3.1. The average total C_0-C_3 alkylphenol concentration (ng g^{-1}) for the whole oil and extracted blend fractions for each crude oil. Number of averaged samples are bracketed. Standard Deviation report in italics where appropriate. Statistical data for all oils given in Appendix 4. nd = not determined.

Further assessment of the alkylphenol extracts from the whole oil, supernatant oil and unbound oil fractions of the A29 crude oils may be gained from assessment of their hindered and non-hindered alkylphenol concentrations (Section 5.1) for each oil. Hindrance of alkylphenols is caused by hydrogen bonding (Macleod *et al.*, 1993). Such analyses are illustrated in Figures 5.3.2 to 5.3.4, where the line on the graph ("parity line", x = y) joins points with equal hindered isomer and non-hindered isomer concentrations. The cross plots of the total yields of hindered and non-hindered alkylphenol isomers (Figs. 5.3.2 to 5.3.4), for these three fractions, predominantly plot in the hindered region, indicating that they are all dominated by hindered alkylphenols.

The C_0-C_3 alkylphenol distribution of the bound oil/emulsion fractions contrast sharply to those of the whole oil, supernatant oil and unbound oil fractions. The total C_0-C_3 alkylphenol concentrations of the bound oil/emulsion fractions, on average, are substantially greater (approximately 147,000 ng g^{-1}) than those for the whole oil sample (approximately 36,000 ng g^{-1}). An example of a C_0-C_3 alkylphenol distribution from a bound oil fraction is illustrated in Figure 5.3.1, which is dominated by phenol (approximately 87,000 ng g^{-1}), with relatively minor C_1 and C_2 alkylphenols (approximate isomer concentrations of 8,000 ng g^{-1}) with the C_3

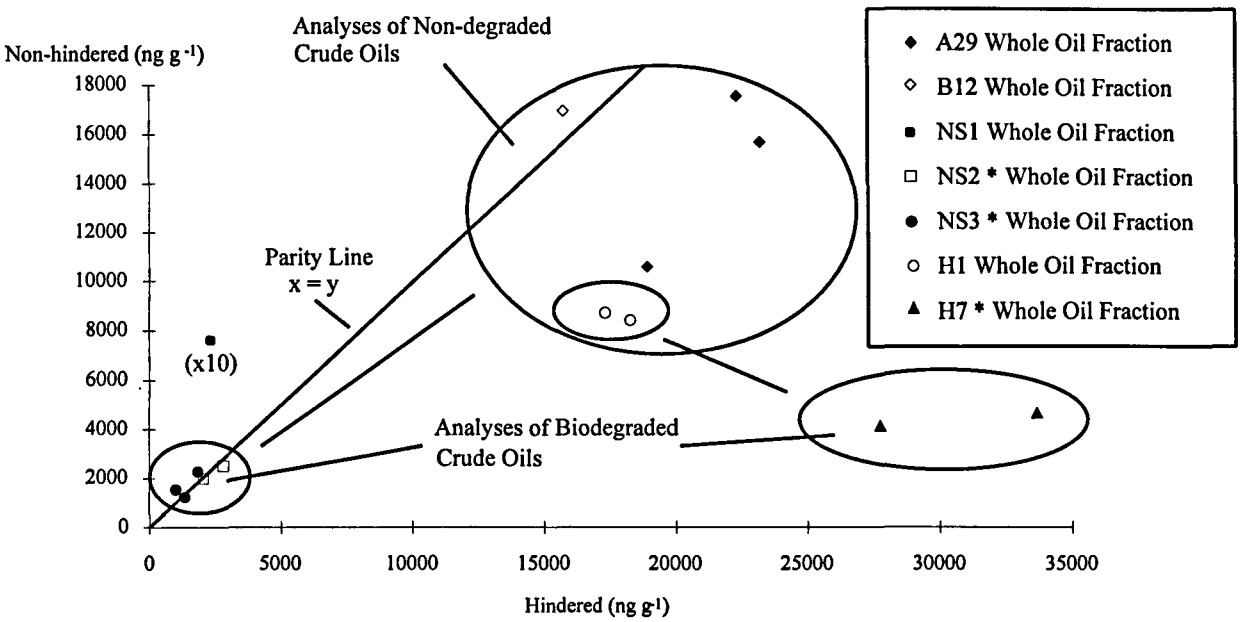

*Figure 5.3.2. Cross plot of hindered and non-hindered C_0-C_3 alkylphenol yields for various crude oils (whole oil fractions). Parity line represents region of equal concentrations of hindered and non-hindered alkylphenol isomers. Arrows indicate alteration of North Sea and Santa Maria Basin (SMB) crude oils with biodegradation. Due to the high concentration of alkylphenols in NS1 they are reported at an order of magnitude lower than actual values, allowing them to be viewed. The NS1 plot occurs on the non-degraded side of the parity line. * = biodegraded crude oils.*

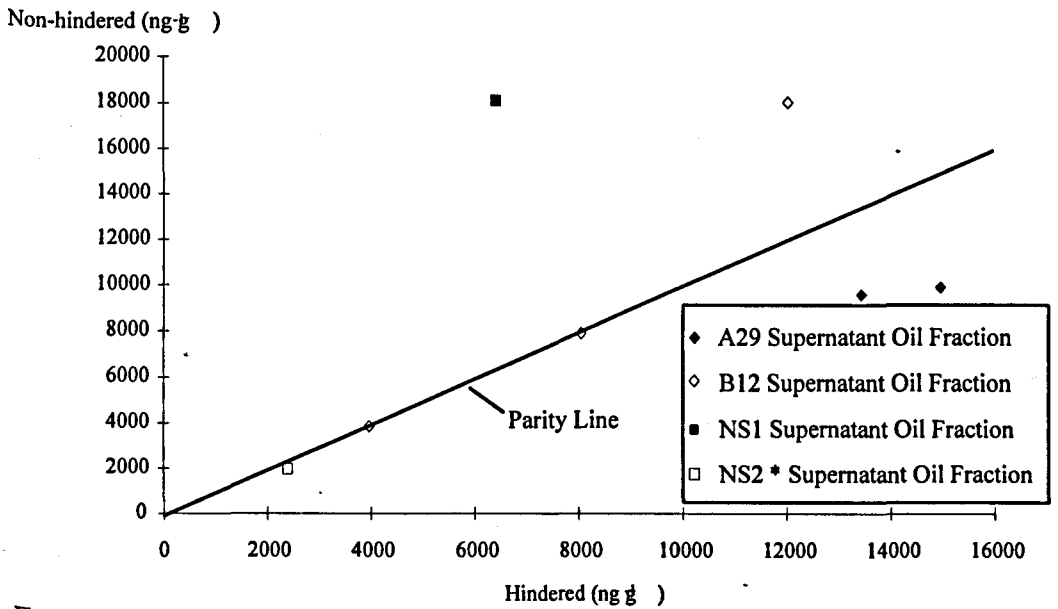

*Figure 5.3.3. Cross plots of the hindered and non-hindered C_0-C_3 alkylphenol yields for the supernatant oil fractions of various crude oils (A29, B12, NS1 & NS2). The parity line represents the region of equal concentrations of hindered and non-hindered alkylphenol isomers. * = biodegraded crude oil.*

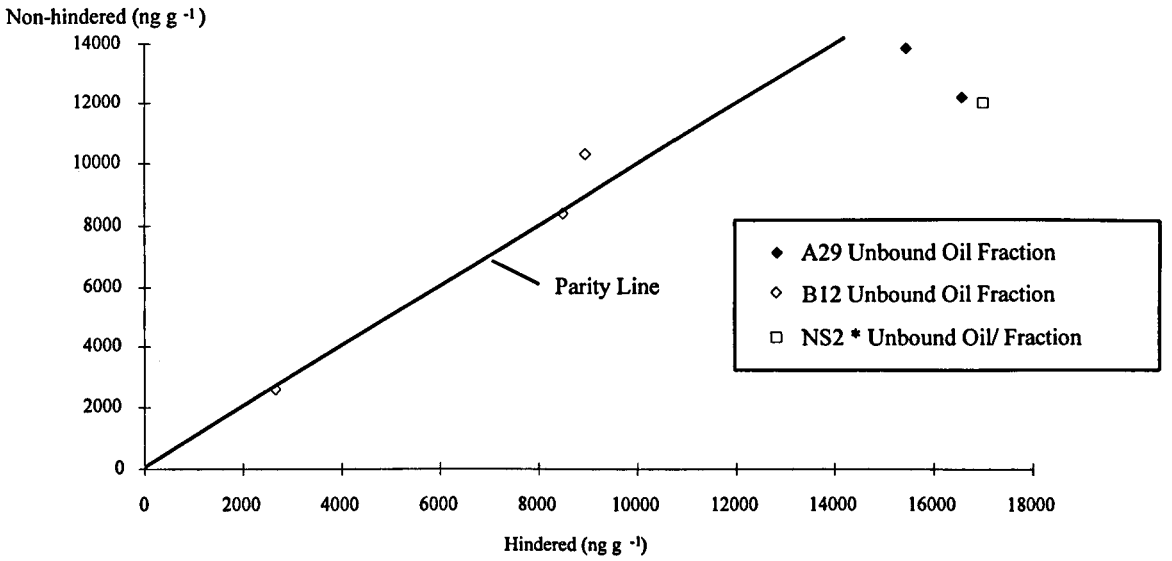

*Figure 5.3.4. Cross plot of hindered and non-hindered C_0-C_3 alkylphenol yields for unbound oil fractions. Parity line represents region of equal concentrations of hindered and non-hindered alkylphenol isomers. * = biodegraded crude oil.*

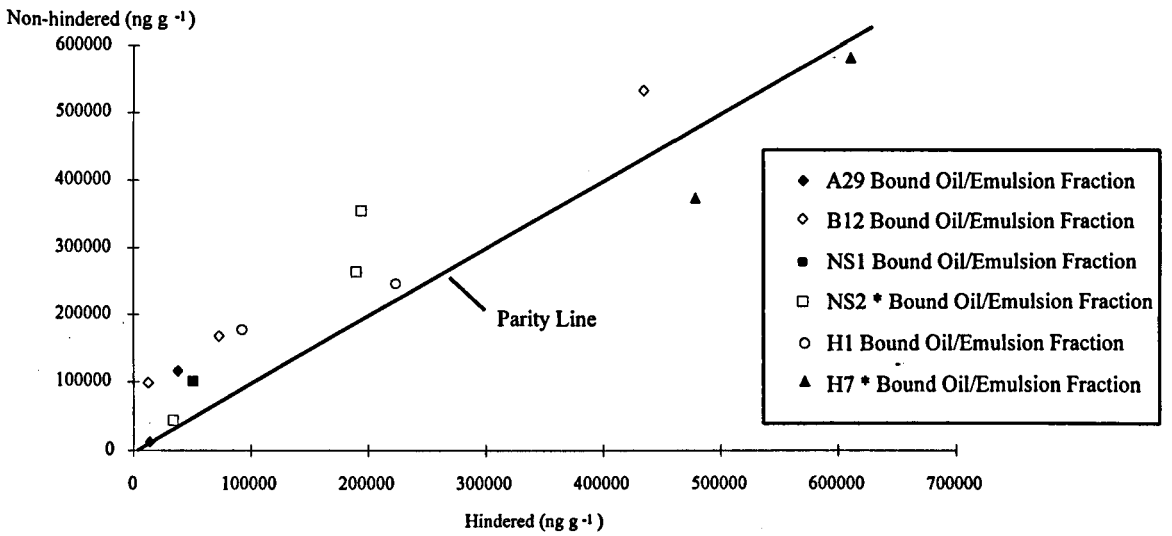

*Figure 5.3.5. Cross plot of hindered and non-hindered C_0-C_3 alkylphenol yields for bound oil and emulsion fractions (highlighted in legend). Parity line represents region of equal concentrations of hindered and non-hindered alkylphenol isomers. * = biodegraded crude oil.*

alkylphenols being absent. The cross plot of the total yields of the hindered and non-hindered C_0-C_3 alkylphenols from the bound oil/emulsion fractions in Figure 5.3.5, plot in the non-hindered region. Therefore, the bound oil/emulsion C_0-C_3 alkylphenol extracts from the A29 North Sea crude oil are enriched with non-hindered alkylphenols, predominantly by the phenol isomer.

5.3.1.2. North Sea Non-Degraded Crude Oil, B12.

Examples of the C_0-C_3 alkylphenol distributions for the B12 whole oil and the extracted blend fractions (supernatant oil, unbound oil & bound oil fractions), are shown in Figure 5.3.6. It may be seen that the whole oil, supernatant oil and unbound oil C_0-C_3 alkylphenols histograms are similar. The total C_0-C_3 alkylphenol yields for the supernatant and unbound oil fractions (approximately 18,000 & 14,000 ng g^{-1} respectively, Table 5.3.1), are approximately half of the total concentrations for the whole oil fraction (33,000 ng g^{-1}, Table 5.3.1). The whole oil, supernatant oil and unbound oil alkylphenol distributions are dominated by the C_1 and C_2 alkylphenol groups (approximately 2,000 ng g^{-1} to 4,000 ng g^{-1} for whole oil; 500 ng g^{-1} to 2,000 ng g^{-1} for supernatant oil and unbound oil fractions), with the C_0 alkylphenol increasing in the unbound oil fraction when compared with the supernatant sample (500 ng g^{-1} to 2,500 ng g^{-1}). The C_3 alkylphenols are minor constituents in these fractions (100 ng g^{-1} to 1,000 ng g^{-1}). The cross plot of the total yields from the hindered versus non-hindered alkylphenols for whole oil, supernatant oil and unbound oil fractions, in Figures 5.3.2 to 5.3.4, show that the fractions predominantly plot in the hindered alkylphenol region.

The total C_0-C_3 alkylphenol concentrations for the bound oil fraction are, on average, an order of magnitude greater than those for the whole oil fraction, being approximately 439,000 ng g-$^{-1}$ The extracted alkylphenol distribution for the bound oil fraction is dominated by phenol (approximately 230,000 ng g^{-1}) followed by the C_1 and C_2 alkylphenol groups in decreasing abundance (approximately 100,000 ng g^{-1} and 50,000 ng g^{-1} respectively). The C_3 alkylphenols are essentially absent. The cross plot of the total yields for the hindered and non-hindered alkylphenols, in Figure 5.3.5, occurs in the non-hindered region.

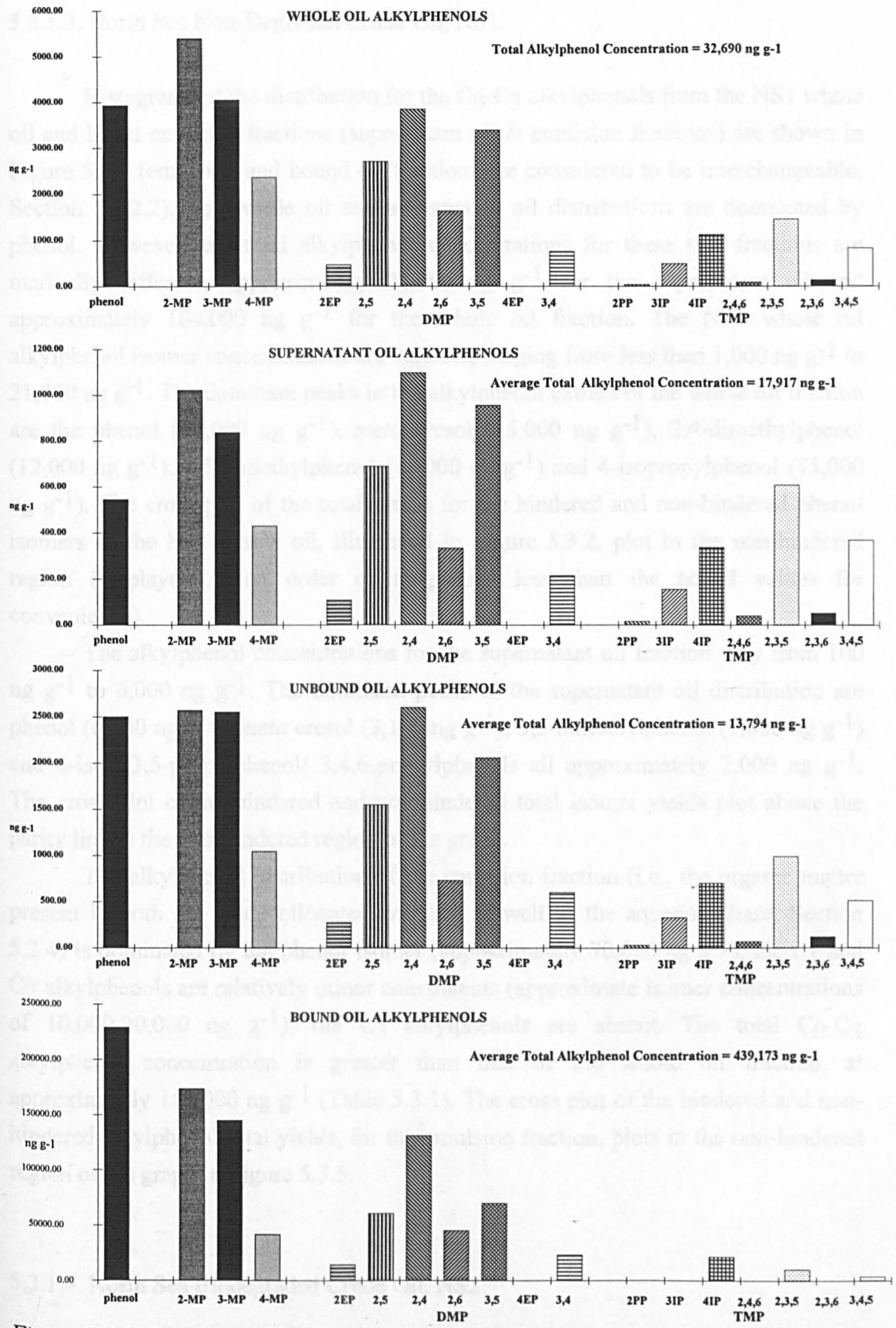

Figure 5.3.6. Examples of C_0-C_3 alkylphenol distributions and concentrations for the Eldfisk B12 whole oil, supernatant oil, unbound oil and bound oil fractions. Average total alkylphenol concentrations are also reported. MP = methylphenol; DMP = dimethylphenol; TMP = trimethylphenol.

5.3.1.3. North Sea Non-Degraded Crude Oil, NS1.

Histograms of the distribution for the C_0-C_3 alkylphenols from the NS1 whole oil and blend extracted fractions (supernatant oil & emulsion fractions) are shown in Figure 5.3.7 (emulsion and bound oil fractions are considered to be interchangeable; Section 5.4.2.2). The whole oil and supernatant oil distributions are dominated by phenol. However, the total alkylphenol concentrations for these two fractions are markedly different, approximately 24,000 ng g^{-1} for the supernatant oil and approximately 104,000 ng g^{-1} for the whole oil fraction. The NS1 whole oil alkylphenol isomer concentrations are variable, ranging from less than 1,000 ng g^{-1} to 21,000 ng g^{-1}. The dominant peaks in the alkylphenol extract of the whole oil fraction are the phenol (21,000 ng g^{-1}), *meta* cresol (15,000 ng g^{-1}), 2,4-dimethylphenol (12,000 ng g^{-1}), 3,5-dimethylphenol (11,000 ng g^{-1}) and 4-isopropylphenol (15,000 ng g^{-1}). The cross plot of the total yields for the hindered and non-hindered phenol isomers of the NS1 whole oil, illustrated in Figure 5.3.2, plot in the non-hindered region (displayed at an order of magnitude less than the actual values for convenience).

The alkylphenol concentrations for the supernatant oil fraction vary from 100 ng g^{-1} to 6,000 ng g^{-1}. The dominant peaks in the supernatant oil distribution are phenol (6,000 ng g^{-1}), *meta* cresol (3,100 ng g^{-1}), 3,5-dimethylphenol (1,800 ng g^{-1}) and 4-iso/2,3,5-propylphenol/ 3,4,6-propylphenols all approximately 2,000 ng g^{-1}. The cross plot of the hindered and non-hindered total isomer yields plot above the parity line in the non-hindered region of the graph.

The alkylphenol distribution of the emulsion fraction (i.e., the organic matter present in both the crude oil/water interface as well as the aqueous phase, Section 5.2.4) is dominated by the phenol isomer (approximately 70,000 ng g^{-1}), the C_1 and C_2 alkylphenols are relatively minor constituents (approximate isomer concentrations of 10,000-20,000 ng g^{-1}), the C_3 alkylphenols are absent. The total C_0-C_3 alkylphenol concentration is greater than that of the whole oil fraction, at approximately 152,000 ng g^{-1} (Table 5.3.1). The cross plot of the hindered and non-hindered alkylphenol total yields, for the emulsion fraction, plots in the non-hindered region of the graph in Figure 5.3.5.

5.3.1.4. North Sea Biodegraded Crude Oil, NS2.

In Figure 5.3.8, the C_0-C_3 alkylphenol distributions for the whole oil and extracted bound oil fractions of the NS2 crude oil are illustrated. The C_0-C_3

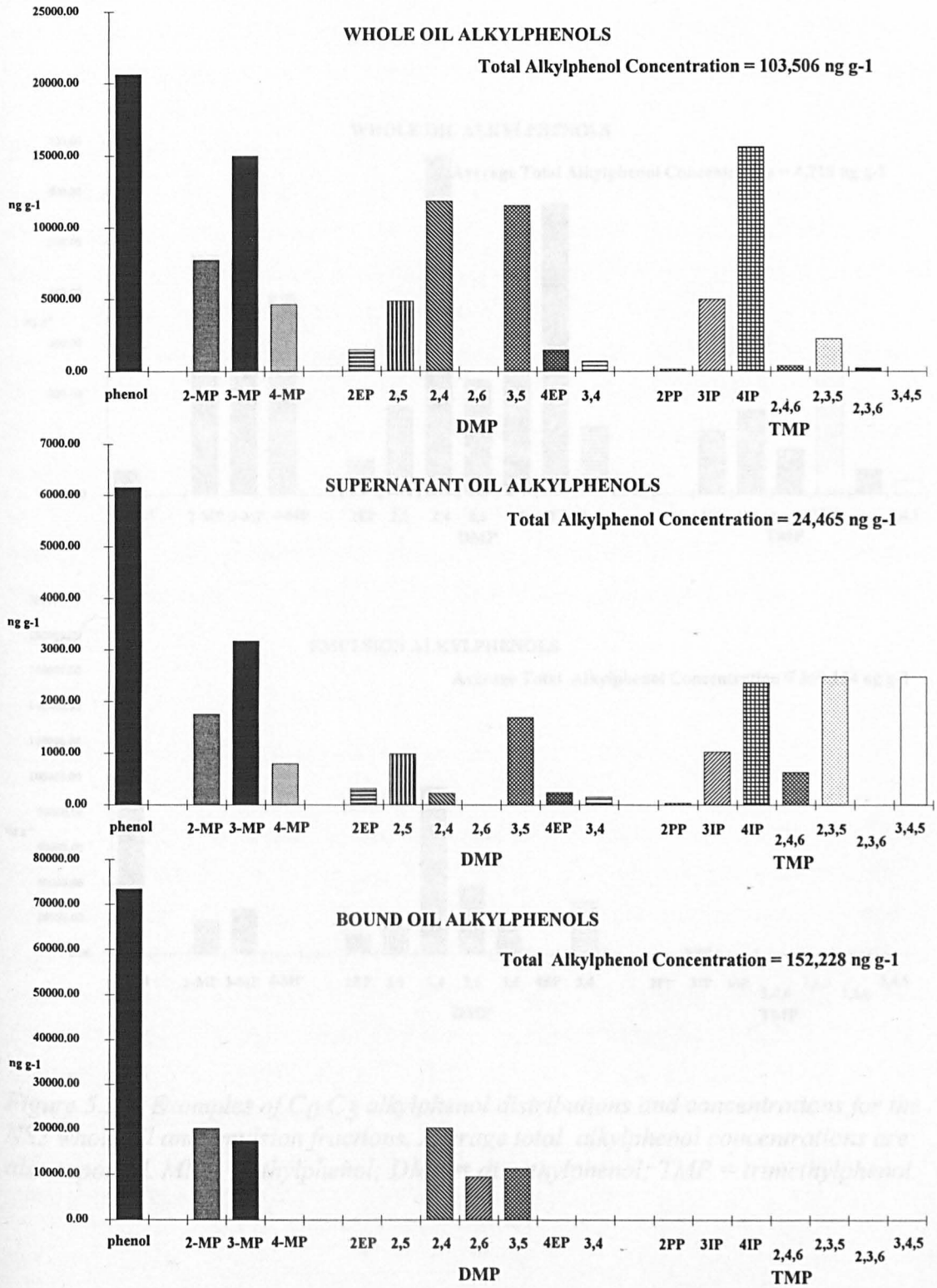

Figure 5.3.7. C_0-C_3 alkylphenol distributions and concentrations for the NS1 whole oil, supernatant oil and bound oil fractions. Total alkylphenol concentrations are also reported. MP = methylphenol; DMP = dimethylphenol; TMP = trimethylphenol.

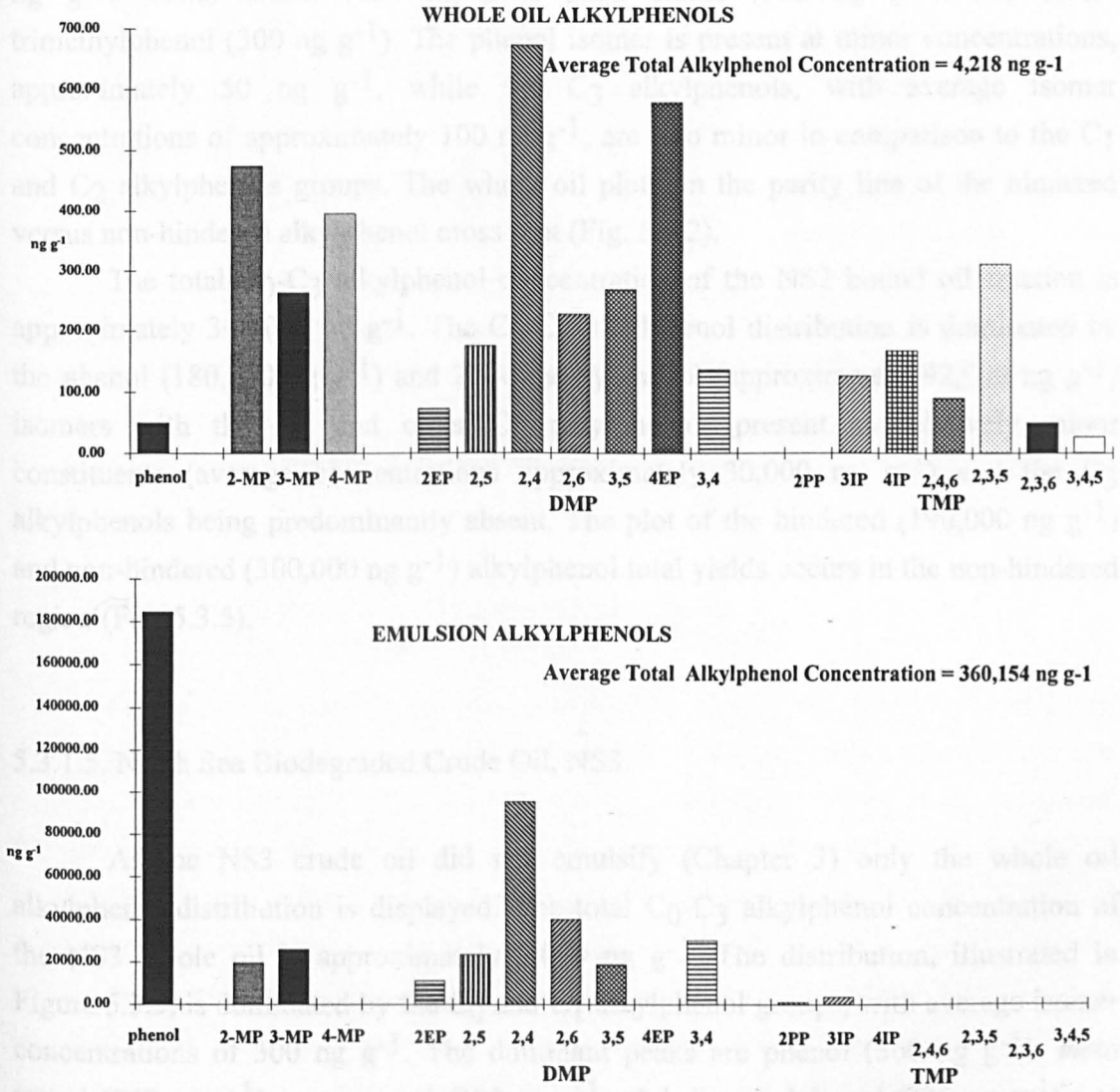

Figure 5.3.8. Examples of C_0-C_3 alkylphenol distributions and concentrations for the NS2 whole oil and emulsion fractions. Average total alkylphenol concentrations are also reported. MP = methylphenol; DMP = dimethylphenol; TMP = trimethylphenol.

alkylphenol extract of the NS2 whole oil has a total concentration of approximately 5,000 ng g^{-1}. The major alkylphenol groups in the alkylphenol distribution are the C_1 and C_2 alkylphenols, with isomer concentrations averaging at approximately 250 ng g^{-1}. The dominant peaks are the 2,4-dimethylphenol (650 ng g^{-1}), 4-ethylphenol (590 ng g^{-1}); *ortho* cresol (480 ng g^{-1}), *para* cresol (390 ng g^{-1}), and 2,3,5-trimethylphenol (300 ng g^{-1}). The phenol isomer is present at minor concentrations, approximately 50 ng g^{-1}, while the C_3 alkylphenols, with average isomer concentrations of approximately 100 ng g^{-1}, are also minor in comparison to the C_1 and C_2 alkylphenols groups. The whole oil plots on the parity line of the hindered versus non-hindered alkylphenol cross plot (Fig. 5.3.2).

The total C_0-C_3 alkylphenol concentration of the NS2 bound oil fraction is approximately 360,000 ng g^{-1}. The C_0-C_3 alkylphenol distribution is dominated by the phenol (180,000 ng g^{-1}) and 2,4-dimethylphenol (approximately 92,000 ng g^{-1}) isomers with the C_1 and other C_2 alkylphenols present as relatively minor constituents (average concentrations approximately 30,000 ng g^{-1}) and the C_3 alkylphenols being predominantly absent. The plot of the hindered (190,000 ng g^{-1}) and non-hindered (300,000 ng g^{-1}) alkylphenol total yields occurs in the non-hindered region (Fig. 5.3.5).

5.3.1.5. North Sea Biodegraded Crude Oil, NS3.

As the NS3 crude oil did not emulsify (Chapter 3) only the whole oil alkylphenol distribution is displayed. The total C_0-C_3 alkylphenol concentration of the NS3 whole oil is approximately 3,000 ng g^{-1}. The distribution, illustrated in Figure 5.3.9, is dominated by the C_0 and C_1 alkylphenol groups, with average isomer concentrations of 300 ng g^{-1}. The dominant peaks are phenol (360 ng g^{-1}), *meta* cresol (340 ng g^{-1}), *para* cresol (300 ng g^{-1}), 2,4-dimethylphenol (325 ng g^{-1}) and 2,3,5-trimethylphenol (300 ng g^{-1}). The majority of the C_2 and C_3 alkylphenol isomer concentrations average 50 ng g^{-1}. The hindered versus non-hindered alkylphenol cross plot, in Figure 5.3.2, plots on the parity line indicating no preferential dominance of either type of phenol in the oil.

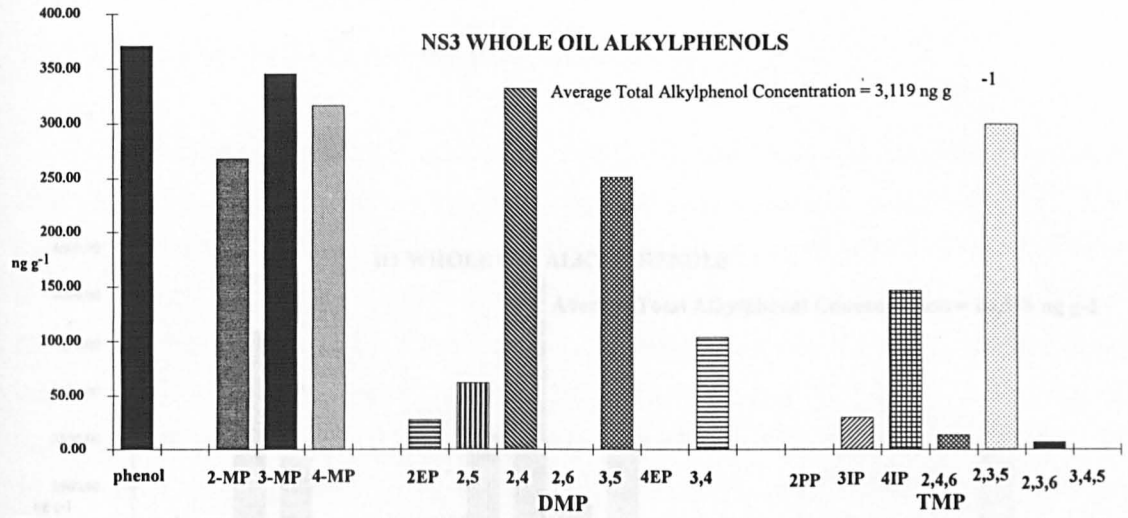

Figure 5.3.9. The C_0-C_3 alkylphenol distribution of the whole oil fraction for the biodegraded North Sea crude oil, NS3. Average total alkylphenol concentration is also reported, MP = methylphenol; DMP = dimethylphenol; TMP = trimethylphenol.

5.3.2. Alkylphenol Distributions for Santa Maria Basin Whole Oil and Blend Oil Fractions.

5.3.2.1. Santa Maria Basin Non-Degraded Crude Oil, H1.

Figure 5.3.10 displays the histograms of the C_0-C_3 alkylphenol distributions from the H1 whole oil and emulsion fractions. The total concentrations for the extracted C_0-C_3 alkylphenols from the non-degraded Santa Maria Basin whole oil fraction is approximately 26,000 ng g^{-1}. The dominant peaks are 2,4-dimethylphenol (4,000 ng g^{-1}) and *ortho* cresol (3,500 ng g^{-1}). The major groups are the C_1 and C_2 alkylphenols, with isomer concentrations averaging 2,000 ng g^{-1}. The C_0 and C_3 alkylphenols are present at lower concentration, with isomer yields ranging from 100 to 2,000 ng g^{-1}, averaging 500 ng g^{-1}. The cross plot of the total yields for hindered alkylphenol isomers (approximately 18,000 ng g^{-1}) and non-hindered alkylphenol isomers (approximately 8,600 ng g^{-1}), in Figure 5.3.2, occurs in the hindered C_0-C_3 alkylphenol region. Therefore, the C_0-C_3 alkylphenol distributions for the H1 whole oil are dominated by hindered alkylphenols.

The total C_0-C_3 alkylphenol yield of the emulsion fraction is approximately 370,000 ng g^{-1}. The distribution is dominated by phenol (approximately 170,000 ng g^{-1}) and 2,4-dimethylphenol (approximately 130,000 ng g^{-1}). The other C_1 and C_2 alkylphenols are present as minor constituents with the C_3 alkylphenols being absent. In Figure 5.3.5 the cross plot of the total yields for the hindered versus non-hindered C_0-C_3 alkylphenols plots in the non-hindered region.

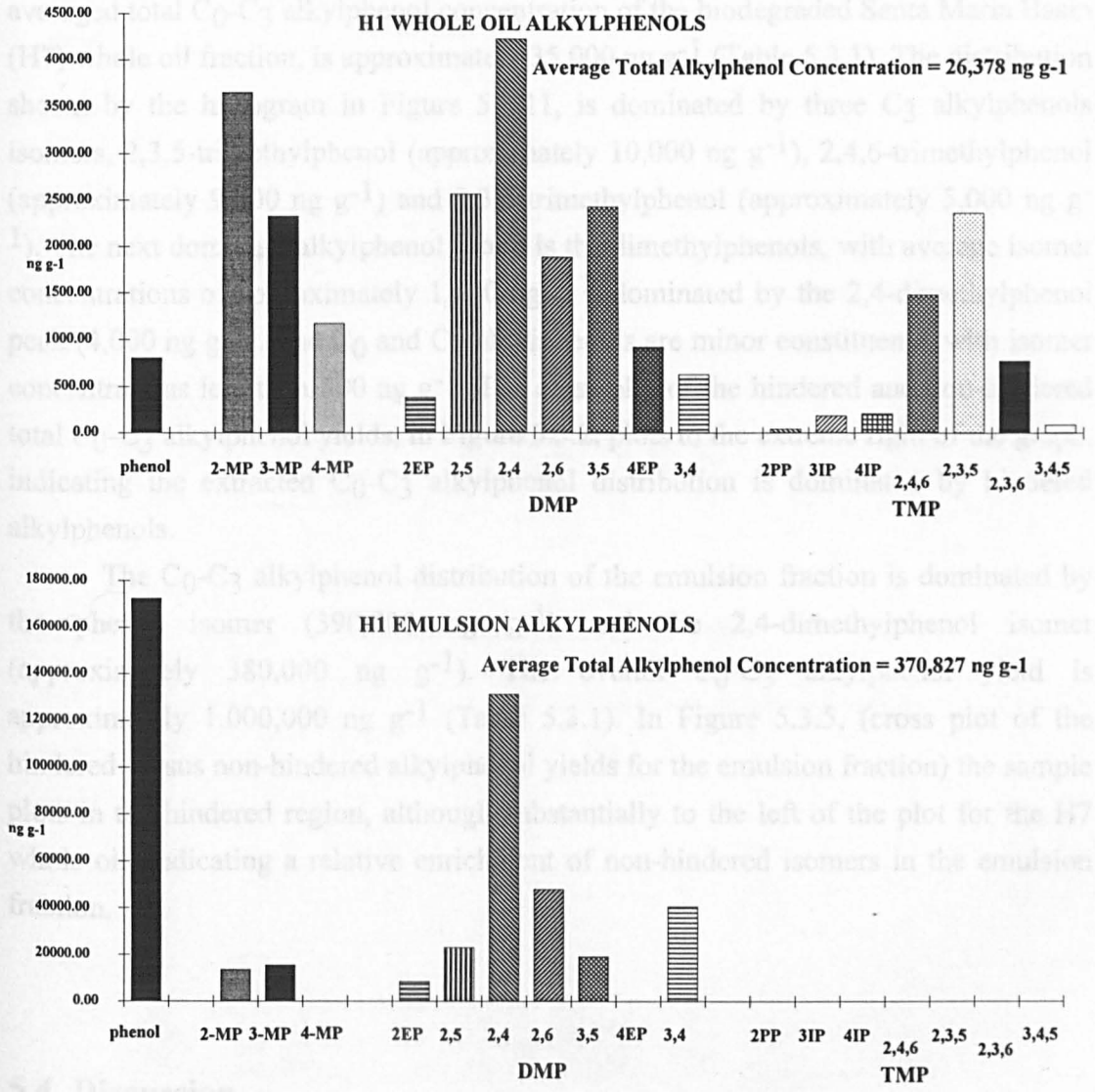

Figure 5.3.10. Examples of the C_0-C_3 alkylphenol distributions and concentrations for the whole oil and emulsion fractions of the non-degraded Santa Maria Basin (SMB) crude oil, H1. Average total alkylphenol concentrations are also reported. MP = methylphenol; DMP = dimethylphenol; TMP = trimethylphenol.

5.3.2.2. Santa Maria Basin Biodegraded Crude Oil, H7.

The alkylphenol distributions for whole oil and extracted emulsion fractions from the H7 crude oil, are represented by the histograms in Figure 5.3.11. The averaged total C_0-C_3 alkylphenol concentration of the biodegraded Santa Maria Basin (H7) whole oil fraction, is approximately 35,000 ng g^{-1} (Table 5.3.1). The distribution shown by the histogram in Figure 5.3.11, is dominated by three C_3 alkylphenols isomers, 2,3,5-trimethylphenol (approximately 10,000 ng g^{-1}), 2,4,6-trimethylphenol (approximately 9,000 ng g^{-1}) and 2,3,6-trimethylphenol (approximately 5,000 ng g^{-1}). The next dominant alkylphenol group is the dimethylphenols, with average isomer concentrations of approximately 1,000 ng g^{-1}, dominated by the 2,4-dimethylphenol peak (4,000 ng g^{-1}). The C_0 and C_1 alkylphenols are minor constituents, with isomer concentrations less than 500 ng g^{-1}. The cross plot of the hindered and non-hindered total C_0-C_3 alkylphenol yields, in Figure 5.3.2, plots to the extreme right of the graph, indicating the extracted C_0-C_3 alkylphenol distribution is dominated by hindered alkylphenols.

The C_0-C_3 alkylphenol distribution of the emulsion fraction is dominated by the phenol isomer (390,000 ng g^{-1}) and the 2,4-dimethylphenol isomer (approximately 380,000 ng g^{-1}). The overall C_0-C_3 alkylphenol yield is approximately 1,000,000 ng g^{-1} (Table 5.3.1). In Figure 5.3.5, (cross plot of the hindered versus non-hindered alkylphenol yields for the emulsion fraction) the sample plots in the hindered region, although substantially to the left of the plot for the H7 whole oil, indicating a relative enrichment of non-hindered isomers in the emulsion fraction.

5.4. Discussion.

Discussion will firstly investigate the C_0-C_3 alkylphenol compositions for the whole oil fractions analysed, assessing the variation of distributions relative to crude oil biodegraded states and water-in-oil emulsion formation/stabilisation ability. Work will then assess alkylphenol distributions of the blend fractions (supernatant oil, unbound oil, emulsion/bound oil fractions), especially any quantitative and qualitative variation between the emulsion/bound oil fractions and the whole oil fractions. Lastly, attention is paid to the relationship between distribution and concentrations of the C_0-C_3 alkylphenols and the crude oil water retention data from Chapter 3.

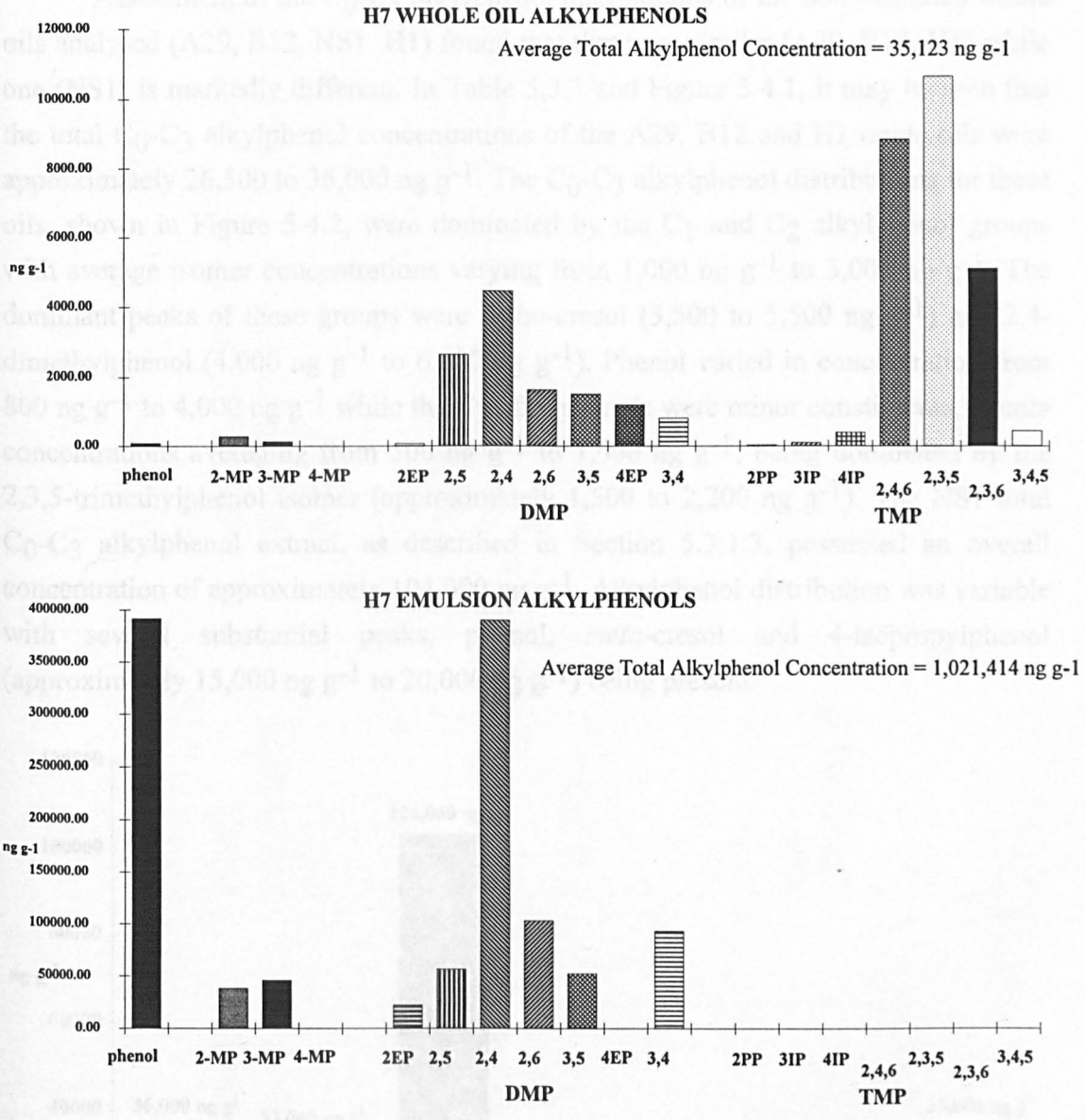

Figure 5.3.11. Examples of the C_0-C_3 alkylphenol distributions and concentrations for the whole oil and emulsion fractions of the biodegraded Santa Maria Basin (SMB) crude oil, H7. Average total alklphenol concentrations also reported. MP = methylphenol; DMP = dimethylphenol; TMP = trimethylphenol.

5.4.1. Alkylphenol Distributions of the Whole Oil Fractions.

5.4.1.1. Non-Degraded Whole Oil Fractions (A29, B12, NS1, H1).

Assessment of the C_0-C_3 alkylphenol distributions of the non-degraded whole oils analysed (A29, B12, NS1, H1) found that three are similar (A29, B12, H1) while one (NS1) is markedly different. In Table 5.3.1 and Figure 5.4.1, it may be seen that the total C_0-C_3 alkylphenol concentrations of the A29, B12 and H1 crude oils were approximately 26,500 to 36,000 ng g^{-1}. The C_0-C_3 alkylphenol distributions for these oils, shown in Figure 5.4.2, were dominated by the C_1 and C_2 alkylphenol groups with average isomer concentrations varying from 1,000 ng g^{-1} to 3,000 ng g^{-1}. The dominant peaks of these groups were *ortho*-cresol (3,500 to 5,500 ng g^{-1}) and 2,4-dimethylphenol (4,000 ng g^{-1} to 6,000 ng g^{-1}). Phenol varied in concentration from 800 ng g^{-1} to 4,000 ng g^{-1} while the C_3 alkylphenols were minor constituents, isomer concentrations averaging from 500 ng g^{-1} to 1,000 ng g^{-1}, being dominated by the 2,3,5-trimethylphenol isomer (approximately 1,500 to 2,200 ng g^{-1}). The NS1 total C_0-C_3 alkylphenol extract, as described in Section 5.3.1.3, possessed an overall concentration of approximately 104,000 ng g^{-1}. Alkylphenol distribution was variable with several substantial peaks, phenol, *meta*-cresol and 4-isopropylphenol (approximately 15,000 ng g^{-1} to 20,000 ng g^{-1}) being present.

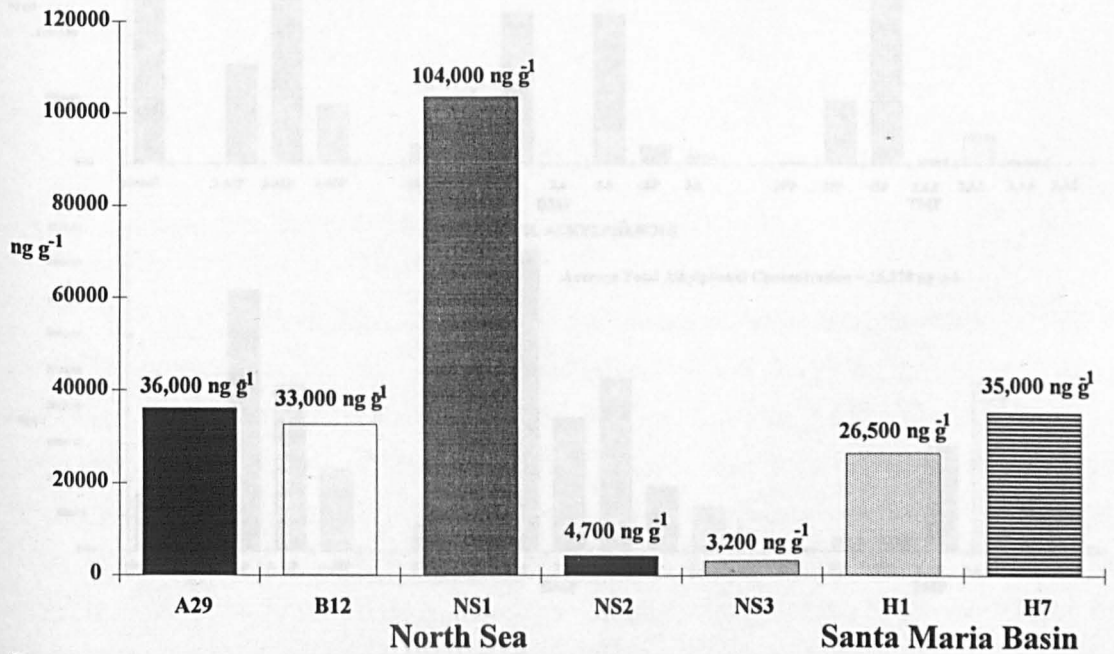

Figure 5.4.1, Histogram of the averaged total C_0-C_3 alkylphenol concentrations (ng g-1) for the whole oils analysed. The averaged C_0-C_3 alkylphenol concentration for each whole oil is also shown above each column. The number of samples averaged per whole oil is shown in Table 5.3.1.

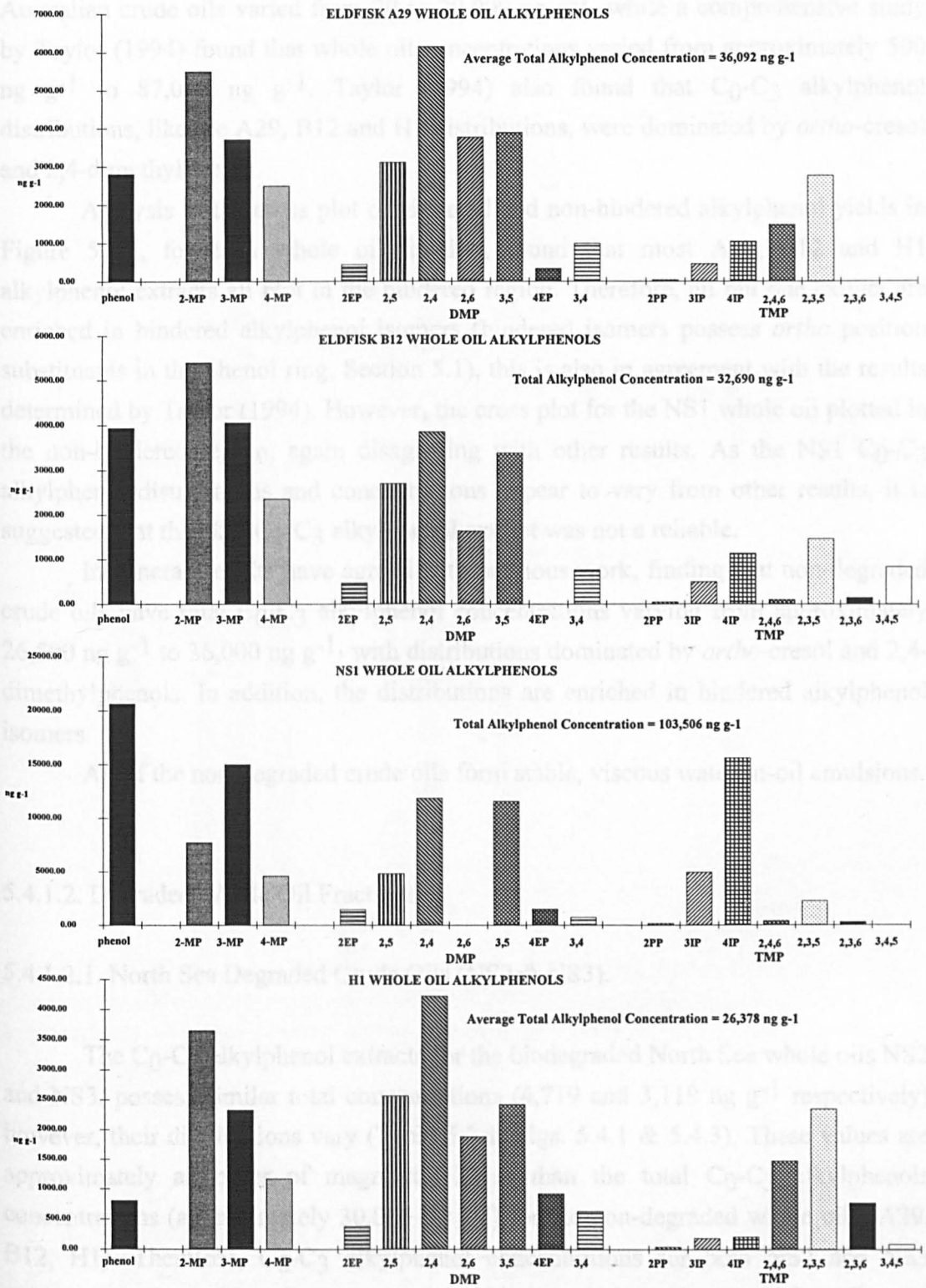

Figure 5.4.2. Examples of the C_0-C_3 alkylphenol distributions and concentrations for non-degraded crude oils (A29, B12, NS1 & H1). Extract concentrations are also shown. MP = methylphenol; DMP = dimethylphenol; TMP = trimethylphenol.

Work by Ioppolo *et al.* (1992) found total alkylphenol concentrations in Australian crude oils varied from 20 to 29,000 ng g^{-1}, while a comprehensive study by Taylor (1994) found that whole oil concentrations varied from approximately 500 ng g^{-1} to 87,000 ng g^{-1}. Taylor (1994) also found that C_0-C_3 alkylphenol distributions, like the A29, B12 and H1 distributions, were dominated by *ortho*-cresol and 2,4-dimethylphenol.

Analysis of the cross plot of hindered and non-hindered alkylphenol yields in Figure 5.3.2, for each whole oil fraction, found that most A29, B12 and H1 alkylphenol extracts all plot in the hindered region. Therefore, all but one extract are enriched in hindered alkylphenol isomers (hindered isomers possess *ortho* position substituents in the phenol ring, Section 5.1), this is also in agreement with the results determined by Taylor (1994). However, the cross plot for the NS1 whole oil plotted in the non-hindered region, again disagreeing with other results. As the NS1 C_0-C_3 alkylphenol distributions and concentrations appear to vary from other results, it is suggested that the NS1 C_0-C_3 alkylphenol extract was not a reliable.

In general, results have agreed with previous work, finding that non-degraded crude oils have total C_0-C_3 alkylphenol concentrations varying from approximately 26,500 ng g^{-1} to 36,000 ng g^{-1}, with distributions dominated by *ortho*-cresol and 2,4-dimethylphenols. In addition, the distributions are enriched in hindered alkylphenol isomers.

All of the non-degraded crude oils form stable, viscous water-in-oil emulsions.

5.4.1.2. Degraded Whole Oil Fractions.

5.4.1.2.1. North Sea Degraded Crude Oils (NS2 & NS3).

The C_0-C_3 alkylphenol extracts for the biodegraded North Sea whole oils NS2 and NS3, possess similar total concentrations (4,719 and 3,119 ng g^{-1} respectively) however, their distributions vary (Table 5.3.1, Figs. 5.4.1 & 5.4.3). These values are approximately an order of magnitude lower than the total C_0-C_3 alkylphenols concentrations (approximately 30,000 ng g^{-1}) for the non-degraded whole oils (A29, B12, H1). Therefore, C_0-C_3 alkylphenol concentrations for both NS2 and NS3 extracts appear to have been reduced by biodegradation. However, the effect of biodegradation on the isomeric distributions of C_0-C_3 alkylphenols was different for the two oils.

The alkylphenol distribution for the NS2 crude oil (Fig. 5.4.3) appears to be similar to those of the non-degraded North Sea crude oils (above), with the *ortho*-

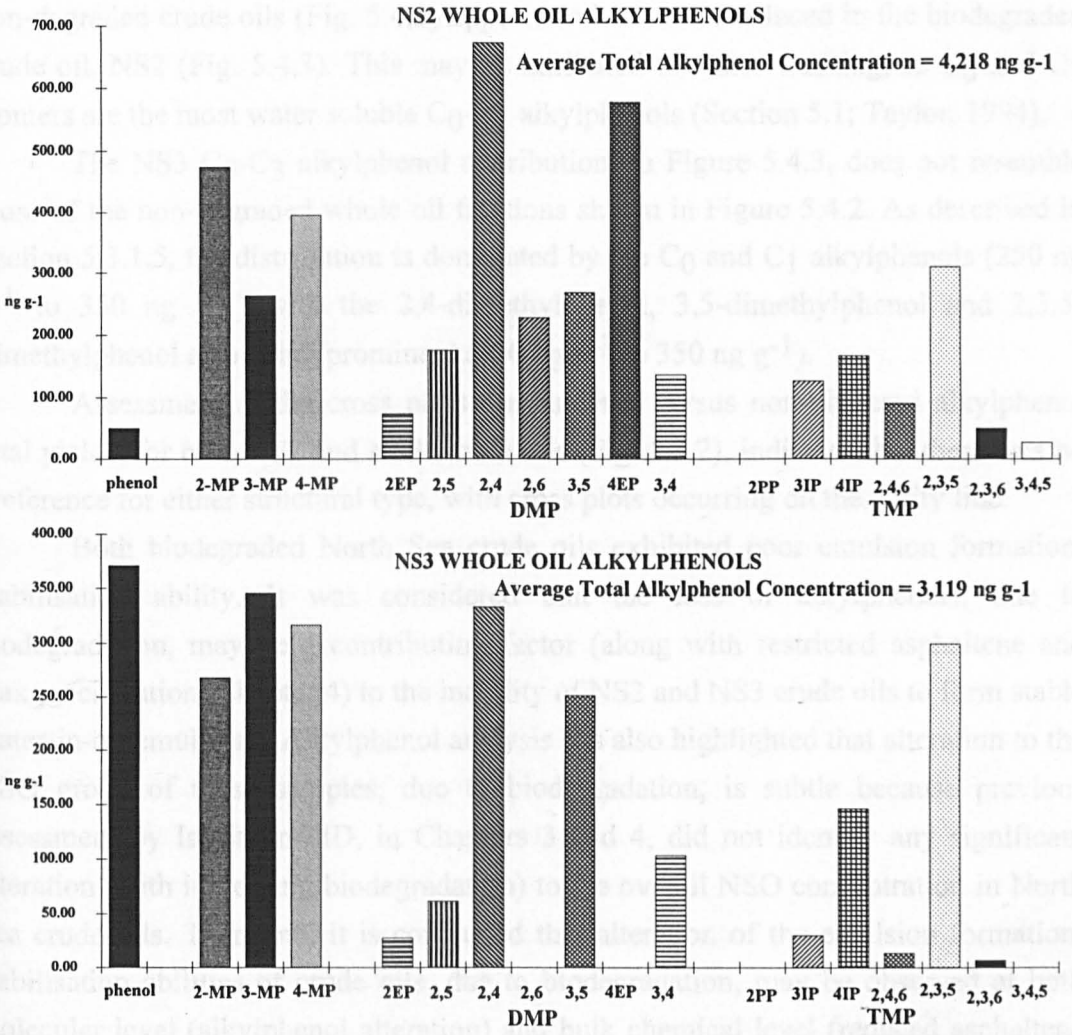

Figure 5.4.3. Examples of the alkylphenol distributions and concentrations of biodegraded North Sea crude oils (NS2 & NS3). Average total alkylphenol concentrations are also shown. MP = nethylphenol; DMP = dimethylphenol; TMP = trimethylphenol.

cresol (480 ng g^{-1}) and 2,4-dimethylphenol (650 ng g^{-1}) peaks being dominant. However, as well as these two peaks the 4-ethylphenol peak was also significant (580 ng g^{-1}). The dominance of C_0 and C_1 alkylphenols over C_2 and C_3 alkylphenols, in non-degraded crude oils (Fig. 5.4.2) appears to have been reduced in the biodegraded crude oil, NS2 (Fig. 5.4.3). This may be attributed to water washing, as C_0 and C_1 isomers are the most water soluble C_0-C_3 alkylphenols (Section 5.1; Taylor, 1994).

The NS3 C_0-C_3 alkylphenol distribution, in Figure 5.4.3, does not resemble those of the non-degraded whole oil fractions shown in Figure 5.4.2. As described in Section 5.3.1.5, the distribution is dominated by the C_0 and C_1 alkylphenols (250 ng g^{-1} to 350 ng g^{-1}) with the 2,4-dimethylphenol, 3,5-dimethylphenol and 2,3,5-trimethylphenol also being prominent (250 ng g^{-1} to 350 ng g^{-1}).

Assessment of the cross plots for hindered versus non-hindered alkylphenol total yields, for both NS2 and NS3 whole oils (Fig. 5.3.2), indicates that there was no preference for either structural type, with cross plots occurring on the parity line.

Both biodegraded North Sea crude oils exhibited poor emulsion formation/ stabilisation ability. It was considered that the loss of alkylphenols, due to biodegradation, may be a contributing factor (along with restricted asphaltene and wax precipitation; Chapter 4) to the inability of NS2 and NS3 crude oils to form stable water-in-oil emulsions. Alkylphenol analysis has also highlighted that alteration to the NSO group of these samples, due to biodegradation, is subtle because previous assessment by Iatroscan-FID, in Chapters 3 and 4, did not identify any significant alteration (with increasing biodegradation) to the overall NSO concentration in North Sea crude oils. Therefore, it is concluded that alteration of the emulsion formation/ stabilisation abilities of crude oils, due to biodegradation, may be observed at both molecular level (alkylphenol alteration) and bulk chemical level (reduced asphaltene precipitation potential and wax content, Chapter 4). It is suggested that biodegradation reduced the emulsion formation/stabilisation ability of North Sea crude oils (NS2 & NS3) by the reduction of the concentration of influential oil-soluble surfactants (alkylphenols), as well as by prevention of asphaltene precipitation and reduction of wax concentration (Chapters 3 & 4).

5.4.1.2.2. Santa Maria Basin Biodegraded Crude Oil, H7.

Unlike the biodegraded North Sea crude oils (NS2 & NS3), the total C_0-C_3 alkylphenols concentration of the biodegraded Santa Maria Basin crude oil, H7, was approximately equal to those of the non-degraded crude oil alkylphenol concentrations (A29, B12 & H1), with an average value of 35,000 ng g^{-1} (Table 5.3.1,

Fig. 5.4.1). However, the alkylphenol distribution for H7, compared with H1 in Figure 5.4.4, is dominated by the 2,4,6-trimethylphenol, 2,3,5-trimethylphenol and 2,3,6-trimethylphenol (approximate isomer concentrations of 5,000 to 11,000 ng g^{-1}) in contrast to the C_0 and C_1 domination distribution for non-degraded crude oils. As the H1 crude oil may be considered to be an example of a non-degraded precursor of the H7 crude oil (Taylor, 1994), an estimation of change in alkylphenol content for H1 crude oil, due to biodegradation, may be established by comparison of H1 and H7 C_0-C_3 alkylphenol concentrations. In Figure 5.4.5, such a comparison has been made. The peaks seen in the histogram represent the H7 alkylphenol concentrations as percentages of their concentrations in the H1 crude oil. For example, the *ortho*-cresol concentration for H7 is divided by the *ortho*-cresol concentration for H1, the result being multiplied by 100%. In Figure 5.4.5 the results from normalisation illustrate the quantitative differences between the H1 and H7 crude oils. The C_0 and C_1 alkylphenols for the H7 oil have reduced relative to H1 concentrations, being 10% of the same isomers in the H1 crude oil. Most of the C_2 alkylphenols, as well as the 2-propylphenol, 3-isopropylphenol and 4-isopropylphenol isomers, from the H7 extracts, possess similar concentrations as those for the H1 crude oil (approximately 100%±50%). However, the C_3 alkylphenols; 2,4,6-trimethylphenol, 2,3,5-trimethylphenol, 2,3,6-trimethylphenol and 3,4,5-trimethylphenol, in the H7 crude oil are approximately 400% to 600% greater than those in the H1 crude oil. In addition to the preferential enrichment of the C_3 alkylphenols, assessment of the cross plots for hindered versus non-hindered alkylphenol total yields (Fig. 5.3.2) indicate that the H7 alkylphenol extract plot upon the extreme right of the graph, with alkylphenol distributions being dominated by hindered phenol isomers. This represents an increase in the hindered alkylphenols in the H7 crude oil when compared with the H1 crude oil, as well as the higher molecular weight alkylphenols, such characteristics are indicative of water washing (Taylor, 1994; Section 6.1).

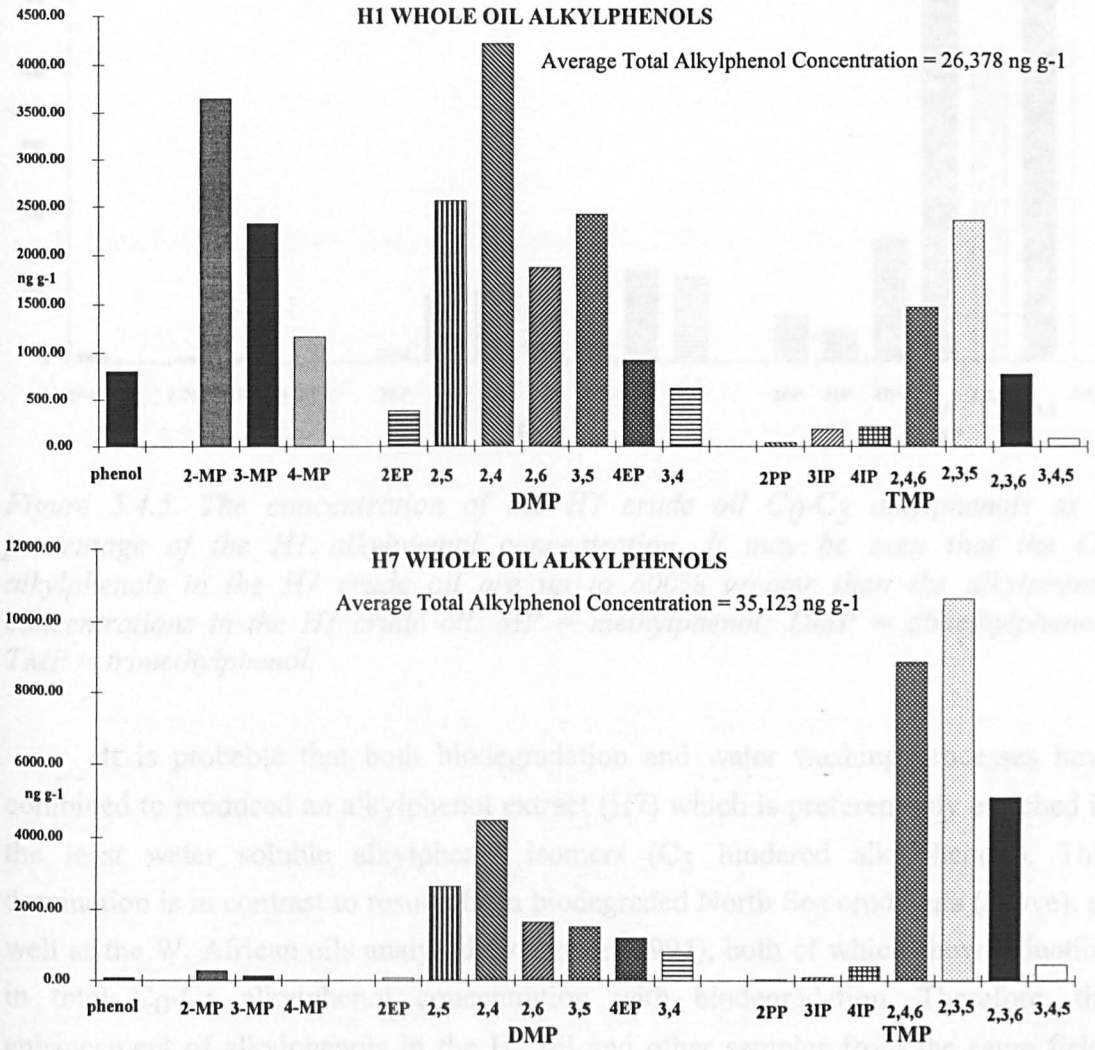

Figure 5.4.4. Examples of the C_0-C_3 alkylphenol distributions and concentrations of normal (H1) and biodegraded (H7) Santa Maria Basin (SMB) crude oils. Average total alkylphenol concentrations are also shown. MP = methylphnol, DMP = dimethylphenol; TMP = trimethylphenol.

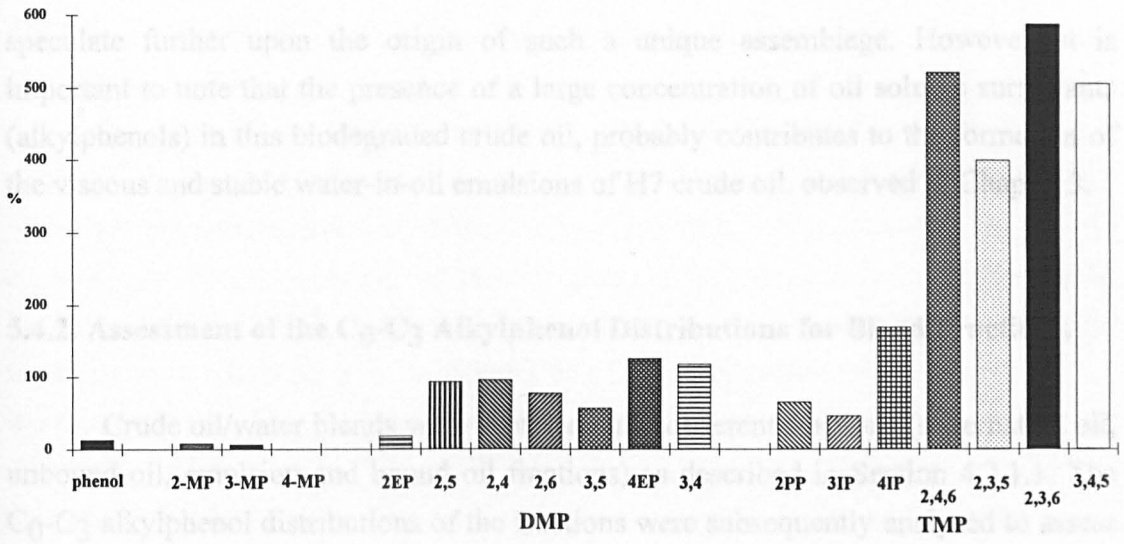

Figure 5.4.5. The concentration of the H7 crude oil C_0-C_3 alkylphenols as a percentage of the H1 alkylphenol concentration. It may be seen that the C_3 alkylphenols in the H7 crude oil are up to 600% greater than the alkylphenol concentrations in the H1 crude oil. MP = methylphenol; DMP = dimethylphenol; TMP = trimethylphenol.

It is probable that both biodegradation and water washing processes have combined to produced an alkylphenol extract (H7) which is preferentially enriched in the least water soluble alkylphenol isomers (C_3 hindered alkylphenols). This domination is in contrast to results from biodegraded North Sea crude oils (above), as well as the W. African oils analysed by Taylor (1994), both of which show reduction in total C_0-C_3 alkylphenol concentration with biodegradation. Therefore, the enhancement of alkylphenols in the H7 oil and other samples from the same field, appears to be unusual (Taylor, 1994).

It is possible that the alkylphenol concentrations and distributions from the H7 crude oil may be attributed to biodegradation. It is known that the microbial degradation of polyaromatic hydrocarbons (PAHs) involves the incorporation of molecular oxygen thereby generating phenols (Gibson & Subramanian, 1984 referred to in Cerniglia, 1992). In addition, work by Cerniglia (1992) has shown that alkylphenols are intermediate products of reactions such as PAH hydroxylation by filamentous fungi, in a monooxygenase system. Also, Gibson (1991) (referred to by Taylor, 1994) has shown that alkylphenols are produced by the biodegradation of toluene. However, detailed work by Taylor (1994) was unable to satisfactorily account for the enrichment of the C_3 alkylphenols in the H7 crude oil and concluded that the C_0-C_3 alkylphenol distribution may be accounted for by "unique reservoir conditions". As this research is not concerned with the generation of C_0-C_3 alkylphenol distributions, merely their effect upon crude oil water uptake, it will not

speculate further upon the origin of such a unique assemblage. However, it is important to note that the presence of a large concentration of oil soluble surfactants (alkylphenols) in this biodegraded crude oil, probably contributes to the formation of the viscous and stable water-in-oil emulsions of H7 crude oil, observed in Chapter 3.

5.4.2. Assessment of the C_0-C_3 Alkylphenol Distributions for Blend Fractions.

Crude oil/water blends were separated into different fractions (supernatant oil, unbound oil, emulsion and bound oil fractions) as described in Section 4.2.1.1. The C_0-C_3 alkylphenol distributions of the fractions were subsequently analysed to assess the alteration due to blending of the oil and water phases.

5.4.2.1. Comparison of Whole Oil, Supernatant Oil and Unbound Oil Fractions.

Assessment of the alkylphenol extracts of the A29 fractions identified that the C_0-C_3 alkylphenol distributions for the whole oil, supernatant oil and unbound oil fractions were similar. In Figure 5.3.1 it is seen that these three fractions are all dominated by *ortho*-cresol (2,800 ng g^{-1} to 5,500 ng g^{-1}) and 2,4-dimethylphenol (4,000 ng g^{-1} to 6,000 ng g^{-1}) although there is an increase in the phenol concentration, for supernatant oil to unbound oil, of 1,500 ng g^{-1} to 3,900 ng g^{-1}. In Figure 5.3.6, the alkylphenol distributions for the B12 crude oil/water blend fractions (supernatant and unbound oil) are dominated by the C_1 and C_2 alkylphenols (100 ng g^{-1} to 2,500 ng g^{-1}) with the C_0 alkylphenol concentration increasing from supernatant oil to unbound oil (600 ng g^{-1} to 2,500 ng g^{-1}).

The increase in the concentration of the phenol, for both A29 and B12 unbound oil fractions, may be attributed to the polarity of the unbound oil fraction prior to alkylphenol extraction. The unbound oil was extracetd in a xylene:heptane solvent mixture (3:1), which possesses a greater polarity than the bulk crude oil. Such an increase in polarity, as reported by Southworth *et al.* (1983) and Taylor (1994), and discussed in Section 5.1, may increase the partition coefficients of the C_0-C_3 alkylphenols. Work by Southworth *et al.* (1983), reported in Table 5.1.1, identified that the partition coefficient of phenol was affected to a lesser degree than that of the C_1-C_3 alkylphenols (C_1-C_3 alkylphenols being retained in the xylene:heptane mix to a greater degree than in the crude oil). Consequently, the increase in the phenol concentration in the total C_0-C_3 alkylphenol recovery is caused by the increased

difficulty of extracting the C_1-C_3 alkylphenols from a higher polarity solvent medium (*i.e.*, xylene:heptane).

In general the total alkylphenol concentrations for the supernatant and unbound oil fractions, even after consideration of standard deviations (Table 5.3.1), were less than those from the whole oil alkylphenols extracts. Again, the greater solvent polarity of the unbound oil medium may account for its reduced extract yields. However, as the alkylphenol extraction conditions for whole oil and supernatant oil fractions were identical, it is considered that the low alkylphenol concentrations for the supernatant oil fraction may be attributed to other factors. It was suspected that the supernatant oil fraction may have lost alkylphenols relative to the whole oil yield by the action of water washing (during blending experiments), or by partition from the oil to the oil/water interfacial film.

The effect of water washing by 3 ml of distilled water, may be assessed by Equation {5.4.1} used by Taylor (1994).

$$C_{of} = \frac{C_{oi}}{1 + Vw/(Vo*Kow)} \quad \{5.4.1\}$$

Cof = concentration of isomer after water washing.
Coi = concentration of isomer prior to water washing.
Vw = volume of water.
Vo = volume of oil.
Kow = oil/water partition coefficient of isomer.

Calculation of each C_0-C_3 alkylphenol isomer concentration, in both water and crude oil phases, was performed for a water:oil ratio of 3:7. These calculated concentrations were summed and the total alkylphenol concentration of the washed crude oil was then compared to the total alkylphenol concentrations of the whole oil and supernatant oil fractions in Table 5.4.1. Results from the comparison show that the calculated alkylphenol concentration in the oil phase is not sufficiently low to explain the C_0-C_3 total alkylphenol concentration of the supernatant oil. Therefore, water washing alone does not account for the low concentration of the supernatant oil fraction. In addition, the low supernatant oil concentrations could not be explained by loss of C_0-C_3 alkylphenols to the bound oil phase. The average bound oil extract weight for A29 and B12 crude oils (approximately 500 ng; discussed below; Table 5.4.2), even when combined with losses due to water washing (above) and analytical errors (standard deviation; Table 5.3.1) do not account for the difference in extract weights for whole oil and supernatant oil fractions.

As mentioned earlier, the only difference between the whole oil and supernatant oil fractions is that the latter has been blended, and then separated from, a water phase. It is therefore suggested that observed losses are due to problems with this procedure. For example, it is possible that the temperature of the crude oil/water blend increased during blending which may have altered the alkylphenol partition coefficients. Such an affect, as observed by Taylor (1994), reduced the alkylphenol concentrations in the oil phase (Section 5.1).

Crude Oils	Whole Oils	Oil Phase (calculated)*	Supernatant Oil	Water Phase (calculated)*
A29	36,092	35,234	23,892	858
B12	32,690	31,678	17,917	1013
NS2	4,218	4,149	4,353	69
H1	26,378	25,906		472
H7	35,123	34,989		134

Table 5.4.1. Comparison of the calculated C_0-C_3 alkylphenol concentrations (ng g^{-1}) for crude oil and water phases (after blending at a water:oil ratio of 3:7) with the actual extracted total C_0-C_3 alkylphenol concentrations (ng g^{-1}) for selected whole oil and supernatant oil fractions. It is seen that the concentration of alkylphenols from the A29 & B12 calculated water washed oil phase (*) is not similar to the alkylphenol concentration for the supernatant oil fraction.*

5.4.2.2. Assessment of the C_0-C_3 Alkylphenol Extracts for Emulsion/Bound Oil Fractions.

One of the main aims of this study was the assessment of the effect of alkylphenols upon the stabilisation of water-in-oil emulsions; consequently, characterisation of alkylphenol distribution in the water-in-oil emulsion is essential. Therefore, analysis of the C_0-C_3 alkylphenol distributions for water-in-oil emulsions was attempted using both the emulsion (containing the bound oil and aqueous phase, Section 4.2.1) and bound oil fractions (organic matter in the interfacial film). Analysis was performed on 9 bound oil fractions and 9 emulsion fractions.

Comparison of the total concentrations for the C_0-C_3 alkylphenol extracts from the bound oil/emulsion fractions, listed in Table 5.3.1, shows that concentrations vary greatly, approximately 150,000 ng g^{-1} to 1,000,000 ng g^{-1}. However, all are substantially greater than the total alkylphenol concentrations for their respective whole oil fractions (3,000 ng g^{-1} to 100,000 ng g^{-1}), many by at least an order of

magnitude. Therefore, it was concluded that the alkylphenol content of the organic matter in the bound oil and emulsion fractions was substantially increased. In addition, it was found that the alkylphenol distributions for most bound oil and emulsion fractions were dominated by the low molecular weight alkylphenols, predominantly phenol itself, although 2,4-dimethylphenol was also a substantial peak.

A cross plot of hindered alkylphenol isomers versus the non-hindered alkylphenol isomers, for all emulsion and bound oil fractions, is shown in Figure 5.3.5. It may be seen that all emulsion and bound oil fractions, except those of the H7 crude oil, plot in the non-hindered region of the cross plot. This change from the alkylphenol distributions of the whole oil fractions, which are dominated by hindered C_0-C_3 alkylphenols illustrated in Figure 5.3.2, to the distributions of the emulsion and bound oil fractions, dominated by non-hindered alkylphenols, indicates preferential enrichment of non-hindered alkylphenols in the water-in-oil emulsion. It must be noted that although the H7 emulsion alkylphenols plotted in the hindered isomer dominated region of the cross plot in Figure 5.3.5, the alkylphenol content of the H7 emulsions were appreciably closer to the parity line than the alkylphenols of H7 whole oil fraction (Fig. 5.3.2), indicating a preferential enrichment of the non-hindered alkylphenols. Therefore, work has shown that overall, the alkylphenols present in the water-in-oil emulsion have been preferentially enriched in the lower molecular weight alkylphenols with non-hindered arrangements and that concentrations are frequently up to an order of magnitude greater than those for whole oil fractions.

However, such analysis gives no indication of the distribution of C_0-C_3 alkylphenols within the water-in-oil emulsion. As discussed in Chapter 1, emulsions in general consist of an oil phase, a water phase and an interfacial film. The oil phase has already been extracted (unbound oil phase) leaving the interfacial film (bound oil) and the aqueous phase (present in the emulsion fraction). The above observations have identified the preferential enrichment of low molecular weight, non-hindered alkylphenols in the water-in-oil emulsions, but not in which phase (aqueous or interfacial). The comparison of the C_0-C_3 alkylphenol extracts for bound oil (organic matter from the interfacial film) and emulsion (organic matter from both aqueous phase and interfacial film) fractions may help identify which phase the alkylphenols are present in.

In Figure 5.4.6 it may be seen that the alkylphenol distributions for bound oil and emulsion fractions for A29 and B12 oils are similar, being dominated by the C_0-alkylphenol (approximately 60,000 to 230,000 ng g^{-1}) with relatively minor quantities of C_1 and C_2 alkylphenols (predominantly 3,000 to 25,000 ng g^{-1} in most extracts with the exception of a B12 fraction with C_1 and C_2 isomer concentrations from

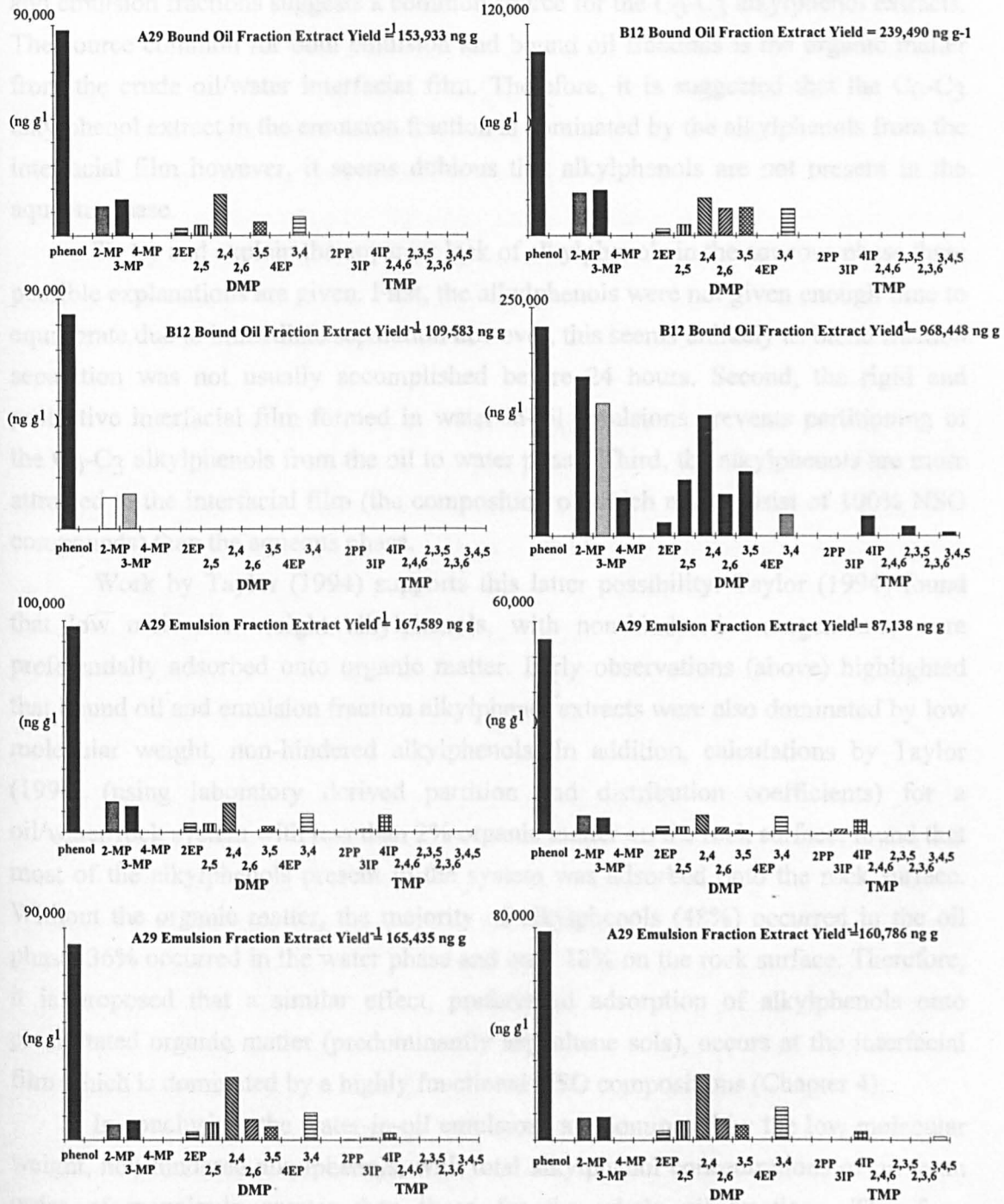

Figure 5.4.6. Comparison of C_0-C_3 alkylphenol distributions for bound oil and emulsion fractions extracted from Eldfisk crude oil/water blends illustrating the common origin of alkylphenols for both fractions. The total concentrations (ng g^{-1}) for extracted C_0-C_3 alkylphenol fractions are also shown. MP = methylphenol; DMP = dimethylphenol; TMP = trimethylphenol.

approximately 10,000 to 170,000 ng g^{-1}). The C_3 alkylphenols are essentially absent in all extracts. Such similarities for both concentrations and distributions of bound oil and emulsion fractions suggests a common source for the C_0-C_3 alkylphenol extracts. The source common for both emulsion and bound oil fractions is the organic matter from the crude oil/water interfacial film. Therefore, it is suggested that the C_0-C_3 alkylphenol extract in the emulsion fraction is dominated by the alkylphenols from the interfacial film however, it seems dubious that alkylphenols are not present in the aqueous phase.

To try and explain the apparent lack of alkylphenols in the aqueous phase three possible explanations are given. First, the alkylphenols were not given enough time to equilibrate due to immediate separation however, this seems unlikely as blend fraction separation was not usually accomplished before 24 hours. Second, the rigid and protective interfacial film formed in water-in-oil emulsions prevents partitioning of the C_0-C_3 alkylphenols from the oil to water phase. Third, the alkylphenols are more attracted to the interfacial film (the composition of which may consist of 100% NSO compounds) than the aqueous phase.

Work by Taylor (1994) supports this latter possibility. Taylor (1994) found that low molecular weight alkylphenols, with non-hindered arrangements, were preferentially adsorbed onto organic matter. Early observations (above) highlighted that bound oil and emulsion fraction alkylphenol extracts were also dominated by low molecular weight, non-hindered alkylphenols. In addition, calculations by Taylor (1994) (using laboratory derived partition and distribution coefficients) for a oil/water/rock system with less than 2% organic matter on the rock surface, found that most of the alkylphenols present in the system was adsorbed onto the rock surface. Without the organic matter, the majority of alkylphenols (48%) occurred in the oil phase, 36% occurred in the water phase and only 18% on the rock surface. Therefore, it is proposed that a similar effect, preferential adsorption of alkylphenols onto precipitated organic matter (predominantly asphaltene sols), occurs at the interfacial film which is dominated by a highly functional NSO compositions (Chapter 4).

In conclusion, the water-in-oil emulsions are dominated by the low molecular weight, non-hindered alkylphenols, with total alkylphenol concentrations of up to an order of magnitude greater than those for the whole oil fractions. Therefore, alkylphenols are preferentially enriched at the oil/water interface, probably aiding the formation of stable water-in-oil emulsions. This enrichment of the interfacial film and not the aqueous phase is suspected to be due to the high polarity of the NSO composition of the interfacial film which may preferentially attract alkylphenols.

5.4.3. Comparison of Results from C_0-C_3 Alkylphenol Analysis and Crude Oil Water Retentive Properties.

Comparison of the observed water retentive behaviours of crude oils, monitored in Chapter 3, with their alkylphenol distributions, characterised in this chapter, was hoped to give some explanation for the observed increase in water retention with increasing biodegradation. The water retentive ability of crude oils is a measure of the sedimentation rate of water and/or emulsion droplets through the crude oil phase and it was considered that the presence of oil-soluble surfactants, such as alkylphenols, would alter such a process by effecting oil/water interactions, droplet growth and thereby sedimentation rate (Jordan & Payne, 1980; Cavello & Chang, 1990).

Three categories of retention were applied to the water sedimentation curves produced in Chapter 3, which are displayed in Table 3.3.2. "Poor" retention, the fastest sedimentation rate, is represented by a drop in the normalised water content (measured from the top of the crude oil/water blend) from 100%R to 40%R or less in under 50 hours. "Moderate" water retention is indicative of a crude oil with normalised water contents which drop from 100%R to less than 40%R in 50 to 100 hours. "Good" water retention, which is the slowest sedimentation rate, exhibits normalised water contents which are maintained at approximately 100-40%R for 100 hours.

Analyses from this chapter found no discernible trend between C_0-C_3 alkylphenol content and water retention abilities for the crude oils analysed (Table 5.4.2). Crude oils which exhibited "poor" water retention, A29, NS1, NS2 and H1 possessed similar alkylphenol distributions, frequently dominated by *ortho*-cresol and 2,4-dimethylphenol however, they were found to possess markedly different total alkylphenol concentrations. As described above, the averaged total alkylphenol concentration of the biodegraded crude oil NS2 was an order of magnitude less than those of the non-degraded crude oils (A29, NS1 & H1). Conversely, the similar C_0-C_3 alkylphenol concentrations of the NS2 and NS3 crude oils are in contrast to their different water retentive properties ("poor" and "good" respectively). Consequently, it appears likely that the increased water retentive abilities of biodegraded crude oils H7 and NS3 are not solely related to their alkylphenol content. In addition, work in Chapters 3 has identified that there is no appreciable correlation between the asphaltene and wax sols content of a crude oil and its water retentive behaviour. Therefore, it seems probable that the chemical composition of crudes, and it's effect upon interfacial film formation between oil and water phases, does not significantly control crude oil water retentive ability.

Crude Oils	Biodegradation State [1]	Total Alkylphenol Concentration (ng g^{-1})	Water Retention Ability [2]	Water-in-Oil (W/O) Emulsion[3]
A29	Non-degraded	36,092	POOR	Forms viscous W/O emulsion
NS1	Non-degraded	103,506	POOR	Forms viscous W/O emulsion
NS2	Mildly degraded	4,218	POOR	Forms both W/O emulsion and water layer
NS3	Extensively degraded	3,119	GOOD	Separate water layer
H1	Non-degraded	26,378	POOR	Forms viscous W/O emulsion
H7	Moderately to extensively degraded	35,123	MODERATE	Forms viscous W/O emulsion

Table 5.4.2. Comparison of total alkylphenol concentration and water retention abilities for crude oils of different biodegraded states. It was found that no relationship could be distinguished. [1] *= Biodegradation state classified using the Volkman et al. (1984) sequence.* [2] *= water retention ability determined in Chapter 3.* [3] *= emulsion formation/stabilisation data determined in Chapter 3..*

5.5. Conclusions.

In general, work suggests that the low molecular weight, non-hindered alkylphenols, have been enhanced in the bound oil fraction (oil/water interfacial film) by approximately an order of magnitude (approximately 150,000 ng g^{-1} to 1,000,000 ng g^{-1}) relative to the whole oil alkylphenol total concentrations (approximately 3,000 ng g^{-1} to 100,000 ng g^{-1}). This implies that alkylphenols are probably associated with the stabilisation of water-in-oil emulsions, in agreement with Acevedo *et al.* (1992) and Hunter & White (1992).

Comparison of the total alkylphenol contents of crude oils with their emulsion formation/stabilisation ability found that poor emulsification was associated with the reduction of the total concentrations C_0-C_3 alkylphenols. Reduction of alkylphenols was attributed to the biodegradation of the crude oils. Therefore, it seems probable

that the reduction of oil-soluble surfactants, such as C_0-C_3 alkylphenols, as well as the reduced presence of precipitated asphaltene and wax sols (Chapter 4) in degraded oils, contributes to the poor emulsion formation and stabilisation abilities of the North Sea crude oils (NS2 & NS3).

However, no such association between crude oil chemical composition and water retention ability was recognised. Water retention was found to be independent of C_0-C_3 alkylphenol distributions. Therefore, no relationship between bulk chemical data/molecular data reported in Chapters 4 and 5, and the water retentive behaviours reported in Chapter 3 was observed. It is was therefore considered probable that water retention was predominantly related to the physicochemical properties of the crude oil (density, viscosity etc.), rather than chemical composition.

CHAPTER 6:

EFFECT OF BIODEGRADATION UPON CRUDE OIL WATER UPTAKE ABILITY

CHAPTER 6: EFFECT OF BIODEGRADATION UPON CRUDE OIL WATER UPTAKE ABILITY.

6.1. Introduction.

In Chapters 3, 4 and 5 the water uptake ability of crude oils was linked to their state of biodegradation. In Chapter 3 it was found that the biodegraded North Sea crude oils analysed had poor emulsification abilities. As well as affecting emulsion formation/stabilisation ability, crude oil biodegradation was also linked with increased water retention by work in Chapter 3. In the previous chapter the retention/biodegradation relationship was suggested to be possibly due to the alteration of the physicochemical properties of crude oil (density, viscosity etc.).

The ability of crude oils to form stable water-in-oil emulsions has been shown to be dependent on their ability to form rigid and protective interfacial films between the oil and water phases (Johansen *et al.*, 1989; Aveyard *et al.*, 1990; Acevedo *et al.* 1992; Schramm, 1992). Work presented in Chapters 3 & 4, related the poor water uptake ability (emulsion formation/stability) of biodegraded North Sea crude oils to their inability to form these rigid and protective interfacial films. This inability was linked to the effect of biodegradation on the bulk chemistry (affecting asphaltene precipitation) and the wax content of crude oils. In addition, Chapter 5 showed that reduction of surfactant groups, such as alkylphenols, probably influences interfacial film formation and hence the emulsion formation/stabilisation ability of crude oils. However, because these results have so far been gained from unrelated North Sea crude oils, a study of the variation of the water uptake ability (both water retention and emulsion formation/stability) of specific crude oils at different biodegradation states is desirable. In this chapter a crude oil is biodegraded in the laboratory and then analysed for changes in water uptake ability using the procedures described in Chapters 2, 3 and 4.

Biodegradation generally results from microbial oxidation of petroleum hydrocarbons, causing enrichment of the non-hydrocarbon, NSO compounds (Palmer, 1993). Therefore, biodegradation produces heavy crude oils with low API gravity and (due to the loss of hydrocarbons) reduced economic value (Connan, 1984).

There are two main types of biodegradation, aerobic and anaerobic, of which aerobic is by far the dominant alteration process in the subsurface (Palmer, 1993). The aerobic biodegradation of subsurface petroleum accumulations occurs at oil/water contacts, with the bacteria existing in the aqueous phase. Biodegradation is enhanced by an ample supply of both nutrients and oxygen, which are predominantly supplied

by flowing water. In addition, biodegradation is also governed by temperature, and it is generally recognised that biodegradation does not often occur above 80°C (Connan, 1984). Therefore, subsurface petroleum biodegradation is often found in shallow, cool (<80°C), petroleum accumulations which are washed by oxygenated, nutrient rich, frequently surface derived waters (Tissot & Welte, 1984). The necessary movement of water at the oil/water contacts results in another alteration process, that of water washing.

Water washing of petroleum is characterised by the selective removal of water soluble petroleum components by hydrocarbon-under-saturated waters (Tissot & Welte, 1984). Consequently, it is observed that the crude oil alteration processes, aerobic biodegradation and water washing, are frequently concurrent (Connan, 1984; Lafargue & Barker, 1988). However, other subsurface petroleum alteration processes, such as reservoir maturation and fractionation of hydrocarbon light ends, may also be mistaken for biodegradation (Larter & Mills, 1989; Palmer, 1993). Therefore, good appreciation of the history of a crude oil is required prior to identification of alteration processes.

At the surface, petroleum is subject to many other alteration processes. The two main surface crude oil alteration processes are biodegradation and evaporation however, other significant processes are dissolution, dispersion into the water column, photochemical oxidation, emulsification, adsorption onto particles, agglomeration and sinking (Jordan & Payne, 1980).

All the above processes may alter the chemical composition of crude oils but it was hoped to assess the influence of aerobic biodegradation alone, as this was considered to be the main alteration process which affected the NS2 and NS3 crude oils (the alteration of both crude oils has been associated with the influx of oxygen rich, meteoric water; Sections 3.1.1.3.5 & 3.1.1.3.6 respectively). However, laboratory based biodegradation is also influenced by two other processes, water washing and evaporation and therefore these, along with aerobic biodegradation, will be described

6.1.1. Alteration of Crude Oil Composition.

This section provides an overview of the crude oil alteration processes; aerobic biodegradation, water washing and evaporation. It does not represent a detailed discussion of these mechanisms and for such the reader should consult the literature (Connan, 1984; Peters & Moldowan, 1993)

6.1.1.1. Aerobic Biodegradation.

Alteration of crude oil composition, by aerobic biodegradation, has been described by Tissot & Welte (1984) as following the sequence {6.1} with progressive removal of:

n-alkanes> isoprenoid alkanes> low ring cycloalkanes> aromatics **{6.1}**

This sequence is well established (Connan, 1984; Palmer, 1993) however exceptions do occur and laboratory experiments by Jones *et al.*, (1983), Jones (1986) and Rowland *et al.*, (1986) have recognised the loss of aromatic hydrocarbons prior to aliphatic hydrocarbons under certain conditions. This preferential removal was suggested by Rowland *et al.* (1986) to be due to different biodegradation mechanisms in reservoir and laboratory environments. However, Connan *et al.*, (1993) attributed preferential aromatic degradation specifically to the lack of nutrients (N, P, O_2).

The above sequence {6.1} is generalised and a more detailed assessment of crude oil hydrocarbon degradation is gained by further analysis of the aliphatic and aromatic hydrocarbons groups.

6.1.1.1.1. Aliphatic Hydrocarbon Group.

Volkman *et al.* (1984) found that biodegradation of the aliphatic hydrocarbon fraction was represented by the following sequence {6.2} of compound class removal:

n-alkanes> acyclic isoprenoid alkanes> C_{14}-C_{16} bicyclic alkanes> steranes> hopanes> diasteranes. **{6.2}**

From this sequence it may be seen that the degree of microbial attack is reduced with increasing branching, alkyl groups and cyclicity of the aliphatic hydrocarbons. In addition, each group (*n*-alkane, *iso*-alkane etc.) will display decreasing rates of reduction with increasing carbon numbers. For example the *n*-C_6 to *n*-C_{15} *n*-alkane fraction will be reduced at a faster rate than the C_{15+} fraction (Walker *et al.*, 1976; Connan, 1984). Taking this into account, Connan (1984) produced a more detailed aliphatic hydrocarbon degradation sequence (Table 6.1.1).

Removal Sequence	Carbon Numbers	Aliphatic Hydrocarbons Degraded
1	C_6-C_{15}	*n*-alkane
2	C_6-C_{15}	isoalkane
3	C_6-C_{15}	cycloalkanes, isoprenoids
4	C_{15}-C_{35}	*n*-alkanes, isoalkanes, anteisoalkanes, cyclohexyl and methylcyclopentylalkanes
5	C_{15}-C_{21}	isoprenoids
6	C_{27}-C_{29}	regular steranes (C_{27}>C_{28}>C_{29})
7	C_{30}-C_{35}	hopane (C_{35}-C_{34}-C_{33}>C_{32}-C_{31}-C_{30} and 22R>22S)
8	C_{27}	diasteranes (20S>20R)
9	C_{28}-C_{29}	diasteranes (C_{28}>C_{29})
10	C_{27}-C_{29}	hopane
11	C_{21}-C_{22}	steranes (C_{21}>C_{22})

Table 6.1.1. Step by step biodegradation of aliphatic hydrocarbons. Adapted from Connan, 1984.

It must be noted that this is not a valid sequence for every instance and variation will be seen, especially for the degradation of steranes and hopanes. Although both steranes and hopanes are resistant, surviving moderate biodegradation, they will eventually be degraded (Seifert & Moldowan, 1979; Seifert *et al.*, 1984).

The order of sterane degradation has been established by observation of both natural and *in vitro* biodegraded crude oils (Seifert & Moldowan, 1979; Goodwin *et al.*, 1983; Chosson *et al.*, 1992). The following sequence has consequently been suggested {6.3}:

Regular Sterane> Diasterane
$C_{27} > C_{28} > C_{29}$
20R > 20S
{6.3}

Therefore, the 20R epimers, due to their biological configuration, are the first to be degraded, while the C_{27} steranes are removed prior to the C_{28} sterane which are removed prior to the C_{29} sterane. Therefore, the first regular sterane to be affected by biodegradation is C_{27} ααα 20R. When the C_{27}-C_{29} steranes have been completely removed the resistant diasteranes may begin to degrade if biodegradation is extreme enough ("severe" degradation; Connan, 1984). However, the recent biomarker review

by Peters and Moldowan (1993) has suggested that the order of sterane degradation, as well as hopane degradation, may vary with the presence of demethylated hopanes (25-nor-17α(H)-hopanes; discussed below), indicating two possible degradation pathways.

In the presence of demethylated hopanes the sterane degradation sequence {6.4} is suggested to be:

$$\alpha\alpha\alpha 20R \;\&\; \alpha\beta\beta 20R > \alpha\alpha\alpha 20S \;\&\; \alpha\beta\beta 20S$$
$$C_{27} > C_{28} > C_{29} > C_{30}$$
$$\{6.4\}$$

This sequence is the result of work by Rullkötter and Wendisch (1982), and McKirdy *et al.* (1983). However, observations by Seifert *et al.* (1984), for the biomarker content of a Greek oil seep, which contained no demethylated hopanes, suggested a different sterane degradation sequence {6.5}:

$$\alpha\alpha\alpha 20R(C_{27}\text{-}C_{29}) > \alpha\alpha\alpha 20S(C_{27}) > \alpha\alpha\alpha 20S(C_{28}) > \alpha\alpha\alpha 20S(C_{29}) \geq \alpha\beta\beta(20R + 20S)(C_{27}\text{-}C_{29})$$
$$\{6.5\}$$

Degradation of hopanes shows that the 22R epimers are more susceptible to degradation than the S configurations (Peters & Moldowan, 1993). However, as mentioned above, Peters and Moldowan (1993) have suggested that the formation of demethylated hopanes may effect the degradative pathway of hopanes. It is suggested that in the absence of the formation of demethylated hopanes the degradation sequence {6.6} of hopanes was:

$$C_{35} > C_{34} > C_{33} > C_{32} > C_{31} > C_{30} > C_{29} > C_{27}$$
$$22R > 22S$$
$$\{6.6\}$$

This was based on work by Goodwin *et al.* (1983), Connan (1984) and Seifert *et al.* (1984). However, results from a homohopane degradation study, by Peters and Moldowan (1991), found that in the presence of demethylated hopanes the overall hopane degradation order was represented by the following sequence {6.7}:

$$C_{27}\text{-}C_{32} > C_{33} > C_{34} > C_{35}$$
$$\{6.7\}$$

However, it must be noted that this sequence {6.7} has only been reported once by Peters and Moldowan (1991) and therefore the findings are tentative (Peters & Moldowan, 1993).

Biodegradation of hopanes has been suggested to produce 25-norhopanes due to the demethylation of the C-10 position (Peters & Moldowan, 1991; Farrimond & Telnæs, *unpublished*). Consequently, it is possible that the presence of 25-norhopanes (10-desmethylhopanes) are an indication of biodegradation (Peters & Moldowan, 1993). However, it remains unclear whether this is a precursor (hopane)/ product (25-norhopane) relationship, or that 25-norhopanes are merely bacterially resistant, being relatively enhanced by the removal of the more abundant and labile 17α-hopanes during biodegradation (Horstad *et al.*, 1992; Moldowan & McCaffrey, 1995).

Whichever hopane or sterane degradation sequence is observed (dependent upon the presence of 25-norhopane) the order in which steranes and hopanes are degraded is controversial. The majority of aliphatic hydrocarbon biodegradation sequences indicate that steranes are degraded prior to hopanes (Volkman *et al.*, 1984; Connan, 1984; Peters & Moldowan, 1993) however, contradictory evidence of hopane group removal before the sterane group has also been observed (Peters & Moldowan, 1991). Therefore, it has been suggested that the degradation of these groups is dependent upon the specific environmental conditions, allowing specific bacteria growth, which will utilise either steranes or hopanes first (Seifert *et al.*, 1984; Peters & Moldowan, 1991; Palmer, 1993).

6.1.1.1.2. Aromatic Hydrocarbon Group.

The degree of biodegradation of aromatic hydrocarbons has been suggested, by many investigators (Walker *et al.*, 1976; Volkman *et al.*, 1984; Rowland *et al.*, 1986), to decrease with increasing aromatic ring number, following the sequence {6.8}:

Monoaromatic> Diaromatic> Triaromatic> Polycyclic aromatic hydrocarbons

{6.8}

Although there is overlap between these groups, Rowland *et al.* (1986) have shown that each group exhibits a decreasing degradation rate with increasing alkylation (C_0>C_1>C_2>C_3 etc.). Work by Wild *et al.* (1991) also recognised some degree of overlap in the above sequence {6.8}. In Figure 6.1.1, Wild *et al.* (1991) found that while the general rate of biodegradation of aromatics is inversely proportional to the

number of aromatic rings present, alkylation may significantly alter the biodegradation rate. For example, it was found that phenanthrene degraded more rapidly than the lower molecular weight compound 2-methylnapthalene.

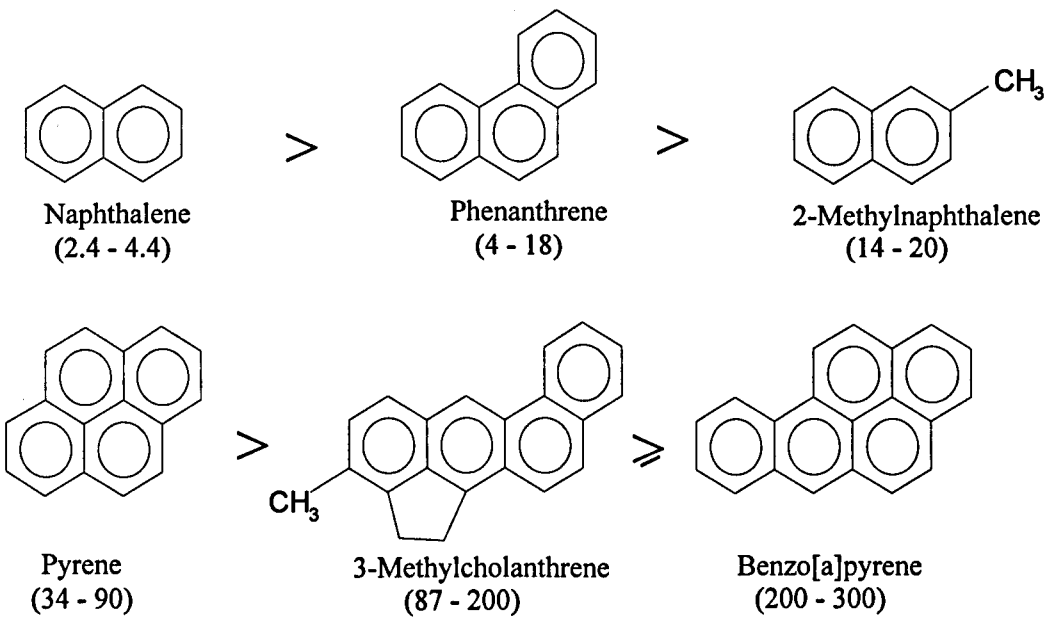

Figure 6.1.1. Aromatic hydrocarbon biodegradation sequence illustrating the effect of alkylation upon biodegradation rate. Half lives in weeks for microbial degradation are bracketed. Arrows indicate an increase in recalcitrance. Data from Wild et al., 1991; figure from Cerniglia, 1992.

It has also been recognised by Raymond *et al.* (1967), that degradation was affected by steric controls, with beta position substituted methylnaphthalene groups (i.e., 2-methylnaphthalene) being degraded at a higher rate than alpha position substituted methylnaphthalenes (*viz*, 1-methylnaphthalene; Fig. 6.1.2). Volkman *et al.* (1984), also observed this preferential removal of beta substituted methylnaphthalene isomers and in addition found that dimethylnaphthalenes (DMN) with opposite substituents (e.g., 2,7-DMN), as well as ethylnaphthalenes, were more resistant to biodegradation than other DMNs (Fig. 6.1.2). Volkman *et al.* (1984) listed the alkylnaphthalene degradation sequence {6.9} as the following:

2MN> 1MN> 2,7-1,7-1,6DMN> 1,3-2,6DMN> 1,4-1,5DMN> 1,2DMN> 2,3DMN> 1EN> 2EN> 1,8DMN **{6.9}**

where MN represents methylnaphthalene, DMN dimethylnaphthalene, and EN ethylnaphthalene.

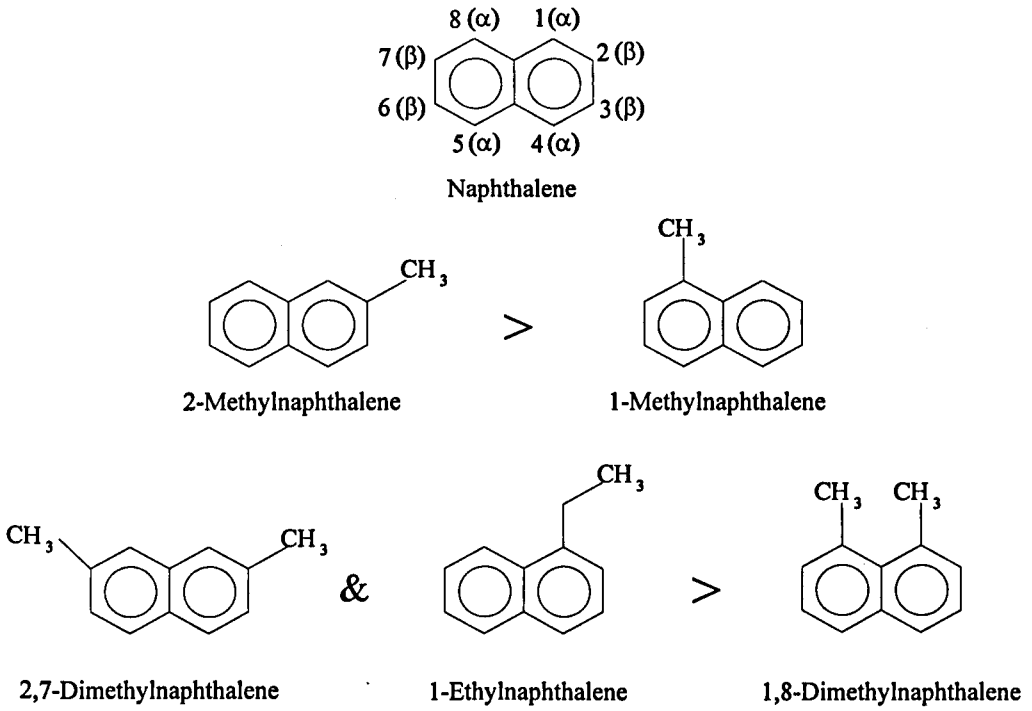

Figure 6.1.2. The effect of substituent positioning on biodegradation rates for alkylnaphthalenes. Arrows indicate an increase in recalcitrance.

Assessment of the degradability of methylphenanthrenes, by Rowland *et al.* (1986), found that they were more resistant to biodegradation than methylnaphthalenes, and at moderate biodegradation were still a valuable maturity parameter. However, phenanthrene should be used with caution as it is susceptible to degradation. The biodegradation of polycyclic aromatic hydrocarbons (PAHs, constituting three or more fused benzene rings in linear, angular and cluster arrangement) have been extensively investigated (Cerniglia 1992 and literature cited therein) due to their general recalcitrance and damaging effects upon ecosystems (Wang *et al.*, 1990; Aronstein *et al.*, 1991). It was found that in general, lower molecular weight PAHs, such as phenanthrene, are degraded rapidly in sediments whereas higher molecular weight PAHs, such as benzo[*a*]pyrene, are quite resistant to microbial attack.

In severely biodegraded crude oils, analysis of total aromatic hydrocarbons may only reliably identify the presence of mono- and tri-aromatic steroids (Volkman *et al.*, 1984). Therefore, the resistance of aromatic steroid hydrocarbons to biodegradation allows maturity assessment of crude oils even at the highest levels of degradation (Peters & Moldowan, 1993).

6.1.1.2. Water Washing.

Water washing is the selective removal of water soluble petroleum species by undersaturated waters (with respect to hydrocarbons) flowing along the oil/water contact (Tissot & Welte, 1984). As mentioned above, water washing frequently accompanies aerobic biodegradation and is usually the only degradative mechanism when either the temperature is greater than 80°C, and generally prohibitive for viable bacterial existence, or when insufficient nutrient and oxygen levels for biodegradation exist (Lafargue & Barker, 1988). Therefore, alteration of crude oil in these circumstances will predominantly be governed by the water solubility of crude oil compound classes. Work by McAuliffe (1979), displayed in Figure 6.1.3, shows that aromatic hydrocarbons (for a given carbon number) are significantly more soluble in water than normal alkanes of the same carbon number. Palmer (1993), lists the removal sequence {6.10} of hydrocarbons, due to water washing as:

1 ring aromatics> naphthalenes> branched alkanes> normal alkanes **{6.10}**

(when all at the same carbon number). It was found that the solubility of each class (naphthalenes, phenols etc.) varied with carbon number, alkylation, unsaturation and branching (Yaws *et al.*, 1990; Varhanícková *et al.*, 1995). Structural differences were also observed to influence dissolution (Eganhouse & Calder, 1976), as ethylnaphthalenes were preferentially removed by water washing when compared with dimethylnaphthalenes. Also, 1-methylnaphthalene was found to be slightly more soluble than 2-methylnaphthalenes. The sequence {6.11} of naphthalene group reduction, due to water washing, was suggested to be:

Naphthalene> 1MN> 2MN> 2EN> 1,5DMN> 2,3DMN> 2,6DMN **{6.11}**

Work by Lafargue and Barker (1988) concluded that water washing in subsurface environments was a major alteration process for crude oil accumulations and was particularly effective in removing the sub C_{15} hydrocarbon fraction on a rapid geological time scale.

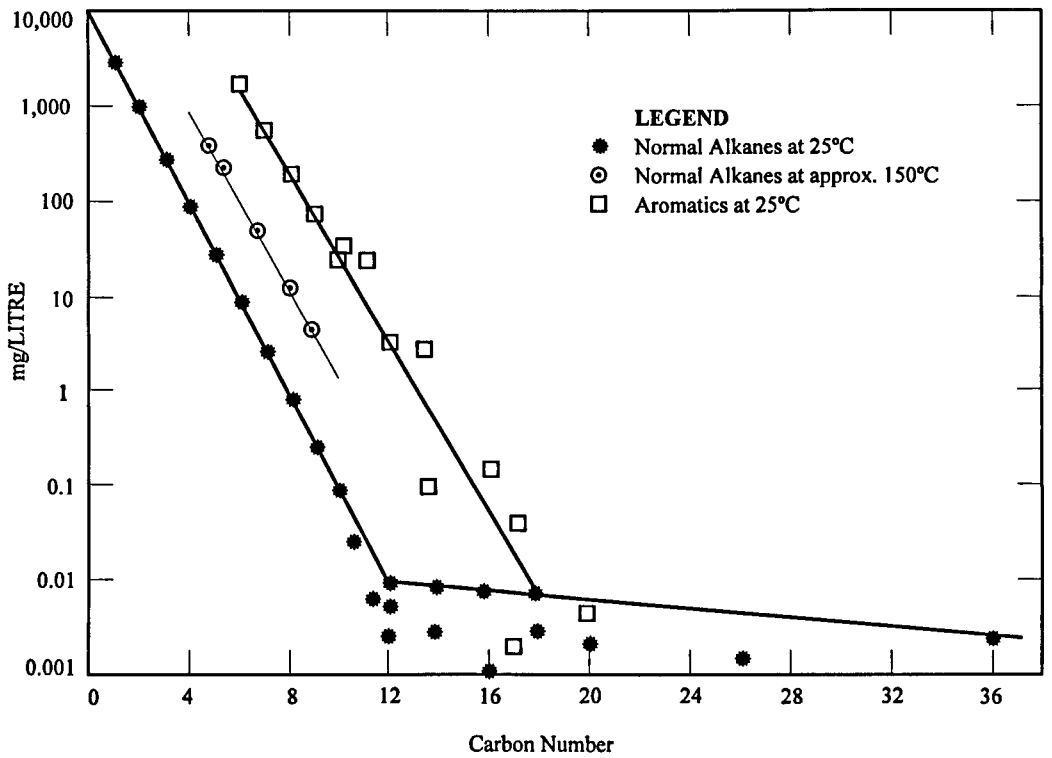

Figure 6.1.3. Solubility of normal alkane and aromatic hydrocarbons in water. Illustrates the greater aqueous solubility of aromatic hydrocarbons compared to n-alkanes. Taken from McAuliffe (1979).

6.1.1.3. Evaporation.

Evaporation causes the majority of the volatile matter of crude oil to be lost within the first 24-28 hours of an oil spillage (Jordan & Payne, 1980). Gundlach *et al.* (1983), in an assessment of the fate of the Amoco Cadiz crude oil, noted that 30% (67,000 tons) of spilled crude oil, was lost by evaporation. Jordan & Payne (1980) noted that on average evaporation accounts for the loss of between 20 and 50% of the composition of crude oil.

In general, most sub C_{15} hydrocarbons, both aliphatic and aromatic, are rapidly lost by evaporation, illustrated in Figure 6.1.4, causing significant crude oil compositional alteration.

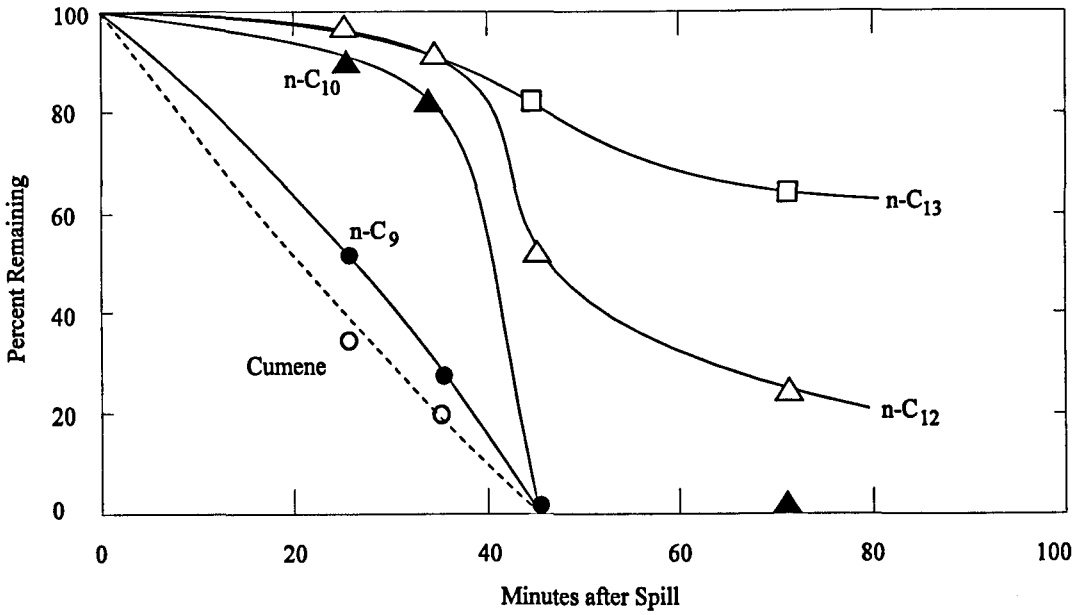

Figure 6.1.4. Percent of low-boiling hydrocarbons remaining in South Louisiana crude oil slicks. Illustrates the rapid loss of low molecular weight components (Jordan & Payne, 1980).

Wheeler (referred to in Jordan & Payne, 1980) suggested that the sub C_{15} hydrocarbon evaporation sequence {6.12} is:

n-alkanes> isoalkanes> cycloalkanes> aromatics **{6.12}**

The evaporation rate of each group, for specific hydrocarbons, being a function of vapour pressure which is inversely related to the molecular weight (McAuliffe, 1977b; Jordan & Payne, 1980). In Figure 6.1.5 (Wheeler referred to in Jordan & Payne, 1980) it may be seen that the aromatic hydrocarbon vapour pressure is slightly less than for *n*-alkanes. Therefore, it is anticipated that *n*-alkane losses, through evaporation, would be greater than those seen for aromatic hydrocarbons. However, due to the greater solubility of the aromatics, their overall loss from the petroleum may even be higher than for the equivalent aliphatic hydrocarbon (Jordan & Payne, 1980). Studies into the quantification of evaporation and dissolution hydrocarbon removal processes, which occur simultaneously in surface environments, has shown that evaporation is dominant over dissolution in the removal of volatile components of an oil slick (McAuliffe, 1977a). In addition, work by Harrison *et al.* (1975), also found that losses, through evaporation, for aromatic hydrocarbons were 100 times greater than from dissolution, while losses for aliphatic hydrocarbons, by evaporation, were 10,000 times greater than by dissolution. It was therefore anticipated that, during this experiment, losses due to evaporation would exceed those attributed to dissolution.

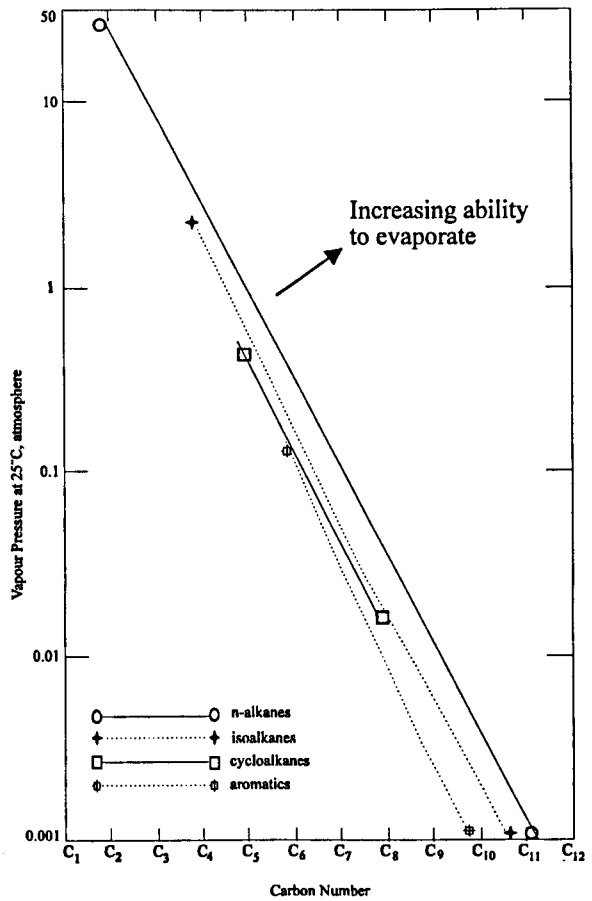

Figure 6.1.5. Vapour pressure as a function of carbon number for alkanes, isoalkanes, cycloalkanes and aromatic hydrocarbons (adapted from Jordan & Payne, 1980). Graph illustrates that n-alkanes are more likely to evaporate than > isoalkanes> cycloalkanes > aromatic hydrocarbons.

6.1.2. Determination of the Extent of Biodegradation.

Assessment of the extent of biodegradation by analysis of the distribution of crude oil fractions (*n*-alkanes, isoprenoids *etc.*), has been in use for many years (Connan, 1984; Volkman *et al.*, 1984). The Volkman *et al.* (1984) scale of biodegradation for reservoired crude oils is the most widely used and lists nine stages of biodegradation, from non-degraded to extreme (Table 6.1.2). However, it has also been realised that biomarker alteration, due to biodegradation, is variable and frequently did not follow the established classifications (Palmer, 1993; Hostettler & Kvenvolden, 1994; Connan, 1984). Peters & Moldowan (1991) also produced a biodegradation scale, listing ten stages of compound class removal. This classification takes into account variable sterane and hopane degradation pathways; however, all scales assume systematic compound class removal. Walker *et al.* (1976), stated that "components of petroleum, although degraded simultaneously, are degraded at

different rates." therefore compound class removal is not in a systematic sequence. This variability is caused by many possible conditions, including crude oil type, biodegradation environment (surface or reservoir conditions), oxygen and nutrient supplies and other alteration processes (listed above).

Stage	Observations	Classification
1	Abundant *n*-alkanes	non-degraded
2	Light-end *n*-alkanes removed	Minor (Mild)
3	>90% *n*-alkanes removed	
4	Alkylcyclohexanes and alkylbenzenes removed; acyclic isoprenoid alkanes and naphthalene reduced	Moderate
5	Isoprenoid alkanes and methylnaphthalenes removed; selective removal of C_2-naphthalenes	
6	C_{14}-C_{16} bicyclic alkanes removed	Extensive
7	>50%(20R)-5α(H),14α(H),17α(H) steranes removed	Very Extensive
8	Distribution of steranes and triaromatic steroids altered, demethylated hopanes abundant	Severe
9	No steranes; demethylated hopanes predominate	Extreme

Table 6.1.2. The Volkman et al. (1984) biodegradation sequence for reservoired crude oils.

6.2. Experimental.

The experimental procedures for this section are illustrated in Figure 6.2.1 and description of the procedures are found below.

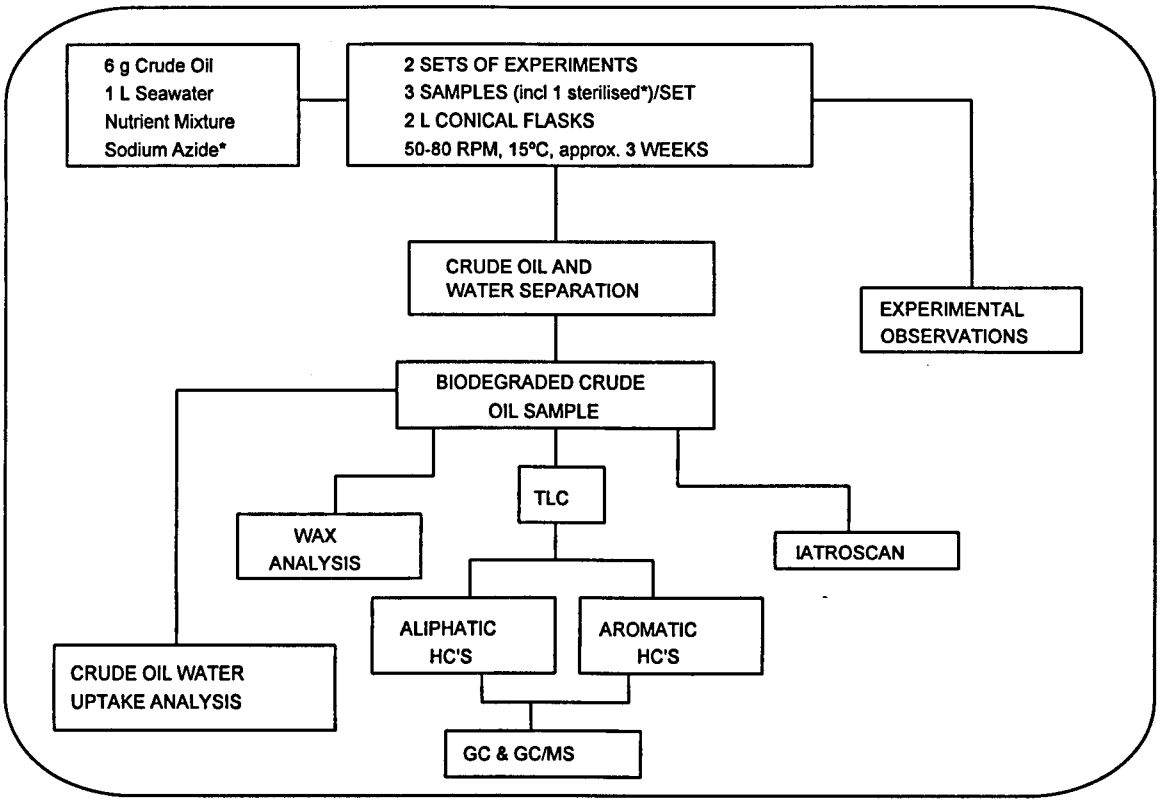

*Figure 6.2.1. Outline of experimental procedures for in-laboratory crude oil biodegradation and subsequent analyses. * Na azide was added to one sample per set.*

6.2.1. Biodegradation.

Biodegradation was performed on two crude oils, a normal North Sea crude oil (Kittiwake) and a biodegraded North Sea crude oil (NS3) using seawater organisms.

Biodegradation experimentation was performed with 6 g of crude oil, 1 L of seawater and a mixture of nutrients (Table 6.2.1) per conical flask.

Nutrients	Weight/litre
$Na_2HPO_4.12H_2O$	9 g
KH_2PO_4	1.5 g
NH_4Cl	4.0 g
$MgSO_4.7H_2O$	0.2 g
Trace Elements	1 ml
Na Azide*(in control samples)	100 mg

*Table 6.2.1. Additional nutrients per 1 L seawater. * Na azide was added to one sample per set.*

The components were added to a 2 L conical flask six flasks (containing six samples) were used for each crude oil biodegradation experiment. For practical reasons each biodegradation experiment was split into two sets, each set consisting of three samples. One sample from each set was sterilised with 200 mg of sodium azide to prevent biogenic activity. These sterilised samples acted as controls to assess the influence of non-biogenic activity, such as water washing, on the crude oils. Both sets were placed on an orbital shaker. Experiments were run at approximately 15°C and at a rotation rate of 50-80 RPM for approximately 3 weeks. Observations were recorded daily to assess any alterations to the samples such as on-set of biodegradation, emulsification and so on.

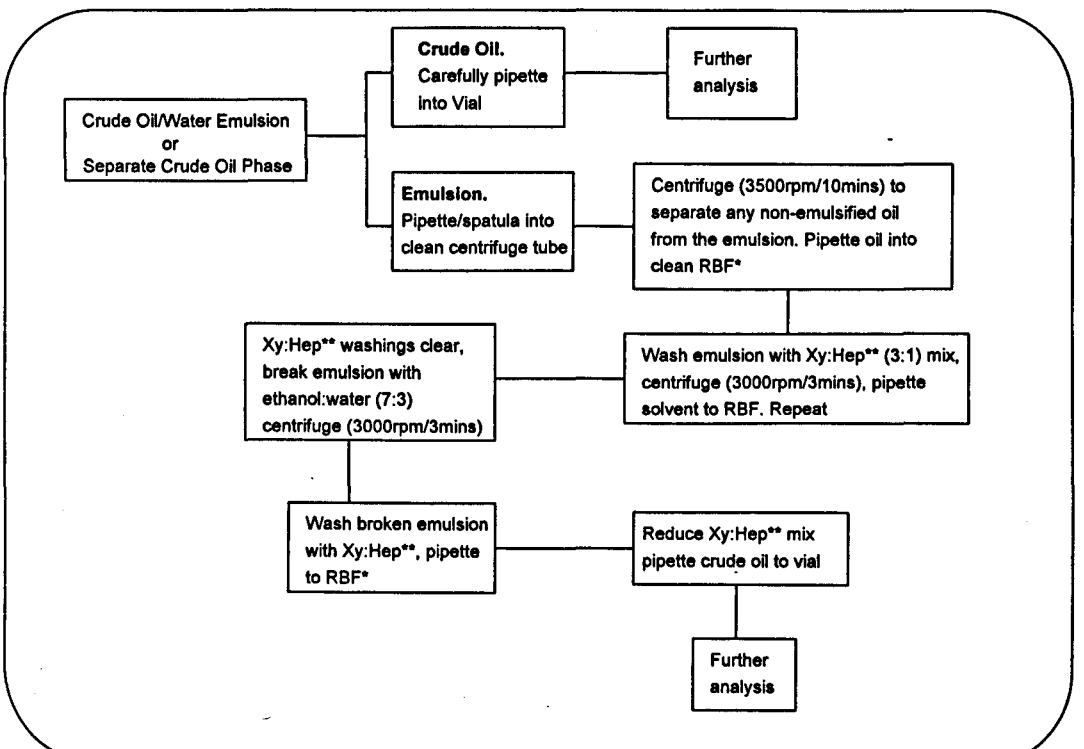

*Figure 6.2.2. Crude oil and water separation process. * = round bottomed flask. ** = xylene:heptane.*

At the end of the incubation period the crude oil in each sample was separated from the aqueous phase (Fig. 6.2.2). There were two possible outcomes of the biodegradation experiment, either a separate oil layer was maintained or a highly viscous, water-in-oil emulsion had formed. If a separate oil layer had been maintained, the oil was carefully pipetted off and centrifuged to ensure that no excess water was present. It was then carefully pipetted into a vial and weighed, ready for further analysis. If a water-in-oil emulsion had formed, then oil and water separation was necessary. Oil and water separation was based on the method used by Acevedo *et al.* (1992).

Firstly, any non-emulsified crude oil was separated by centrifugation (3,500 RPM/10 minutes) and carefully pipetted into a clean round bottomed flask (RBF). The emulsion was then repeatedly extracted with a xylene:heptane (3:1) mixture until the extracts were relatively colourless (it was impractical to wait until the extracts were completely colourless because the time needed would have been prohibitive). Initial extracts sometimes required centrifuging to aid separation of the solvent and emulsion phases. The extracts were pipetted into a clean RBF. Once the emulsion had been extracted, removing the crude oil trapped in the emulsion matrix which is not actually part of the interfacial film, the emulsion was then broken (demulsified, the oil and water phases separated) by addition of 10 ml ethanol:water (70:30) mixture and centrifuged at 3,000 RPM/3 minutes. The broken emulsion was then washed again with a xylene:heptane (3:1) mixture, to remove any organics released by demulsification. The washings were added to the RBF and reduced by rotary evaporation. An aliquot of the oil extract was weighed. The separated crude oil was then ready for further analysis.

6.2.2. Crude Oil Water Uptake Analysis (COWUA).

The water uptake analysis of crude oil samples followed the procedure used in Chapter 3.

6.2.3. Wax Extraction and Analysis.

Wax extraction followed the procedure in Chapter 4. However, the high temperature gas chromatography (HTGC) analysis differed slightly. HTGC of the wax extracts was performed on a Carlo Erba 5160 gas chromatograph. On-column injection was used with no secondary cooling. The instrument was fitted with a flame

ionisation detector (FID) at a temperature of 450°C. The chromatographic column used was a SGE aluminium clad, HT-5, fused silica column (25 m x 0.33 mm, film thickness 0.1 μm). Hydrogen pressure was 50 kPa. The temperature program started at 60°C for 2 minutes, increased to 450°C at 6°C/min, with the final temperature being maintained for 20 minutes. Prior to analysis, the gas chromatographic column was conditioned by slowly increasing the final temperature from 300°C to 450°C, over three conditioning runs. Before analysing the wax extracts, the column was calibrated with Fisons wax standards, P Wax and FT Wax. Injected sample size was 1 μl. In addition, analyses of wax extracts were performed with an internal standard (3.5 μg eicosene per 1 mg sample), which was added to the wax extract prior to high temperature gas chromatography.

6.2.4. Iatroscan-FID Analysis.

Iatroscan-FID analysis followed the procedure detailed in Chapter 4.

6.2.5. Aliphatic and Aromatic Hydrocarbon Fraction Extraction and Analysis.

Thin Layer Chromatography (TLC) was used to fractionate the samples into aliphatic and aromatic (3 rings or less) hydrocarbon extracts. The TLC plates, 20 cm x 20 cm, were coated (0.5 mm thickness) with silica gel (Kiesel gel, 60G) and activated at 120°C for 4 hours before use. The plates were then cleaned using ethyl acetate and then reactivated at 120°C for 2 hours. The plates were developed in petroleum ether. The aliphatic and aromatic hydrocarbon bands were scraped off the plates and desorbed from the silica using light petroleum for the aliphatic hydrocarbons and dichloromethane for the aromatic hydrocarbons.

The aliphatic and aromatic hydrocarbon fractions were both analysed on a Carlo Erba 5160 gas chromatograph. On-column injection was used and the instrument was fitted with flame ionisation detectors (FID). Both hydrocarbon fractions were analysed on HP-5 coated fused silica columns (30 m x 0.25 mm, with a film thickness of 0.25 μm). All analyses were made using the temperature programme of 50°C (2 mins) to 300°C (20 mins) at 4°C/min, using a hydrogen carrier gas pressure of 50 kPa. Before injection, the samples were diluted with dichloromethane, using approximately 10 mg aliphatic and aromatic hydrocarbons per 1 ml DCM, 0.5 μl was injected.

Gas chromatography/mass spectrometry analysis was performed on a Hewlett Packard, 5890 Gas Chromatograph coupled to a Hewlett Packard 5972 Mass Selective Detector (MSD). Sample size was 1 µl, injected by split/splitless injection (280°C) onto a HP-5 fused silica column (30 m x 0.25 mm, with a film thickness of 0.25 µm), with a helium carrier gas pressure of 25 kPa. A temperature programme of 40°C to 300°C (20 minutes) at a rate of 4°C/min was used. Ionisation voltage was 70 ev and the voltage of the electron multiplier was 1600 V. Analysis mode was selective ion monitoring (SIM) for both the aliphatic and aromatic hydrocarbon fractions from the Kittiwake whole oil and biodegraded samples 3 and 5 only. The ions monitored are listed in Appendix 5, Tables A5.1 and A5.2.

6.3. Results.

The results from the biodegradation of the Kittiwake and NS3 crude oils are summarised below. The experiments on both crude oils were monitored visually for emulsion formation but only the Kittiwake crude oil was also assessed by wax, Iatroscan-FID, GC and GC/MS analyses (the NS3 crude oil was not assessed as it reacted as expected during biodegradation, *i.e.*, it did not form an emulsion). It was not possible to extract enough biodegraded crude oil to perform Crude Oil Water Uptake Analysis (COWUA). This was due to the biodegraded samples forming viscous water-in-oil emulsions. The oil samples used for COWUA have to be solvent free to ensure that their water retentive and emulsion formation/stabilisation characteristics are not altered. Therefore, only physical emulsion separation and extraction processes, such as centrifuging, were possible. This processes was unable to "break" the emulsion and therefore, insufficient yields (approximately 0.5 g) for COWUA were produced.

6.3.1. Experimental Observations.

Observations of the biodegradation experiments are illustrated schematically in Figures 6.3.1 & 6.3.2. It may be seen in Figure 6.3.1, that there was no visual change in either of the control samples (1 & 4), throughout the experiment. The biodegradation of samples 2, 3, 5 and 6 commenced between 2 to 5 days after initiation of the experiment.

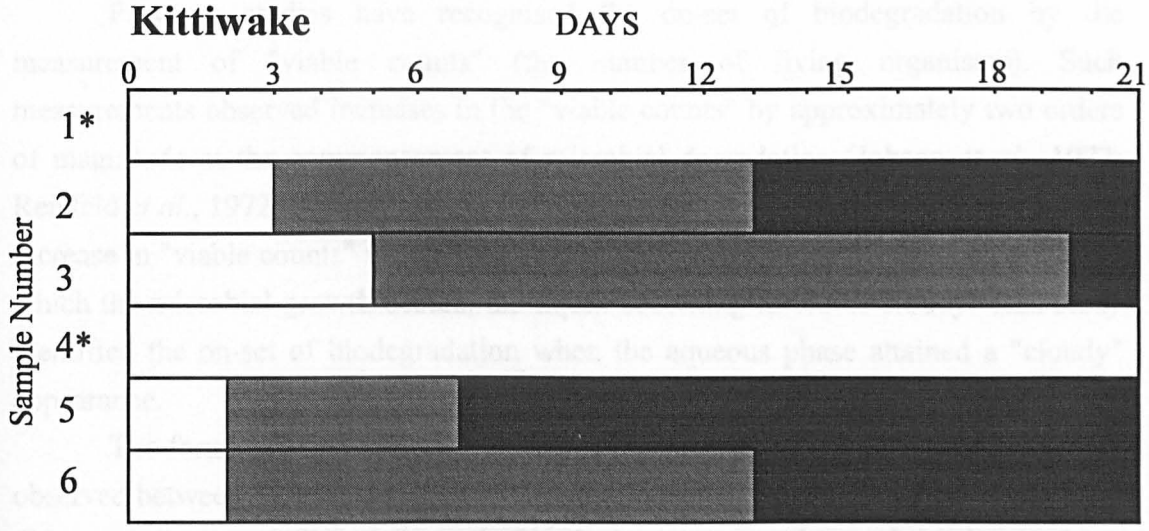

*Figure 6.3.1. Schematic illustration of experimental observations for the in-laboratory biodegradation of Kittiwake crude oil. * = control samples*

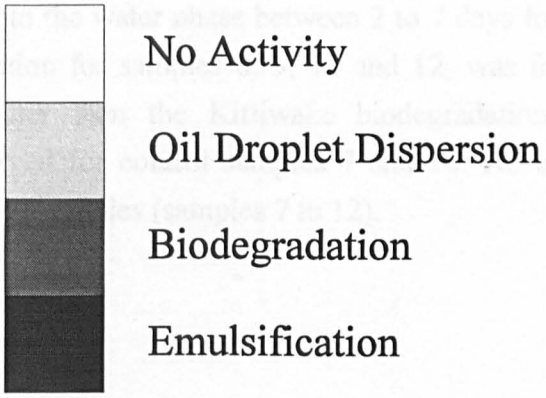

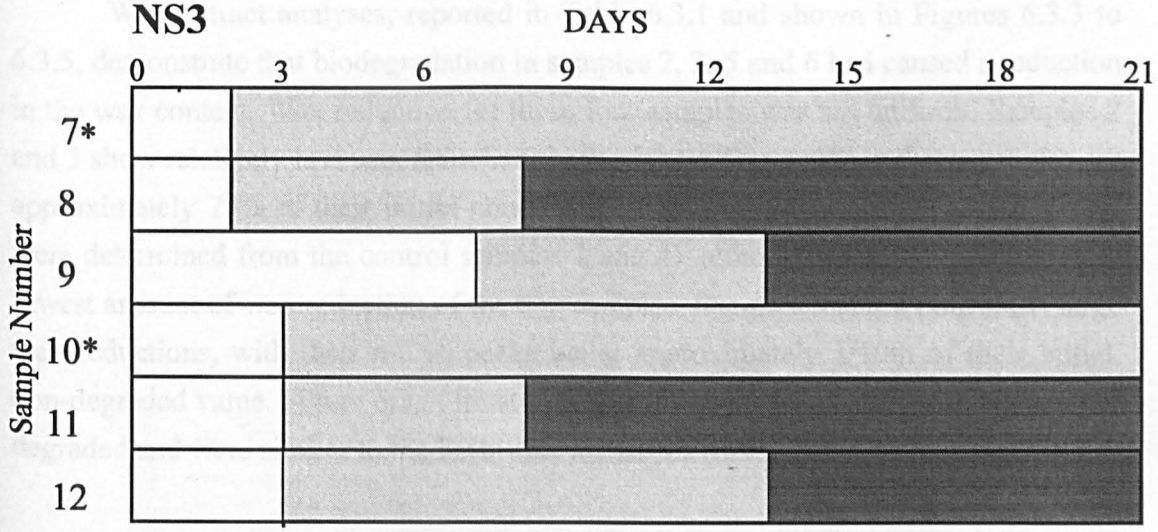

*Figure 6.3.2. Schematic illustration of experimental observations for the in-laboratory biodegradattion of NS3 crude oil. * = control samples*

Previous studies have recognised the on-set of biodegradation by the measurement of "viable counts" (the number of living organisms). Such measurements observed increases in the "viable counts" by approximately two orders of magnitude at the commencement of microbial degradation (Jobson *et al.*, 1972; Reisfeld *et al.*, 1972; Bailey *et al.*, 1973b). Jones (1979) identified that this substantial increase in "viable counts" was related to the visual alteration of the liquid medium in which the microbial growth occurs, the liquid becoming turbid or cloudy. This study identified the on-set of biodegradation when the aqueous phase attained a "cloudy" appearance.

The formation of water-in-crude oil emulsions, for samples 2, 3, 5 and 6, was observed between 7 and 19 days after commencement. The emulsification of sample 3 did not commence until near the end of analysis and it was observed that its emulsion thickness was less than that of the emulsions for samples 2, 5 and 6.

Observations of the NS3 experiment, shown in Figure 6.3.2, indicate that oil droplets were dispersed into the water phase between 2 to 7 days for samples 7 to 12. The on-set of biodegradation for samples 8, 9, 11 and 12, was from 8 to 13 days, approximately 9 days later than the Kittiwake biodegradation experiment. No biodegradation was observed for control samples 7 and 10. No emulsification was observed for any of the NS3 samples (samples 7 to 12).

6.3.2. Wax Analysis.

Wax extract analyses, reported in Table 6.3.1 and shown in Figures 6.3.3 to 6.3.5, demonstrate that biodegradation in samples 2, 3, 5 and 6 had caused a reduction in the wax content. Wax reduction for these four samples was not uniform. Samples 2 and 3 show relatively low wax reduction, both of the n-C_{30} peaks in these samples are approximately 75% of their initial non-degraded concentration (non-degraded values were determined from the control samples 1 and 4), although sample 3 exhibited the lowest amount of wax reduction of the two samples. Samples 5 and 6 both show large wax reductions, with their n-C_{30} peaks being approximately 1/10th of their initial, non-degraded value. Figure 6.3.5, illustrates that the control samples 1 and 4 were not degraded and were similar to the Kittiwake whole oil wax extract.

Samples	Wax Analysis		Iatroscan-FID				GC peak heights (mm) and molecular ratios								
	n-C_{30} (mg)	% of original	Aliphatic HC	Aromatic HC	Resins	Asph	n-C_{17}	Pristane (Pr)	n-C_{18}	Phytane (Ph)	UCM	Pr/Ph	n-C_{17}/ Pr	n-C_{18}/ Ph	Ph/ UCM
WO	8×10^{-4}	100	36	49	12	4	43	12	39	11	-	0.8	3.58	3.55	-
1*	8×10^{-4}	100	40	50	9	2	44	12	43	15	-	0.8	3.67	2.87	-
2	0.6×10^{-4}	7.25	22	60	15	3	-	15	-	30	22	0.5	-	-	1.36
3	5.4×10^{-4}	67.5	34	49	13	4	18	38	19	53	10	0.72	0.47	0.36	5.3
4*	8×10^{-4}	100	37	45	13	5	44	11	39	15	-	0.73	4	2.6	-
5	0.9×10^{-4}	11.5	20	65	12	3	-	11	-	24	38	0.46	-	-	0.63
6	0.6×10^{-4}	7.5	21	63	12	4	-	17	-	35	28	0.49	-	-	1.25

*Table 6.3.1. Results from the wax, Iatroscan and gas chromatogaphic analyses of Kittiwake oil samples. WO = whole oil; HC = hydrocarbon; UCM = unresolved complex mixture; Asph = Asphaltene. * = control samples.. - = not determined.*

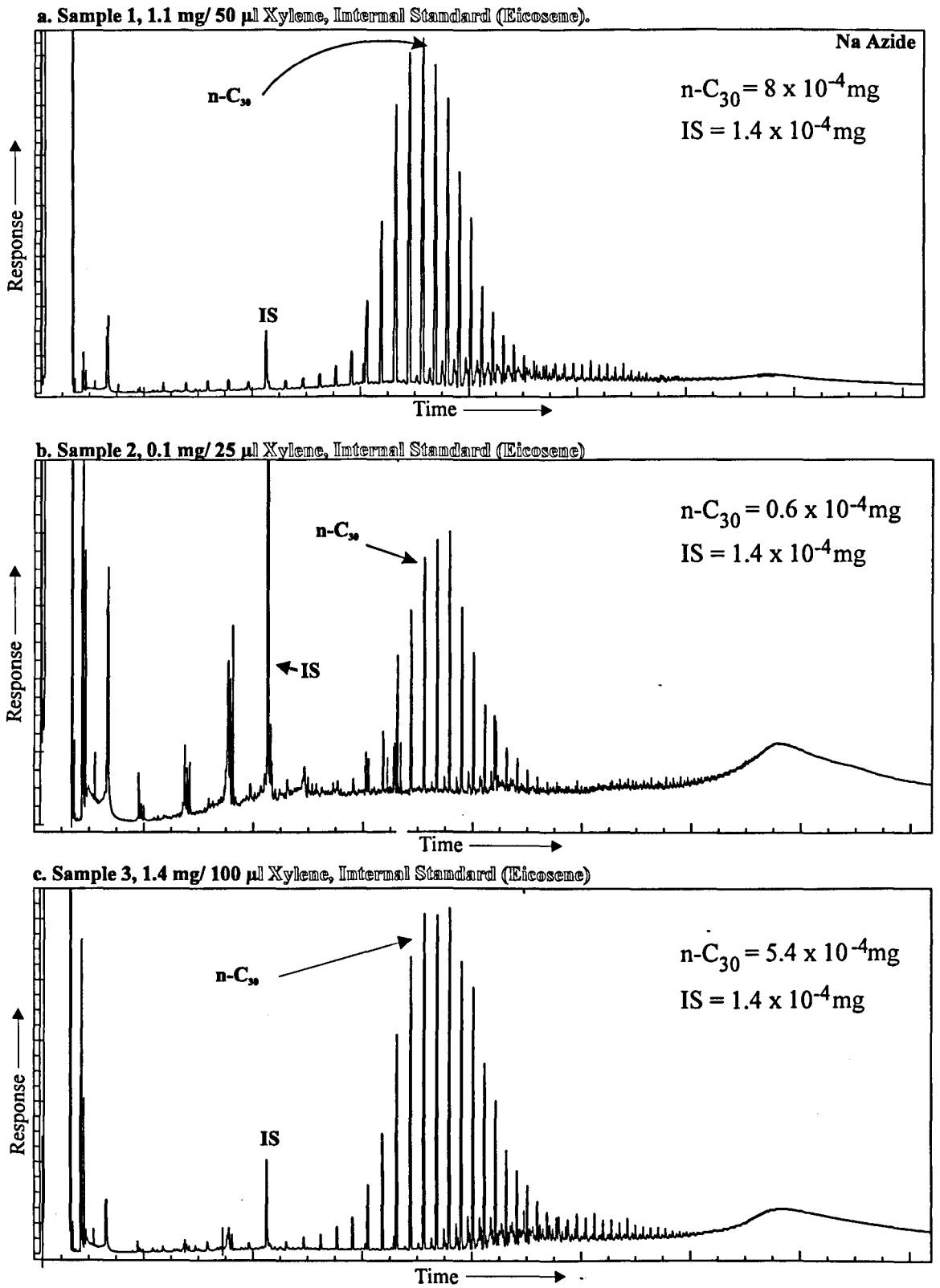

Figure 6.3.3(a,b,c). Kittiwake biodegradation set 1. Wax extracts analysed by high temperature gas chromatography (HTGC). IS = internal standard. Calculated n-C_{30} and IS contents (mg) are illustrated.

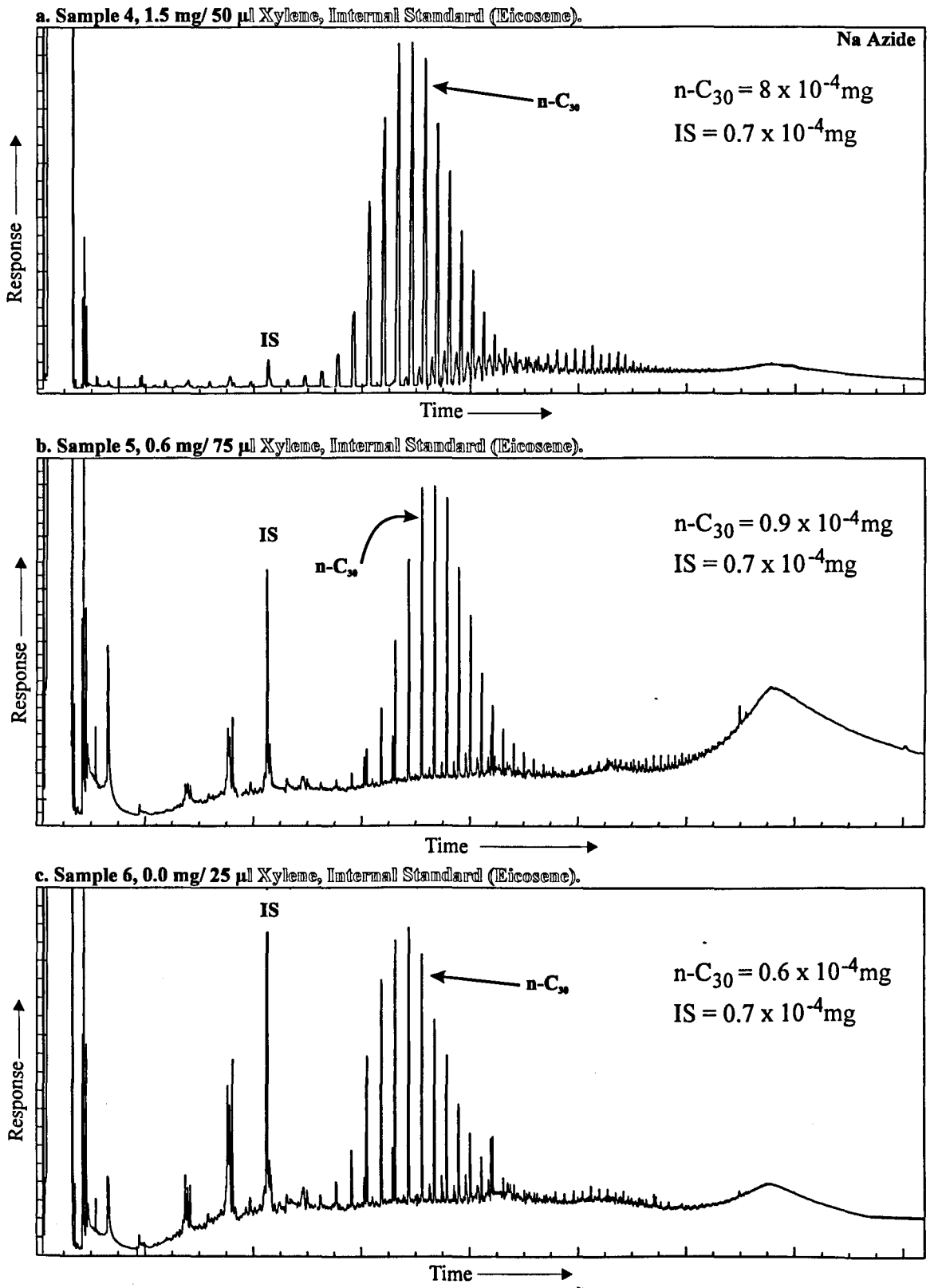

Figure 6.3.4(a,b,c). Kittiwake biodegradation set 2. Wax extracts analysed by high temperature gas chromatography (HTGC). IS = internal standard. Calculated n-C_{30} and IS contents (mg) are illustrated.

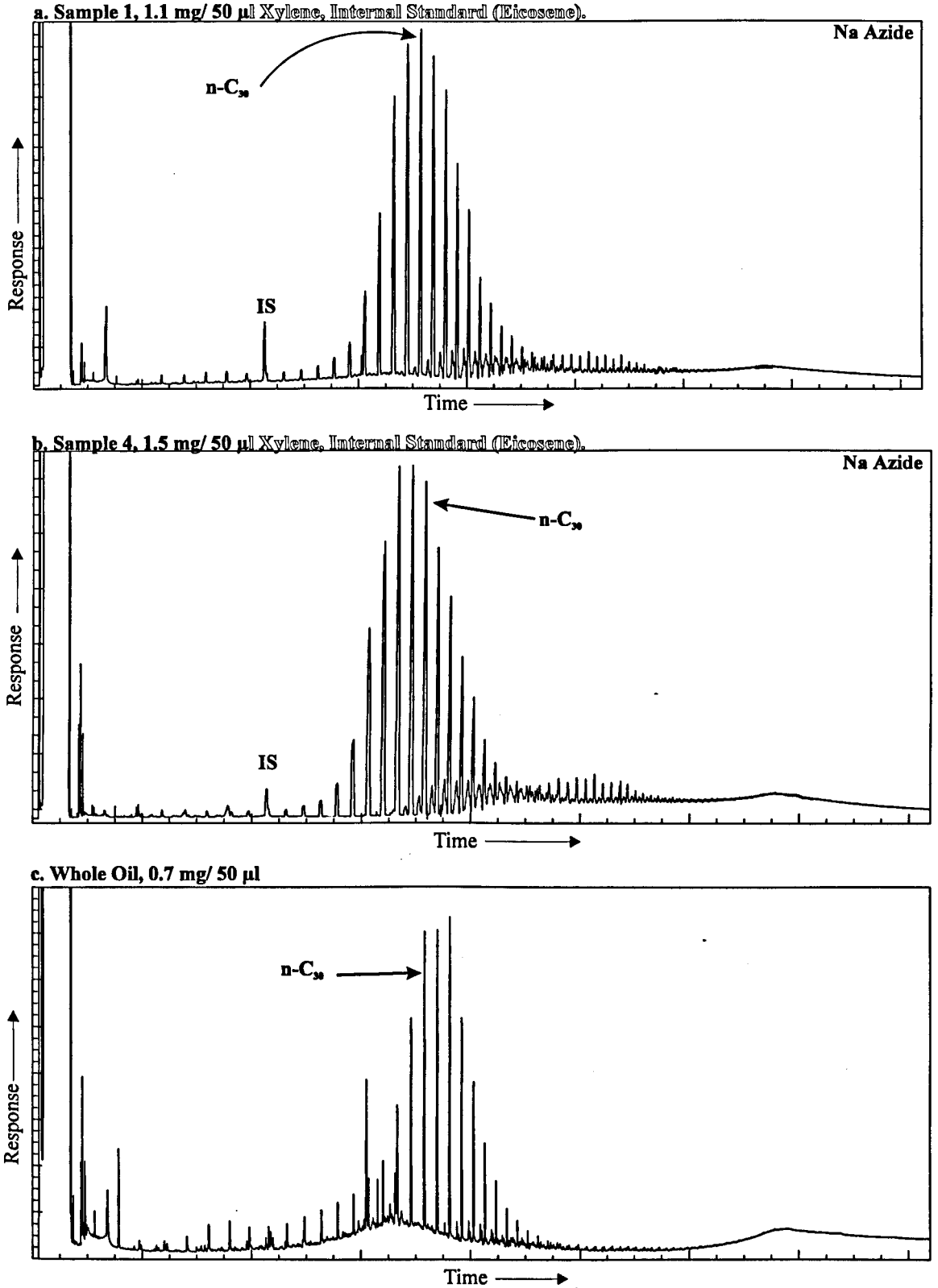

Figure 6.3.5(a,b,c). Comparison of the wax extract HTGCs for the control samples and whole oil sample IS = internal standard. Calculated n-C_{30} and IS contents (mg) are illustrated.

6.3.3. Iatroscan Analysis.

The Iatroscan results, illustrated in the histogram in Figure 6.3.6 and Table 6.3.1, show that samples 1, 3 and 4 possess similar bulk chemistries to the Kittiwake whole oil. Samples 2, 5 and 6, all show large reductions in their aliphatic hydrocarbon concentration (approximately 35% to 20% content), with the aromatic hydrocarbons abundances being enhanced in the samples (approximately 50% to 60% content). The asphaltene and resin contents of all samples are similar, at approximately 4% and 13%, respectively.

6.3.4. Gas Chromatographic Analysis of Aliphatic and Aromatic Hydrocarbon Fractions.

The gas chromatograms of the aliphatic hydrocarbon fractions of all samples, including the Kittiwake whole oil, are displayed in Figures 6.3.7 to 6.3.9 with values for peak heights and molecular ratios listed in Table 6.3.1. Both Figures 6.3.7 and 6.3.8 clearly show that the extent of biodegradation in samples 2, 3, 5 and 6 is not uniform. Figure 6.3.10, a cross plot of *n*-C_{17}/Pr and *n*-C_{18}/Ph ratios, also illustrates that biodegradation was variable with samples 2, 5 and 6 being degraded to a greater degree than sample 3, which in turn was degraded to a greater degree than the control samples and whole oil sample.

In addition, the height of the unresolved complex mixture (UCM), or "hump", may also be used as a biodegradation parameter when compared with the phytane peak height (Taylor, 1994). The relative increase in the UCM height (measured at its maximum, illustrated on Figs. 6.3.7 to 6.3.9) has been related to increasing biodegradation by many authors (Jones *et al.*, 1983; Connan, 1984; Volkman *et al.*, 1984).

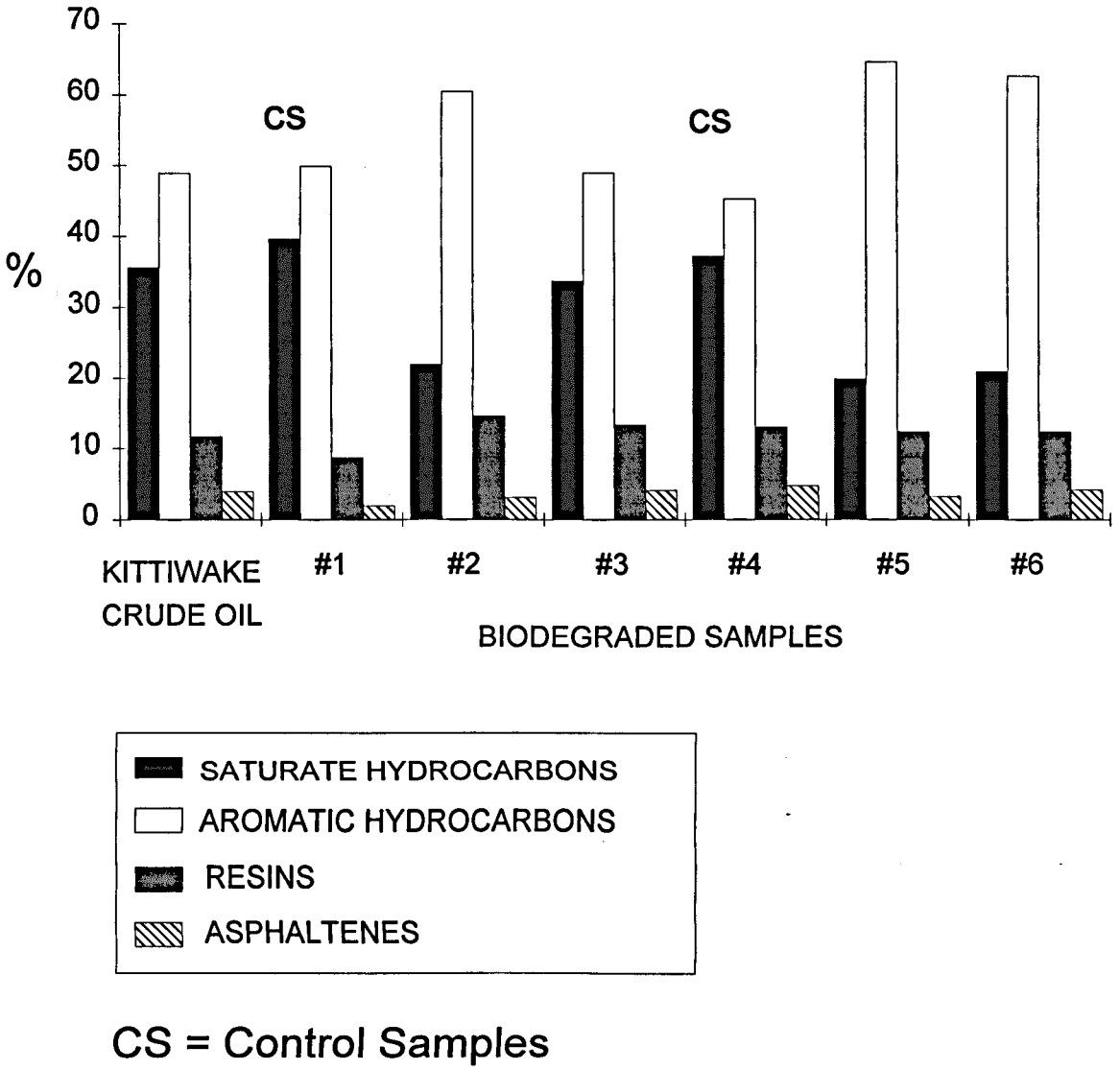

Figure 6.3.6. Iatroscan-FID results for Kittiwake biodegradation experiments.

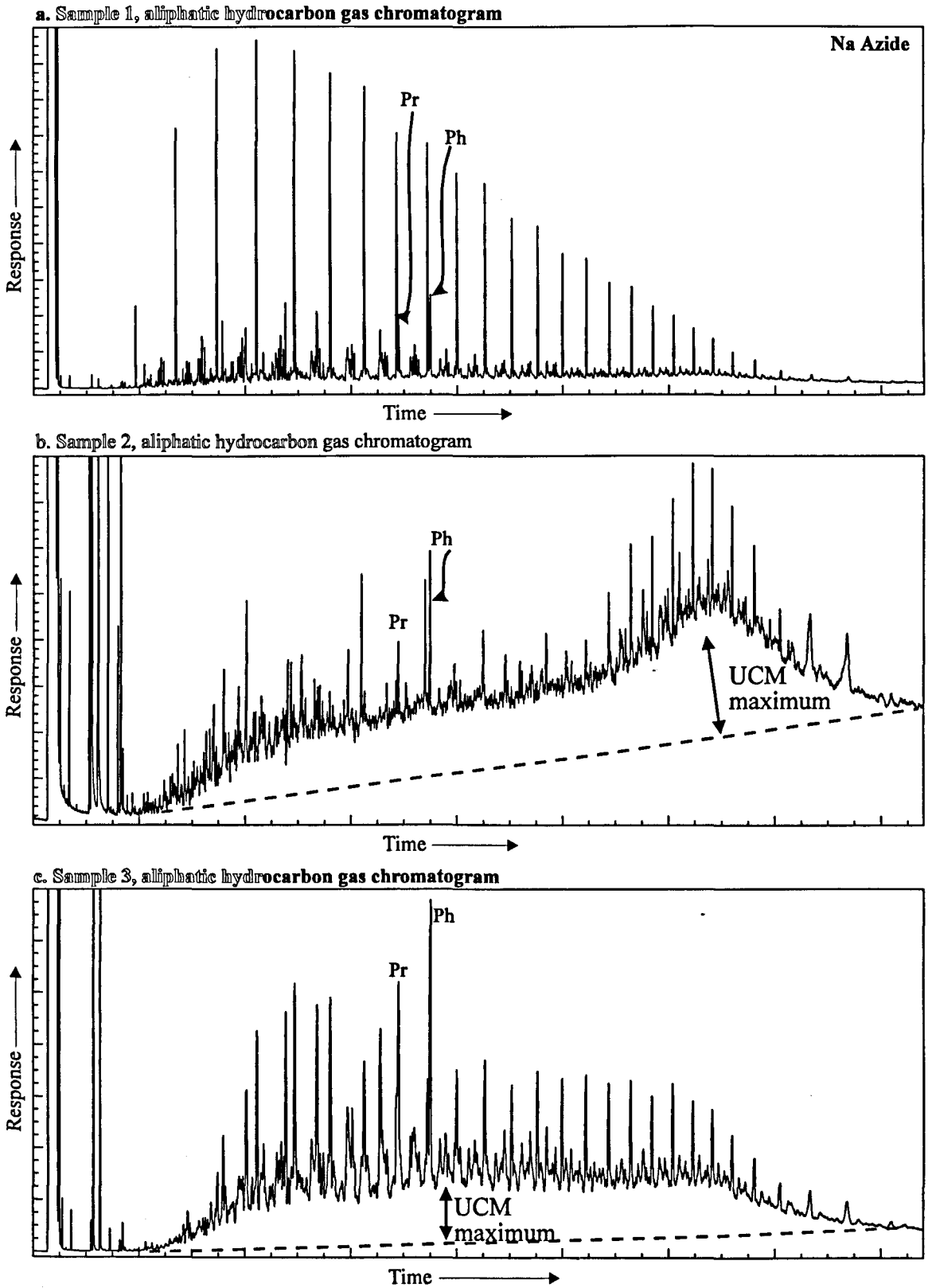

Figure 6.3.7(a,b,c). Kittiwake biodegradation set 1. Aliphatic hydrocarbon gas chromatograms. Pr = pristane; Ph = phytane..

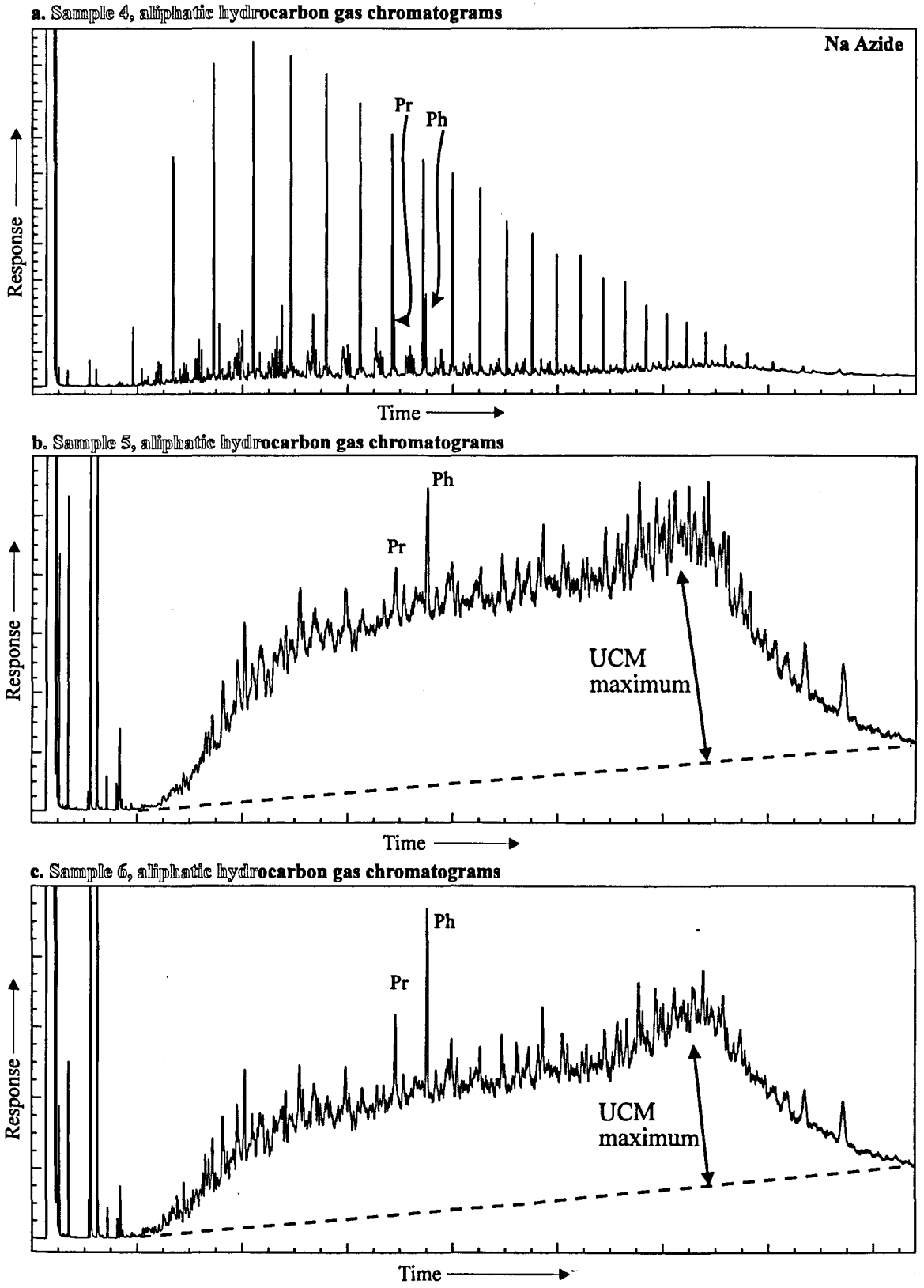

Figure 6.3.8(a,b,c). Kittiwake biodegradation set 2. Aliphatic hydrocarbon gas chromatograms. Pr = pristane; Ph = phytane..

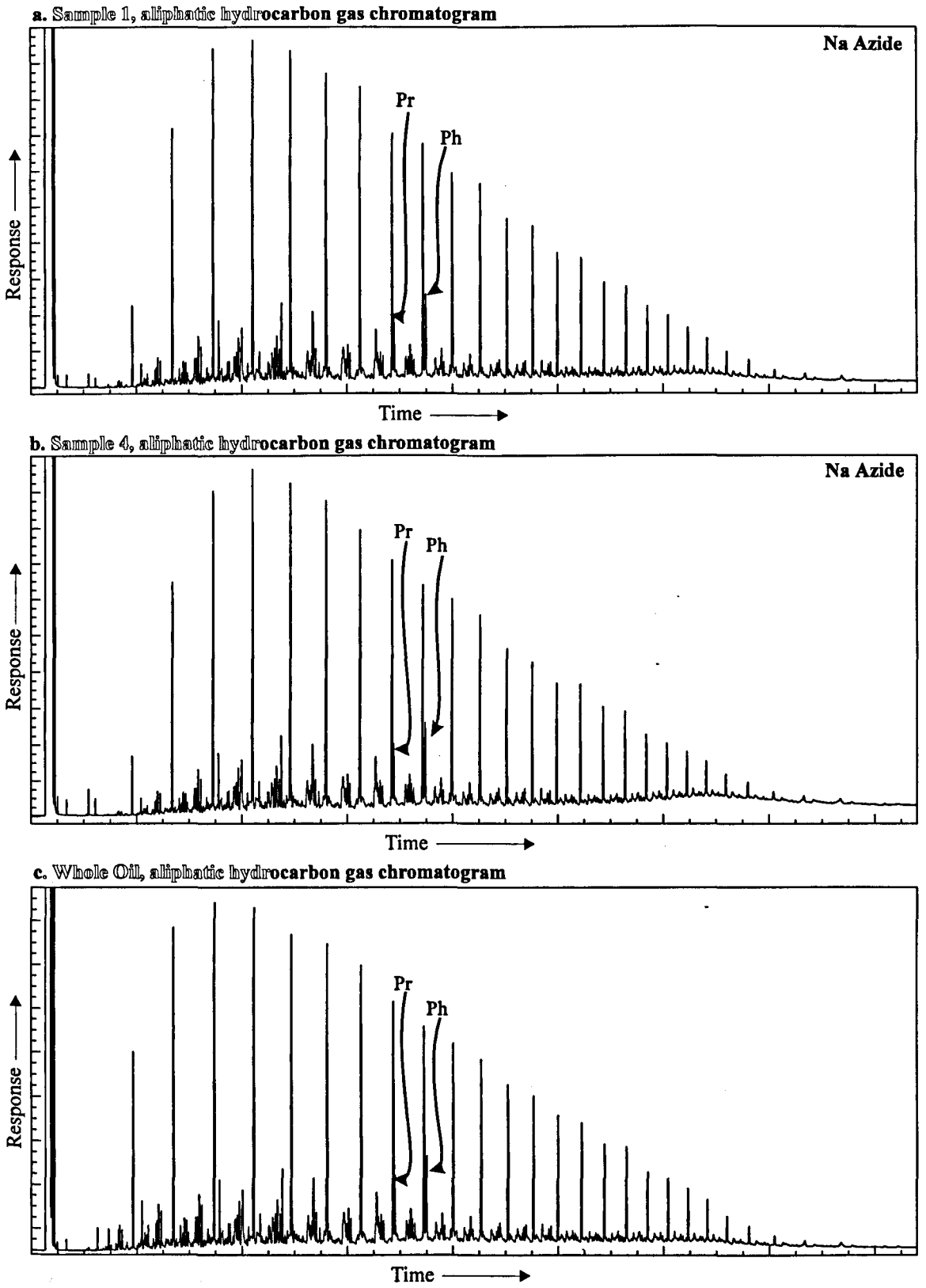

Figure 6.3.9(a,b,c). Comparison of sterilised samples with Kittiwake crude oil. Aliphatic hydrocarbon gas chromatograms. Pr = pristane; Ph = phytane..

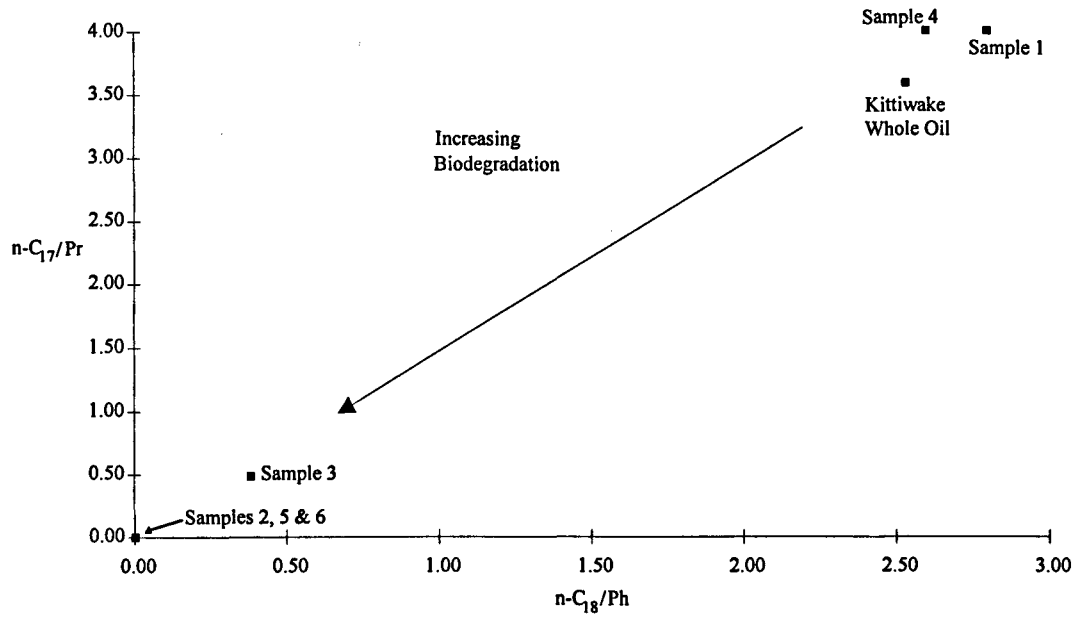

Figure 6.3.10. Comparison of n-C_{17}/Pr and n-C_{18}/Ph aliphatic hydrocarbon ratios, indicating increasing biodegradation. Ratios calculated from gas chromatogram peaks heights (Figs. 6.3.7 to 6.3.9; listed in Table 6.3.1).

Control samples 1 and 4, as well as the Kittiwake whole oil sample, were considered "non-degraded" while increasing order of degradation went from sample 3 ("mild-moderate", no isoprenoid reduction), sample 2 ("moderate", isoprenoid reduction) and samples 5 and 6 ("moderate to extensive", extensive aliphatic hydrocarbon reduction).

Sample 3 has a pristane/phytane ratio of 0.72, almost identical to that of the non-degraded samples however, its *n*-C_{18}/phytane ratio has greatly decreased from the non-degraded value of 3.55 to 0.36, due to *n*-alkane reduction. In addition, a UCM had formed, with a phytane/UCM ratio of 5.3. The *n*-alkane distribution for sample 3 ranges from *n*-C_{12} upwards, although aliphatic hydrocarbons up to *n*-C_{28}, are seen to have been greatly reduced when compared to the aliphatic hydrocarbon gas chromatogram for the Kittiwake whole oil.

The majority of the aliphatic hydrocarbons for sample 2 have been reduced and are not detectable by gas chromatographic analysis. Consequently the *n*-C_{18}/phytane ratio, for this sample, may not be calculated, however, alkanes are still visible from *n*-C_{24} upwards. However, the pristane/phytane ratio is lower than in sample 3, at 0.51, and the phytane/UCM value has reduced from 5.3 (sample 3) to 1.36. Both these ratios imply biodegradation of the isoprenoids and therefore, sample 2 is classified as moderately biodegraded.

Samples 5 and 6 show almost total depletion of the normal aliphatic hydrocarbons with only a very small concentration of alkanes above the *n*-C_{24} alkane peak, being identifiable. The pristane/phytane ratio is the same as that for sample 2

(approximately 0.5) however, the phytane/UCM values have decreased from 1.36 to 0.63 and 1.25 respectively. Due to the extensive reduction of the *n*-alkanes both are classified as moderately-extensively degraded (Volkman *et al.*, 1984) however, the phytane/UCM values indicate that sample 5 has been degraded to a greater degree than sample 6.

The comparison of the control samples 1 and 4, with the Kittiwake whole oil, may be seen in Figure 6.3.9. This shows that there is little, or no, difference between the saturated hydrocarbon fractions of these samples. All three samples display similar pristane/phytane and *n*-C_{18}/phytane ratios with UCMs not being observed. The *n*-C_{10} and *n*-C_{11} aliphatic hydrocarbons are slightly reduced in the saturate hydrocarbon fractions for samples 1 and 4 when compared to the Kittiwake whole oil saturate hydrocarbon fraction; however, these are probably due to evaporation effects upon samples 1 and 4 during work up procedures.

The aromatic hydrocarbon gas chromatograms for samples 1 to 6, in Figures 6.3.11 and 6.3.12, show slight differences in alkylnaphthalene concentrations which will be addressed in Section 6.3.6.1. In Figure 6.3.13, the comparison between the control samples 1 and 4, and the Kittiwake whole oil aromatic hydrocarbon fractions, indicates that a slight difference does exist between the control samples and the Kittiwake whole oil. Again probably due to the effects of work-up procedures in samples 1 and 4.

6.3.5. Gas Chromatography/Mass Spectrometry Analysis for Aliphatic Hydrocarbon Fractions.

Gas chromatography/mass spectrometry (GC/MS) analysis of the aliphatic hydrocarbon fractions for samples 3, 5 and the Kittiwake whole oil, provided more accurate assessment of biodegradation affects, and other alteration processes (water washing and evaporation), than gas chromatographic analysis.

The aliphatic hydrocarbons used for the assessment of biodegradation and maturation of the samples, and their diagnostic ions, are listed in Appendix 5, Table A5.1. The biomarker and molecular aliphatic hydrocarbon ratios used, references (where known) and their alteration during incubation is highlighted in Table 6.3.2. These ratios were chosen predominantly because of their previous use for assessment of crude oil biodegradation. More detailed biomarker and molecular ratio data, for both aliphatic and aromatic hydrocarbons, along with their applications as either maturity, source correlation or biodegradation indicators, is given in Table 6.3.3.

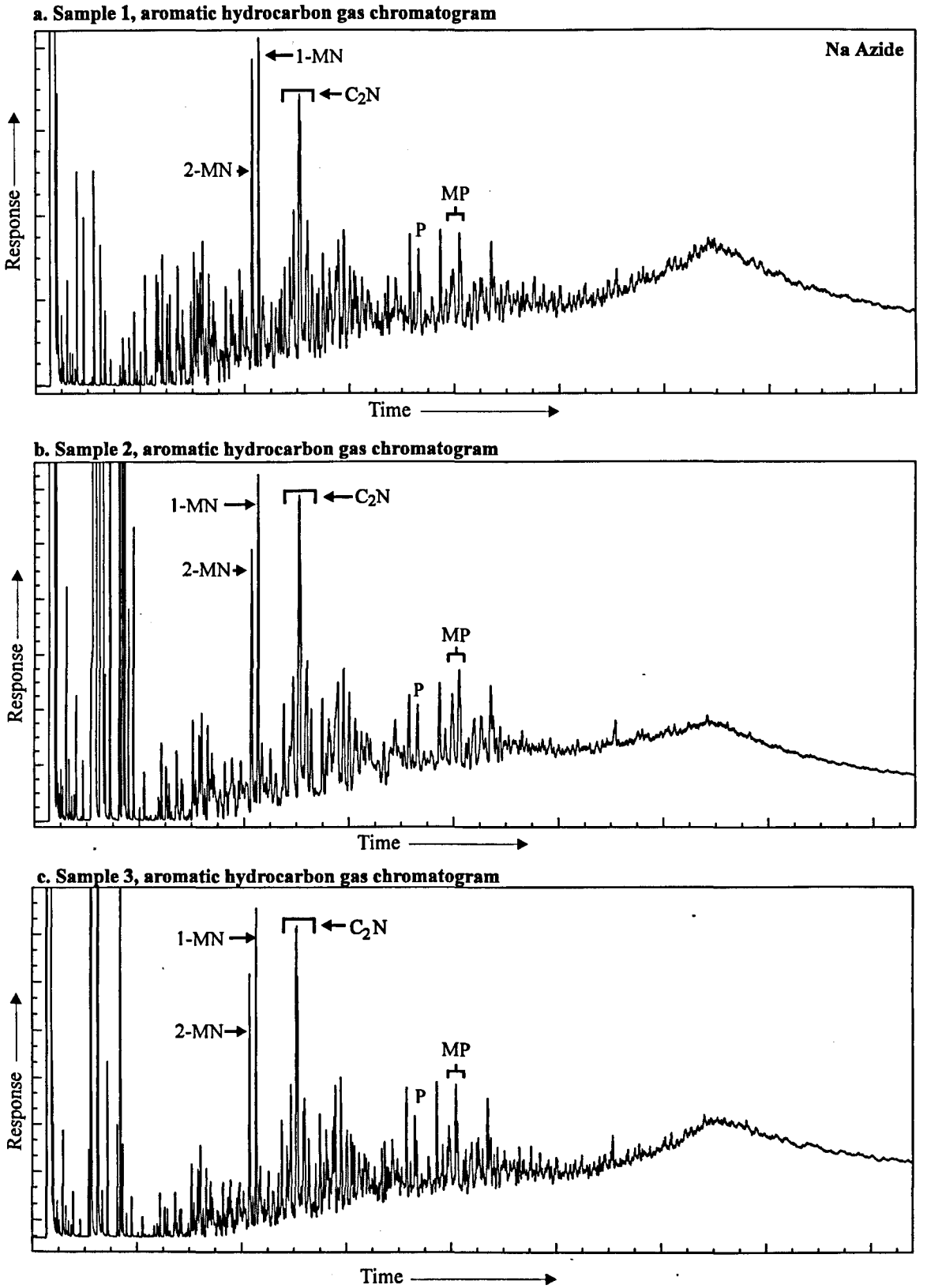

Figure 6.3.11(a,b,c). Kittiwake biodegradation set 1. Aromatic hydrocarbon gas chromatograms. MN = methylnaphthalene; C_2N = C_2 naphthalene; P = phenanthrene; MP = methylphenanthrene.

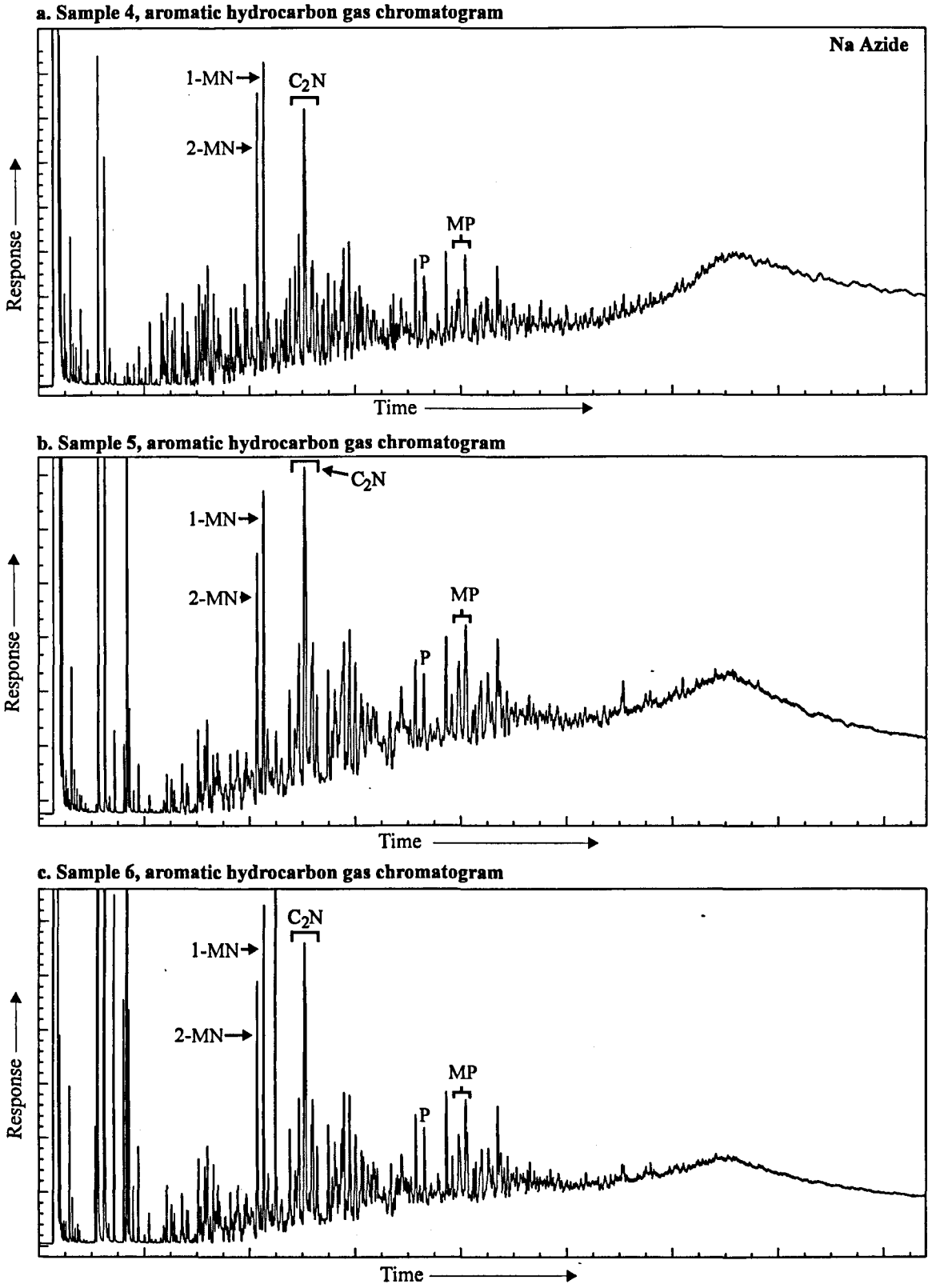

Figure 6.3.12(a,b,c). Kittiwake biodegradation set 2. Aromatic hydrocarbon gas chromatograms. MN = methylnaphthalene; C_2N = C_2 naphthalene; P = phenanthrene; MP = methylphenanthrene.

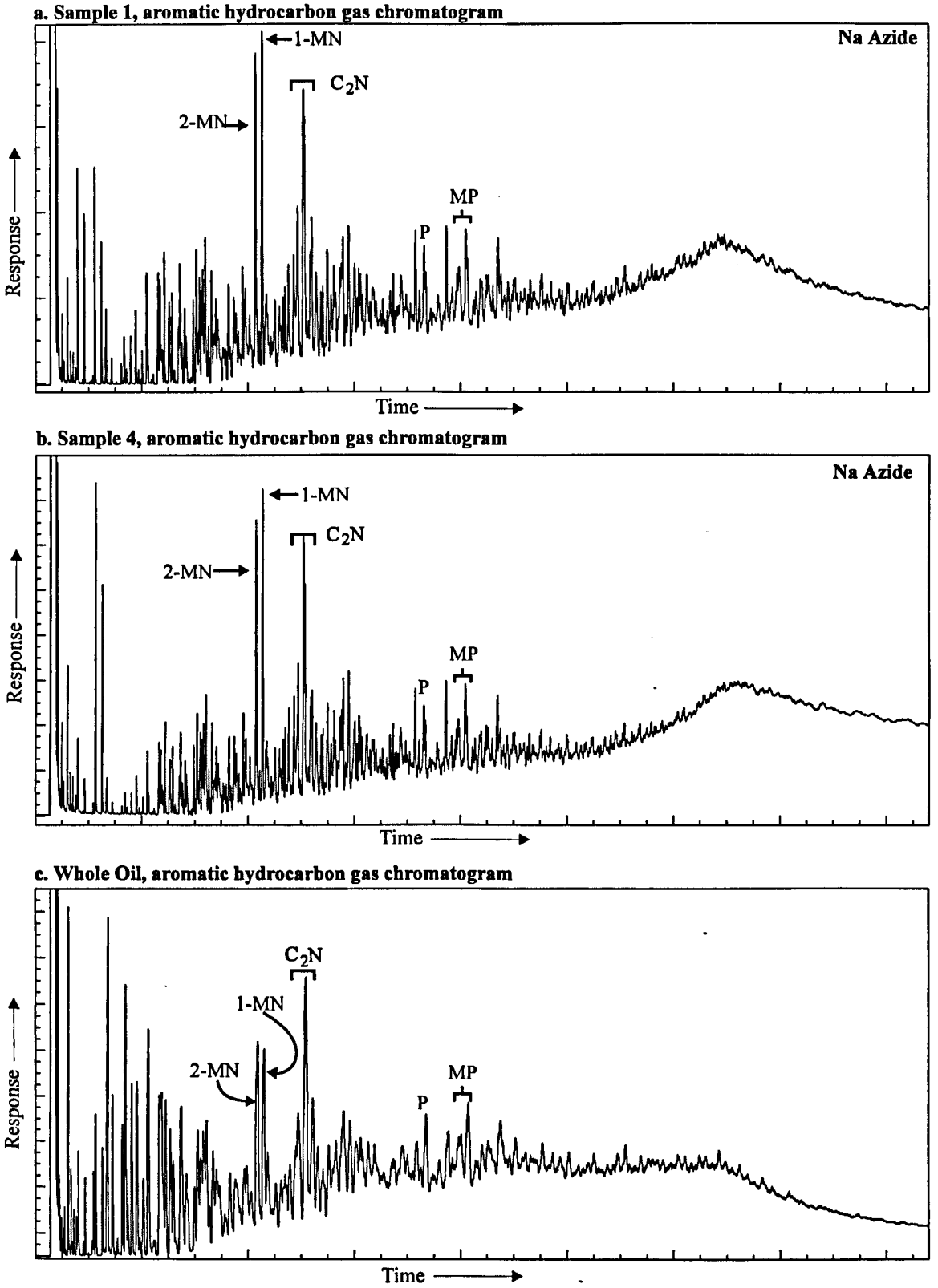

Figure 6.3.13(a,b,c). Comparison of control samples with Kittiwake whole oil sample. Aromatic hydrocarbon gas chromatograms. MN = methylnaphthalene; C_2N = C_2 naphthalene; P = phenanthrene; MP = methylphenanthrene.

	KITTIWAKE	SAMPLE #3	SAMPLE #5
Biodegradation*			
n-C_{17}/Pr	3.62	0.64	0.55
n-C_{18}/Ph	1.87	0.38	0.11
n-C_{18}/C_{30} αβ-hopane	53.70	8.21	0.38
Ph/C_{30} αβ-hopane	28.72	21.37	3.40
Tm/C_{30} αβ-hopane	0.10	0.11	0.13
N/N+P	0.51	0.29	0.23
2-MN/2-MN + P	0.63	0.49	0.44
2,6+2,7-DMN/2,6+2,7-DMN + P	0.50	0.44	0.39
1,3,5 + 1,4,6-TMN/1,3,5 + 1,4,6-TMN + P	0.42	0.42	0.40
P/DBT	0.91	0.83	0.88
4-MDBT/DBT (MDR4)	0.98	1.01	1.01
C_{27}ααα R sterane/C_{30} αβ-hopane	0.26	0.28	0.23
Source Correlation			
Homohopane Indices			
C_{31}αβ(S+R)/[SUM, C_{31}αβ(S+R) to C_{35}αβ(S+R)]	27.32%	26.46%	26.34%
C_{32}αβ(S+R)/[SUM, C_{31}αβ(S+R) to C_{35}αβ(S+R)]	21.42%	20.84%	22.20%
C_{33}αβ(S+R)/[SUM, C_{31}αβ(S+R) to C_{35}αβ(S+R)]	17.43%	17.95%	17.35%
C_{34}αβ(S+R)/[SUM, C_{31}αβ(S+R) to C_{35}αβ(S+R)]	13.88%	14.37%	13.70%
C_{35}αβ(S+R)/[SUM, C_{31}αβ(S+R) to C_{35}αβ(S+R)]	19.95%	20.38%	20.42%
C_{27}αααR/C_{29}αααR	0.94%	1.02%	0.82%
Maturity Parameters			
Pr/Ph	0.47	0.58	0.29
Ts/Ts + Tm	0.82	0.79	0.78
C_{30}βα/C_{30}βα + C_{30}αβ	0.02	nd	nd
C_{31}αβS/C_{31}αβS + C_{31}αβR	0.57	0.58	0.59
C_{32}αβS/C_{32}αβS + C_{32}αβR	0.63	0.61	0.59
C_{29}αααS/C_{29}αααS + C_{29}αααR	0.53	0.54	0.54
C_{29}αββ(S+R)/C_{29}αββ(S+R) + C_{29}ααα(S+R)	0.55	0.53	0.53
2-MN/1-MN (MNR)	0.78	0.65	0.59
2,3,6-TMN/1,3,5+1,4,6-TMN (TNR)	0.43	0.36	0.42
1.5(2-MP + 3-MP)/(P + 1-MP + 9-MP) (MPI)	0.41	0.41	0.40
Calculate Vitrinite Reflectance			
Rm = 0.60(MPI) + 0.4	0.65	0.65	0.64
(2-MP + 3-MP)/(2-MP + 3-MP + 1-MP + 9-MP) (MPDF1)	0.31	0.31	0.31
4-MDBT/1-MDBT (MDR)	2.75	2.62	2.62
C_{20} TA 20R/C_{20} TA 20R + C_{28} TA 20R	0.64	0.65	0.66

Table 6.3.3. Biodegradation, source correlation and maturity information from the GC/MS analyses of Kittiwake whole oil, samples 3 and sample 5. Values gained from biomarker and molecular ratios from both aliphatic and aromatic hydrocarbons. Peak areas are given in Appendix 5, Tables A5.1 and A5.2.

	Reference	m/z	Results found in these Experiments
Biodegradation			
n-C_{17}/Pr	Bailey *et al.*, 1973a	85	Decrease
n-C_{18}/Ph	Bailey *et al.*, 1973a	85	Decrease
n-C_{18}/C_{30} αβ	Pritchard *et al.*, 1992	85/191	Decrease
Ph/C_{30} αβ	Pritchard *et al.*, 1992	85/191	Decrease
Tm/C_{30} αβ		191	Increase
Maturation			
C_{31} αβ S/(S+R)	Mackenzie, 1984	191	Slight Increase
C_{32} αβ S/(S+R)	Mackenzie, 1984	191	Slight Decrease
Ts/Ts+Tm	Peters & Moldowan, 1993	191	Decrease
C_{29} αββ/(C_{29} αββ+ααα)	Mackenzie, 1984	217	Constant
C_{29} ααα 20S/(20S+20R)	Mackenzie, 1984	217	Constant

Table 6.3.2. Aliphatic hydrocarbon biomarker and molecular ratios, and their alteration with biodegradation. Detailed ratio values are given in Table 6.3.3. Individual peak areas for aliphatic hydrocarbons analysed are given in Table A5.1.

6.3.5.1. Aliphatic Hydrocarbon Biomarker Assessment of Crude Oil Biodegradation.

For the assessment of the influence of biodegradation on aliphatic hydrocarbons, the regular hopane, C_{30} αβ, was used as a constant with which to evaluate aliphatic hydrocarbon reduction, due to biodegradation. The C_{30} αβ hopane has been used in other studies as a recalcitrant biomarker, not being affected by biodegradation, unless degradation is "severe" (Pritchard *et al.*, 1992; Bragg *et al.*, 1994; Palmer, 1994). Phytane, which was observed not to alter through the initial stages of biodegradation ("mild", "mild-moderate", Fig. 6.3.7), was also used as constant but only for those stages in which it has not been degraded, *i.e.*, "mild" and "mild to moderate" biodegradation stages.

The compounds used to assess biodegradation, were the *n*-C_{18} alkane, phytane (for biodegradation stages "moderate" and above) and trisnorhopane (Tm).

The values for the *n*-C_{18}/C_{30} αβ, Ph/C_{30} αβ and Tm/C_{30} αβ ratios, and their variation with increasing biodegradation, are illustrated in the graph in Figure 6.3.14, and Table 6.3.3, while the cross plot of the *n*-C_{17}/Pr and *n*-C_{18}/Ph ratios is shown in Figure 6.3.15.

In Figure 6.3.14 and Table 6.3.3, the results for sample 3 show that the *n*-C_{18}/C_{30} αβ values have been reduced by approximately 80% of the initial non-degraded value, while the Ph/C_{30} αβ ratio has been reduced by approximately 25% of

the initial value. The Tm/C_{30} αβ ratio exhibits a slight increase. In Figure 6.3.15 the cross plot of the *n*-C_{17}/Pr and *n*-C_{18}/Ph ratios indicating a substantial reduction of both *n*-alkanes. Overall, results show that both aliphatic hydrocarbon groups, n-alkanes and isoprenoids, have been reduced by biodegradation therefore, according to Volkman *et al.* (1984), sample 3 is classified as "moderately" biodegraded, and not "mild-moderately" biodegraded as defined in Section 6.3.4. In addition, the occurrence of isoprenoid reduction nullifies the use of the *n*-C_{17}/Pr and *n*-C_{18}/Ph ratios for accurate assessment of biodegradation in sample 3.

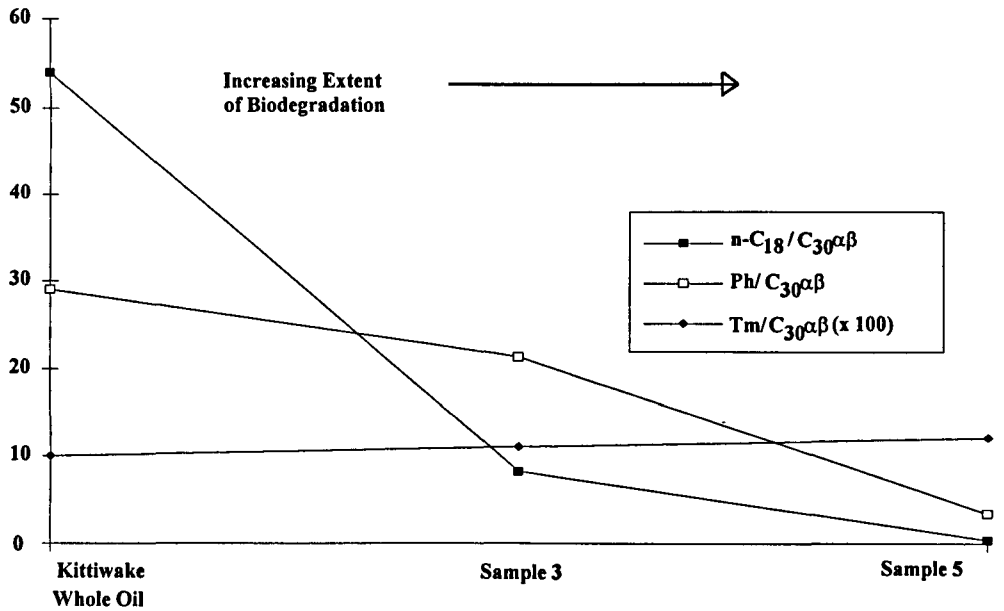

Figure 6.3.14. Variation of aliphatic hydrocarbon ratios highlighting loss of n-C_{18} and phytane with increasing biodegradation.

The results for sample 5, in Figure 6.3.14 and Tables 6.3.2 and 6.3.3, indicate that both *n*-C_{18}/C_{30} αβ and Ph/C_{30} αβ ratios have both been substantially reduced from their initial non-degraded values, by approximately 99% and 90%, respectively. The Tm/C_{30} αβ ratio again exhibits a slight increase. The almost total removal of *n*-alkanes and isoprenoids suggests that sample 5 is "moderately-extensively" biodegraded.

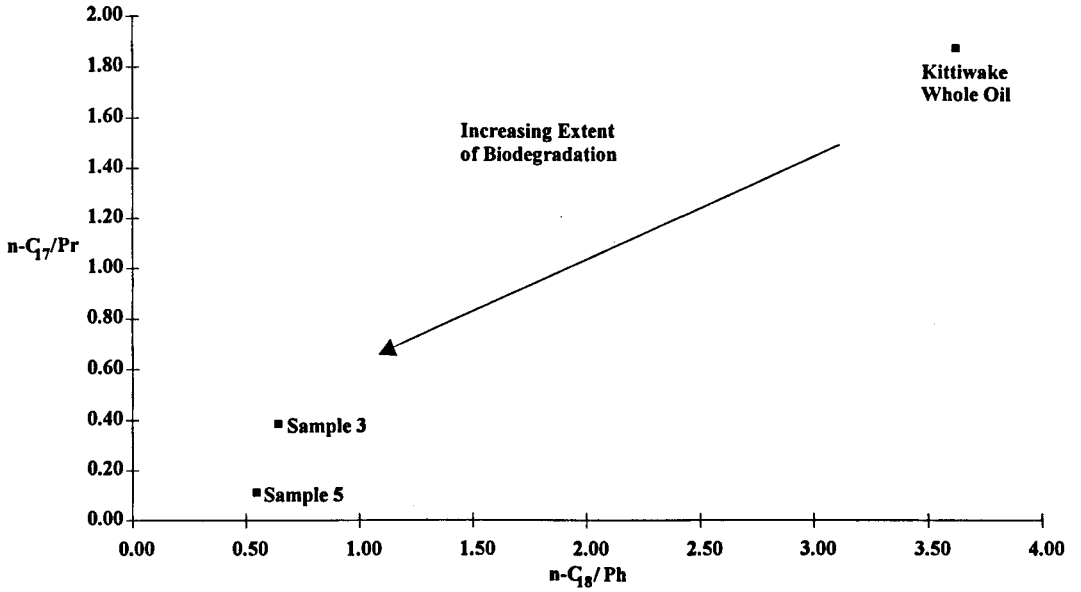

Figure 6.3.15. Comparison of n-C17/Pr and n-C18/Ph aliphatic hydrocarbon ratios indicating increasing extent of biodegradation. Ratios calculated from peaks areas, measured from gas chromatography/mass chromatograms

The Tm/C_{30} αβ ratio illustrates (Fig. 6.3.14, Tables 6.3.2 & 6.3.3) a slow, constant increase with increased degradation, from the non-degraded Kittiwake whole oil to sample 5 and therefore, cannot be related to any particular stage of biodegradation. This slight increase signifies that either Tm is increasing, or C_{30} αβ is decreasing. It seems likely that hopane is decreasing in accordance with previous work upon hopane biodegradation by Seifert *et al.* (1984), who also identified that Tm exhibited a greater resistance to biodegradation than the higher hopane homologs. However, it must be stressed that this apparent hopane reduction is insignificant and does not suggest a higher biodegradation level (i.e., "severe" to "extreme"). Support for this is gained by examination of the relative abundances of the homohopanes (C_{31}-C_{35}). Examination of their percentages, in Table 6.3.3, and illustrated in Figure 6.3.16, could not identify any biodegradational alterations. Further assessment was performed by examining the C_{27}ααα R regular sterane relative to the abundance of the C_{30}αβ hopane. In Table 6.3.3 a slight reduction for the C_{27}ααα R (0.26 to 0.23) is observed, (also for C_{27}ααα R/C_{29}ααα R ratio, 0.94 to 0.82) this may cautiously suggest that sample 5 should be categorised no higher than "extensive" biodegradation, as 50%+ of the ααα R steranes are still present (Volkman *et al.*, 1984).

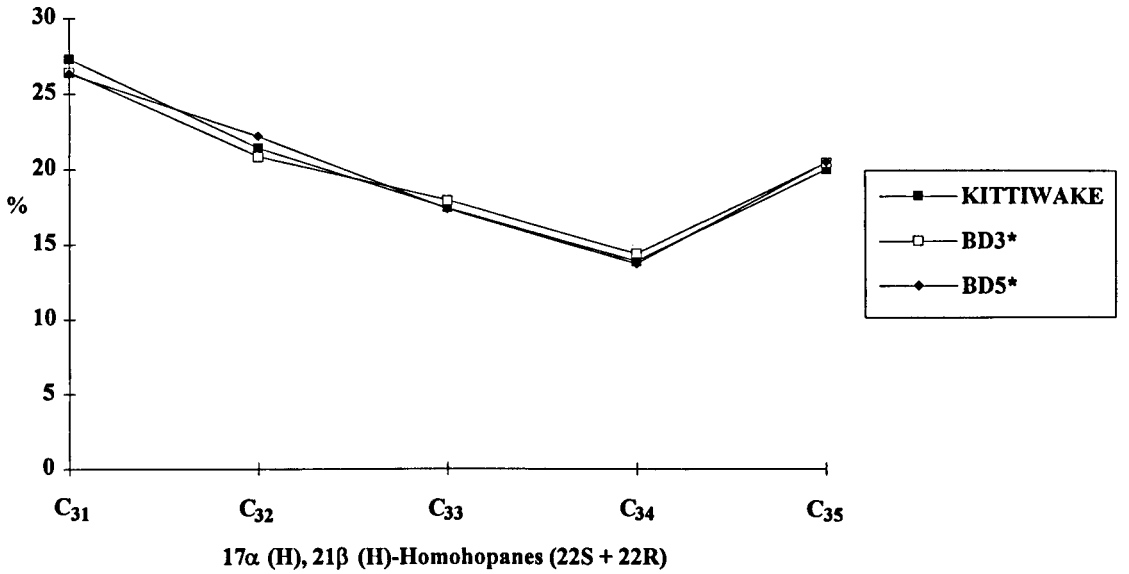

*Figure 6.3.16. The relative abundances (%) of C_{31}-C_{35} 17α(H), 21β(H) (22S+22R) homohopanes (normalised to total C_{31}-C_{35} homohopanes) in the oils analysed in this chapter. Note the high C_{35} homohopane percentages indicating high redox conditions at the source rock depositional environment (Peters & Moldowan, 1991). Kittiwake = whole oil sample; * = biodegraded crude oil, BD3 = sample 3; BD5 = sample 5.*

In conclusion, from the GC and GC/MS analyses, samples 2 and 3 are classed as "moderately" biodegraded and sample 6, which showed a large reduction of the ratios involving both Ph and *n*-C_{18} aliphatic hydrocarbons in Figure 6.3.10, is classed as "moderately to extensively" biodegraded. Sample 5 possibly exhibited the initial stages of ααα R sterane degradation and is classed as "extensively" degraded.

6.3.5.2. Aliphatic Hydrocarbon Biomarkers Assessment of Crude Oil Maturity.

The hopane and sterane maturity ratios for the saturate fractions of the Kittiwake crude oils, in Table 6.3.3, indicate oil was expelled during early generation stage (Section 3.1.1.3.2., Fig. 3.1.4). However, the Ts/(Ts+Tm) hopane ratio differs from this, suggesting that crude oil was produced at the peak generation stage (Peters & Moldowan, 1993).

6.3.6. Gas Chromatography/Mass Spectrometry Analysis of Aromatic Hydrocarbon Fractions.

The aromatic hydrocarbons used, and their diagnostic ions, for the assessment of the biodegradation and maturation of the samples are listed and identified in

Appendix 5, Table A5.2. The molecular aromatic hydrocarbon ratios used, their original references (where known) and their alteration during incubation are highlighted in Table 6.3.4. More detailed molecular ratio data, for both aliphatic and aromatic hydrocarbons, along with their applications as either maturity, source correlation or biodegradation indicators, are given in Table 6.3.3.

	Reference	**m/z**	**Results found in these Experiments**
Maturity			
MPI	Radke *et al.*, 1982	178, 192	Constant
MPDF1	Kvalheim *et al.*, 1987	192	Constant
Biodegradation			
N/(N+P)		128/178	Large Decrease
2-MN/(2-MN+P)		142/178	Decrease
2-MN/1-MN	Radke *et al.*, 1982	142	Decrease
2,6+2,7-DMN/(2,6+2,7-DMN+P)		156/178	Slight Decrease
1,3,5+1,4,6-TMN/ (1,3,5+1,4,6-TMN+P)		170/178	Constant
4-MDBT/DBT	Radke *et al.*, 1982	184/198	Slight Decrease
P/DBT		178/184	Constant

Table 6.3.4. Aromatic hydrocarbon fraction ratios and their variation with biodegradation. Detailed ratio values are given in Table 6.3.3. Individual peak areas for aromatic hydrocarbons analysed are given in Table A5.2.

6.3.6.1. Aromatic Hydrocarbon Ratio Assessment of Crude Oil Biodegradation.

The aromatic hydrocarbon ratios used to assess the increasing extent of biodegradation are shown in Tables 6.3.3 and 6.3.4. The only major alteration was seen for the alkylnaphthalenes (Fig. 6.3.17), whose ratios with phenanthrene decreased with increasing biodegradation. The amount of alkylnaphthalene reduction decreased with increasing molecular weight of the naphthalene compounds. The naphthalene ratio (N/N+P) decreased by 54% (0.51 to 0.23), methylnaphthalene ratio (2-MN/2-MN+P) decreased by 30% (0.63 to 0.44), dimethylnaphthalene ratio (2,6+2,7-DMN/2,6+2,7-DMN+P) decreased by 22% (0.50 to 0.39) and trimethylnaphthalene (1,3,5+1,4,6-TMN/1,3,5+1,4,6-TMN+P) by 5% (0.42 to 0.40). The effects of steric differences, as well as molecular weight differences, were

observed in the biodegradation rates. Therefore, both samples 3 and 5 displayed large reduction of both the naphthalene and methylnaphthalene ratios, with only slight reduction for the dimethylnaphthalene ratio. According to the Volkman *et al.* (1984) scale (Table 6.1.2), both possessed "moderately" degraded compositions, agreeing with observations from aliphatic hydrocarbon analysis for sample 3 but not for sample 5.

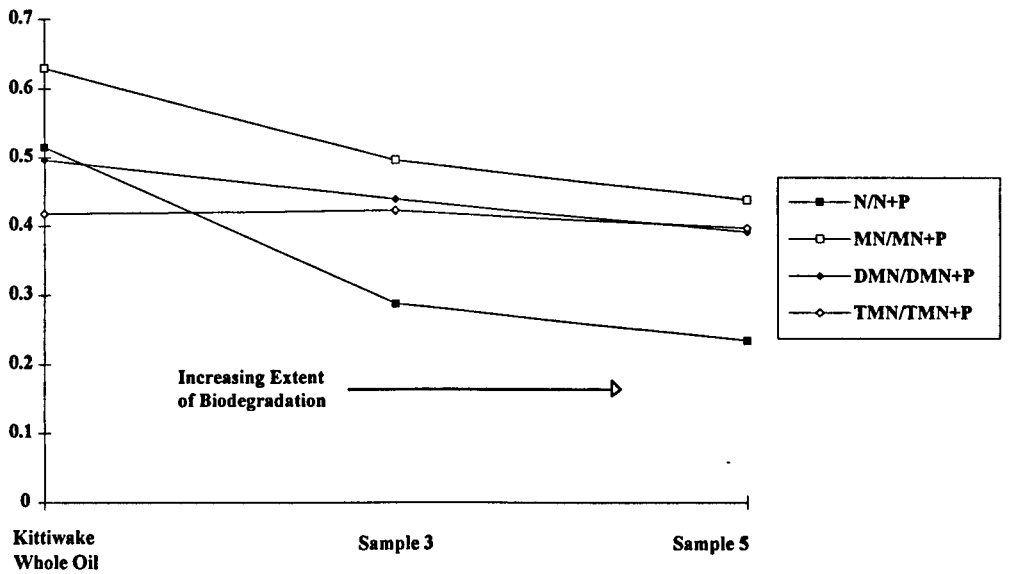

Figure 6.3.17. Variation of alkylnaphthalenes (N, MN, DMN, TMN) versus phenanthrene, indicating an increasing extent of biodegradation from Kittiwake whole oil > sample 3 > sample 5.

Figure 6.3.18 shows that 2-methylnaphthalene preferentially degrades before 1-methylnaphthalene. In Tables 6.3.3 and 6.3.4 no alteration, with increasing biodegradation, occurs to the phenanthrene group, while the methylphenanthrene index (MPI, Radke *et al.*, 1982) and methylphenanthrene distribution fraction 1 (MPDF1, Kvalheim *et al.*, 1987) ratios also remained constant. The dibenzothiophene (DBT) group also showed no alteration with biodegradation, as indicated by the phenanthrene/dibenzothiophene ratio.

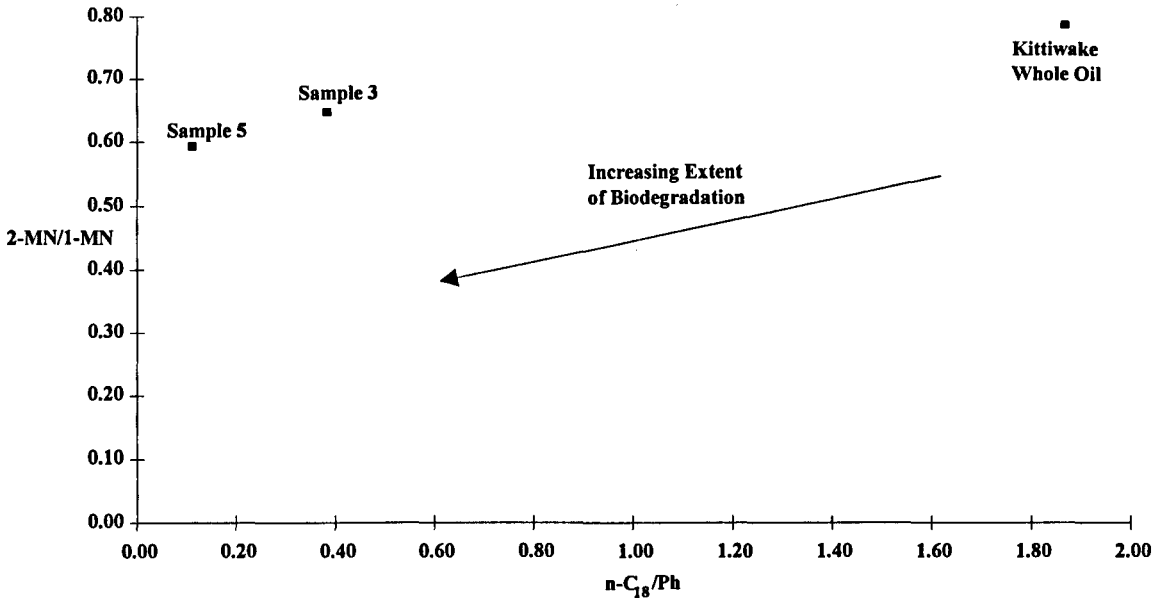

Figure 6.3.18. Aliphatic ratio, n-C18/Ph, plotted against the aromatic hydrocarbon ratio, 2-MN/1-MN, indicating preferential loss of 2-MN with increasing biodegradation. In agreement with Volkman et al. (1984).

6.3.6.2. Aromatic Hydrocarbon Ratio Assessment of Crude Oil Maturity.

The MPI calculated vitrinite reflectance (Radke *et al.*, 1982) was approximately 0.64% Ro, in agreement with other aromatic maturity parameters (TNR, MDR; Table 6.3.3). These were also in agreement with the majority of the aliphatic hydrocarbon biomarker ratios (Section 6.3.5.2). Therefore, the Kittiwake represents a mature crude oil from early generation.

6.4. Discussion.

Assessment of the effect of biodegradation on the water uptake behaviour of NS3 and Kittiwake crude oils will be performed in two stages. First, discussion of the extent of biodegradation upon the aliphatic and aromatic hydrocarbon fractions, by comparison with established models and second, the effect of biodegradation on emulsifiers (sols and surfactants) and therefore, emulsification ability of crude oils.

6.4.1. Effect of Biodegradation on Aliphatic and Aromatic Hydrocarbon Fractions.

Assessment of the aliphatic hydrocarbon gas chromatograms (Figs. 6.3.7 to 6.3.9; Table 6.4.1) of the biodegraded and non-biodegraded samples indicates that four stages of the Volkman *et al.* (1984) classification are present. These stages are the "non-degraded" stage for the Kittiwake whole oil and samples 1 and 4; sample 3 is classed as "mild-moderately" biodegraded, sample 2 is classed as "moderate" and samples 5 and 6 are classed as "moderate to extensively" degraded. However, assessment of the data generated from the aliphatic hydrocarbon gas chromatography/mass spectrometry (Fig. 6.3.14; Tables 6.3.2 & 6.3.3) indicate that sample 3, is actually a "moderately" biodegraded sample, because isoprenoid degradation has occurred. In addition, GC/MS analysis of sample 5 suggested that the $C_{27}\alpha\alpha\alpha R$ sterane may have been slightly degraded, possibly indicating the on-set of the "extensive" biodegradation stage.

Samples	GC	GC/MS	
	Ali. HC	Ali. HC	Arom. HC
WO	Non-degraded	Non-degraded	Non-degraded
1*	Non-degraded	nd	nd
2	Moderate	nd	nd
3	Mild-moderate	Moderate	Moderate
4*	Non-degraded	nd	nd
5	Moderate-extensive	Extensive	Moderate
6	Moderate-extensive	nd	nd

*Table 6.4.1. The determined biodegraded states of samples (Volkman et al., 1984) from GC & GC/MS analyses. Ali HC = aliphatic hydrocarbons; Arom. HC = aromatic hydrocarbons. nd = not determined. * = Control samples (Section 6.2.1).*

Assessment of the variation of the aromatic hydrocarbon fractions showed little alteration. The alkylnaphthalenes appeared to be the only compounds affected. This group may be affected by either water washing or microbial degradation. Naphthalene reduction due to work up procedures and evaporation were discounted because increased alkylnaphthalene reduction was related to increased degradation. It was considered that the effect of water washing may be significant, as the most degraded and most emulsified sample (sample 5), would have been exposed to the greatest amount of water. The more emulsified a sample the greater its oil/water interfacial area. As sample 5 was emulsified to a greater degree than sample 3 it has had a greater oil/water interfacial area and therefore has been exposed to the greatest

amount of water washing. Consequently, water washing may account for the increased reduction of the alkylnaphthalene group with increasing degradation. However, comparison of 2-methylnaphthalene (beta substituted) and 1-methylnapthalene (alpha substituted) in Figure 6.3.18, indicates that 2-methylnaphthalene has been reduced to the greatest degree. This reduction is characteristic of biodegradation, as water washing will tend to reduce 1-methylnaphthalene before 2-methylnaphthalene (Eganhouse & Calder, 1976; Volkman *et al.*, 1984). It was concluded that as reduction of the high molecular weight alkylnaphthalenes progressed at a slower rate than the low molecular weight alkylnaphthalenes, biodegradation was restricted by molecular size, in agreement with Rowland *et al.* (1986) (Section 6.1.1.1.2). The Volkman *et al.* (1984) classification scheme uses alkylnaphthalene reduction, in particular selective C_2 naphthalene reduction, to indicate "moderate" degradation, therefore, both samples 3 and 5 were classified as "moderately" biodegraded. The biodegradation state of sample 5 determined by aromatic hydrocarbon is therefore lower than that determined by aliphatic hydrocarbons. The biodegraded state of sample 3 is unaltered.

Of the three hydrocarbon groups analysed (n-alkane, isoprenoid & aromatic hydrocarbon) it has been observed that the n-alkanes were degraded to the greatest degree followed by the isoprenoids and then by the aromatic hydrocarbons, which only exhibited substantial reduction of the C_0 and C_1 alkylnaphthalenes. Overall, it was seen that reduction sequence {6.13} for these experiments was:

n-alkane> iso-alkane> aromatics {6.13}

Therefore, the biodegradation sequence was in general agreement with Tissot & Welte (1984), Connan (1984) and Volkman *et al.* (1984). However, it is probable that n-alkanes and isoprenoid alkanes were reduced simultaneously as seen in a previous assessment of surface biodegradation by Pritchard *et al.* (1992). This is suggested because the *n*-alkanes have not been fully removed (i.e., *n*-C_{17} & *n*-C_{18} still present) before degradation of the isoprenoid alkanes commenced. This is not in agreement with Volkman *et al.* (1984) and therefore, it must be re-emphasised that the Volkman *et al.* (1984) classification was for subsurface crude oil biodegradation.

6.4.2. Effect of Biodegradation on Crude Oil Emulsifiers and Emulsification.

As discussed in the previous chapters, water-in-oil emulsions are stabilised by the formation of rigid and protective interfacial films between the oil and water phases, caused by the accumulation of emulsifiers (Schramm, 1992). The most

influential emulsifiers in the stabilisation of water-in-oil emulsions are the asphaltene and wax sols (Graham *et al.*, 1983; Eley *et al.*, 1987). Chapter 4 related the varying emulsifying ability of North Sea crude oils in terms of the asphaltene solubility in the bulk phase, as well as the concentration of the wax fraction. It was found that the biodegraded North Sea crude oils, which are characterised by high asphaltene solubility and low wax content, were unable to form stable water-in-oil emulsions. During the course of the biodegradation experiments in this chapter it was expected that the solubility of the asphaltenes in the crude oil, as well as the crude oil wax contents, would both be affected by the reduction of *n*-alkanes (see Section 1.2.2.1 for explanation of asphaltene precipitation; Section 4.4.2.2 for explanation of wax precipitation), thereby altering emulsion formation/stabilisation abilities. This was confirmed by Iatroscan-FID analysis (Fig. 6.3.6) which showed reduction of the *n*-alkane content (asphaltene and resin contents remain generally unchanged, any alteration probably being within analytical error) and by wax extraction analysis (Figs. 6.3.3 to 6.3.5).

Iatroscan analysis found that the concentration of the aromatic hydrocarbon fractions, in the samples analysed, increased with increasing biodegradation while the content of the aliphatic hydrocarbon fraction was reduced. This will increase the solubility of the asphaltene group in the crude oil, referred to by Leontaritis (1989) as increasing the "solvent power" of the crude oils, thereby making asphaltene precipitation unlikely (Section 1.2.2.1). Therefore, the ability of asphaltene particles to accumulate at the oil/water interface, thereby assisting the stabilisation of water-in-oil emulsions, would probably be reduced.

Wax analysis found that biodegradation reduced the wax concentration of sample 5 by an order of magnitude (wax content of sample 3 being reduced by approximately 30%; Table 6.3.1) and therefore, the ability of the wax fraction to stabilise the interface would also be reduced. Overall, the Iatroscan and wax results from the laboratory biodegradation experiments were similar to those for the reservoir degraded North Sea crude oils (NS2 & NS3), which did not form stable, water-in-crude oil emulsions. Therefore, it would be expected that the laboratory biodegraded crude oil samples from this experiment would behave similarly to the North Sea biodegraded crude oils, characterised in Chapters 3, 4 & 5. However, all laboratory biodegraded crude oils were found to form stable water-in-crude oil emulsions. In addition, it was found that the most stable emulsions were those which contained the most biodegraded crude oils. Consequently, this means that either the relationship between biodegradation and emulsification, identified in Chapter 3, does not apply or the biodegraded samples in this experiment, and the resultant emulsions, were not

comparable with the reservoir biodegraded North Sea crude oils in the previous sample set.

Experimental observations, Figures 6.3.1 and 6.3.2 (Section 6.3.1), shows that during the biodegradation experiments the "moderately" and "moderately to extensively" biodegraded samples, 2, 5 & 6, all formed thick, viscous and very stable water-in-crude oil emulsions. The "mildly" degraded sample 3 formed a poor, relatively unstable, water-in-crude oil emulsion while the non-biodegraded controls, samples 1 & 4, did not emulsify. As the presence of emulsifiers (asphaltene and wax particles) is generally reduced by biodegradation their ability to stabilise emulsions, especially for the most degraded samples (*i.e.*, samples 5 & 6), will probably be reduced. It is therefore concluded that other factors were responsible for the emulsification observed during experimentation.

Consideration of the process of biodegradation may explain why emulsions were formed. Biodegradation products from *Pseudomonas* sp., were reported by Zajic & Supplisson (1972) and Zajic *et al.* (1974), as being responsible for the emulsification of Bunker C oil (heavy fuel oil). The products were generated from the aliphatic hydrocarbons and were characterised as high molecular weight polysaccharides. In addition, other crude oil biodegradation experiments, such as those by Jobson *et al.* (1972), also observed emulsification of biodegrading crude oils. Generation of emulsifiers, during biodegradation, was shown by Connan (1984), who identified different bacterial strains as being responsible for aerobic biodegradation of specific aliphatic and aromatic hydrocarbons. Biodegradation, and therefore surfactant generation, is not restricted to bacteria or aerobic conditions. For example Payne & Philips (1985a) noted that microbial degradation was also attributed to fungi and yeast as well as bacteria. Bumpus *et al.* (1985) also noted the effect of white rot fungi while Connan *et al.* (1993) reported anaerobic biodegradation in Congo petroleum reservoirs was attributed to sulphate reducing bacteria. Work on the biodegradation of polycyclic aromatic hydrocarbons (PAHs), reviewed by Cerniglia (1992), lists many pathways and products for biodegradation with both procaryotes and eucaryotes differing in their biodegradation mechanisms. Predominantly, most mechanisms produce alcohols and acids, both of which are ideal emulsifiers, which reduce interfacial tension (the effect of surfactants on emulsion stability is discussed in Section 1.2.1). Therefore, the products from the biodegradation of aliphatic and aromatic hydrocarbons, by many hundreds of species of bacteria, yeast and filamentous fungi, common to many environments, potentially aid emulsion formation/stabilisation.

The reduction of the interfacial tension consequently results in the amount of emulsification energy needed to form a stable water-in-oil emulsion being reduced (Section 1.2.1). Whereas previous emulsions have been emulsified after large amounts

of shear energy have been applied to the crude oil and water phases (Chapters 2 & 3, Johansen *et al.*, 1989), the emulsification of biodegrading crude oils reported in this chapter only required a small amount of shear energy (50-80 RPM). Therefore, there are two types of emulsion formation processes identified by this research first, the high energy input, by use of the Ultra-Turrax dispersing tool (Chapter 2, Johansen *et al.*, 1989) and second, the reduced energy input combined with high surfactant concentration, described in this chapter. In addition, it is important to note the difference between "biodegrading" samples, which are still associated with their degradation products, and "biodegraded" samples, such as NS2 and NS3, which have probably lost their degradation products during in-reservoir degradation. The difference in the emulsification ability of the "biodegrading" crude oils is therefore probably due to the presence of surfactants. These surfactants are not present in the "biodegraded" NS2 and NS3 crude oils, presumably because they have partitioned into the water phase in the reservoir due to their water solubility (Chapter 5). Consequently, the NS3 and NS2 biodegraded crude oils do not emulsify (consequences for crude oil spillage are briefly discussed below).

The ability to generate surfactants, during biodegradation, will depend upon the crude oil composition, whether or not it is easily biodegradable (therefore, easy surfactant generation). In Figure 6.3.2, the visual observations of the NS3 crude oil biodegradation experiment, illustrates that the crude oil did not form an emulsion at any time, even though biodegradation did occur. The "clouding" of the samples, marking the commencement of biodegradation of the NS3 crude oil (discussed in Section 6.3.1) was approximately 9 days later than the Kittiwake experiment. It has previously been reported that the initial state of crude oil effects its rate of degradation (Walker *et al.*, 1976). In general, "heavy" crude oils, such as NS3, were found to degrade at a slower rate than "light" oils (Westlake *et al.*, 1978). This slowness of degradation, and lack of emulsification, is thought to be due to the lack of easily degradable components in the NS3 crude oil, such as low molecular weight n-alkanes. Slow degradation rate implies slower generation of surfactant by-products. Consequently, the resultant low concentration of surfactants would probably not be able to sufficiently lower the interfacial tension between the crude oil and water phases, for the low energy input to cause emulsification.

6.4.2.1. Influence of Biodegradation upon Crude Oil Spills and Emulsification.

Results contained within this thesis indicate that the chemical alteration of crude oil by biodegradation may affect its ability to form stable water-in-oil

emulsions. The implication for crude oil spillage and clean up operations is now considered.

The majority of crude oil spillages, such as the *Torrey Canyon* (Jordan & Payne, 1980), *Amoco Cadiz* (Gundlach *et al.*, 1983) and *Exxon Valdez* (Bragg *et al.*, 1992), form highly viscous water-in-oil emulsions, frequently referred to as "mousses" or "chocolate mousses". These emulsions are extremely problematic affecting clean up due to increased viscosity (Bridié *et al.*, 1980) and by increasing the quantity of contaminant to be recovered and disposed. Water uptake by crude oil may increase the contaminated volume by five times (Schramm, 1992; Bridié *et al.*, 1980). In addition, bioremediation techniques are hampered by the restriction of nutrients at the oil and water interface, essential for biodegradation (Atlas *et al.*, 1981; Bragg *et al.*, 1992). Consequently, identification of whether or not a crude oil will form such an emulsion may significantly affect clean up operations.

These hazardous emulsions may be formed by two mechanisms. The first and most commonly considered mechanism is attributed to the stabilising effect of asphaltene particles at the oil/water interface, in accordance with work by Bobra *et al.* (1992; Chapter 1). The second mechanism is due to the generation of significant quantities of surfactants during the biodegradation of spilled crude oil, suggested by Zajic *et al.* (1972; Section 6.4.2). Work in this thesis has assessed these mechanisms with both being found to be influenced by the biodegraded state of the crude oil.

The first mechanism was assessed in Chapters 3, 4 & 5. Results suggested that an observed lack of emulsification for biodegraded crude oils was due to the reduced presence of emulsifiers (asphaltene sols, wax sols and oil-soluble surfactants). The second mechanism was assessed in this chapter which analysed the ability of crude oil to emulsify during in-laboratory biodegradation. It was observed that non-degraded crude oils formed stable water-in-oil emulsions while previously biodegraded crude oil (NS3) did not (Section 6.4.2). This lack of emulsification was probably due to the absence of easily degradable components necessary for the formation of surfactants.

Therefore, it is suggested that previously biodegraded crude oils are less likely to emulsify. This characteristic may have been observed during the *Braer* spillage. In this instance the spilled crude oil, which was biodegraded before spillage, did not emulsify, dispersing quickly (Wolff *et al.*, 1993). Although the dispersal of the *Braer* spillage was suggested to be due prevalent weather conditions (hurricane force winds: Wolff *et al.*, 1993; Farmer & Li, 1994) it is considered here that the chemistry of the crude oil was the one of the main reasons for lack of emulsification.

6.5. Conclusions.

Laboratory biodegradation of crude oil samples was successful and it was recognised that the non-degraded Kittiwake crude oil formed an emulsion during laboratory degradation while the biodegraded NS3 crude oil did not. Subsequent chemical analysis of Kittiwake samples was able to characterise the extent of biodegradation with the order of degradation loosely following the Volkman *et al.* (1984) biodegradation sequence. However, COWUA was unable to be performed because of poor sample recovery due to the emulsification of the Kittiwake crude oil samples.

Laboratory biodegradation of the Kittiwake crude oil samples produced compositions with low wax content and probably poor asphaltene precipitation. Therefore, the stabilisation of emulsions by the precipitation of asphaltene and wax sols was thought to be unlikely. Consequently, the subsequent emulsification of the biodegraded Kittiwake crude oil samples was attributed to the generation, during biodegradation, of surfactant by-products.

Observations of the laboratory biodegradation of the degraded NS3 crude oil found that although biodegradation occurred no emulsification was observed. This lack of emulsification was attributed to insufficient surfactant generation during biodegradation. It was consequently suggested that the spillage of biodegraded crude oil was possibly less likely to form stable water-in-oil emulsions than spillage of non-degraded crude oil.

CHAPTER 7:

OVERALL RESULTS AND FURTHER WORK

Chapter 7. Overall Conclusions and Suggested Further Work.

7.1. Conclusions.

The aim of this study was to assess the water uptake ability of various crude oils and then to relate this to their chemical composition.

Assessment of the water uptake ability was achieved by the use of a set of procedures based around the Karl Fischer titration technique. The results showed that crude oil water uptake may be characterised by crude oil water retention (water sedimentation rate) and crude oil emulsion formation/stabilisation (degree of oil & water separation) ability. Both of these water uptake abilities were found to vary with the extent of crude oil biodegradation. Non-biodegraded crude oils exhibited "poor" water retention (rapid water or emulsion sedimentation) and formed stable water-in-oil emulsions, while degraded crude oils exhibited higher water retentive capability (slower sedimentation) yet possessed varied emulsification ability. Consequently, organic geochemical analyses attempted to relate variations in water uptake characteristics to crude oil composition. Analyses were also attempted on oils that were biodegraded in the laboratory.

7.1.1. Water Retention Ability of Crude Oils.

Crude oil water retention characterisation was based upon assessment of the water sedimentation rate from the top of oil/water blends which contained 30% added water. This enabled oils to be categorised in a basic water retention ability classification scheme ("poor", "moderate" or "good"). Analysis of the variation of water retention ability with increasing biodegradation found that the most biodegraded crude oils exhibited the slowest sedimentation rate ("good" and "moderate" water retention, respectively), whilst non-degraded crude oils exhibited the quickest sedimentation ("poor" water retention).

Two possibilities were considered for the observed water retention characteristics. First, the increased presence of emulsifying compounds (asphaltene and wax sols as well as surfactants) with increased degree of biodegradation of the crude oil, were proposed to strengthen oil/water interfacial film formation, as well as increasing oil and water interaction (Schramm, 1992). This would slow water content sedimentation (increasing the water retention) due to prevention, or retardation, of water and/or emulsion droplet growth (Aveyard et al., 1990; Cavello & Chang, 1990).

Since it has been reported that biodegradation increases the NSO content of crude oils, increased crude oil water retention ability may be attributed to this particular group (Connan, 1984).

Second, crude oil water retention ability may be due to alteration of the physicochemical properties of the crude oil, i.e., viscosity and density. Therefore, as biodegradation has been considered to increase viscosity and density of crude oils, it was suggested that physical changes resulting from biodegradation in the crude oil may also explain increased water retention (Tissot & Welte, 1984).

Initial observations identified that increased water retention was related to the API gravity of the crude oil. API gravities for both North Sea and Santa Maria Basin crude oils were observed to be inversely related to water retention values (Fig. 3.4.1). However, since many factors alter crude oil API gravity (*e.g.*, source rock type, maturation history, reservoir conditions and crude oil composition), it could not be reliably concluded whether the correlation was attributed to geochemical or physicochemical crude oil properties. Therefore, geochemical assessment of crude oil bulk chemistry was performed in order to identify any correlations between crude oil emulsifier content and water retention.

In contradiction to the initial possibly assessment of crude oil bulk chemistry found that the presence of both asphaltene and wax sols, in crude oil, reduced with increasing biodegradation. This was attributed to the actual degradation of the wax components and the increased solubility of asphaltenes in an increasingly more polar crude oil medium. In addition, no reliable relationship between NSO surfactants and water retention could be identified, with NSO bulk concentrations generally remaining unaltered.

Results from bulk geochemical analyses subsequently suggest that either (1) there was no relationship between the crude oil composition (asphaltenes, waxes and NSO components) and the reported water retention values, and that retention was predominantly governed by physicochemical properties; or (2) subtle alteration, not determined by bulk geochemical studies, had occurred to the NSO composition during biodegradation. However, a subsequent and more detailed organic geochemical analysis of an influential oil soluble surfactant group (the C_0-C_3 alkylphenols) was also unable to provide an explanation for the relationship between water retention and biodegradation. Consequently, it is suggested that the observed water retention values were more likely to be related to the physicochemical properties (viscosity, density etc.) of crude oils, which are related to the overall oil composition rather than specific compound classes in the oil.

7.1.2. Crude Oil Emulsion Formation/ Stabilisation Ability.

The majority of the crude oils analysed were found to possess similar emulsion formation/stabilisation ability. Most crude oils, except for the biodegraded North Sea crude oils (NS2 & NS3), formed stable, viscous, water-in-oil emulsions (emulsion type identified by Freeze-Fracture Replication).

The lack of emulsion formation/stabilisation for the biodegraded North Sea crude oils (NS2 & NS3), when blended with water, indicated that the stabilising influence of the emulsifiers had probably been affected by biodegradation. Compositional assessment of various crude oils (with differing degrees of biodegradation) and water-in-oil emulsions, resolved this phenomenon. Emulsifiers (asphaltene sols, wax sols and alkylphenols) were found to be preferentially enriched within water-in-oil emulsions while their presence in crude oils was considered to be strongly influenced by the effect of biodegradation.

7.1.3. Formation and Stabilisation of Emulsions.

It was shown that the organic matter in the crude oil/water interfacial film (bound oil fraction), was preferentially enriched with both asphaltene and wax groups, implying their involvement in the stabilisation of water-in-oil emulsions. The asphaltene content in the bound oil fractions varied from 45% to 80%, with the overall NSO content being approximately 80%. Analysis of the aliphatic hydrocarbon fraction, separated by TLC from the bound oil fractions, identified the enrichment of waxes from approximately *n*-C_{30} upwards when compared with the whole oil fractions.

Total C_0-C_3 alkylphenol concentrations at the crude oil/water interface were an order of magnitude greater than those in the whole oil alkylphenol extracts. Therefore, the involvement of the C_0-C_3 alkylphenols in the formation and stabilisation of water-in-oil emulsions, as with asphaltenes and waxes, was indicated. It was observed that C_0-C_3 alkylphenol enrichment in the emulsions was by the low molecular weight, non-hindered alkylphenols. Further work is necessary to identify the exact role of C_0-C_3 alkylphenols in emulsion stabilisation; however, the preferential enrichment of alkylphenols in the water-in-oil emulsion was possibly associated with the attraction of the alkylphenols to the highly polar organic matter content of the interface (frequently up to 80% asphaltenes).

Therefore, from the above it is suggested that asphaltenes, waxes and oil-soluble surfactants (such as C_0-C_3 alkylphenols) are associated with the formation of

stable water-in-oil emulsions. This association was examined in biodegraded North Sea crude oils with poor emulsion formation/stabilisation ability.

7.1.4. Effect of Biodegradation upon Crude Oil Emulsifiers.

Crude oil bulk chemistry indicated that in contrast to the North Sea non-biodegraded oils the biodegraded crude oils (NS2 & NS3) were unlikely to precipitate asphaltenes. This was attributed to the increase in asphaltene solubility in crude oil, due to the reduction of the apolar content (aliphatic hydrocarbons). Detailed high temperature gas chromatography (HTGC) of extracted wax fractions also indicated that the high molecular weight *n*-alkane distributions had been drastically reduced by biodegradation. This was best illustrated by examination of Santa Maria Basin crude oils which found that wax contents were reduced by an order of magnitude due to biodegradation.

No relationship between bulk NSO content and emulsification ability of North Sea crude oils could be established by bulk chemical assessment. However, analysis of the biodegraded NS2 and NS3 crude oils found that C_0-C_3 alkylphenol contents had been reduced by an order of magnitude, in comparison with non-degraded North Sea crude oils.

Examination of Santa Maria Basin crude oils found that the biodegraded crude oils were characterised by both reduced asphaltene precipitation potential (as were all Santa Maria Basin oils compared with non-degraded North Sea crude oils) as well as reduced wax content, yet still formed stable water-in-oil emulsions. Bulk chemical analyses also highlighted that the NSO concentrations were high for all oils (49% to 69%). Detailed analysis of the alkylphenols observed that the total alkylphenol concentrations, unlike those for the NS2 and NS3 crude oils, were not reduced by biodegradation. Therefore, the ability of biodegraded Santa Maria Basin crude oils to form stable, viscous water-in-oil emulsion, despite the probable reduced presence of precipitated asphaltene and wax sols, was attributed to surfactant activity (large surfactant concentration being suggested by the high NSO content of the crude oil)

7.1.5. Effect of Laboratory Biodegradation on Water Uptake.

In-laboratory crude oil biodegradation was performed in order to assess the variation of crude oil water uptake with increasing extent of biodegradation, under controlled conditions. Unfortunately, insufficient biodegraded crude oil was extracted from the biodegradation experiments and consequently water retention data, from COWUA, could not be attained. However, information was gained concerning the emulsion formation/stabilisation ability of crude oils, with inferences for crude oil spillage scenarios.

The formation of viscous water-in-oil emulsions after oil spill incidents, such as that involving the *Torrey Canyon*, are generally attributed to the precipitation of asphaltene sols (Bobra *et al.*, 1992). However, the laboratory biodegradation experiments in this work suggested an alternative mechanism. The laboratory degradation of a non-degraded North Sea crude oil, and the probable reduction of the stabilising potential of asphaltene and wax sols, did not deter the subsequent formation of stable water-in-oil emulsions. Consequently, emulsification ability was not attributed to the mechanical stabilisation effects of asphaltene and wax sols, but to the probable generation of surfactants, a mechanism previously suggested by Zajic *et al.* (1972 & 1974). The lack of emulsion formation during the laboratory degradation of a biodegraded North Sea crude oil (NS3), was suggested to be due to insufficient surfactant generation. Poor surfactant production was attributed to the absence of the majority of the easily biodegradable hydrocarbons (*i.e.*, low molecular weight alkanes), which were lost during earlier, in-reservoir biodegradation. Therefore, it was suggested that the spillage of previously biodegraded crude oils, as with the *Braer* tanker disaster, were probably less likely to form viscous water-in-oil emulsions (mousses). This was due to (1) the lack of emulsifying agents (*i.e.*, the biodegradation state of the crude oil indicating a reduced presence of asphaltene and wax sols, as well as oil-soluble surfactants), and (2) the lack of easily biodegradable hydrocarbons preventing significant surfactant generation.

7.2. Suggestions for Further Work.

From assessment of the results gained during this investigation a number of suggestions for further research may be offered.

1. Several physicochemical and geochemical analyses of the crude oils used in this study may help to resolve further the relationship between crude oil chemical composition and water uptake ability. Physicochemical analyses, primarily of crude oil viscosity and density, may illustrate the influence of these properties upon the water retentive ability of crude oils. This may potentially aid the precise identification of oils which physically retain high water quantities and therefore increase production and refinery costs in the petroleum industry.

Additional geochemical analyses may be performed to determine the total acid numbers (TAN) of the crude oils analysed. This may be achieved accurately and rapidly by the use of automated titration procedures which may be easily performed on the Metrohm 702SM Titrino. As acids represent influential emulsifier groups resolution of their relationship with crude oil water uptake ability may prove useful.

2. Assessment of the effect of biodegradation upon the C_0-C_3 alkylphenol content of crude oils illustrated two possibilities; first, the reduction of the C_0-C_3 alkylphenol distribution, as for biodegraded North Sea crude oil; second, the apparent enrichment of the C_3 hindered alkylphenols, as for the biodegraded Santa Maria Basin crude oil, H7. It is therefore suggested that analyses of both natural and laboratory degraded crude oils, using established methods may help to explain conflicting observations found in this and other studies.

3. The controlled biodegradation of a specific crude oil, followed by assessment of its water uptake ability at varying biodegradation states may help to add support to the results gained in this investigation. This was attempted in Chapter 6 of this thesis; however, emulsification subsequently reduced the usable sample size (*i.e.*, the amount of degraded crude oil which could be recovered and used in crude oil water uptake analysis). It is therefore suggested that this experiment should be repeated using larger crude oil sample sizes in order to be able to extract enough usable biodegraded sample (approximately 4 g).

REFERENCES

ACEVEDO, S., LAYRISSE, I., & RIVAS, H., 1984. Isolation and characterisation of natural surfactants present in extra heavy crude oils. *Journal of Dispresion Science and Technology*, **5**(1), 1-18.

ACEVEDO, S., MENDEZ, B., RAJAS, A., LAYRISSE, T., & RIVAS, H., 1985. Asphaltene and resins from the Orinoco Basin. *FUEL*, **64**, 1741-1747.

ACEVEDO, S., ESCOBAR, G., GUTIÉRREZ, L., & RIVAS, H., 1992. Isolation and characterisation of natural surfactants from extra heavy crude oils, asphaltenes and maltenes. Interpretation of their interfacial tension-pH behaviour in terms of ion pair formation. *FUEL*, **71**, 619-623.

ANDERSON, S.I. & BIRDI, K.S., 1991. Aggregation of asphaltenes as determined by calorimetry. *Journal of Colloid and Interface Science*, **142**(2), 497-502.

ARONSON, M.P. & PETKO, M.F., 1993. Highly concentrated water-in-oil emulsions. Influence of electrolyte on their properties and stability. *Journal of Colloidal and Interface Science*, **159**(1), 134-149.

ARONSTEIN, B.N., CALVILLO, Y.M. & ALEXANDER, M., 1991. Effects of surfactants at low concentrations on the desorption and biodegradation of sorbed aromatic compounds in soil. *Environmental Science & Technology*, **25**, 1728-1731.

ATLAS, R.M., BOEHM, P.D., & CALDER, J.A., 1981. Chemical and biological weathering of oil, from the Amoco Cadiz spillage, within the Littoral zone. *Estuarine, Coastal and Shelf Science*, **12**, 589-608.

AVEYARD, R., BINKS, B.P., FLETCHER, P.D.I., & LU, J.R., 1990. The resolution of water-in-crude oil emulsions by the addition of low molar mass demulsifiers. *Journal of Colloid and Interface Science*, **139**(1), 128-135.

BABU, D.R., HORNOF, V., & NEALE, G., 1984. Effects of temperature and time on interfacial tension behaviour between heavy oils and alkaline solutions. *The Canadian Journal of Chemical Engineering*, **62**, 156-159.

BAILEY, N.J.L., KROUSE, H.R., EVANS, C.R. & ROGERS, M.A., 1973a. Alteration of crude oil by waters and bacteria: Evidence from geochemical and isotope studies. *Bulletin of the American Association of Petroleum Geologist*, **57**, 1276-1290.

BAILEY, N.J.L., JOBSON, A.M. & ROGERS, M.A., 1973b. Bacterial degradation of crude oil: Comparison of field and experimental data. *Chemical Geology*, **11**, 203-221.

BECHER, P., 1966. *EMULSIONS: Theory and Practice*. (2nd Edition), Chapman & Hall Ltd., London, 440pp.

References.

BEHAR, F.H. & ALBRECHT, P., 1984. Correlations between carboxylic acids and hydrocarbons in several crude oils. Alteration by biodegradation. *Organic Geochemistry*, **6**, 597-604.

BERRIDGE, S.A., THEW, M.T., & LORISTON-CLARKE, A.G., 1968. The formation and stability of emulsions of water-in-crude oil petroleum and similar stocks. *Journal of the Institute of Petroleum*, **54**, 333-357.

BHARDWAJ, A. & HARTLAND, S., 1994. Dynamics of emulsification and demulsification of water-in-crude oil emulsions. *Journal of Industrial Engineering and Chemical Research*, **33**, 1271-1279.

BHATNAGAR, S.S., 1920. Studies in emulsions. Part I, A new method of determining the inversion of phases. *Journal of the Chemical Society, Transactions*, **67**, 542-549.

BISHOP, A.N., PHILP, R.P. & ALLEN, J., 1994. Prediction of wax deposition via early recognition of high molecular weight hydrocarbons (>C_{40}) concentrations. *Society of Petroleum Engineers*, SPE **30077**, 15pp.

BÍZEK, V., HORÁCEK, J. & PROCHÁZKA, J., 1992. Extraction of Phenols: I. Distribution of Individual Phenols Between Organic Solvents and Water or Aqueous Solvents. *The Canadian Journal of Chemical Engineering*, **70**, 341-349.

BOBRA, M.A., 1989. A Catalogue of Crude Oil and Oil Product Properties. *Environment Canada Report EE-114*, 195pp.

BOBRA, M.A., 1990. A study of the formation of water-in-oil emulsions. *Proceedings of 1990 Artic and Marine Oilspill Program Technical Seminar*, Edmonton, Alberta, Ministry of Supply and Services Canada, Cat. No. EN 40-11/5-1990, 87-117.

BOBRA, M.A., FINGAS, M., & TENNYSON, E., 1992. When oil spills emulsify. *CHEMTECH*, April, 236-241.

BOUSSIGNAULT, M., 1837. Mémoire sur la composition du bitume. *Ann. Chim. Phys.* **II**, 64-141.

BRAGG, J.R., PRINCE, R.C., WILKINSON, J.B. & ATLAS, R.M., 1992. Bioremediation: for shoreline cleanup following the 1989 Alaskan oil spill. *Exxon Company, U.S.A., Houston, Texas, 94pp.*

BRAGG, J.R., PRINCE, R.C., HARNER, E.J., & ATLAS, R.M., 1994. Effectiveness of bioremediation for the Exxon Valdez oil spill. NATURE, 368, 413-418.

References.

BRAUER, P.R. & WASAN, D.T., 1982. The role of emulsification phenomena in alkaline waterflooding of heavy crude oils. *American Chemical Society*, 215-226.

BRIDIÉ, A.L., WANDERS, TH.H., ZEGVELD, W., & VAN DER HEIJDE, H.B., 1980. Formation, prevention and breaking of seawater-in-crude oil emulsions "Chocolate Mousses". *Marine Pollution Bulletin*, **11**, 343-348.

BROWN, S., 1990. Jurassic. *In:* GLENNIE, K.W. (ed) *Introduction to the petroleum geology of the North Sea (3rd Edition), Blackwell Scientific Publications, London*, 219-254.

BUMPUS, J.A., TIEN, M., WRIGHT, D. & AUST, S.D., 1985. Oxidation of persistent environmemtal pollutants by a White Rot fungus. *Science*, **228**, 1434-1436.

CAVELLO, J.L. & CHANG, D.L., 1990. Emulsion preparation and stability. *Chemical Engineering Progress*, 54-59.

CERNIGLIA, C.E., 1992. Biodegradation of polycyclic aromatic hydrocarbons. *Biodegradation*, 3, 351-368.

CHAN, M. & YEN, T.F., 1982. A chemical equilibrium model for interfacial activity of crude oil in aqueous alkaline solution: The effects of pH, alkali and salt. *The Canadian Journal of Chemical Engineering*, **60**, 305-308.

CHIOU, C.T. & SCHMEDDING, D.V., 1982. Partitioning of Organic Compounds in Octanol-Water Systems. *Environ. Sci. Technol.*, **16** (1), 4-10.

CHIOU, C.T., FREED, V.H., SCHMEDDING, D.W. & KOHNERT, R.L., 1977. *Environ. Sci. Technol.*, **11**, 475-487.

CHOSSON, P., CONNAN, J., DESSORT, D. & LANAU, C., 1992. In *vitro* biodegradation of steranes and terpanes: A clue to understanding geological situations. *In:* MOLDOWAN, ALBRECHT & PHILPS (eds) *Biological Markers in Sediments and Petroleum*. Prentice Hall, Englewood Cliffs, New Jersey, 320-349.

CONNAN, J., 1984. Biodegradation of crude oils in reservoirs. *In* BROOKS, J. & WELTE, D.H. (eds) *Advances in Petroleum Geochemistry, Volume 1, Academic Press, London*, 299-335.

CONNAN, J., DESSORT, D. & MAGOT, M., 1993. Advances in our knowledge of alteration of hydrocarbons in reservoirs. *Presentation to the 16th international meeting of The European Association of Organic Geochemists, 20-24th September 1993, Stavanger, Norway.*

CORNFORD, C., 1990. Source rocks and hydrocarbons of the North Sea. *In:* GLENNIE, K.W. (ed) *Introduction to the petroleum geology of the North Sea (3rd Edition), Blackwell Scientific Publications, London*, 294-361.

References.

DE BOER, R.B., LEERLOOYER, K., EIGNER, M.R.P. & VAN BERGEN, A.R.D., 1995. Screening of crude oils for asphalt precipitation: Theory, practice, and the selection of inhibitors. *SPE Production & Facilities*, **10**(1), 55-61.

DEL RIO, J.C. & PHILP, R.P., 1992. Oligomerization of fatty acids as a possible source for high molecular weight hydrocarbons and sulphur-containing compounds in sediments. *Organic Geochemistry*, **18**(6), 869-880.

DEL RIO, J.C., PHILP, R.P. & ALLEN, J., 1992. Nature and geochemistry of high molecular weight hydrocarbons (above C40) in oils and solid bitumens. *Organic Geochemistry*, **18**(4), 541-553.

DIDYK, B.M., SIMONEIT, B.R.T., BRASSELL, S.C. & EGLINTON, G., 1978. Organic geochemical indicators of palaeoenvironmental conditions of sedimentation. *Nature*, **272**, 216-222.

EGANHOUSE, R.P. & CALDER, J.A., 1976. The solubility of medium molecular weight aromatic hydrocarbons and the effects of hydrocarbon co-solutes and salinity. *Geochemica et Cosmochemica Acta*, **40**, 555-561.

ELEY, D.D. HEY, M.J., LEE, M.A., 1987. Rheological studies of asphaltene films adsorbed at the oil/water interface. *Colloids and Surfaces*, **24**, 173-182.

ELEY, D.D., HEY, M.J., & SYMONDS, J.D., 1988. Emulsions of water-in-asphatene-containing oils. 1. Droplet size distribution and emulsified rates. *Colloids and Surfaces*, **32**, 87-101.

ELEY, D.D., HEY, M.J., SYMONDS, J.D., & WILLISON, J.H.M., 1976. Electron micrography of emulsions of water-in-crude oil petroleum. *Journal of Colloid and Interface Sciences*, **54**(3), 462-466.

FARMER, D. & LI, M., 1994. Oil dispersion by turbulence and coherent circulations. *Ocean Engineering*, **21**(6), 575-586.

FARRIMOND & TELNÆS **unpublished**

FINE, L.W. & BEALL, H., 1990. *Chemistry for Engineers and Scientists*. Saunders College Publishing, London, 1006pp.

FISCHER, K., 1935. New Method for the Volumetric Determination of Water Content in Liquids and Solids. (In German). *Agnew. Chem.*, **48**, 394-408.

FOLEY, J.P., 1988. Separation of *m* and *p* cresol and other methylated phenols in shale oil by reversed phase liquid chromatography with electrochemical detection. *Journal of Chromatography*, **441**, 347-354.

GIBSON, D.T., 1991. The role of oxygenases in the microbial oxidation of aromatic compounds. *ACS Abstracts*, 201, AGFD46.

References.

GIBSON, D.T. & SUBRAMANIAN, V., 1984. Microbial degradation of aromatic hydrocarbons. *In:* GIBSON, D.T. (ed) *Microbial Degradation of Organic Compounds, Marcel Dekker, New York,* 181-252.

GIULIANO, F.A (ed), 1981. *Introduction to Oil and Gas Technology* (2nd edition). Intercomp Resource Development Inc., Houston, Texas, 547pp.

GOLUMBIC, C., ORCHIN, M., & WELLER, S., 1949. Partition studies on phenols. I. Relation between partition coefficient and ionization constant. *Journal of the American Chemical Society*, **71**, 2624-2627.

GONZÁLEZ, G. & LOUVISSE, A.M.T., 1991. The adsorption of asphaltenes and it's effect on oil production. *SPE 21039.*

GOODWIN, N.S., PARK, P.J.D. & RAWLINSON, A.P., 1983. Crude oil biodegradation under simulated and natural conditions. *In:* BJORØY, M. *et al.* (eds), *Advances in Organic Geochemistry, 1981, John Wiley, Chichester*, 650-658.

GRAHAM, D.E., STOCKWELL, A., & THOMPSON, D.G., 1983. Chemical demulsification of produced crude oil emulsions. *In:*OGDEN, P.H. (ed) *Chemicals in the Oil Industry. The Royal Society of Chemistry, London*, 73-91.

GUNDLACH, E.R., BOEHM, P.D., MARCHAND, M., ATLAS, R.M., WARD, D.M., & WOLFE, D.A., 1983. The fate of Amoco Cadiz oil. *Science*, **221**, 122-129.

HALLAM, A., 1987. Mesozoic marine organic-rich shales. *In:* BROOKS, J. & FLEET, A.J. (eds) *Marine petroleum source rocks, The Geological Society, Blackwell Scientific, London*, 251-262.

HANCOCK, J.M., 1990. Cretaceous. *In:* GLENNIE, K.W. (ed) *Introduction to the petroleum geology of the North Sea (3rd Edition), Blackwell Scientific Publications, London*, 255-272.

HANSTVEIT, A.O., 1992. Biodegradability of petroleum waxes and beeswax in an adapted CO_2 evolution test. *Chemosphere*, **25**(4), 605-620.

HARRISON, W., WINNIK, M.A., KWONG, P.T.Y., & MACKAY, D., 1975. Disappearance of aromatic and aliphatic components from small sea-surface slicks. *Environmental Science & Technology*, **9**(3), 231-234.

HORSTAD, I., LARTER, S.R. & MILLS, N., 1995. Migration of hydrocarbons in the Tampen Spur area, Norwegian North Sea: a reservoir geochemical evaluation. *In:* CUBITT, J.M. & ENGLAND, W.A. (eds) *The Geochemistry of Reservoirs, Geological Society Special Publication*, **86**, 159-183.

HOSTETTLER, F.D. & KVENVOLDEN, K.A., 1994. Geochemical changes in crude oil spilled from the Exxon Valdez supertanker into Prince William Sound, Alaska. *Organic Geochemistry*, **21**(8/9), 927-936.

References.

HUANG, W.Y. & MEINSCHEIN, W.G., 1979. Sterols as ecological indicators. *Geochimica et Cosmochimica Acta.*, **43**, 739-745.

HUNTER, R.J. & WHITE, L.R., 1992. *Foundations of colloid science.* Clarendon Press, New York. 2 vols., 1120pp.

IOPPOLO, M., ALEXANDER, R. & KAGI, R.I., 1992. Identification and analysis of C_0-C_3 phenols in some Australian crude oils. *Organic Geochemistry*, **18**(5), 603-609.

ISAACS, E.E. & CHOW, R.S., 1992. Practical aspects of emulsion stability. *In: Emulsion in the Petroleum Industry, American Chemical Society*, chapter 2, 51-77.

ISRAELACHVILI, J.N., 1991. *Intermolecular and surface forces.* Academic Press, London, 450pp.

JAMALUDDIN, A.K.M., NAZARKO, T.W., SILLS, S. & FUHR, B.J., 1995. Deasphalted oil - A natural solvent. *Paper SPE 28994 presented at the 1995 International Symposium on Oilfield Chemistry, San Antonio, Texas, February 14 - 17.*

JENNINGS, H.R., 1975. A study of caustic solution-crude oil interfacial tensions. *Society of Petroleum Engineers Journal*, **15**, 197-202.

JOBSON, A., COOK, F.D. & WESTLAKE, D.W.S., 1972. Microbial utilisation of crude oil. *Applied Microbiology*, **23**(6), 1082-1089.

JOHANSEN, E.J., SKJÄRVÖ, M., LUND, T., SJÖBLOM, J., SÖDERLUND, H., & BOSTRÖM, G., 1989. Water-in-crude oil emulsions from tthe Norwegian Continental Shelf. Part 1, Formation, characterisation and stability correlation. *Colloids and Surfaces*, **34**, 353-370.

JONES, D.M., 1986. Biodegradation of Geochemical Markers in Pollution Studies. *Unpublished PhD Thesis, University of Newcastle upon Tyne.*

JONES, D.M., DOUGLAS, A.G., PARKES, R.J., TAYLOR, J., GIGER, W. & SCHAFFNER, C., 1983. The recognition of biodegraded petroleum-derived aromatic hydrocarbons in recent marine sediments. *Marine Pollution Bulletin*, **14**(3), 103-108.

JONES, J.G., 1979. A guide to methods for estimating microbial numbers and biomass in fresh water. *Freshwater Biological Association, Scientific Publication* **39**. 112pp.

JONES, T.J., NEUSTADLER, E.L., & WHITTINGHAM, K.P., 1978. Water-in-crude oil emulsion stability and emulsion destabilisation by chemical demulsifiers. *The Journal of Canadian Petroleum Technology*, **April-June**, 100-108.

References.

JORDAN, R.E. & PAYNE, J.R., 1980. *Fate and Weathering of Petroleum Spills in the Marine Envronment.* Ann Arbor Science, Ann Arbor, Michigan, 174pp.

KAWANAKA, S., LEONTARITIS, K.J., PARK, S.J., & MANSOORI, G.A., 1989. Thermodynamic and colloidal models of asphaltene flocculation. *American Chemical Society in Oil Field Chemistry*, **24**, 443-458.

KIZLING, J. & KRONBERG, B., 1990. On the formation and stability of concentrated water-in-oil emulsions, Aphrons. *Colloids and Surfaces*, **50**, 131-140.

KRAWCZYK, M.A., WASAN, D.T., & SHETTY, C.S., 1991. Chemical demulsification of petroleum emulsions using oil-soluble demulsifiers. *Industrial and Engineering Chemistry Research*, **30**, 367-375.

KVALHEIM, O.M., CHRISTY, A.A., TELNÆS, N. & BJØRSETH, A., 1987. Maturity determination of organic matter in coals using the methylphenanthrene distribution. *Geochimica et Cosmochimica Acta*, **51**, 1883-1888.

LAFARGUE, E. & BARKER, C., 1988. Effect of water washing on crude oil compositions. *Bulletin of the American Association of Petroleum Geologists*, **72**(3), 263-276.

LARTER, S.R. & APLIN, A.C., 1995. Reservoir geochemistry: methods, applications and oppprtunities. *In:* CUBITT & ENGLAND (eds) *The Geochemistry of Reservoirs, Geological Society Special Publication*, **86**, 5-32.

LARTER, S.R. & MILLS, N., 1992. Phase controlled molecular fractionations in migrating petroleum charge. *In:* ENGLAND, W.A. & FLEET, A.J., (eds) *Petroleum Migration. Geological Society, London, Special Publication*, **59**, 137-147.

LAWRENCE, A.S.C. & KILLNER, W., 1948. Emulsions of seawater in admiralty fuel oil with special reference to their demulsification. *Journal of the Institute of Petroleum*, **34**, 821-856.

LEO, A., HANSCH, C. & ELKINS, D., 1972. Partition coefficients and their uses. *Chemical Reviews*, **71**(6), 525-557.

LEONTARITIS, K.J., 1988. Asphaltene deposition: A thermodynamic-colloidal model. *PhD Thesis, University of Illinois.*

LEONTARITIS, K.J., 1989. Asphaltene deposition: A comprehensive description of problem manifestations and modelling approaches. *Society of Petroleum Engineers*, **SPE 18892**, 599-613.

References.

LI, M. & LARTER, S.R., 1993. Interactions of organic nitrogen species with mineral/water and organic networks: Implications to petroleum geochemistry. *205th American Chemical Society Meetin Abstracts*, American Chemical Society.

LHIOREAU, C., BRIANT, J. & TINDY, R., 1967. Influence de la pression sur la flocculation des asphaltènes. *Rev. Inst. Fr. Pétrol.*, **22**, 797-806.

LYMAN, W.J., REEHL, W.F. & ROSENBLATT, D.H., (eds) 1982. Handbook of chemical property estimation methods. Environmental behaviour of organic compounds. McGraw-Hill, New York.

MACKAY, G.D.M., MCLEAN, A.Y., BETANCOURT, J., & JOHNSON, B.D., 1973. The formation of water-in-oil emulsions subsequent to an oil spill. *Journal of the Institute of Petroleum*, **59**, 164-172

MACKENZIE, A.S., 1984. Applications of biological markers in petroleum geochemistry. *In:* BROOKS, J. & WELTE, D. (eds) *Advances in Petroleum Geochemistry, Academic Press, London*, **1**, 115-214.

MACKENZIE,A.S., LAMB, C.A. & MAXWELL, J.R., 1982. Chemical fossils: The gological fate of steroids. *Science*, **217**, 491-504.

MACLEOD, G., TAYLOR, P.N., LARTER, S.R. & APLIN, A.C., 1993. Dissolved organics in formation waters: Insights into water-oil-rock ratios in petroleum systems. *In:* PARNELL, J., RUFFELL, A. & MOLES N., (eds), *Geofluids 93: International conference on fluid evolution, migration and interaction in rocks. Geological Society, London*, 18-20.

MACLEOD, S.K., 1991. Moisture determination using Karl Fischer titrations. *Analytical Chemistry*, **63**(10), 557-565.

MADIAN, E.S., MOELYODIHARDJO, T., SNAVELY, E.S. & JAN, R.J., 1995. Treating of produced water for surface discharge at the Arun gas condensation field. *Paper SPE 28946 presented at the 1995 SPE International Symposium on Oilfield Chemistry, San Antonio, Texas, February 14-17.*

MASON, P.C., BURWOOD, R. & MYCKE, B., 1995. The reservoir geochemistry and petroleum charging histories of Palaeogene-reservoired fields in the Outer Witch Ground Garben. *In:* CUBITT & ENGLAND (eds) *The Geochemistry of Reservoirs, Geological Society Special Publication*, **86**, 281-301.

MCAULIFFE, C.D., 1977a. Dispersal and alteration of oil discharged on a water surface. *In:* WOLFE, D.A. (ed) *Fate and effects of petroleum hydrocarbons in marine ecosystems and organisms, Pergamen Press, Oxford*, 19-35.

References.

MCAULIFFE, C.D., 1977b. Evaporation and solution of C_2 to C_{10} hydrocarbons from crude oils on the sea surface. *In:* WOLFE, D.A. (ed) *Fate and effects of petroleum hydrocarbons in marine ecosystems and organisms, Pergamen Press, Oxford*, 363-372.

MCAULIFFE, C.D., 1979. Chemical and physical constraints on petroleum migration with emphasis on hydrocarbon solubilites in water. *In:* ROBERTS (III), W.H. & CORDELL, R.J. (eds) *Physical and chemical constraints upon petroleum migration. AAPG, continuing education source notes series 8, C-1 to C-39.*

MCKIRDY, D.M., ALDERIDGE, A.K. & YPMA, P.J.M., 1983. A geochemical comparison of some crude oils from Pre-Ordovician carbonate rocks. *In:* BJORØY, M. *et al.* (eds), *Advances in Organic Geochemistry, 1981, John Wiley, Chichester*, 99-107.

MIKULA, R.J., 1992. Emulsion characterisation. *In: Emulsions in the Petroleum Industry, American Chemical Society*, 78-129 .

MISRA, S., BARUAH,S. & SINGH,K., 1995. Paraffin problems in crude oil production and transportation: A review. *SPE Production & Facilities*, **10**(1), 50-54.

MOLDOWAN, J.M. & MCCAFFREY, M.A., 1995. A novel microbial hydrocarbon degradation pathway revealed by hopane demethylation in a petroleum reservoir. *Geochimica et Cosmochimica Acta.* **59**(9), 1891-1894.

MYERS, D., 1991. *Surfaces, interfaces and colloids: principles and applications.* VCH Publishers, New York, 433pp.

NG, F.T.T. & TSAKIRI, S.K., 1992. Activation of water in emulsion for catalytic desulphurisation of benzothiophene. *FUEL*, **71**, 1309-1317.

OREN, J.J. & MACKAY, G.D.M., 1977. Electrolyte and pH effect on emulsion stability of water-in-petroleum oils. *FUEL*, **56**, 382-384.

ORR, W.L., 1986. Kerogen/ asphaltene/ sulphur relationships in sulphur-rich Monterey oils. *Organic Geochemistry*, **10**, 499-516.

PALMER, S.E., 1984. Effect of water washing on C_{15+} hydrocarbon fraction of crude oils from Northwestern Palawan, Philippines. *Bulletin of the American Association of Petroleum Geologists*, **68**, 137-149.

PALMER, S.E., 1993. Effect of biodegradation and water washing on crude oil composition. *In:* ENGEL, M.H. & MACKO, S.A. (eds) *Organic Geochemistry*, Plenum Press, New York, 511-533.

PAPIRER, E., BOURGEOIS, C., SIFFERT, B., & BALARD, H., 1982. Chemical nature and water/oil emulsifying properties of asphaltenes. *FUEL*, **61**, 732-734.

References.

PATIENCE, R.L. & CLAXTON, M.J., 1993. Bond energies in alkyl-substituted organic sulphur compounds. *In:* Øygard (ed) *Organic Geochemistry: Poster sessions from the 16th International Meeting on Organic Geochemisty*, EAOG, Stavanger, 217-219.

PAULS, R.E., BAMBACHT, M.E., CHERLYNLAVAUGHN, B., SCHEPPELE, S.E. & CRONAUER, D.C., 1990. Distribution and Characterisation of Phenolics in Distillates Derived from Two-Stage Coal Liquefacton. *Energy & Fuels*, **4**, 236-242.

PAYNE, J.R. & PHILLIPS, C.R., 1985a. *Petroleum Spills in the Marine Environment. The Chemistry and Formation of Water-in-Oil Emulsions and Tar Balls*. Lewis Publishers Inc., Chelsea, Michigan, 148pp.

PAYNE, J.R. & PHILLIPS, C.R., 1985b. Photochemistry of petroleum in water. *Environmental Science & Technology*, **19**(7), 569-579.

PETERS, K.E. & MOLDOWAN, J.M., 1991. Effects of source, thermal maturity, and biodegradation on the distribution and isomerisation of homohopanes in petroleum. *Organic Geochemistry*, **17**(1), 47-61.

PETERS, K.E. & MOLDOWAN, J.M., 1993. *The biomarker guide*. Prentice Hall, New Jersey, 363pp.

PHILP, R.P. & BISHOP, A.N., 1995. Exploration and Reservoir Geochemistry: Concepts, applications and results. *Proceedings of PETROTECH-95, New Delhi Technology Trends in Petroleum Industry*, 57-79.

POYNTER, W.G. & BARRIOS, R.J., 1994. Coulometric Karl Fischer titration simplifies water content testing. *Oil & Gas Journal*, Apr 11, 53-55.

PRICE, L.C., 1976. Aqueous Solubility of Petroleum as Applied to its Origin and Primary Migrtion. *Bulletin of the American Association of Petroleum Geologists*, **60**(2), 213-244.

PRITCHARD, P.H., MUELLER, J.G., ROGERS, J.C., KREMER, F.V., & GLASER, J.A., 1992. Oil spill bioremediation: experiences, lessons and results from the Exxon Valdez oil spill in Alaska. *Biodegradation*, **3**, 315-335.

RADKE, M., WELTE, D.H., & WILLSCH, H., 1982. Geochemical study on a well in the Western Canadian Basin: Relation of the aromatic distribution pattern to maturity of organic matter. *Geochimica et Cosmochimica Acta*, **46**, 1-10.

REISFELD, A., ROSENBERG, E. & GUTNICK, D., 1972. Microbial Degradation of crude oil: Factors affecting the dispersion in sea water by mixed and pure cultures. *Applied Microbiology*, **24**(3), 363-368.

References.

ROBARDS, A.W. & SLEYTR, U.B., 1985. Low temperature methods in biological electron microscopy. *In:* GLAUERT, A.M., (ed) *Practical Methods in Electron Microscopy, Elsevier, Oxford*, **10**,

RØNNINGSEN, H.P., 1995. Correlations for predicting viscosity of W/O-emulsions based on North Sea crude oils. *Paper SPE 28968 presented the 1995 SPE International Symposium on Oilfield Chemistry, San Antonio, Texas, February 14-17.*

ROWLAND, S.J., ALEXANDER, R., KAGI, R.I., JONES, D.M. & DOUGLAS, A.G., 1986. Microbial degradation of aromatic components of crude oils: A comparison of laboratory and field observations. *Organic Geochemistry*, **9**(4), 153-161.

ROSENBERG, E., LEGMANN, R., KUSHMARO, A., TAUBE, R., ADLER, E., & RON, E.Z., 1992. Petroleum bioremediation - a multiphase problem. *Biodegradation*, **3**, 337-350.

RUDIN, J., BERNARD, C. WASAN, D.T., 1994. Effect of Added Surfactant on Interfacial Tension and Spontaneous Emulsification in Alkali/Acidic Systems. *Ind. Eng. Chem. Res.*, **33**, 1150-1158.

RULLKÖTTER, J. & WENDISCH, D., 1982. Microbial alteration of 17α(H)-hopane in Madagascar asphalts: Removal of C-10 methyl group and ring opening. *Geochimica et Cosmochimica Acta*, **46**, 1543-1553.

SANDVIK, E.I., YOUNG, W.A. & CURRY, D.J., 1991. Expulsion from hydrocarbon sources: the role of organic absorption. *Org, Geochem.*, **19**(1-3), 77-87.

SCHOLZ, E., 1984. *Karl Fischer Titration determination of water. Chemical laboratory practice*. Springer-Verlag, Berlin, 138pp.

SCHOLZ, E., 1985. Karl Fischer titrations of aldehydes and ketones. *American Chemical Society*, **57**, 2965-2971.

SCHRAMM, L.L., 1992. Petroleum emulsions, basic principles. *In: Emulsions in the Petroleum Industry, American Chemical Society*, 1-49.

SEIFERT, W.K. & MOLDOWAN, J.M., 1979. The effect of biodegradation on steranes and terpanes in crude oils. *Geochimica et Cosmochimica Acta*, **43**, 111-126.

SEIFERT, W.K., MOLDOWAN, J.M. & DEMAISON, G.J., 1984. Source correlation of biodegraded oils. *Organic Geochemistry*, **6**, 633-643.

SHAW, D.J., 1980. *Introduction to colloid and surface chemistry*. (2nd Edition), Butterworth, London, 272pp

SHEU, E.Y. & SHIELDS M.B., 1995. Asphaltene surface activity at oil/water interfaces. *Paper SPE 28995 presented at the International Symposium on Oilfield Chemistry, San Antonio, Texas, February 14-17.*

SHEU, E.Y., DE TAR, M.M. & STORM, D.A., 1992b. Interfacial properties of asphaltenes. *FUEL*, **71**, 1277-1281.

SHEU, E.Y., DE TAR, M.M., STORM, D.A., & DECANIO, S.J., 1992a. Aggregation and kinetics of asphaltenes in organic solvents. *FUEL*, **71**, 299-302.

SHIU, W.Y., BOBRA, M., BOBRA, A.M., MAIJANEN, A., SUNTIO, L. & MACKAY, D., 1990. The Water Solubility of Crude Oils and Petroleum Products. *Oil & Chemical Pollution*, **7**, 57-84.

SIFFERT, B., BOURGEOIS, C., & PAPIRER, E., 1984, Structure and water-oil emulsifying properties of asphaltenes. *FUEL*, **63**, 834-837.

SJÖBLOM, J., SÖDERLUND, H., LINDBLAD, S., JOHANSEN, E.J., & SKJÄRVÖ, I.M., 1990. Water-in-crude oil emulsions from the Norwegian continental shelf. Part II. Chemical destabilisation and interfacial tensions. *Colloid & Polymer Science*, **268**, 389-398.

SJÖBLOM, J., NINGYUAN, L.M., HÖILAND, H., & JOHANSEN, E.J., 1990. Water-in-crude oil emulsions from the Norwegian continental shelf. Part III. A comparative destabilisation of model systems. *Colloids and Surfaces*, **46**, 127-139.

SOUTHWORTH, G.R., HERBES, S.E. & ALLEN, C.P., 1983. Evaluating a mass transfer model for the dissolution of organics from oil films into water. *Water Research*, **17**(11), 1647-1651.

SPEIGHT, J.G., 1980. The Chemistry and Technology of Petroleum. *In:* HEINEMANN, H. (ed) *Chemical Industries, Marcel Dekker, Inc., New York*, **3**, 498pp.

SPEIGHT, J.G. & MOSCHOPEDIS, S.E., 1979. On the molecular nature of petroleum asphaltenes. *In:* BUNGER & LI (eds) *Chemistry of Asphaltenes.* Advances in Chemistry Series 195: American Chemical Society, Washington D.C., 1-15.

SPEIGHT, J.G., LONG, R.B., & TROWBRIDGE, T.D., 1984. Factors influencing the separation of asphaltenes from heavy petroleum feedstocks. *FUEL*, **63**, 616-620.

STAISS, F., BÖHM, R. & RAINER, K., 1991. Improved demulsifier chemistry: A novel approach in the dehydration of crude oil. *SPE Production Engineering*, **8**, 334-338.

STODDART, D.P., 1993. Petroleum and nitrogen compound reservoir geochemistry of the Eldfisk chalk reservoir. *Unpublished PhD Thesis, University of Newcastle upon Tyne.*

References.

STOSUR, G.J., SINGER, M.I., LUHNING, R.W., & YURKO, W.J., 1990. Enhanced oil recovery in North America: Status and prospects. *Energy Sources*, **12**, 429-437.

SURKALO, H., 1990. Enhanced Alkaline Flooding. *JPT*, Jan, 6-7.

TAYLOR, K.C, & SCHRAMM, L.L., 1990. Measurement of short-term low dynamic interfacial tensions: Applications to surfactant enhanced alkaline flooding in enhanced oil recovery. *Colloids and Surfaces*, **47**, 245-253.

TAYLOR, P.N., 1994. Controls on the occurrence of phenols in petroleums and waters. *Unpublished PhD Thesis, University of Newcastle upon Tyne.*

TAYLOR, S.E., 1992a. Use of surface tension measurements to evaluate aggregation of asphaltenes in organic solvents. *FUEL*, **71**(2), 1338-1339.

TAYLOR, S.E., 1992b. Resolving crude oil emulsions. *Chemistry and Industry*, **20**, 770-773.

THOMPSON, D.G., TAYLOR, A.S., & GRAHAM, D.E., 1985. Emulsification and demulsification related to crude oil production. *Colloids and Surfaces*, **15**, 175-189.

TISSOT, B.P. & WELTE, D.H., 1984. *Petroleum Formation and Occurrence.* (2nd Edition), Springer-Verlag, Berlin, 699pp.

TISSOT, B.P., DEROO, G. & HOOD, A., 1978. Geochemical study of the Uinta Basin: Formation of petroleum from the Green River formation. *Geochimica et Cosmochimica Acta*, **42**, 1469-1485.

TISSOT, B.P., PELET, R. & UNGERER, PH., 1987. Thermal History of Sedimentary Basins, Maturation Indices, and Kinetics of Oil and Gas Generation. *Bulletin of the American Association of Petroleum Geologists*, **71**(12), 1445-1466.

TISSOT, B., DURAND, B., ESPITALIÉ, J. & COMBAZ, A., 1974. Influence of Nature and Diagenesis of Organic Matter in Formation of Petroleum. *Bulletin of the American Association of Petroleum Geologists*, **58**(3), 499-506.

TYSON, R.V., 1995. *Sedimentary organic matter.* Chapman & Hall, London, 615pp

VAN DER WAARDEN, M., 1957. Stability of emulsions of water in mineral oils containing asphaltenes. *Kolloid-Zeitschrift*, **156**, 116-122.

VARHANÍCKOVÁ, D., SHIU, W-Y. & MACKAY, D., 1995. Aqueous solubilities of alkylphenols and methoxyphenols at 25°C. *Journal of Chemical Engineering Data*, **40**, 448-451.

VOLKMAN, J.K., 1986, A review of sterol markers for marine and terrigenous organic matter. *Organic Geochemistry*, **9**(2), 83-99.

References.

VOLKMAN, J.K., ALEXANDER, R., KAGI, R.I., ROWLAND, S.J. & SHEPPARD, P.N., 1984. Biodegradation of aromatic hydrocarbons in crude oils from the Barrow Sub-basin of Western Australia. *Organic Geochemistry*, **6**, 619-632.

WALKER, J.D., PETRAKIS, L., & COLWELL, R.R., 1976. Comparison of the biodegradability of crude and fuel oils. *Canadian Journal Microbiology*, **22**, 598-602.

WANG, X., YU, X. & BARTHA, R., 1990. Effect of bioremediation on polycyclic aromatic hydrocarbon residues in soil. *Environmental Science & Technology*, **24**(7), 1086-1089.

WEERS, J.G. & ARLAUSKAS, R.A., 1995. Sedimentation field-flow fractionation studies of Oswald ripening in fluorocarbon emulsions containing two disperse phase components. *Langmuir*, **11**, 474-477.

WESTLAKE *ET AL.*, 1978. *Can. J. Microbiol.* **24**, 254-260.

WILD, S.R., BERROW, M.L. & JONES, K.C., 1991. The persistence of polynuclear aromatic hydrocarbons (PAHs) in sewage sludge amended agricultural soils. *Environmental Pollution*, **72**, 141-157.

WILHELMS, A. & LARTER, S.R., 1994a. Origin of tar mats in petroleum reservoirs. Part I: introduction and case studies. *Marine Petroleum Geology*, **11**(4), 418-441.

WILHELMS, A. & LARTER, S.R., 1994b. Origin of tar mats in petroleum reservoirs. Part II: formation mechanisms for tar mats. *Marine Petroleum Geology*, **11**(4), 442-456.

WILSON A.J., 1989. *Foams: Physics, Chemistry and Structure*, Springer-Verlag, Berlin, 345pp.

WOLFF, G.A., PRESTON, M.R., HARRIMAN, G. & ROWLAND, S.J., 1993. Some preliminary observations after the wreck of the oil tanker Braer in Shetland. *Marine Pollution Bulletin*, **26**(10), 567-571.

YAWS, C.L., YANG, H-C., HOPPER, J.R. & HANSEN, K.C., 1990. 232 hydrocarbons: water solubility data. *Chemical Engineering*, **April**, 177-182.

ZAJIC, J.E. & SUPPLISSON, B., 1972. Emulsification and degradation of "Bunker C" fuel oil by microorganisms. *Biotechnology and Bioengineering*, **14**, 331-343.

ZAJIC, J.E., SUPPLISSON, B. & VOLESKY, B., 1974. Bacterial degradation and emulsification of No. 6 fuel oil. *Environmental Science & Technology*, **6**(7), 664-668.

APPENDIX 1

APPENDIX 1.

KARL FISCHER ANALYSIS - OPERATIONAL GUIDE

A1.1. Inroduction.

This guide is to be used in conjunction with the Metrohm 702SM Titrino and Ultra-Turrax (T25) manuals. Both pieces of equipment are expensive and easily damaged and therefore the guide and manuals should be read fully before operation. For explanation of the selection of both the equipment and method, please refer to the Chapter 2.

The procedure established in this guide is for the Karl Fischer Water Determination Technique. Assessesment is made of the water content of crude oil/water blends and results are plotted against time from blending of the water and oil phases.

A1.2. Hazards.

There are four hazardous materials used in this procedure. The reagent; the reaction medium, containing Solvent Solution and Xylene, and the crude oil. The reagent, Karl Fischer Titrant U (BDH# 19280, Pyridine Free), is HARMFUL and flammable; contact to the skin and eyes, inhalation and swallowing should all be avoided. The Solvent Solution (Karl Fischer Solvent Solution, BDH# 19266, Pyridine Free) of the reaction medium is TOXIC and highly flammable; inhalation, swallowing, contact with skin and eyes should be avoided. Xylene is HARMFUL and flammable; contact with the skin and eyes, inhalation and swallowing should be avoided. Crude oil is TOXIC and HARMFUL; contact with skin and eyes, inhalation and swallowing should be avoided. In the event of contact with the skin the effected area should be washed with copious amounts of soap and water. If irritation persists seek medical advice. Seek immediate medical advice in the event of inhalation, swallowing or contact with the eyes. If you feel unwell during or after this analysis seek medical advice. ANALYSIS MUST BE PERFORMED IN A FUME CUPBOARD.

A1.3. Storage and Disposal of Karl Fischer Waste.

The chemical composition of the various reagents in this procedure are protected industrial secrets. However, it is known that there is NO chloroform present. As the waste reacts with some metals it should be stored in glass containers.

A1.4. Loading of Operational Method onto Metrohm 702SM Titrino.

1. PRESS **<user method>** of the remote keypad (Fig. 2.2.2) to give prompt "recall method".
2. PRESS **ENTER** to give prompt "method name".
3. PRESS **<select>** until the relevant method name appears. The method used for Karl Fischer analysis is "18".
4. When the correct method name appears PRESS **ENTER**. The method is then loaded.

A1.5. Computer Settings for Method 18.

To alter any of the following variables either; 1. enter the relevant variable and PRESS **ENTER**, or PRESS **<select>** until the relevant parameter appears and then PRESS **ENTER**. Once the method has been loaded these settings should not need altering unless a change of sample or conditions requires it.

Parameters Section.
parameters:

SET1 = OFF, only one endpoint (EP) is generated in this procedure.
EP at U = 250 mV. Endpoint (EP) Limit at which reagent addition either ceases or commences. 250 mV is a high setting to encourage rapid endpoint determination (see Fig. 2.2.4).
dynamics = 10 mV. Dynamic Limit. Distance from the endpoint (EP) at which the titration slows. As oils may give drifting or even vanishing EP's, due to side reactions, it is essential that the EP is reached quickly therefore the dynamics setting's limit is small at 10 mV from the EP (250 mV) (Fig. 2.2.4).
max.rate = MAX (maximum rate for a 10 ml burette is 30 ml/min).
min.rate = 45 µl/min. Minimum possible titration rate. This parameter determines the addition rate at the beginning and end of titrations. This

parameter influences the titration speed and therefore it's accuracy. A small minimum rate results in a slower titration therefore, this method is set at 45 µl/min (quite high), to encourage rapid titration.

stop.crit = drift. Either drift or time (t(delay) or time stop) is used as stop criteria. They are the parameters which determine when the titration has finished. Drift refers to variation of the potential difference measurements at the electrode.

stop drift = 30 µl/min. When EP is reached and drift limit is reached then titration ceases. Drift is the amount the variation after the EP is acquired.

titration parameters:

titr.direction = "-" (negative) and refers to the direction to lower mV. The titration will therefore decrease the potential difference.

start V = "abs", absolute start volume in ml.

start V = start volume 0 ml.

dos.rate = MAX. Reagent dispensing rate for the start volume.

pause = 0 s. Waiting time, e.g., for equilibrium of the electrode after the start.

I(pol) + connection of electrodes = 50 µA

electrode test = ON, test for polarised electrodes, performed on changeover from inactive standby state to a measurement.

temperature = 25°C. Titration temperature.

stop conditions: conditions for titration termination, if this is not normal i.e., after attainment of EP (i.e., if it overruns due to side reactions).

stopV = abs maximum amount of reagent added during a titration.

stop V = 50 ml (therefore the cell wouldn't overflow).

filling rate = MAX. Burette filling rate after titration, or during recharge. (30 ml/min).

statistics: calculations, mean, absolute and relative sd's.

status = ON, if doing statistics.

mean = mean value calculation for "n" single results, n=3.

res.tab = original. Result table, .

preselections: for the titration sequence.

conditioning = ON, between the titrations the reaction medium potential difference is maintain below the "stop drift" limit. If this limit is exceeded the Metrohm does not allow titration to take place. When conditioning is performed, the volume drift can be displayed.

display drift = ON

req.ident = id1, of no real importance to this method.

req.smpl size = ON. The sample size for these titrations is measured as a weight (grams).

activate pulse = OFF.

Configuration

peripheral units

send to = Seiko

balance = Sartorius (even though not connected)

record = U

auxilliaries

dialog = English

date
time
run number = 0
auto start = OFF
start delay = 0
device label = blank
program = 702.0010

RS232 settings

baud rate = 9600
data bit = 8
stop bit = 1
parity = none
handshake = HWs
RS control = ON

common variable

C30 = usually approximately 5 (see reagent calibration)
C31-C39 = blank

Calculations

RS1=EP1*C30*C01/C00;4;%
RS1 = calculated water percentage of sample.
EP1 = amount of reagent used to complete the titration.
C30 = reagent reactivity (see reagent calibration)
C01 = 0.1 (constant)
C00 = sample weight
4 = results given to four decimal places.
% = results given as percent.

Sample Data

id 1 or C21 = usually blank (same for id's 2&3; C22 &23)

C-fmla

C01 = 0.1

def:

formula

RS1=EP1*C30*C01/C00
RS1 decimal places 4
RS1 unit %

common variables

report

report:full:full;

mean

MN1=RS1

A1.6. Basic Preparations.

Stirrer Rate = 4
Dispenser Rate = 10
Level of Reagent. The reagent used in this method was BDH# 19280 ET, Titrant U (Pyridine Free).
Level of Reaction Medium (60:40; Xylene:Solvent Solution) Check levels in bottle and titration vessels. The solvent solution used in this method was BDH# 19266, Karl Fischer Solvent Solution (Pyridine Free). The Xylene used in this method was SLR grade. The level for the titration vessel was approximately 3 cm depth. The reaction medium in the titration vessel was changed after two titrations.
Condition of water adsorbent molecular sieve. If the molecular sieve is pink it needs replacing with dry, blue, molecular sieve. The pink material should be dried in an oven until it is dehydrated and a blue colour. It is then ready for use.
Condition of Septum. The septum in the Titration Vessel should be intact and whole, not torn.

A1.7. REAGENT CALIBRATION.

1. Fill titration vessel with reaction medium to approximately 3 cm depth.
2. PRESS **START** on either the main panel or the remote keypad. The Metrohm neutralises the water present in the reaction medium. At neutralisation the voltage response should return to within the pre-set limits, i.e., 30 µl/min. Shake the titration vessel to rinse the reaction medium around the insides of the vessel. The Metrohm neutralises any water from the inside of the vessel. The voltage should return to 3 µ l/min, or less before titration.
3. Clean Syringe by washing with solvent, putting in drying oven and allowing to cool in a desiccator.
4. Sample approximately 20 µl of distilled water with the clean syringe.
5. Weigh the syringe.
6. PRESS **START** twice to give prompt "sample weight".
7. Push the syringe through the septum on the titration vessel until the needle tip is in the reaction medium.
8. Inject the water sample.
9. Remove the syringe from the titration vessel and re-weighed.

10. Calculate the weight of water injected into the vessel. Enter the weight into the computer using the remote keypad. PRESS **ENTER**. The Metrohm automatically titres the water sample and prints out the result on the thermal printer. The endpoint voltage reading (mV) should ideally be between 30 - 80 mV. If the voltage reading is above 100 mV then the electrode needs cleaning in methanol before further use. After titration the voltage should return to 3 µl/min or less before continuing.
11. Repeat steps 4 - 10 once more.
12. PRESS **STOP** and change the reaction medium. Shake reaction medium's bottle before using.
13. PRESS **START**. Remmeber, voltage response should be 3 µl/min or less before continuing.
14. Repeat steps 4 - 13 three times.
15. PRESS **STOP**.
16. Calculate the reagents titre for each titration. In the calculation assume the water content (RS1) is 100%.

$$C30 = \frac{RS1 \times C00}{EP \times C01}$$

C30 = Reagents Titre.
RS1 = Water Content (100%).
C00 = Sample Weight.
EP = (ENDPOINT) gives the amount of reagent used for titration.
C01 = Constant (0.1).

17. Calculate the mean of all the results from step 16. However, remove any spurious results (usually the 1st and 2nd titration may be dubious).
18. Enter the mean into the computer. To achieve this PRESS **<Configuration>** on the remote keypad four times to give the prompt **"Common Variables"**, PRESS **ENTER** to give C30, enter the mean, PRESS **ENTER**, PRESS **QUIT** twice.
19. Check the C30 reading by printing out the parameters. Print out is achieved by PRESSING **<Print>** on remote keypad, PRESS **<Configuration>** (or any other variable to be printed out) on the remote keypad and then PRESS **ENTER**.
20. The Metrohm is now ready for use.

A1.8. Sample Preparation.

A1.8.1. Homogenisation of the Crude Oil Sample.

1. An ultra-turrax (T25) high speed dispenser, with an S25N-18G dispersion tool, is used to homogenise the crude oil sample (Figs. 2.2.5 & 2.2.6).
2. Place the end of the dispersion tool into the sample container, 10 mm from it's base.
3. The ultra-turrax RPM should be increased slowly after starting and decreased slowly before stopping.
4. Homogenise the water and oil mixture for 3 minutes at 13,000 to 18,000 RPM.
5. Remove the dispersion tool from the sample jar.
6. The mixture is now ready for removal of a aliquot (approximately 6 g) for blending with water.

A1.8.2. Water Addition.

1. Add approximately 6 g of crude oil to a BDH #215/0073/33, 28.25 ml vial.
2. Calculate the amount of water necessary to give either 5, 10, 20 or 30% water content in a water and oil mixture containing 6 g of crude oil. E.g., To make a 30% water content mixture using 6g of crude oil approximately 2.6g (2.6ml) of water is needed.

A1.8.3. Homogenisation of Water and Oil Mixtures.

1. An ultra-turrax (T25) high speed dispenser, with an S25N-10G VS dispersion tool, is used to homogenise the water and oil mixtures (Figs. 2.2.5 & 2.2.6).
2. Place the end of the dispersion tool into the vial, 10 mm from it's base.
3. The ultra-turrax RPM should be increased slowly after starting and decreased slowly before stopping.
4. Homogenise the water and oil mixture for 3 minutes at 13,000 to 18,000 RPM.
5. Remove the dispersion tool from the vial.
6. The mixture is now ready for immediate sampling.

A1.8.4. Cleaning the Dispersion Tool.

1. Place the end of the dispersion tool into a vial containing dichloromethane (DCM).
2. Activate the ultra-turrax at approximately 2,000 RPM for a few seconds.
3. Replace the DCM and repeat steps 1 & 2.
4. Carefully follow the dismantling instructions which accompanied the dispersion tool.
5. Clean all the components in DCM.
6. Allow components to dry and then carefully re-assemble the dispersion tool. DO NOT OVER TIGHTEN.
7. If the dispersion tool is abnormally loud during operation, or the sample is overheating, the "bearing bush" component may need replacing.
8. IF CLEANING WITH AQUEOUS PHASE DO NOT WET THE SHAFT BEARINGS AND DO NOT LEAVE ANY COMPONENT IN A DAMP CONDITION.

A1.9. Sample Analysis.

A1.9.1. Sampling Strategy.

There were two sampling strategies employed during the use of the Karl Fischer Water Determination Technique. The first sampled only from the top of the water and oil blend, as show in Figure 2.2.9, with an intense sampling frequency which is listed in Table 2.2.1.

The superseding sampling strategy sampled separately from both the top and bottom of each water and oil blend, shown in Figure 3.2.2, along with the less intense sampling frequency.

A1.9.2. Sampling Procedure.

1. Ensure titration vessel contains 3 cm of reaction medium.
2. PRESS START and wait for the voltage to return to 3 µl/min or less (Display reads "OK" when below 30 µl/min ("stop drift" parameter, section A1.5)).
3. Secure the sample vial in a clamp (Fig. 2.2.10).
4. Secure the syringe in a clamp, directly above the sample vial (Fig. 2.2.10).

5. Lower the syringe into the vial, take approximately 100 µl of water and oil blend from the appropriate sampling sites (according to the sampling strategy in use). If more than one sampling site per water and oil blend then each sample site must be sampled with a separate syringe.
6. Weight the syringe.
7. PRESS **START** twice to give prompt "sample weight".
8. Push syringe through the septum on the titration vessel until the needle tip is in the neutralised reaction medium (Fig. 2.2.11).
9. Inject the sample (Fig. 2.2.11).
10. Withdraw needle from reaction medium BUT not from the titration vessel. Take in approximately 50 µl to remove any drops of oil/water mixture from the needle tip. Remove syringe from the titration vessel and re-weigh (Fig. 2.2.11).
11. Calculate the sample weight.
12. Enter the weight and PRESS **ENTER.**
13. After completing two titrations PRESS **STOP** and change the reaction medium.
14. Repeat steps 1 - 13 for all samples.

A1.10. Maintenance.

1. To avoid the Reagent crystallising in the burette and associated tubes, the apparatus should be used weekly. In the event of the reagent crystallising wash the affected areas with Methanol. Pay particular attention to the Stopcock. DO NOT attempt to dismantle the stopcock, refer to manual.
2. Leave the titration vessel in 3 cm of methanol.
3. If the apparatus is not going to be used for a long period of time the Metrohm should be cleaned out by following the instructions in the manual.

APPENDIX 2

Table A2.1. Peak areas for the n-alkanes, isoprenoids, pentacyclic triterpanes and steranes analysed from the North Sea crude oils.

Compounds, Abbreviations and Diagnostic Ions	A29	B12	KITTIWAKE	NINIAN	NS1	NS2	NS3
m/z 85							
n-C_{17}	208280	190030	428939	152708	191310	32081	0
Pristane (Pr)	84610	64997	118346	83076	111161	149280	50393
n-C_{18}	198255	170225	467417	131344	148772	29041	0
Phytane (Ph)	97260	67361	250040	89498	111389	143255	55821
m/z 191							
18α(H), 22, 29, 30-trisnorneohopane (Ts)	1397	1212	3847	1331	1814	2077	3467
17α(H), 22, 29, 30-trisnorhopane (Tm)	793	701	855	797	985	1316	2031
C_{29}, 17α(H), 21β(H), 30-norhopane (C_{29}αβ)	4113	2600	4329	3087	3987	4603	9152
C_{29}, 17β(H), 21α(H), 30-norhopane (C_{29}βα)	687	320	985	650	711	1307	1410
C_{30}, 17α(H), 21β(H)-hopane (C_{30}αβ)	8504	5242	8705	6015	7028	9308	10780
C_{30}, 17β(H), 21α(H)-hopane (C_{30}βα)	941	645	200	578	835	907	1505
C_{31}, 17α(H), 21β(H)-homohopane(22S) (C_{31}αβS)	3430	2178	5297	3244	3437	3821	5492
C_{31}, 17α(H), 21β(H)-homohopane (22R) (C_{31}αβR)	2703	1731	3960	2309	2749	2788	3554
C_{32}, 17α(H), 21β(H)-bishomohopane (22S) (C_{32}αβS)	2768	1636	4565	2334	2865	2794	4556
C_{32}, 17α(H), 21β(H)-bishomohopane (22R) (C_{32}αβR)	1683	1029	2692	1556	1796	1728	2790
C_{33}, 17α(H), 21β(H)-trishomohopane (22S) (C_{33}αβS)	2319	1256	3738	1691	2155	2251	3826
C_{33}, 17α(H), 21β(H)-trishomohopane (22R) (C_{33}αβR)	1398	898	2168	1185	1453	1486	2492
C_{34}, 17α(H), 21β(H)-tetrakishomohopane (22S) (C_{34}αβS)	1185	709	2865	1035	1503	1389	3008
C_{34}, 17α(H), 21β(H)-tetrakishomohopane (22R) (C_{34}αβR)	1019	472	1836	788	1074	1065	1789
C_{35}, 17α(H), 21β(H)-pentakishomohopane (22S) (C_{35}αβS)	727	453	4220	1126	1955	1433	3785
C_{35}, 17α(H), 21β(H)-pentakishomohopane (22R) (C_{35}αβR)	661	368	2538	791	1220	877	2295
m/z 217							
C_{27}, 24 ethyl 5α(H), 14α(H), 17α(H)-cholestane(20R) (C_{27}αααR)	1027	810	2293	927	1209	2015	934
C_{28}, 24 ethyl 5α(H), 14α(H), 17α(H)-cholestane(20R) (C_{28}αααR)	872	833	1393	967	841	2216	1434
C_{29}, 24 ethyl 5α(H), 14α(H), 17α(H)-cholestane(20S) (C_{29}αααS)	813	912	2119	1321	943	2542	1984
C_{29}, 24 ethyl 5α(H), 14α(H), 17α(H)-cholestane(20R) (C_{29}αααR)	1083	772	2429	863	1105	2009	1771
C_{29}, 24 ethyl 5α(H), 14β(H), 17β(H)-cholestane(20S) (C_{29}αββR)	749	958	2429	1631	1293	2815	2753
C_{29}, 24 ethyl 5α(H), 14β(H), 17β(H)-cholestane(20R) (C_{29}αββR)	1256	1007	3195	1488	1516	3095	3193

Table A2.2. Peak areas for the n-alkanes, isoprenoids, pentacyclic triterpanes and steranes analsyed for SMB crude oils.			
Compounds, Abbreviations and Diagnostic Ions	H1	H7	MONTEREY
m/z 85			
n-C_{17}	420617	0	141625
Pristane (Pr)	181861	0	160702
n-C_{18}	437676	0	161038
Phytane (Ph)	310000	0	251904
m/z 191			
18α(H), 22, 29, 30-trisnorneohopane (Ts)	6108	9139	6060
17α(H), 22, 29, 30-trisnorhopane (Tm)	28556	34387	23842
C_{29}, 17α(H), 21β(H), 30-norhopane ($C_{29}\alpha\beta$)	44346	60174	45931
C_{29}, 17β(H), 21α(H), 30-norhopane ($C_{29}\beta\alpha$)	5000	11556	8406
C_{30}, 17α(H), 21β(H)-hopane ($C_{30}\alpha\beta$)	61947	84101	64840
C_{30}, 17β(H), 21α(H)-hopane ($C_{30}\beta\alpha$)	6546	21462	11706
C_{31}, 17α(H), 21β(H)-homohopane(22S) ($C_{31}\alpha\beta S$)	24141	27292	22457
C_{31}, 17α(H), 21β(H)-homohopane (22R) ($C_{31}\alpha\beta R$)	17064	19445	30500
C_{32}, 17α(H), 21β(H)-bishomohopane (22S) ($C_{32}\alpha\beta S$)	14641	22132	18469
C_{32}, 17α(H), 21β(H)-bishomohopane (22R) ($C_{32}\alpha\beta R$)	14007	18221	14259
C_{33}, 17α(H), 21β(H)-trishomohopane (22S) ($C_{33}\alpha\beta S$)	11754	15609	13312
C_{33}, 17α(H), 21β(H)-trishomohopane (22R) ($C_{33}\alpha\beta R$)	7394	9717	8528
C_{34}, 17α(H), 21β(H)-tetrakishomohopane (22S) ($C_{34}\alpha\beta S$)	6882	10000	7571
C_{34}, 17α(H), 21β(H)-tetrakishomohopane (22R) ($C_{34}\alpha\beta R$)	5012	7000	6001
C_{35}, 17α(H), 21β(H)-pentakishomohopane (22S) ($C_{35}\alpha\beta S$)	7936	11339	11738
C_{35}, 17α(H), 21β(H)-pentakishomohopane (22R) ($C_{35}\alpha\beta R$)	7310	10834	9645
m/z 217			
C_{27}, 24 ethyl 5α(H), 14α(H), 17α(H)-cholestane(20R) ($C_{27}\alpha\alpha\alpha R$)	57329	93519	52261
C_{28}, 24 ethyl 5α(H), 14α(H), 17α(H)-cholestane(20R) ($C_{28}\alpha\alpha\alpha R$)	32083	56942	42309
C_{29}, 24 ethyl 5α(H), 14α(H), 17α(H)-cholestane(20S) ($C_{29}\alpha\alpha\alpha S$)	19680	32999	23036
C_{29}, 24 ethyl 5α(H), 14α(H), 17α(H)-cholestane(20R) ($C_{29}\alpha\alpha\alpha R$)	27165	47913	36029
C_{29}, 24 ethyl 5α(H), 14β(H), 17β(H)-cholestane(20S) ($C_{29}\alpha\beta\beta R$)	25286	30639	22782
C_{29}, 24 ethyl 5α(H), 14β(H), 17β(H)-cholestane(20R) ($C_{29}\alpha\beta\beta R$)	19585	31505	24145

Table A2.3. Peak areas for the aromatic molecules analysed from North Sea crude oils.					
Compounds, Abbreviations and Diagnostic Ions	A29	KITTIWAKE	NS1	NS2	NS3
m/z 128					
Naphthalene (N)	202592	240358	73261	147519	13112
m/z 142					
2-methylnaphthalene (2-MN)	305704	385611	175483	382475	28458
1-methylnaphthalene (1-MN)	281138	491523	147710	302897	30189
m/z 156					
2-ethylnaphthalene (2-EN)	23465	67872	19273	40361	3590
1-ethylnaphthalene (1-EN)	15943	37002	13283	28360	4656
2,6 + 2,7-dimethylnaphthalene (2,6+2,7-DMN)	161795	223170	121795	228725	37799
1,6-dimethylnaphthalene (1,6-DMN)	197336	235248	144339	249556	39903
1,5-dimethylnaphthalene (1,5-DMN)	61659	134510	47506	79599	18084
m/z 170					
1,3,5 + 1,4,6-trimethylnaphthalene (1,3,5+1,4,6-TMN)	70888	162709	61717	118828	18028
2,3,6-trimethylnaphthalene (2,3,6-TMN)	54765	69311	53420	69413	16716
m/z 178					
Phenanthrene (P)	79881	227002	81915	91009	21577
m/z 192					
3-methylphenanthrene (3-MP)	33056	79381	30189	38135	12983
2-methylphenanthrene (2-MP)	41935	86142	37729	48722	18439
9-methylphenanthrene (9-MP)	56398	227930	54967	69840	28724
1-methylphenanthrene (1-MP)	59760	147814	41727	62046	18484
m/z 184					
Dibenzothiophene (DBT)	16415	249513	22936	38517	12949
m/z 198					
4-methyldibenzothiophene (4-MDBT)	25615	244561	35935	47401	21198
1-methyldibenzothiophene (1-MDBT)	9454	89007	12389	14365	10530
m/z 231					
C_{20}-triaromatic steroid (20R) (C_{20} TA 20R)	5136	13698	4936	6873	4399
C_{28}-triaromatic steroid (20R) (C_{28} TA 20R)	9213	7689	9804	13660	10302

Table A2.4. Peak areas for the molecules analysed from the SMB crude oils.			
Compounds, Abbreviations and Diagnostic Ions	H1	H7	MONTEREY
m/z 128			
Naphthalene (N)	95702	115023	46472
m/z 142			
2-methylnaphthalene (2-MN)	236331	315667	126676
1-methylnaphthalene (1-MN)	204669	232722	101459
m/z 156			
2-ethylnaphthalene (2-EN)	30543	28708	11811
1-ethylnaphthalene (1-EN)	17930	15961	8585
2,6 + 2,7-dimethylnaphthalene (2,6+2,7-DMN)	169468	208084	85202
1,6-dimethylnaphthalene (1,6-DMN)	211981	205967	105453
1,5-dimethylnaphthalene (1,5-DMN)	52563	45172	22276
m/z 170			
1,3,5 + 1,4,6-trimethylnaphthalene (1,3,5+1,4,6-TMN)	63167	64808	31660
2,3,6-trimethylnaphthalene (2,3,6-TMN)	79286	87391	39491
m/z 178			
Phenanthrene (P)	61454	54548	22298
m/z 192			
3-methylphenanthrene (3-MP)	32602	29582	10079
2-methylphenanthrene (2-MP)	48272	42476	12514
9-methylphenanthrene (9-MP)	45120	34643	12763
1-methylphenanthrene (1-MP)	38668	30299	8909
m/z 184			
Dibenzothiophene (DBT)	93570	62361	32991
m/z 198			
4-methyldibenzothiophene (4-MDBT)	103065	61834	29742
1-methyldibenzothiophene (1-MDBT)	31399	19752	10732
m/z 231			
C_{20}-triaromatic steroid (20R) (C_{20} TA 20R)	14480	12102	3960
C_{28}-triaromatic steroid (20R) (C_{28} TA 20R)	2503	15290	10235

	A29	B12	KITTIWAKE	NINIAN	NS1	NS2	NS3
Biodegradation*							
n-C_{17}/Pr	2.46	2.92	3.62	1.84	1.72	0.22	0
n-C_{18}/Ph	2.04	2.53	1.87	1.47	1.34	0.20	0
n-C_{18}/C_{30} αβ-hopane	23.31	32.47	53.70	21.84	21.17	3.12	0
Ph/C_{30} αβ-hopane	11.44	12.85	28.72	14.88	15.85	15.39	5.18
Tm/C_{30} αβ-hopane	0.09	0.13	0.10	0.13	0.14	0.14	0.19
N/N+P	0.72	nd	0.51	nd	0.47	0.62	0.38
2-MN/2-MN + P	0.79	nd	0.63	nd	0.68	0.81	0.57
2,6+2,7-DMN/2,6+2,7-DMN + P	0.67	nd	0.50	nd	0.60	0.72	0.64
1,3,5 + 1,4,6-TMN/1,3,5 + 1,4,6-TMN + P	0.47	nd	0.42	nd	0.43	0.57	0.46
P/DBT	4.87	nd	0.91	nd	3.57	2.36	1.67
4-MDBT/DBT (MDR4)	1.56	nd	0.98	nd	1.57	1.23	1.64
Source Correlation**							
Homohopane Indices							
C_{31}αβ(S+R)/[SUM, C_{31}αβ(S+R) to C_{35}αβ(S+R)]	34.28	36.43	27.32	34.58	30.61	33.66	26.93
C_{32}αβ(S+R)/[SUM, C_{31}αβ(S+R) to C_{35}αβ(S+R)]	24.88	24.84	21.42	24.22	23.07	23.03	21.87
C_{33}αβ(S+R)/[SUM, C_{31}αβ(S+R) to C_{35}αβ(S+R)]	20.77	20.07	17.43	17.91	17.86	19.04	18.81
C_{34}αβ(S+R)/[SUM, C_{31}αβ(S+R) to C_{35}αβ(S+R)]	12.32	11.01	13.88	11.35	12.75	12.50	14.28
C_{35}αβ(S+R)/[SUM, C_{31}αβ(S+R) to C_{35}αβ(S+R)]	7.76	7.65	19.95	11.93	15.71	11.77	18.10
C_{27}ααα R/C_{29}ααα R	0.95	1.05	0.94	1.07	1.09	1.00	0.53

*Table A2.5. Results of the biomarker and molecular parameters used to assess extent of biodegradation and source correlation of North Sea crude oils in this study.Abbreviations identified in Tables A2.5 to A2.8. * = biodegradation parameters are discussed* in Chapter 6.. *nd = not determined.*

	A29	B12	KITTIWAKE	NINIAN	NS1	NS2	NS3
Maturity Parametesr							
Pr/Ph	0.87	0.96	0.47	0.93	1.00	1.04	0.90
Ts/Ts + Tm	0.64	0.63	0.82	0.63	0.65	0.61	0.63
$C_{30}\beta\alpha/C_{30}\beta\alpha + C_{30}\alpha\beta$	0.10	0.11	0.02	0.09	0.11	0.09	0.12
$C_{31}\alpha\beta S/C_{31}\alpha\beta S + C_{31}\alpha\beta R$	0.56	0.56	0.57	0.58	0.56	0.58	0.61
$C_{32}\alpha\beta S/C_{32}\alpha\beta S + C_{32}\alpha\beta R$	0.62	0.61	0.63	0.60	0.61	0.62	0.62
$C_{29}\alpha\alpha\alpha S/C_{29}\alpha\alpha\alpha S + C_{29}\alpha\alpha\alpha R$	0.57	0.46	0.53	0.40	0.54	0.44	0.47
$C_{29}\alpha\beta\beta(S+R)/C_{29}\alpha\beta\beta(S+R) + C_{29}\alpha\alpha\alpha(S+R)$	0.51	0.54	0.55	0.59	0.58	0.57	0.61
2-MN/1-MN (MNR)	1.09	nd	0.78	nd	1.19	1.26	0.94
2,3,6-TMN/1,3,5+1,4,6-TMN (TNR)	0.77	nd	0.43	nd	0.87	0.58	0.93
1.5(2-MP + 3-MP)/(P + 1-MP + 9-MP) (MPI)	0.57	nd	0.41	nd	0.57	0.58	0.69
Calculate Vitrinite Reflectance							
Rm = 0.60(MPI) + 0.4	0.74	nd	0.65	nd	0.74	0.75	0.81
(2-MP + 3-MP)/(2-MP + 3-MP + 1-MP + 9-MP) (MPDF1)	0.39	nd	0.31	nd	0.41	0.40	0.40
4-MDBT/1-MDBT (MDR)	2.71	nd	2.75	nd	2.90	3.30	2.01
C_{20} TA 20R/C_{20} TA 20R + C_{28} TA 20R	0.36	nd	0.64	nd	0.34	0.34	0.30

Table A2.6. Results of the biomarker and molecular parameters used to assess the maturities of the North Sea crude oils in this study. Abbreviations identified in Tables A2.1 to A2.4. nd = not determined.

	H1	H7	MONTEREY
Biodegradation*			
n-C_{17}/Pr	2.31	0	0.88
n-C_{18}/Ph	1.41	0	0.64
n-C_{18}/C_{30} αβ-hopane	7.07	0	2.48
Ph/C_{30} αβ-hopane	5.01	0	3.89
Tm/C_{30} αβ-hopane	0.46	0.41	0.37
N/N+P	0.61	0.68	0.68
2-MN/2-MN + P	0.79	0.85	0.85
2,6+2,7-DMN/2,6+2,7-DMN + P	0.73	0.79	0.79
1,3,5 + 1,4,6-TMN/1,3,5 + 1,4,6-TMN + P	0.51	0.54	0.59
P/DBT	0.66	0.87	0.68
4-MDBT/DBT (MDR4)	1.10	0.99	0.90
Source Correlation**			
Homohopane Indices			
C_{31}αβ(S+R)/[SUM, C_{31}αβ(S+R) to C_{35}αβ(S+R)]	35.48	30.83	37.17
C_{32}αβ(S+R)/[SUM, C_{31}αβ(S+R) to C_{35}αβ(S+R)]	24.67	26.62	22.97
C_{33}αβ(S+R)/[SUM, C_{31}αβ(S+R) to C_{35}αβ(S+R)]	16.49	16.71	15.33
C_{34}αβ(S+R)/[SUM, C_{31}αβ(S+R) to C_{35}αβ(S+R)]	10.24	11.22	9.53
C_{35}αβ(S+R)/[SUM, C_{31}αβ(S+R) to C_{35}αβ(S+R)]	13.13	14.63	15.01
C_{27}ααα R/C_{29}ααα R	2.11	1.95	1.45

*Table A2.7. Results of the biomarker and molecular parameters used to assess extent of biodegradation and source correlation of SMB crude oils in this study. Abbreviations identified in Tables A2.1 to A2.4. * = biodegradation parameters are discussed in Chapter 6.*

	H1	H7	MONTEREY
Maturity Parametesr			
Pr/Ph	0.59	0	0.64
Ts/Ts + Tm	0.18	0.21	0.20
$C_{30}\beta\alpha/C_{30}\beta\alpha + C_{30}\alpha\beta$	0.10	0.20	0.15
$C_{31}\alpha\beta S/C_{31}\alpha\beta S + C_{31}\alpha\beta R$	0.59	0.58	0.42
$C_{32}\alpha\beta S/C_{32}\alpha\beta S + C_{32}\alpha\beta R$	0.51	0.55	0.56
$C_{29}\alpha\alpha\alpha S/C_{29}\alpha\alpha\alpha S + C_{29}\alpha\alpha\alpha R$	0.58	0.59	0.61
$C_{29}\alpha\beta\beta(S+R)/C_{29}\alpha\beta\beta(S+R) + C_{29}\alpha\alpha\alpha(S+R)$	0.49	0.43	0.44
2-MN/1-MN (MNR)	1.16	1.36	1.25
2,3,6-TMN/1,3,5+1,4,6-TMN (TNR)	1.26	1.35	1.25
1.5(2-MP + 3-MP)/(P + 1-MP + 9-MP) (MPI)	0.84	0.91	0.77
Calculate Vitrinite Reflectance			
Rm = 0.60(MPI) + 0.4	0.90	0.94	0.86
(2-MP + 3-MP)/(2-MP + 3-MP + 1-MP + 9-MP) (MPDF1)	0.49	0.53	0.51
4-MDBT/1-MDBT (MDR)	3.28	3.13	2.77
C_{20} TA 20R/C_{20} TA 20R + C_{28} TA 20R	0.85	0.44	0.28

Table A2.8. Results of the biomarker and molecular parameters used to assess the maturities of the SMB crude oils in this study. Abbreviations identified in Tables A2.1 to A2.4.

APPENDIX 3

5% Added Water Content					10% Added Water Content				
Sampling Time (Hours)	Number of Analyses	Mean %R	Standard Deviation	+/- Error	Sampling Time (Hours)	Number of Analyses	Mean %R	Standard Deviation	+/- Error
0	2	92.1		2.98	0	4	92.43	10.23	
0.18	2	95.34		2.4	0.15	4	89.8	15.4	
0.35	2	81.12		4.63	0.34	4	82.58	13.46	
0.67	2	98.02		1.49	0.5	4	93.56	21.92	
1	2	88.98		9.3	0.98	4	91.58	11.1	
2	2	99.84		5.82	1.98	4	90.14	16.94	
3.03	2	71.68		1.59	3	4	84.87	19.25	
25.88	2	66.89		8.4	5.98	4	84.2	11.54	
46.85	2	70.07		6.03	8.73	4	83.24	5.99	
70.73	2	56.34		14.79	11.53	4	69.86	14.23	
97.32	2	49.88		10.97	23.4	4	46.69	23.61	
120.35	2	18.07		12.78	48.02	4	6.27	2.76	
					71.2	4	4.09	3.22	
					95.6	4	12.01	14.72	
					121.12	4	1.32	1.74	
					146.22	4	0.82	0.67	
					167.13	4	0.9	1.76	
					191.33	4	1.72	1.83	
					215.95	2	0.87		0.87

Table A3.1a. Statistical data for COWUA of Eldfisk crude oil/distilled water blends containing 5 & 10% added water.

20% Added Water Content					30% Added Water Content				
Sampling Time (Hours)	Number of Analyses	Mean %R	Standard Deviation	+/- Error	Sampling Time (Hours)	Number of Analyses	Mean %R	Standard Deviation	+/- Error
0	4	82.16	13.09		0	4	86.84	5.75	
0.17	4	70.27	27.57		0.17	4	93.3	2.53	
0.3	4	42.98	29.8		0.32	4	85.77	4.01	
0.64	4	46.25	27.94		0.65	4	84.76	6.82	
0.97	4	43.73	32.55		0.97	4	93.83	2.87	
1.98	4	38.05	25.4		1.95	4	86	4.57	
2.97	4	36.07	25.2		2.94	4	87.25	5.13	
5.98	4	32.7	27.28		6	4	83.77	1.82	
8.72	4	26.25	14.47		8.38	4	82.64	6.25	
11.48	4	25.46	16.1		11.1	4	80.04	3.18	
23.37	4	9.13	7.59		23.03	4	32.46	34.42	
47.98	4	3.96	2.2		47.03	4	5.58	4.83	
71.15	4	3.29	3.48		70.82	4	5.9	9.4	
95.33	4	2.58	2.72		95.05	4	0.65	0.63	
121.15	4	0.8	0.62		120.83	4	0.46	0.56	
146.18	4	1.6	1.31		145.83	4	0.46	0.47	
167.12	4	1.48	1.79		166.83	4	0.07	0.1	
191.33	4	0.97	0.67		191	4	0.73	0.9	
215.92	2	2.72		1.27	215.6	2	0.01	0.01	0.01

Table A3.1b. Statistical data for COWUA of Eldfisk crude oil/distilled water blends containing 20 & 30% added water.

5% Added Water Content					10% Added Water Content				
Sampling Time (Hours)	Number of Analyses	Mean %R	Standard Deviation	+/- Error	Sampling Time (Hours)	Number of Analyses	Mean %R	Standard Deviation	+/- Error
0	2	141.04		4.33	0	2	115.34		0.01
0.18	2	173.36		5.04	0.15	2	124.09		3.18
0.32	2	190.65		1.18	0.32	2	122.69		1.35
0.67	2	214.12		19.77	0.48	2	134.88		5.97
0.97	2	194.41		2.32	0.98	2	126.1		1.46
1.98	2	202.73		16.62	1.98	2	136.49		3.15
2.77	2	189.12		7.84	2.75	2	133.77		8.87
5.67	2	182.46		8.82	5.65	2	130.07		6.73
7.9	2	183.74		1.99	7.9	2	121.26		2.08
11.18	2	165.3		14.68	11.15	2	98.14		30.72
23.33	2	140.17		3.87	23.68	2	67.68		33.54
46.58	2	151.89		22.07	46.6	2	16.74		15.81
71.02	2	141.64		9.88	71.02	2	9.54		7.78
94.48	2	131.33		3.61	94.47	2	19.69		6.48
121.77	2	92.37		7.54	121.75	2	14.95		14.87
145.92	2	118		7.87	145.95	2	7.03		3.25
167.5	2	91.48		0.78	167.52	2	10.89		7.17
191.5	2	111.42		7.19	191.48	2	17.71		9.36
218.55	2	124.48		1.07	218.65	2	16.62		8.12

Table A3.2a. Statistical data for COWUA of Ninian crude oil/distilled water blends containing 5 & 10% added water.

20% Added Water Content					30% Added Water Content				
Sampling Time (Hours)	**Number of Analyses**	**Mean %R**	**Standard Deviation**	**+/- Error**	**Sampling Time (Hours)**	**Number of Analyses**	**Mean %R**	**Standard Deviation**	**+/- Error**
0	2	99.87		7.69	0	2	104.34		0.61
0.1	2	108.85		4.18	0.15	2	104.08		0.45
0.32	2	104.97		4.64	0.3	2	104.71		0.1
0.63	2	105.77		5.96	0.65	2	103.72		3.33
0.97	2	108.07		2.81	0.98	2	106.91		3.75
1.97	2	110.37		0.48	1.98	2	107.34		0.83
2.72	2	111.94		2.65	4.1	2	89.16		30.01
5.63	2	98.45		1.85	5.3	2	54.48		18.73
7.87	2	91.68		12.56	7.53	2	32.29		15.91
11.88	2	11.73		12.38	10.78	2	9.48		10.49
23.28	2	7.08		7.66	22.95	2	10.96		13.19
46.57	2	13.97		17.84	46.23	2	6.59		8.32
70.98	2	10.11		10.43	70.65	2	16.73		11.95
94.45	2	19.07		7.69	94.15	2	72.76		2.25
121.72	2	37.81		14.1	121.38	2	9.77		10.2
145.98	2	61.03		13.28	145.68	2	56.42		14.04
167.52	2	11.64		12.36	167.22	2	11.34		1.86
191.48	2	11.43		13.63	191.17	2	17.46		17.47
218.72	2	13.53		5.57	218.45	2	13.47		16.44

Table A3.2b. Statistical data for COWUA of Ninian crude oil/distilled water blends containing 20 & 30% added water.

NS1 30% Added Water Content					NS2 30% Added Water Content, Top Sample				
Sampling Time (Hours)	**Number of Analyses**	**Mean %R**	**Standard Deviation**	**+/- Error**	**Sampling Time (Hours)**	**Number of Analyses**	**Mean %R**	**Standard Deviation**	**+/- Error**
0	2	102.07		0.96	0	2	106.04		0.24
0.17	2	101.8		1.47	2.67	2	98.26		0.54
0.33	2	105.05		0.64	5.73	2	83.55		3.47
0.62	2	101.33		0.96	8.45	2	67.05		3.21
0.95	2	100.05		4.12	22.95	2	22.11		3.47
2.02	2	103.84		1.18	47.87	2	5.71		1.21
2.97	2	103.77		3.51					
5.88	2	109.74		0.26	**NS2 30% Added Water Content, Bottom Sample**				
8.78	2	96.69		1.44	0	2	99.08		0.86
11.62	2	79.13		5.56	3.01	2	102.06		0.2
25.93	2	22.01		4.78	6	2	94.7		0.11
51.33	2	8.93		4.91	8.3	2	115.41		9.19
75.6	2	3.56		3.56	23.1	2	148.43		15.43
96.33	2	0.41		0.41	49.01	2	197.93		9.31

Table A3.3. Statistical data for COWUA of NS1 and NS2 crude oil/distilled water blends containing 30% added water. Samples were taken from the top and bottom of the NS2 blends.

5% Added Water Content					10% Added Water Content				
Sampling Time (Hours)	**Number of Analyses**	**Mean %R**	**Standard Deviation**	**+/- Error**	**Sampling Time (Hours)**	**Number of Analyses**	**Mean %R**	**Standard Deviation**	**+/- Error**
0	2	111.4		5.92	0	4	103.51	8.13	
0.18	2	108.4		1.82	0.15	4	109.23	1.24	
0.32	2	115.72		2.63	0.48	4	114.09	7.03	
0.65	2	116.8		5.48	0.67	4	103.8	7.21	
0.95	2	119.55		2.66	0.97	4	112.44	3.7	
1.97	2	107.58		3.77	2.02	4	110.95	3.86	
2.93	2	112.76		2.36	3.02	4	111.37	6.71	
5.9	2	116.6		0.55	5.95	4	103.82	12.65	
8.9	2	118.26		1.08	8.28	2	96.46	15.41	
					12.35	1	92.91	0	
21.45	2	111.54		15.48	24.37	4	107.84	2.7	
47.98	2	100.29		9.45	49.48	4	101.9	16.16	
71.73	2	112.52		2.83	75.13	4	97.38	10.74	
97.7	2	113.08		79.96	101.7	4	93.45	14.99	
121.27	2	109.41		77.37	121.18	4	95.32	10.77	
142.77	2	104.1		73.61	148.22	4	94.7	6.89	
168.63	2	104.54		73.92	168.78	4	77.13	23.58	
					194.3	3	70.15	13.17	
					217.92	3	61.5	3.17	

Table A3.4a. Statistical data for COWUA of NS3 crude oil/distilled water blends containing 5 & 10% added water.

20% Added Water Content					30% Added Water Content				
Sampling Time (Hours)	Number of Analyses	Mean %R	Standard Deviation	+/- Error	Sampling Time (Hours)	Number of Analyses	Mean %R	Standard Deviation	+/- Error
0	4	89.36	14.59		0	4	95.27	10.51	
0.15	4	86.83	10.48		0.13	4	95.26	1.58	
0.32	4	87.59	15.1		0.33	4	85.11	17.94	
0.65	4	76.78	36.97		0.68	4	81.57	22.66	
0.97	4	85.6	22.61		0.92	4	85.87	29.06	
2.02	4	78.03	25.01		1.95	4	79.13	11.83	
3.03	4	99.75	6.53		3	4	57.92	26.43	
5.97	4	86.79	15.37		5.35	4	60.97	29.43	
8.27	2	81.59		13.64	8.93	2	96.64		7.07
12.35	1	71.37			12.02	1	49.95		
24.37	4	88.77	15.03		24.08	4	65.18	23.28	
49.5	4	84.52	16.58		49.25	4	49.85	5.49	
75.13	4	88.55	16.65		74.82	4	48.54	12.06	
101.87	4	84.78	16.92		101.78	4	47.23	9.4	
121.52	4	77.28	18.71		121.27	4	43.33	6.35	
148.42	4	64.31	25.05		148.77	4	31	12.59	
169.75	4	53.77	39.43		169.77	4	33.52	14.51	
194.47	3	41.54	43.48		194.4	3	14.19	5.76	
218.47	3	42.41	33.46		218.35	3	21.47	5.14	

Table A3.4b. Statistical data for COWUA of NS3 crude oil/distilled water blends containing 20 & 30% added water.

5% Added Water Content					10% Added Water Content				
Sampling Time (Hours)	Number of Analyses	Mean %R	Standard Deviation	+/- Error	Sampling Time (Hours)	Number of Analyses	Mean %R	Standard Deviation	+/- Error
0	3	103.75	18.42		0	3	94.78	6.57	
0.13	3	124.66	39.07		0.15	3	97.51	4.63	
0.3	3	98.49	11.07		0.32	3	100.41	7.28	
0.65	3	113.51	10.46		0.65	3	100.61	4.66	
0.98	3	119.26	4.22		1	3	99.41	9.28	
1.97	3	117.36	11.92		2.02	3	99.73	1.4	
2.97	3	119.73	4.25		3	3	101.42	5.18	
6.22	3	117.33	2.51		6.22	3	100.01	3.43	
8.83	3	117.51	5.25		8.83	3	84.84	25.89	
11.15	3	127	24.04		11.17	3	87.65	21.77	
25.95	3	112.79	7.92		25.95	3	67.75	34.09	
50.1	3	58.12	37.49		51.08	3	26.7	10.76	
74.07	3	53.05	15.44		74.17	3	21.34	5.04	
95.65	3	36.24	9.67		95.65	3	19.82	7.96	
124.33	3	22.02	14.18		124.35	3	14.56	6.18	
147.4	3	20.59	5.54		147.42	3	10.65	2.76	
169.95	3	19.64	12.87		169.98	3	10.75	3.87	
190.26	3	20.12	8.17		190.98	3	9.32	4.99	
243.36	2	23.33		10.22	243.42	2	7.65		0.98

Table A3.5a. Statistical data for COWUA of Monterey crude oil/distilled water blends containing 5 and 10% added water.

20% Added Water Content					30% Added Water Content				
Sampling Time (Hours)	Number of Analyses	Mean %R	Standard Deviation	+/- Error	Sampling Time (Hours)	Number of Analyses	Mean %R	Standard Deviation	+/- Error
0	3	94.7	4.13		0	3	97.21	0.13	
0.15	3	99.15	4.98		0.12	3	94.89	11.84	
0.33	3	95	3.22		0.28	3	101.32	7.44	
0.65	3	100.22	7.46		0.65	3	99.53	3.84	
1	3	98.8	1.65		0.98	3	103.48	4.1	
2	3	97.49	1.9		1.93	3	99.87	1.91	
3.02	3	98.36	4.41		2.9	3	101.42	2.55	
6.22	3	95.59	0.43		5.85	3	97.98	1.12	
8.85	3	88.12	17.76		8.4	3	99.42	1.72	
11.17	3	80.1	35.71		10.8	3	101.19	1.6	
25.95	3	59.76	40.4		25.57	3	95.14	5.92	
51.07	3	22.23	10.11		50.72	3	69	35.7	
74.15	3	17.06	8.78		73.77	3	63.89	58.14	
95.63	3	9.64	9.34		95.27	3	11.99	10.14	
124.57	3	12.71	4.48		123.97	3	27.58	39.96	
147.42	3	8.92	5.32		147.12	3	49.95	59.92	
170	3	8.1	2.45		169.63	3	4.39	2.75	
191.58	3	8.76	4.04		191.68	3	26.89	43.4	
243.45	2	1.36		0.29	243.13	2	0.86		0.63

Table A3.5b. Statistical data for COWUA of Monterey crude oil/distilled water blends containing 20 and 30% added water.

H1, 30% Added Water Content, Top Sample					H7, 30% Added Water Content, Top Sample				
Sampling Time (Hours)	Number of Analyses	Mean %R	Standard Deviation	+/- Error	Sampling Time (Hours)	Number of Analyses	Mean %R	Standard Deviation	+/- Error
0	2	98.67		0.18	0	2	99.09		0.81
2.85	2	100.4		2.54	2.88	2	99.64		0.91
5.65	2	53.49		0.94	5.67	2	95.4		2.62
10.65	2	7.07		7.07	10.37	2	94.96		1.88
25.15	2	0.36		0.36	24.88	2	96.26		3.32
51.28	2	0		0	50.98	2	30.71		0.94
73.08	2	0		0	72.82	2	16.88		4.11
H1, 30% Added Water Content, Bottom Sample					H7, 30% Added Water Content, Bottom Sample				
0	2	100.05		0.44	0	2	98.52		1.08
2.85	2	101.42		2.04	2.88	2	103.38		0.42
5.65	2	100.95		5.16	5.67	2	96.08		2.84
10.65	2	99.86		1.67	10.37	2	100.3		0.01
25.15	2	124		13.12	24.88	2	107.6		1.89
51.28	2	139.79		5.07	50.98	2	128.22		0.83
73.08	2	123.93		49.42	72.82	2	147.5		1.66

Table A3.6. Statistical data for COWUA of H1 and H7 crude oil/distilled water blends containing 30% added water. Samples were taken from the top and bottom of all blends.

APPENDIX 4

Isomers	Isomer Concentrations (ng g^{-1})											
	Whole Oil			Supernatant Oil		Unbound Oil		Bound Oil/Emulsion				
phenol	2,790.43	1,065.87	4,887.07	1,500.97	1,558.24	2,065.65	3,905.54	83,070.93	87,812.12	97,064	54,997.32	78,494.24
2-MP	5,494.95	4,158.74	6,206.94	2,754.99	3,209.29	2,956.06	2,833.08	6,385.63	12,300.17	14,631.36	5,039.38	8,398.05
3-MP	3,699.54	2,638.57	3,958.22	2,201.79	2,222.96	2,958.69	2,593.33	8,304.67	15,283.31	12,328.24	4,490.87	8,766.2
4-MP	2,493.88	1,786.23	2,670.91	1,481.33	1,496.15	1,674.29	1,442.71	0	0	0	0	0
2-EP	443.08	325.17	386.88	280.28	277.65	395.93	360.91	3,537.31	3,149.91	4,453.16	2,144.63	3,581.2
2,5-DMP	3,104.5	2,399.47	2,612.35	2,005.78	1,981.61	2,585.09	2,382.9	7,432.4	4,338.12	4,152.4	1,976.47	7,130.46
2,4-DMP	6,152.98	5,125.48	5,621.25	3,534.47	4,077.6	4,624.15	4,138.08	26,658.87	17,488.08	13,861.54	5,255.87	24,741.99
2,6-DMP	3,764.56	2,586.73	3,207.16	2,401.19	2,169.23	2,698.11	2,303.85	8,700.44	0	0	1,867.34	7,736.23
3,5-DMP	3,881.03	2,567.62	3,252.16	2,532.93	2,372	3,377.46	2,992.65	5,497.34	5,729.91	2,830.22	1,073.53	5,342.42
4-EP	335.89	649.2	705.89	185.55	0	0	0	0	0	0	0	0
3,4-DMP	997.83	760.99	870.01	626.2	617.28	861.31	911.26	11,660.18	7,831.41	8,798.96	4,922.14	12,029.17
2-PP	33.1	31.54	31.09	27.51	27.07	37.54	0	290.75	0	0	88.38	0
3-iPP	464.38	298.91	333.97	307.9	303.91	362.11	430.73	927.98	0	1,360.84	1,335.06	0
4-iPP	1,048.14	708.07	804.55	695.91	686.36	840.52	901.67	2,968.87	0	8,108.53	3,947.25	3,113.07
2,4,6TMP	1,484.91	1,504.72	1,473.89	678.95	832.88	897.79	790.41	0	0	0	0	0
2,3,5TMP	2,746.85	2,188.77	2,192.4	1,748.64	1,921.88	2,399.16	2,233.25	0	0	0	0	0
2,3,6TMP	0	623.82	573.85	0	468.95	0	410.53	0	0	0	0	0
3,4,5TMP	0	68.93	62.96	0	597.59	0	619.44	0	0	0	0	1,453.31
Total	23,224.92	18,944.44	22,305.79	13,431.81	14,966.14	16,593.84	15,453	53,005.41	37,276.28	37,098.46	16,372.07	51,587.93
Total	15,711.12	10,544.4	17,545.74	9,532.57	9,854.5	12,140.04	13,797.34	112,429.97	116,656.75	130,490.79	70,766.17	109,198.41
Extract	38,936.04	29,488.84	39,851.53	22,964.38	24,820.63	28,733.88	29,250.34	165,435.38	153,933.03	167,589.25	87,138.23	160,786.34
Average	36,092.14			23,892.51		28,992.11		146,976.45				
Standard	5,736.91							33,857.57				
+/- Error				928.13		258.23						

Table A4.1. Statistical data for Eldfisk, A29, C_0-C_3 alkylphenol analyses.

Isomers	Isomer Concentrations (ng g^{-1})									
	WholeOil	Supernatant Oil			Unbound Oil			Bound Oil/Emulsion		
phenol	3,932.36	544.95	1,368.94	2,763	2,500.18	605.89	1,557.4	228,856.44	108,578.58	83,955.53
2-methylphenol	5,395.63	1,021.5	2,382.33	3,362.22	2,568.65	693.81	1,361.13	173,474.77	24,975.2	12,136.09
3-methylphenol	4,049.17	835.11	1,883.34	2,761.8	2,551.57	759.42	1,713.51	144,667.57	26,537.03	13,491.63
4-methylphenol	2,361.93	429.51	1,163.77	1,563.49	1,046.77	0	0	41,659.01	0	0
2-ethylphenol	464.88	107.89	254.16	411.6	277.22	85.02	422.57	14,528.7	3,833.16	0
2,5-dimethylphenol	2,701.24	689.59	1,434.59	2,040.69	1,549.11	483.78	1,701.58	60,612.68	6,348.18	0
2,4-dimethylphenol	3,848.39	1,096.51	2,213.85	2,972.8	2,599.2	767.43	2,939.67	130,972.86	21,747.4	0
2,6-dimethylphenol	1,633.52	334.05	508.56	1,167.58	732.94	215.53	1,116.99	45,146.32	15,751.89	0
3,5-dimethylphenol	3,385.44	956.29	1,832	2,627.85	2,058.46	666.31	2,410.72	69,922.07	16,314.36	0
4-ethylphenol	0	0	0	5,305.36	0	0	0	0	0	0
3,4-dimethylphenol	755.28	214.21	443.52	706.96	599.11	178.59	992.44	23,141.58	15,404.41	0
2-propylphenol	42.57	15.18	28.44	35.96	32.37	0	31.14	0	0	0
3-isopropylphenol	489.78	154.93	288.16	376.16	331.4	113.02	274.33	0	0	0
4-isopropylphenol	1,120.11	336.71	273.88	1,046.72	701.75	271.25	852.75	21,575.74	0	0
2,4,6-trimethylphenol	93.13	39.96	71.74	241.15	71.74	31.06	115.58	0	0	0
2,3,5-trimethylphenol	1,447.96	607.57	1,047.01	1,582.61	990.14	375.5	788.16	10,150.53	0	0
2,3,6-trimethylphenol	138.46	51.9	108.27	215.56	118.78	0	0	0	0	0
3,4,5-trimethylphenol	831.01	369.6	621.42	841.32	510.86	0	619.33	3,739.97	0	0
Total Hindered	15,765.78	3,964.14	8,048.97	12,030.16	8,940.16	2,652.13	8,476.83	434,885.85	72,655.83	12,136.09
Total Non-hindered	16,925.09	3,841.31	7,875.03	17,992.67	10,300.11	2,594.47	8,420.49	533,562.38	166,834.39	97,447.15
Extract Totals	32,690.87	7,805.45	15,924	30,022.83	19,240.27	5,246.59	16,897.31	968,448.23	239,490.22	109,583.24
Average Totals	32,690.87	17,917.43			13,794.73			439,173.9		
Standard Deviation		11,242.03			7,495.02			462,944.32		

Table A4.2. Statistical data for Eldfisk, B12, C_0-C_3 alkylphenol analyses.

Isomers	Isomer Concentrations (ng g^{-1})		
	Whole Oil	**Supernatant Oil**	**Bound Oil/Emulsion**
phenol	20,617.77	6,151.96	73,383.28
2-methylphenol	7,725.58	1,752.07	20,231.91
3-methylphenol	14,981.11	3,164.77	17,413.6
4-methylphenol	4,616.07	796.14	0
2-ethylphenol	1,480.87	318.92	0
2,5-dimethylphenol	4,824.31	978.41	0
2,4-dimethylphenol	11,827.94	222.57	20,324.19
2,6-dimethylphenol	0	0	9,545.37
3,5-dimethylphenol	11,538.3	1,687.97	11,329.92
4-ethylphenol	1,483.42	243.05	0
3,4-dimethylphenol	716.44	153.92	0
2-propylphenol	157.48	34.04	0
3-isopropylphenol	4,974.83	1,023.31	0
4-isopropylphenol	15,613.84	2,362.1	0
2,4,6-trimethylphenol	403.05	630.57	0
2,3,5-trimethylphenol	2,284.3	2,472.68	0
2,3,6-trimethylphenol	261.42	0	0
3,4,5-trimethylphenol	0	2,472.68	0
Total Hindered	28,964.95	6,409.27	50,101.47
Total Non-hindered	74,541.78	18,055.91	102,126.8
Extract Totals	103,506.73	24,465.18	152,228.28
Average Totals			

Table A4.3. Statistical data for NS1 C_0-C_3 alkylphenol analyses.

Isomers	Isomer Concentrations (ng g-1)						
	Whole Oil		Supernatant Oil	Unbound Oil	Bound Oil/Emulsion		
phenol	134	50.05	150.53	1,960.87	30,715.17	184,653.19	183,006.73
2-methylphenol	664.45	474.51	600.31	1,780.06	8,414	19,644.97	88,882.98
3-methylphenol	331.64	263.27	309.32	1,372.7	7,225.29	25,947.78	97,016.84
4-methylphenol	592.7	395.04	436.49	763.02	0	0	0
2-ethylphenol	121.5	72.99	107.64	1,759.21	0	11,336.15	23,444.23
2,5-dimethylphenol	263.1	175.1	238.15	3,755.81	0	23,540.44	32,220.38
2,4-dimethylphenol	946.85	671.77	1,002.19	6,335.33	13,103.28	95,071.98	34,506.44
2,6-dimethylphenol	280.04	227.53	0	2,985.62	11,719.64	39,868.62	14,928.62
3,5-dimethylphenol	507.26	268.39	397.75	3,443.2	4,514.52	18,864.58	43,352.77
4-ethylphenol	0	577.7	0	0	0	0	0
3,4-dimethylphenol	160.17	136.13	164.36	4,129.44	2,979.89	30,200.37	30,806.01
2-propylphenol	0	0	0	0	0	920.19	0
3-isopropylphenol	257.77	126.22	97.86	107.5	0	3,578.91	0
4-isopropylphenol	277.18	167.39	201.94	200.65	0	0	0
2,4,6-trimethylphenol	127.19	90.82	70.45	0	0	0	0
2,3,5-trimethylphenol	451.84	309.74	383.88	199.25	0	0	0
2,3,6-trimethylphenol	0	49.93	0	201.23	0	0	0
3,4,5-trimethylphenol	233.61	27.12	192.48	0	0	0	0
Total Hindered	2,854.98	2,072.39	2,402.61	17,016.51	33,236.92	190,382.36	193,982.65
Total Non-hindered	2,494.33	2,011.31	1,950.74	11,977.38	45,434.86	263,244.83	354,182.35
Extract Totals	5,349.31	4,083.7	4,353.35	28,993.9	78,671.79	453,627.19	548,165
Average Totals	4,716.5				360,154.66		
Standard Deviation					248,311.91		
+/- Error	632.81						

Table A4.4. Statistical data for NS2 C_0-C_3 alkylphenol analyses.

Isomers	Isomer Concentrations (ng g-1)		
	Whole Oil		
phenol	272.34	1,003.19	370.9
2-methylphenol	498.17	937.36	268.04
3-methylphenol	381.99	670.91	345.65
4-methylphenol	0	0	316.43
2-ethylphenol	25.89	32.25	27.82
2,5-dimethylphenol	62.67	67.36	61.68
2,4-dimethylphenol	372.25	424.93	332.84
2,6-dimethylphenol	0	0	0
3,5-dimethylphenol	172.88	233.06	251.28
4-ethylphenol	168.92	0	0
3,4-dimethylphenol	96.71	116.75	103.64
2-propylphenol	0	0	0
3-isopropylphenol	28.32	39.75	30.2
4-isopropylphenol	95.37	120.63	146.36
2,4,6-trimethylphenol	65.75	74.28	13.81
2,3,5-trimethylphenol	304.73	338.56	299.3
2,3,6-trimethylphenol	18.45	11.23	6.94
3,4,5-trimethylphenol	72.21	77.67	0
Total Hindered	1,347.91	1,885.97	1,010.42
Total Non-hindered	1,288.75	2,261.96	1,564.46
Extract Totals	2,636.66	4,147.93	2,574.88
Average Totals	3,119.82		
Standard Deviation	890.9		

Table A4.5. Statistical data for NS3 C_0-C_3 alkylphenol analyses.

Isomers	Isomer Concentrations (ng g-1)				Isomer Concentrations (ng g-1)			
	Whole Oil		Bound Oil/Emulsion		Whole Oil		Bound Oil/Emulsion	
phenol	800.51	714.98	172,394.46	89,601.97	79.67	115.24	391,515.89	108,284.81
2-methylphenol	3,648.99	3,725.76	13,483.9	24,711.79	278.24	312.91	38,109.7	44,896.23
3-methylphenol	2,322.56	2,331.29	15,373.2	28,893.16	132.77	154.85	45,563.84	46,758.21
4-methylphenol	1,169.09	795.29	0	0	0	0	0	0
2-ethylphenol	379.9	406.52	8,356.06	12,198.21	75.67	67.88	22,074.08	32,594.41
2,5-dimethylphenol	2,559.29	2,683.07	22,965.63	22,277.07	2,643.38	2,240.23	56,630.02	79,967.25
2,4-dimethylphenol	4,220.11	4,284.28	131,029.85	29,463.81	4,461.59	3,664.19	389,768.83	238,797.12
2,6-dimethylphenol	1,877.31	2,230.98	47,918.6	3,436.93	1,635	1,541.75	102,966.41	81,162.79
3,5-dimethylphenol	2,421.41	2,527.93	19,089.23	12,029.25	1,508.89	1,289.48	52,125.9	71,887.74
4-ethylphenol	919.9	887.51	0	0	1,199.54	1,059.49	0	0
3,4-dimethylphenol	626.16	656.57	40,494.71	47,937.32	812.33	694.24	92,623.11	147,103.57
2-propylphenol	41.59	42.88	0	0	27.47	27.04	0	0
3-isopropylphenol	185.72	191.19	0	0	91.42	81.45	0	0
4-isopropylphenol	208.78	225.61	0	0	397.89	332.23	0	0
2,4,6-trimethylphenol	1,475.84	1,602.86	0	0	8,851.19	7,120.74	0	0
2,3,5-trimethylphenol	2,352.87	2,491.46	0	0	10,640.86	8,610.44	0	0
2,3,6-trimethylphenol	773.11	808.38	0	0	5,110.69	4,149.73	0	0
3,4,5-trimethylphenol	86.2	80.34	0	0	446.98	392.52	0	0
Total Hindered	17,329.01	18,276.19	223,754.05	92,087.81	33,724.09	27,734.91	609,549.04	477,417.81
Total Non-hindered	8,740.33	8,410.71	247,351.6	178,461.69	4,669.48	4,119.51	581,828.75	374,034.33
Extract Totals	26,069.33	26,686.9	471,105.65	270,549.5	38,393.57	31,854.42	1,191,377.78	851,452.13
Average Totals	26,378.12		370,827.57		35,123.99		1,021,414.96	
Standard Deviation								
Percent Error	308.79		100,278.08		3,269.58		169,962.79	

Table A4.6. Statistical data for H1 and H7 C_0-C_3 alkylphenol analyses.

APPENDIX 5

Table A5.1. Peak areas for the n-alkanes, isoprenoids, pentacyclic triterpanes and steranes analsyed for oils in Chapter 6.			
Compounds, Abbreviations and Diagnostic Ions	KITTIWAKE	SAMPLE #3	SAMPLE #5
m/z 85			
n-C_{17}	428939	78279	3250
Pristane (Pr)	118346	121484	5944
n-C_{18}	467417	80389	2324
Phytane (Ph)	250040	209202	20838
m/z 191			
18α(H), 22, 29, 30-trisnorneohopane (Ts)	3847	4138	2729
17α(H), 22, 29, 30-trisnorhopane (Tm)	855	1107	507
C_{29}, 17α(H), 21β(H), 30-norhopane ($C_{29}\alpha\beta$)	4329	4262	2799
C_{29}, 17β(H), 21α(H), 30-norhopane ($C_{29}\beta\alpha$)	985	984	507
C_{30}, 17α(H), 21β(H)-hopane ($C_{30}\alpha\beta$)	8705	9790	6130
C_{30}, 17β(H), 21α(H)-hopane ($C_{30}\beta\alpha$)	200	nd	nd
C_{31}, 17α(H), 21β(H)-homohopane(22S) ($C_{31}\alpha\beta S$)	5297	5745	3690
C_{31}, 17α(H), 21β(H)-homohopane (22R) ($C_{31}\alpha\beta R$)	3960	4167	2528
C_{32}, 17α(H), 21β(H)-bishomohopane (22S) ($C_{32}\alpha\beta S$)	4565	4775	3111
C_{32}, 17α(H), 21β(H)-bishomohopane (22R) ($C_{32}\alpha\beta R$)	2692	3034	2130
C_{33}, 17α(H), 21β(H)-trishomohopane (22S) ($C_{33}\alpha\beta S$)	3738	4119	2525
C_{33}, 17α(H), 21β(H)-trishomohopane (22R) ($C_{33}\alpha\beta R$)	2168	2605	1572
C_{34}, 17α(H), 21β(H)-tetrakishomohopane (22S) ($C_{34}\alpha\beta S$)	2865	3274	2052
C_{34}, 17α(H), 21β(H)-tetrakishomohopane (22R) ($C_{34}\alpha\beta R$)	1836	2111	1182
C_{35}, 17α(H), 21β(H)-pentakishomohopane (22S) ($C_{35}\alpha\beta S$)	4220	4484	3031
C_{35}, 17α(H), 21β(H)-pentakishomohopane (22R) ($C_{35}\alpha\beta R$)	2538	3152	1789
m/z 217			
C_{27}, 24 ethyl 5α(H), 14α(H), 17α(H)-cholestane(20R) ($C_{27}\alpha\alpha\alpha R$)	2293	2771	1434
C_{28}, 24 ethyl 5α(H), 14α(H), 17α(H)-cholestane(20R) ($C_{28}\alpha\alpha\alpha R$)	1393	1567	760
C_{29}, 24 ethyl 5α(H), 14α(H), 17α(H)-cholestane(20S) ($C_{29}\alpha\alpha\alpha S$)	2119	2374	1494
C_{29}, 24 ethyl 5α(H), 14α(H), 17α(H)-cholestane(20R) ($C_{29}\alpha\alpha\alpha R$)	2429	2730	1755
C_{29}, 24 ethyl 5α(H), 14β(H), 17β(H)-cholestane(20S) ($C_{29}\alpha\beta\beta R$)	2429	2059	1421
C_{29}, 24 ethyl 5α(H), 14β(H), 17β(H)-cholestane(20R) ($C_{29}\alpha\beta\beta R$)	3195	3708	2212

Table A5.2. Peak areas for the molecules analysed from the crude oils in Chapter 6.			
Compounds, Abbreviations and Diagnostic Ions	KITTIWAKE	SAMPLE #3	SAMPLE #5
m/z 128			
Naphthalene (N)	240358	95198	88174
m/z 142			
2-methylnaphthalene (2-MN)	385611	230869	224008
1-methylnaphthalene (1-MN)	491523	357304	377124
m/z 156			
2-ethylnaphthalene (2-EN)	67872	31689	24843
1-ethylnaphthalene (1-EN)	37002	33498	35681
2,6 + 2,7-dimethylnaphthalene (2,6+2,7-DMN)	223170	183537	184702
1,6-dimethylnaphthalene (1,6-DMN)	235248	252043	264705
1,5-dimethylnaphthalene (1,5-DMN)	134510	124513	144484
m/z 170			
1,3,5 + 1,4,6-trimethylnaphthalene (1,3,5+1,4,6-TMN)	162709	171773	189308
2,3,6-trimethylnaphthalene (2,3,6-TMN)	69311	61587	79533
m/z 178			
Phenanthrene (P)	227002	235694	289873
m/z 192			
3-methylphenanthrene (3-MP)	79381	82682	95510
2-methylphenanthrene (2-MP)	86142	84729	100118
9-methylphenanthrene (9-MP)	227930	231630	263584
1-methylphenanthrene (1-MP)	147814	142384	181171
m/z 184			
Dibenzothiophene (DBT)	249513	283833	329302
m/z 198			
4-methyldibenzothiophene (4-MDBT)	244561	285128	331568
1-methyldibenzothiophene (1-MDBT)	89007	108699	126729
m/z 231			
C_{20}-triaromatic steroid (20R) (C_{20} TA 20R)	13698	15756	18765
C_{28}-triaromatic steroid (20R) (C_{28} TA 20R)	7689	8573	9622

	KITTIWAKE	SAMPLE #3	SAMPLE #5
Biodegradation*			
n-C_{17}/Pr	3.62	0.64	0.55
n-C_{18}/Ph	1.87	0.38	0.11
n-C_{18}/C_{30} αβ-hopane	53.70	8.21	0.38
Ph/C_{30} αβ-hopane	28.72	21.37	3.40
Tm/C_{30} αβ-hopane	0.10	0.11	0.13
N/N+P	0.51	0.29	0.23
2-MN/2-MN + P	0.63	0.49	0.44
2,6+2,7-DMN/2,6+2,7-DMN + P	0.50	0.44	0.39
1,3,5 + 1,4,6-TMN/1,3,5 + 1,4,6-TMN + P	0.42	0.42	0.40
P/DBT	0.91	0.83	0.88
4-MDBT/DBT (MDR4)	0.98	1.01	1.01
Source Correlation**			
Homohopane Indices			
C_{31}αβ(S+R)/[SUM, C_{31}αβ(S+R) to C_{35}αβ(S+R)]	27.32	26.46	26.34
C_{32}αβ(S+R)/[SUM, C_{31}αβ(S+R) to C_{35}αβ(S+R)]	21.42	20.84	22.20
C_{33}αβ(S+R)/[SUM, C_{31}αβ(S+R) to C_{35}αβ(S+R)]	17.43	17.95	17.35
C_{34}αβ(S+R)/[SUM, C_{31}αβ(S+R) to C_{35}αβ(S+R)]	13.88	14.37	13.70
C_{35}αβ(S+R)/[SUM, C_{31}αβ(S+R) to C_{35}αβ(S+R)]	19.95	20.38	20.42
C_{27}ααα R/C_{29}ααα R	0.94	1.02	0.82

*Table A5.3. Results of the biomarker and molecular parameters used to assess extent of biodegradation and source correlation of crude oils in Chapter 6. Key to abbreviations is given in Tables A5.1 and A5.2. * = biodegradation parameters are discussed in Chapter 6. nd = not determined.*

	KITTIWAKE	SAMPLE #3	SAMPLE #5
Maturity Parametesr			
Pr/Ph	0.47	0.58	0.29
Ts/Ts + Tm	0.82	0.79	0.78
$C_{30}\beta\alpha/C_{30}\beta\alpha + C_{30}\alpha\beta$	0.02	nd	nd
$C_{31}\alpha\beta S/C_{31}\alpha\beta S + C_{31}\alpha\beta R$	0.57	0.58	0.59
$C_{32}\alpha\beta S/C_{32}\alpha\beta S + C_{32}\alpha\beta R$	0.63	0.61	0.59
$C_{29}\alpha\alpha\alpha S/C_{29}\alpha\alpha\alpha S + C_{29}\alpha\alpha\alpha R$	0.53	0.54	0.54
$C_{29}\alpha\beta\beta(S+R)/C_{29}\alpha\beta\beta(S+R) + C_{29}\alpha\alpha\alpha(S+R)$	0.55	0.53	0.53
2-MN/1-MN (MNR)	0.78	0.65	0.59
2,3,6-TMN/1,3,5+1,4,6-TMN (TNR)	0.43	0.36	0.42
1.5(2-MP + 3-MP)/(P + 1-MP + 9-MP) (MPI)	0.41	0.41	0.40
Calculate Vitrinite Reflectance			
Rm = 0.60(MPI) + 0.4	0.65	0.65	0.64
(2-MP + 3-MP)/(2-MP + 3-MP + 1-MP + 9-MP) (MPDF1)	0.31	0.31	0.31
4-MDBT/1-MDBT (MDR)	2.75	2.62	2.62
C_{20} TA 20R/C_{20} TA 20R + C_{28} TA 20R	0.64	0.65	0.66

Table A5.4. Results of the biomarker and molecular parameters used to assess the maturities of the crude oils in Chapter 6. Key to abbreviations is given in Tables A5.1 and A5.2. nd = not determined.